Spring 1994

# Behavior of biaxially loaded concrete-encased composite columns

Pedro Ricardo Munoz
*New Jersey Institute of Technology*

# Copyright Warning & Restrictions

The copyright law of the United States (Title 17, United States Code) governs the making of photocopies or other reproductions of copyrighted material.

Under certain conditions specified in the law, libraries and archives are authorized to furnish a photocopy or other reproduction. One of these specified conditions is that the photocopy or reproduction is not to be "used for any purpose other than private study, scholarship, or research." If a, user makes a request for, or later uses, a photocopy or reproduction for purposes in excess of "fair use" that user may be liable for copyright infringement,

This institution reserves the right to refuse to accept a copying order if, in its judgment, fulfillment of the order would involve violation of copyright law.

Please Note: The author retains the copyright while the New Jersey Institute of Technology reserves the right to distribute this thesis or dissertation

Printing note: If you do not wish to print this page, then select "Pages from: first page # to: last page #" on the print dialog screen

## ABSTRACT

## BEHAVIOR OF BIAXIALLY LOADED CONCRETE-ENCASED COMPOSITE COLUMNS

by
**Pedro Ricardo Muñoz**

The theory of nonlinear behavior of biaxially loaded short and slender composite columns is used to study the load-deformation and moment-curvature of four pin-ended composite column specimens tested under axial compressive load and biaxial bending moments in a single curvature. The accuracy of the test results is verified by comparison with analytical results obtained by a method of analysis that includes the nonlinear material properties of concrete and steel and covers the ascending and descending branches of the linear segmented column specimen. A computational method is presented to model the analytical behavior of the biaxially loaded composite column. Its validity is verified by the comparisons with other analytical methods, and the results of experimental tests from four different authors.

A generalized interaction equation for the analysis and design of composite columns is presented. Its validity is verified by comparing the results of existing design examples and some test results with the results obtained from the equation.

A comparative review of the available design methods currently being used in the United States is presented. Their major differences, compatibilities and inconsistences are highlighted and discussed.

Finally some design recommendations are proposed for the analysis and design of biaxially loaded concrete-encased composite columns.

# BEHAVIOR OF BIAXIALLY LOADED CONCRETE-ENCASED COMPOSITE COLUMNS

by
Pedro Ricardo Muñoz

A Dissertation
Submitted to the Faculty of
New Jersey Institute of Technology
in Partial Fulfillment of the Requirements for the Degree of
Doctor of Philosophy

Department of Civil and
Environmental Engineering

May 1994

## APPROVAL PAGE

## BEHAVIOR OF BIAXIALLY LOADED CONCRETE-ENCASED COMPOSITE COLUMNS

**Pedro Ricardo Muñoz**

---

Dr. C. T. Thomas Hsu, Dissertation Advisor — Date
Professor of Civil and Environmental Engineering, NJIT

---

Dr. Methi Wecharatana, Committee Member — Date
Professor of Civil and Environmental Engineering, NJIT

---

Dr. Ala Saadeghvaziri, Committee Member — Date
Associate Professor of Civil and Environmental Engineering, NJIT

---

Prof. Ed. Dauenheimer, Committee Member — Date
Professor of Civil and Environmental Engineering, NJIT

---

Dr. Rong Chen, Committee Member — Date
Professor of Mechanical Engineering, NJIT

## BIOGRAPHICAL SKETCH

**Author:** Pedro Ricardo Muñoz

**Degree:** Doctor of Philosophy in Civil Engineering

**Date:** May, 1994

**Undergraduate and Graduate Education:**

- Doctor of Philosophy in Civil Engineering,
  New Jersey Institute of Technology, Newark, NJ, 1994
- Master of Science in Civil Engineering,
  New Jersey Institute of Technology, Newark, NJ, 1987
- Graduate Studies in Structural Engineering,
  National University of Colombia, Colombia, (1980-1983)
- Bachelor of Science in Civil Engineering,
  University of Cartagena, Cartagena, Colombia, 1979
- Proficiency Degree in English as a Second Language,
  Colombo-American Bilingual Center, Colombia 1984-1985

**Major:** Civil Engineering

**Presentations and Publications:**

- Speaker at the Spring 1991 CEE Seminar sponsored by the Civil and Environmental Engineering Department of NJIT, presenting the topic of Composite Columns, April 1991.

**Professional Experience:**

- 1988 to present. Structural Design Engineer.
  PAUL BECK ASSOCIATES, Structural Engineers, Wayne, New Jersey.
- 1980 to 1985 Structural Design Engineer.
  Ingetec S.A., Consulting Engineers, Bogota, Colombia (South-America).
- 1979 to 1980 Assistant Engineer.
  Arca Ltda., Civil Engineers, Cartagena, Colombia (South-America).

## BIOGRAPHICAL SKETCH
## (Continued)

- 1977 to 1978 Contractor's Assistant
  Vikingos S.A., Fishing Company, Cartagena, Colombia (South-America).

**Educational Experience:**

- Teaching Assistant, Civil and Environmental Engineering Department of New Jersey Institute of Technology, 1986-1988

- Hydraulics Laboratory Assistant, Civil Engineering Department, Cartagena University, Colombia, (South America) 1978.

**Professional Membership:**

- American Society of Civil Engineers, student member
- American Concrete Institute, student member
- Colombian Society of Engineers

This dissertation is dedicated to my beloved
parents Angel Maria and Bolivia Cristina, brothers, sisters,
relatives, and friends.

## ACKNOWLEDGMENT

The Author would like to express his most sincere and profound note of gratitude to his Dissertation Advisor, Professor Cheng-Tzu Thomas Hsu, for his wise and strong academic guidance, constant moral support, and considerate and friendly personal interaction; for providing his very valuable time and advice during the experimental part of this research work, and for partially funding and promoting the Author to a Teaching Assistantship position during the early years of his Doctoral studies at NJIT.

The Author thanks the Civil and Environmental Engineering Department of NJIT for awarding the author a Teaching Assistantship during 1986 to 1988.

Immense gratitude and appreciation is expressed to the members of the Advisory Committee for reviewing and providing the final approval to this Dissertation work.

Special Thanks to the following people:

Mr. Paul C. Beck, P.E., for providing the Author with very valuable engineering experience and job opportunity. Mrs. Theresa C. Soltis, for typing part of the manuscript, All the fellow coworkers and staff at Paul Beck Associates and NJIT: Mr. M. Celeb, Mr. M. Yakowt, Mr. A. Gerchanovich, Dr. B.Y. Bahn, Dr. X.Y. Xing and Mrs Xing, Dr. W.H. Tsao, Dr. L.S.M. Hsu, Dr. G. Wang, Mr. A. Hussain, Mr. M. Faisal, Mr. J. Eimess, Mr. A. Luke and Dr. Herman A. Estrin.

## TABLE OF CONTENTS

## LIST OF TABLES

**Table** **Page**

**Table** **Page**

## LIST OF FIGURES

**Figure** **Page**

**Figure** **Page**

**Figure** **Page**

## LIST OF PHOTOGRAPHS

## LIST OF SYMBOLS AND NOTATIONS

| | |
|---|---|
| $a$ | depth of equivalent rectangular stress block = $\beta_1$ c |
| $a_k$ | cross sectional area of small element k |
| $A_c$ | net area of concrete |
| $A_{sr}$,$A_r$ | area of longitudinal reinforcing bars |
| $A_s$ | area of structural steel shapes |
| $A_t$ | area of structural steel shape, pipe, or tubing in a composite section |
| $A_g$ | gross area of cross section |
| $A_w$ | area of web of rolled steel shape |
| $A/C$ | aggregate-cement ratio |
| $AS2$ | cross sectional area of one leg of a lateral tie |
| $b$ | width of compression side of cross section |
| $B_1$,$B_2$ | bending factors for combined flexure and axial loads for firs order analysis |
| $B2$,$D2$ | short and long lateral ties dimensions |
| $c$ | distance from extreme compression section fiber to the neutral axis |
| $c_1$,$c_2$,$c_3$ | numerical coefficients for concrete-filled pipe or tubing, and for concrete encased steel shapes by LRFD |
| $c_r$ | edge distance from face of section to centroid of reinforcing bars |
| $C_1$ | confinement coefficient, function of lateral ties size and spacing |
| $C_c$ | resultant compressive axial strength provided by concrete |
| $C_m$ | coefficient applied to the bending moment term in the interaction equation |
| $C_{mx}$,$C_{my}$ | coefficient applied to the bending moment about the x and y axis |
| $C_{si}$ | compressive axial strength provided by the ith steel bar of the cross section |

## LIST OF SYMBOLS AND NOTATIONS
**(Continued)**

$dA$ small differential element area of cross section

$e_{byx}$ eccentricity along the x axis for the corresponding balance load $P_{nby}$

$e_{bxy}$ eccentricity along the y axis for the corresponding balance load $P_{nbx}$

$e_x, e_y$ eccentricities of the axial load along the x and y axis respectively

$E_c$ modulus of elasticity of concrete in compression

$EI$ flexural stiffness of a compressive cross section

$E_{ct}$ modulus of elasticity of concrete in tension

$E_s$ modulus of elasticity of steel

$(E_s)_k$ secant modulus of elasticity of element k

$E_{t1}, E_{t2}, E_{t3}$ concrete modulus of elasticity at tensile strain limit values of $e_1, e_2, e_3$

$E_m$ modified modulus of elasticity for composite members by LRFD

$F_a$ allowable axial stress

$F_b$ allowable bending stress

$F_{cr}$ critical stress for a steel section by LRFD

$F'_e$ reduced Euler buckling stress by LRFD

$F_{my}$ modified yield stress for composite members by LRFD

$F_{mc}$ modified allowable stress for composite section by LRFD

$F_{mcr}$ modified critical stress for composite section

$F_y$ specified minimum yield stress of steel shape, pipe or tubing

$F_{yr}$ specified minimum yield stress of longitudinal reinforcing bars

$f_a$ calculated axial stress

## LIST OF SYMBOLS AND NOTATIONS
**(Continued)**

$f_b$ calculated bending stress

$f'_c$ compressive strength of concrete, measured at 28 days after casting

$f_t$ modulus of rupture of concrete

$f_y$ specified yield stress of reinforcing steel bars

$h$ length of column segment

$h_1,h_2$ thickness of cross section parallel and perpendicular to plane of bending

$H$ horizontal force applied at a story

$i$ denotes the number of segments along the length of a column

$I_g$ moment of inertia of gross concrete section about centroidal axis, neglecting reinforcement

$I_m$ modified moment of inertia of the composite cross section

$I_t,I_s$ moment of inertia of structural steel shape, pipe or tubing about centroidal axis of composite member cross section

$I_{sr},I_{se}$ moment of inertia of steel rebars about centroidal axis of section

$j$ denotes the number of joints along the length of a column

$k$ subscript denoting cross section element number

$k_x,k_y$ rotational stiffness coefficients about the x and y axis respectively

$K$ effective length factor for compression cross sections

$L$ column length at a story

$M_{1b},M_{2b}$ smaller and larger bending moments at end of unbraced column

$M_{bxy}$ bending moment in the y-axis corresponding to the balanced load $P_{nbx}$

$M_{byx}$ bending moment in the x-axis corresponding to the balanced load $P_{nby}$

## LIST OF SYMBOLS AND NOTATIONS
**(Continued)**

$M_{fx}$,$M_{fy}$ bending moment shape factors about the x and y axis respectively

$M_{nb}$ nominal balanced moment for bending at an inclined plane to the major axis

$M_{nbx}$ nominal balanced moment for bending about the x axis

$M_{nby}$ nominal balanced moment for bending about the y axis

$M_{nt}$,$M_{lt}$ required flexural strength of member with and without member translation

$M_{RA}$,$M_{RB}$ restraining moments at ends a and b of a compression member

$M_u$ factored bending moment at cross section

$M_{ux}$,$M_{uy}$ required flexural strength about the x and y axis respectively

$M_x$,$M_y$ bending moments in the x and y planes respectively

$M_{XA}$,$M_{XB}$ final bending moments at restrained ends a and b about the x-axis

$M_{YA}$,$M_{YB}$ final bending moments at restrained ends a and b about the y-axis

$n$ number of cross section elements

$P$ axial load

$P_d$ design strength axial compressive or tensile load by LRFD

$P_e$ Euler axial buckling strength by LRFD

$P_{cr}$ critical buckling Euler load

$P_{crx}$,$P_{cry}$ critical buckling Euler load about the x and y axis

$P_{mcr}$ modified critical buckling Euler load for a composite section

$P_o^{(+)}$ maximum axial compressive load of a composite cross section

$P_o^{(-)}$ maximum axial tensile load of a composite cross section

$P_n$ nominal axial compressive strength

## LIST OF SYMBOLS AND NOTATIONS
**(Continued)**

| | |
|---|---|
| $P_{NJIT}$ | axial load from the Generalized Interaction Equation of Failure Surface |
| $P_{nb}$ | nominal balanced load for bending about an inclined plane to the major axis |
| $P_{nbx}$ | nominal balanced load for bending about the x axis |
| $P_{nby}$ | nominal balanced load for bending about the y axis |
| $P_t$ | experimental or testing ultimate load of cross section |
| $P_u$ | factored axial load at given eccentricity $\leq \phi P_n$ |
| $r_m$ | modified radius of gyration for composite sections by LRFD |
| $r_{mc}$ | modified radius of gyration for composite sections |
| $SP$ | spacing of the ties |
| $S_{sc}$ | elastic section modulus for the steel shape of composite columns |
| $S_{ij}$ | element of the stiffness matrix in terms of the secant modulus of elasticity |
| $S_m$ | modified section modulus for composite columns |
| $s$ | joint number along the deflected column length |
| $t$ | overall depth of cross section |
| $T_{si}$ | tensile axial strength provided by the ith steel element of the cross section |
| $u,v$ | lateral deflections along the x and y axis respectively |
| $x,y$ | coordinates of a point at a cross section along the x and y axis respectively |
| $x_c,y_c$ | coordinates of the point of application of the resultant compressive force |
| $x_k,y_k$ | coordinates of element k along the x and y axis respectively |
| $x_{si},y_{si}$ | coordinates of each steel element respect to the plastic centroid |
| $w$ | unit weight of concrete |

## LIST OF SYMBOLS AND NOTATIONS
**(Continued)**

$W/C$ water-cement ratio

$\alpha$ coefficient to define the shape of the load-moment interaction diagram

$\alpha_{cx}, \alpha_{cy}$ coefficient to define the shape of the compression controlled region of the load-moment interaction diagram respect to the x and y axis respectively

$\alpha_{tx}, \alpha_{ty}$ coefficient to define the shape of the tension controlled region of the load-moment interaction diagram respect to the x and y axis respectively

$\beta$ coefficient to define the shape of the load-contour diagram at a constant axial load $P_n$

$\beta_d$ ratio of maximum factored axial dead load to maximum total factored axial load

$\beta_1$ factor for determining depth of concrete compressive stress block

$\delta$ lateral deflection of cross section

$\delta_{mfx}, \delta_{mfy}$ moment magnification factor for x and y bending moments respectively

$\Delta$ lateral midheight translation of center line of compression member

$\Delta_{oh}$ lateral translation of columns supporting a story

$\varepsilon$ strain at a point of a cross section

$\varepsilon_c$ compressive strain of concrete

$\varepsilon_{cu}$ ultimate compressive strain of concrete

$\varepsilon_{cu}^{I}, \varepsilon_{cu}^{II}, \varepsilon_{cu}^{III}$ concrete compressive strain limit values

$\varepsilon_k$ strain at element k of a cross section

$\varepsilon_o$ strain at the plastic centroid of a cross section

$\varepsilon_t$ tensile strain of concrete

$\varepsilon_1, \varepsilon_2, \varepsilon_3$ tensile strain limit values of concrete

## LIST OF SYMBOLS AND NOTATIONS
**(Continued)**

| | |
|---|---|
| $\lambda_g$ | slenderness ratio of concrete gross section of a composite column |
| $\theta$ | angular direction of the neutral axis |
| $\theta_a, \theta_b$ | angular rotations of ends a and b of a compression member |
| $\rho_g$ | percentage of steel rebar area to gross concrete area |
| $\rho_s$ | percentage of steel rebar and steel shape area to gross concrete area |
| $\lambda_c$ | column slender parameter for steel shapes and composite sections by LRFD |
| $\lambda_{mc}$ | column slender parameter for composite sections |
| $\sigma$ | stress at a point in the cross section |
| $\sigma_c$ | stress value of concrete in compression |
| $\sigma_k$ | stress at element k of a cross section |
| $\phi$ | curvature of cross section and strength reduction factor |
| $\phi_b$ | strength reduction factor for flexure |
| $\phi_c$ | resistance factor design for axial compressive strength of composite section |
| $\phi_x, \phi_y$ | curvatures of a cross section in the x and y planes respectively |

## LIST OF CONVERSION FACTORS

1 ft. = 0.3048 m

1 in. = 25.4 mm

1 yd = 0.9144 m

1 sq ft = 0.092903 $m^2$

1 sq in. = 645.16 $mm^2$

1 cu ft = 0.0283168 $m^3$

1 lbf = 4.448 N

1 tonf = 2,240.1 lbsf

1 lbm = 0.5 kg

1 psf = 48 Pa

1 psi = 6.895 kPa

1 ksi = 6.895 MPa

1 kip = 4.448 kN

1 short ton = 907 kgf

1 gal.(U.S.) = 0.004 $m^3$

1 mi = 1.60634 km

# CHAPTER 1

# INTRODUCTION

A composite column is a structural member that uses a combination of structural steel shapes, pipes or tubes with or without reinforcing steel bars and reinforced concrete to provide adequate load carrying capacity to sustain either axial compressive loads alone or a combination of axial loads and bending moments. The interactive and integral behavior of concrete and the structural steel elements makes the composite column a very cost effective and structural efficient member among the wide range of structural elements in building and bridge constructions.

A typical example of a composite column subjected to bending moments around two major perpendicular axes due to wind, earthquake, or unbalanced live loads and in combination with axial compressible loads could be found in bridge piers and at the corners of a three-dimensional building frame, as shown in Fig. 1.1. We could also find those columns subjected to bending moments in combination with axial tensile loads, in which case it would be necessary to have a design method that includes the overall range of combinations of axial load and bending moments.

## 1.1 General Concept of Composite Columns

Composite columns may be of two kinds:(1)Concrete-filled pipe and tubular steel columns, and (2) concrete-encased steel columns, as shown in Figs. 1.2(a) to (d). Fig. 1.2(a) and (b) shows a composite column in which the steel pipe and tube serve both as form and reinforcement. The column may be reinforced with longitudinal bars

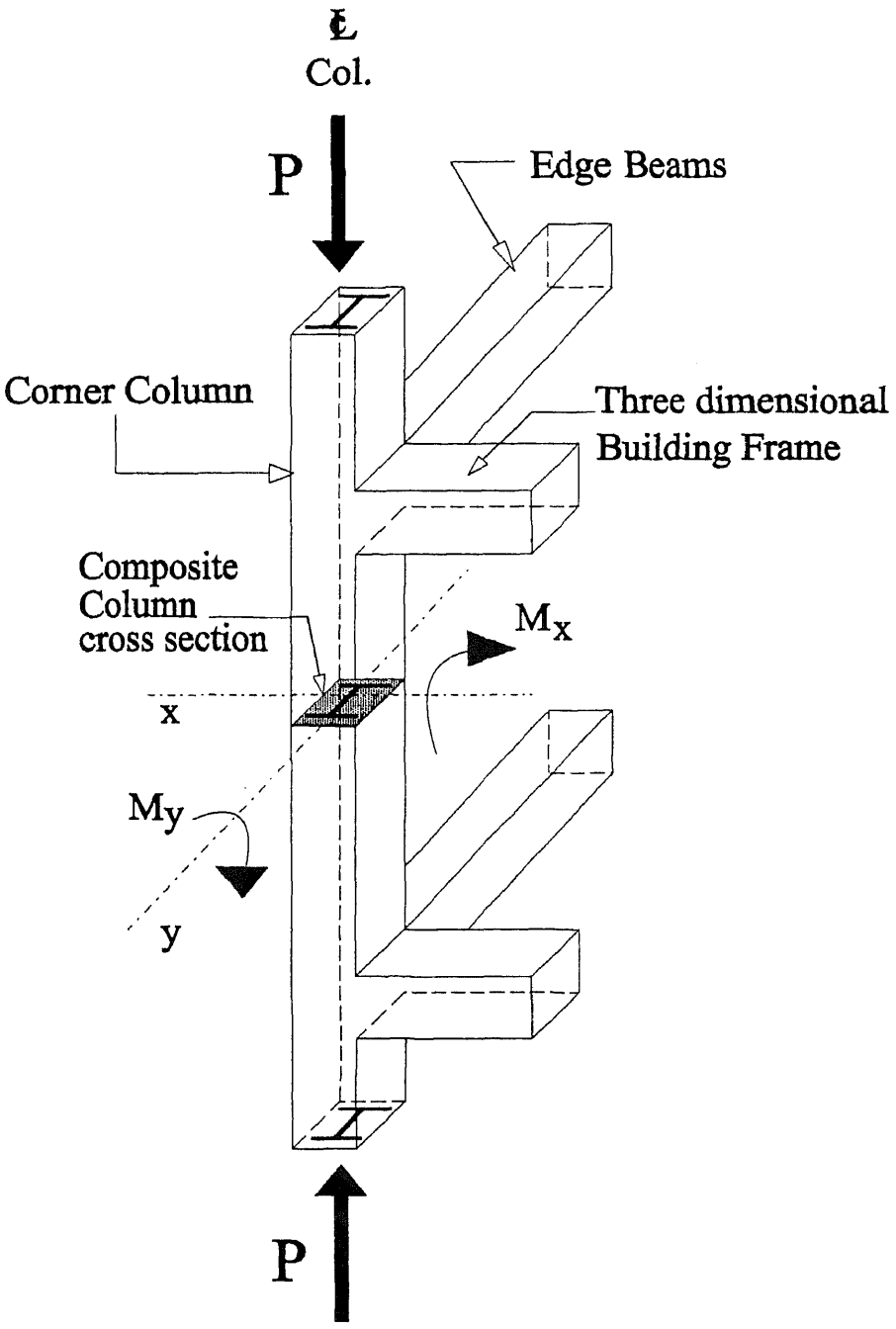


**Figure 1.1** A Typical three-dimensional structural building frame

and have shear studs welded to the structural steel shape in order to maintain the elements together as a unit. Fig. 1.2(c) shows a wide flange structural steel shape encased by concrete and reinforced with longitudinal bars, in some cases shear studs are welded to the steel to improve shear transfer between steel and surrounding concrete. In early 1950's, structural steel shapes were encased by plain concrete without longitudinal bars, such encasement was used mainly for fireproofing purposes. A very low-strength concrete was used and no intention was made to use the concrete's contribution to load-carrying capacity and column stiffness properties.

Figure 1.2 (d) shows a circular reinforced concrete-encased structural steel shape with longitudinal bars and shear studs. The composite columns shown in Figs. 1.2 (c) and (d) describe one of the major applications and advantages of using the steel core for construction purposes, the erection of the structural steel framing speeds-up the overall building construction after which the concrete encasement completes the composite construction system. Figs. 1.2 (e),(f) and (g) show typical configurations for built up sections consisting of two or more structural steel shapes, basically channels and angles that could be laced or battened together forming one piece.

It is important to note that the use of composite columns in a framing system enhances the rigidity of the building and provides significant shear resistance to strong earthquakes and other lateral loads. Composite columns can be used very effectively in high-rise building systems to reduce the size of the main columns of the building and increase the usable space of the floor plan.

Other types of composite columns include the exterior columns of a framed-tube concrete-encased steel structure that takes advantage of the architectural

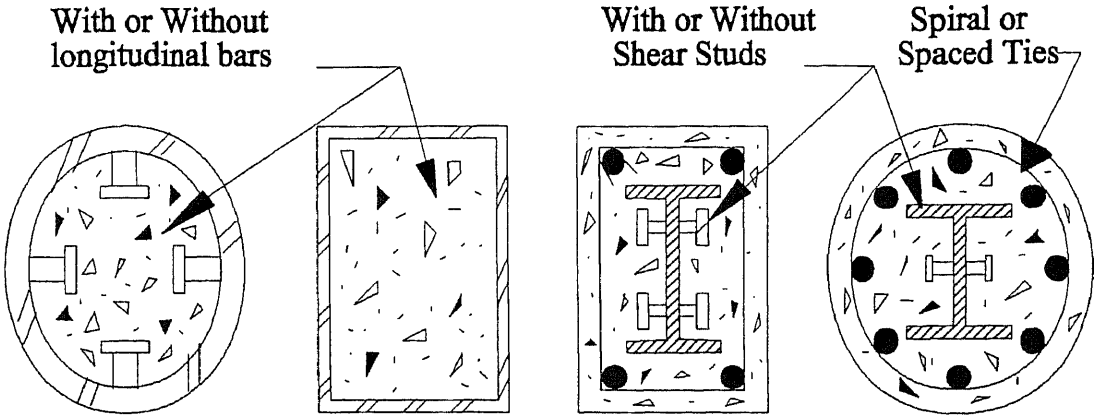


(a) Concrete filled Pipe Column

(b) Concrete filled Tubular Column

(c) Reinforced Concrete with encased wide flange steel shape

(d) Circular Reinforced Concrete with encased wide flange steel shape

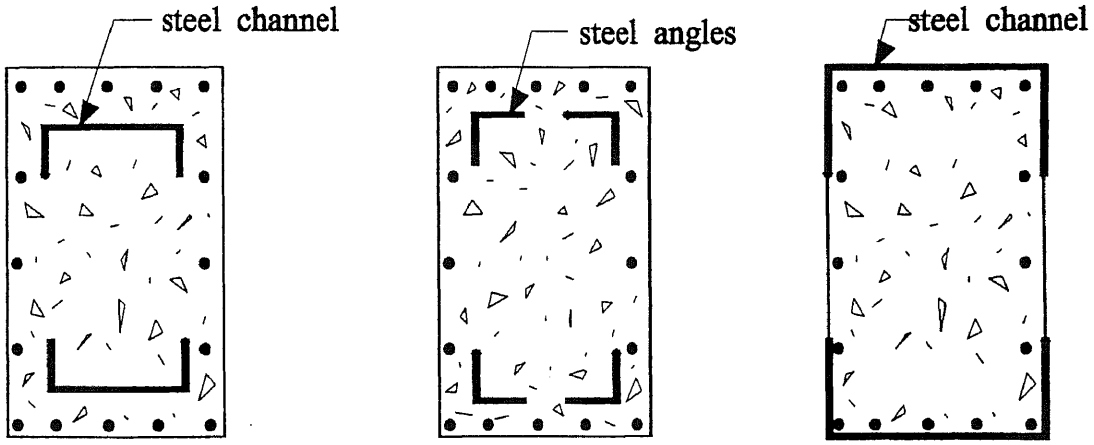


e ) Reinforced concrete with encased steel channel shape

f ) Reinforced concrete with encased steel angles shapes

g ) Reinforced concrete partially encased steel channel shape

**Figure 1.2** Composite Column Types

embedded bent steel plate cladding to provide a composite section. Some special applications include the use of large structural steel shapes encased in concrete shear wall or basement walls to increase the lateral stiffness.

The general design approach of short composite columns is basically the same as for typical reinforced concrete columns. Special procedures are applied to the case of slender composite columns, where some parameters such as: the stiffness of the composite cross section, the radius of gyration, the allowable axial composite stress and the structural stability among other parameters differ considerably from those of slender reinforced concrete columns.

In order to obtain an adequate and safe design of composite columns, it is necessary that the interaction between the structural steel shape and the surrounding concrete must be satisfied by providing shear connectors such as lugs, plates, or small reinforcing rods welded to the structural steel shape previous to concrete casting.

### 1.2 Historical Background, Development and Applications

In early 1900's, concrete was used to encase steel columns and beams, and as a fill material for floor systems. In those applications, concrete was mainly used to provide fire protection for steel and finishes or flat surfaces for columns, beams and floors.

Johnston (106) presented a compilation of the most relevant and important information on the topic of composite columns for the Structural Stability Research Council. Some of the materials are herein summarized and introduced as part of the literature review.

Historically, the definition of composite columns was intended to designate all concrete columns that were reinforced with anything different from reinforcing rods,

and its use preceded that of reinforced concrete columns by about 20 years.

Built up composite columns consisting of two or more structural steel sections or cast iron encased in concrete were used in the early developments of composite columns, they were used long time before the typical concrete encased single steel I-section became very popular in the 1940's.

In the early 1900's Emperger (58), Burr (24), Mensch (140,141), Talbot and Lord (213), Withey (229), and Molitor (142) reported tests on composite columns containing steel and cast iron reinforcement that were the basis for the very first proposed formulas to predict the strength of composite columns. The first reported tests on built up composite columns under concentric loading were presented by Emperger (58) in 1905.

Composite Columns in the early 1920's were reinforced with cast iron cores, and the designers relied on actual load tests of the specific type of cross section to be used without any analytical approach.

Tucker (214) advocated the use of a strength formula for short concrete columns, where the ultimate strength was the sum of the concrete and reinforcement capacity, with a linear interaction due to the column height. Tucker included the safety factors and made reference to statistical correlation with strength based on field tests. Tucker's recommendations were a fundamental contribution to the concrete column technology with great impact on the design methods and procedures implemented around the 1970's.

In 1930, Mensch (143) demonstrated that the cast-iron cores developed higher ultimate stresses than those by the steel shapes, and concluded that the cast iron would provide the most cost effective type of reinforcement for the composite cross

section. Almost the same time when the cast-iron was being used as the main reinforcement for concrete columns, the steel producers were developing a way to produce reinforcing rods with better physical properties and stronger. They were less expensive than those of the cast-iron reinforcement.

The history of the first applications of composite columns in the construction industry dates back to the 1940's. The current design standards and specifications are originated from either the steel or concrete design approach of that time and were always addressed in the United States by the American Institute of Steel Construction (AISC), and the American Concrete Institute (ACI) for the steel and concrete industry, respectively.

In 1940's and 1950's, composite construction started to develop rapidly, and solid concrete slabs with encased steel beams were used extensively, with considerable composite action allowed in some instances. The appearance and application of mechanical shear connectors in late 1950's encouraged the development of composite structural systems.

Until the 1950's, fireproofing of the steel-framework was achieved by encasing the steel columns in a low-strength mix of concrete but with no contribution of the concrete to the strength of the column. Faber (71), and Stevens (201) performed tests on encased columns that showed the economical advantage on using a better quality (higher compressive strength) concrete that could allow the use of the columns as a composite structural member.

The development of sprayed-on fire protection in 1960's substantially eliminated the use of composite columns for anything but very special and specific uses; and since then, its use is very limited in current practice. McDevitt and Viest

(149) in 1972, presented a Report summarizing the progress and developments on Composite Columns from 1960 up to the early 1970's.

In 1960's and 1970's, the rapid development of the high-rise building industry and the need to provide more rigid structural systems to sustain very severe lateral loading due to seismic and wind conditions set the grounds for a widespread use of mixed steel-concrete systems as a viable alternative in terms of cost and construction process than the traditional all steel or all concrete structural framing systems. In 1980's and 1990's, the composite column started to play a major role in the development of some of the most important and tallest high-rise buildings in the United States, Japan and other parts of the world.

In 1969, Khan (149) started using mixed steel-concrete into a single system for the lateral load resisting system of mid and high-rise buildings. One of his first applications features the use of composite exterior columns and spandrel beams for a 20-story mid-rise building in Chicago.

As stated by Iyengar (102) in 1977 the British Standard BS449 permitted some compressive stress in the concrete for the axially loaded columns and a further increase in steel stress was permitted by a larger radius of gyration for the encased column. The structural composite behavior was generally ignored in the strength calculations.

In United States of America a joint Structural Specifications Liaison Committee (SSLC) was organized in 1978 under the direction of George Winter to evaluate the acceptability of a common composite column design procedure that would be acceptable to the steel and concrete industry. The Structural Stability Research Council (SSRC) in 1979 published a report where they recommended the

use of a parabolic type of interaction equation for a combined axial load and uniaxial bending moment.

Furlong (72) in 1983 presented a comparison of the interaction diagrams obtained by the different recommendations of the ACI, AISC, and SSLC. He also described the Steel Industry Specifications (AISC and LRFD), and the Concrete Industry Specifications (ACI) applicable to the design of composite columns. Three different sets of provisions were compared and the applicability of each method was discussed.

In China 1983, Xi et al. (236) presented a paper describing the various shapes of composite columns being used in China, where steel members are filled with concrete to provide the columns to support the new factory buildings.

In Japan, the reinforced concrete industry have incorporated the use of light structural steel shapes such as angles, T-sections, and channels, which are very weak as slender structural steel columns due to their torsional and flexural buckling tendency, into reinforced concrete members in order to provide a composite column with a stronger structural capacity. The Japanese called these types of composite columns as Steel Reinforced Concrete (SRC) members. Due to the large seismic forces that the columns have to carry under the working stresses design conditions, the SRC columns usually result in a stocky cross section.

Composite Columns and Composite Construction in Japan are often identified as SRC Structures (steel-frame-reinforced concrete structures), and have been widely used in the Building Construction Industry since the 1923 Kanto Earthquake. Composite Columns are recognized for their great energy absorption capacity and resistance to Earthquake loads. Abe (14) presented an outline of the structural

system used for the SRC Elevated Station Structures of the new Bullet Trains in Japan.

Recent research work on Composite Steel Reinforced Concrete Buildings in Japan in 1984 were presented by Wakabayashi (230,233). In 1977, Wakabayashi (232), proposed a new design method for composite columns by extending the concept of superimposed strength that led the researchers in Japan to undertaking theoretical and experimental investigations of slender composite columns.

Extensive documentation on the State of the Art applications of composite construction in Japan has been presented by the Japanese Society of Civil Engineers in a report prepared by the subcommittee on Steel-Concrete Composite construction (108) and the Architectural Institute of Japan.

Lu, Slutter, and Yen (128) in 1984, presented the results of the recent research on composite structures for buildings and bridge applications carried out at Lehigh University during the past six years. Some of the topics covered among others include the strength of steel stud anchors and composite beam-to-column joints which are directly related to the behavior of composite columns.

Roik and Bergmann (176) in 1984 described a computational procedure to obtain the basic points of an interaction diagram for encased steel shape columns based on a plastic stress distribution for both steel and concrete.

Later in 1986 the AISC (13) adopted expressions for limit strength of composite columns and included them in the new Load and Resistance Factor Design Method (LRFD), using a linear interaction formula for the Axial Load and Bending Moment relationship.

Griffis (81) in 1986 presented a paper on which he discussed some design

considerations for composite-frame construction. Two case studies of high-rise buildings with composite-frame were described. Erection procedures, stability, and strength resistance were highlighted. A summary of research needs, basic design questions over the responsibilities of the structural designer on the proper design criteria being assumed in the overall composite-frame structural system and potential future research were discussed

Iyengar and Iqbal (102) in 1987 discussed several topics of composite construction, including the composite columns. They also presented a brief description of historical development of composite construction.

Some of the most relevant applications of composite columns in building industry in the United States and some other parts of the world are herein presented to demonstrate that this very strong structural element could offer to the engineering construction industry, specially in tall buildings and bridges. A brief description of the Building Projects where the Composite Columns have been used is presented below:

A. - The 775-ft-tall FIRST BANK PLACE TOWER in Minneapolis, 53-story high, (ENR, July 29, 1991, pp.24-25), features four massive steel-and-concrete composite supercolumns that are responsible for the overall load carrying capacity of the building under all gravity, lateral, and torsional loads.

B.- The 794-ft-tall MELLON BANK CENTER in Philadelphia, 54-story high, (ENR, July 19,1990, pp.30-32), features a composite structural system that joins steel and concrete throughout the building in both the perimeter columns and the core. L-shape structural steel encased composite columns are used at the corners of the building core to sustain the total wind and gravity forces.

C.- The 619-ft-tall ONE DETROIT CENTER TOWER in Detroit, 44-story high,

(ENR, October 18, 1990, pp.22), features eight full-height super-columns, two at each corner of the building. Each super-column is the composite type with structural steel shapes encased in 8000-psi concrete.

D.- The 1,209-ft-tall BANK OF CHINA's HONG KONG, 73-story high, (ENR, October 13, 1988, pp.36-46), is a composite space frame with four steel-concrete megastructure composite columns at the four corners of the building and some megastructure fully composite diagonal transfer columns.

E.- The TWO UNION SQUARE Office Complex in Seattle, Washington (Civil Engineering Magazine, ASCE, October 1990, pp. 83-84), features a large concrete column wrapped in steel shells, with concrete of 19,000 psi.

F.- The proposed MIGLIN-BEITLER TOWER in Chicago (potentially the world's tallest building at close to 2,000 ft.) will have a concrete core surrounded by a steel frame. Composite columns will consist of steel erection columns encased in concrete.

G.- The FIRST CITY TOWER, a 49-story high-rise building in Houston, features a very complete composite structural system, including: a) Composite floor-framing system, b) Composite stub girder system, c) Composite columns, d) Composite lateral framing resisting system, e) Composite shear walls, and f) Composite construction system. The use of Steel and Concrete in a mixed system produced a cost-effective design and expedited the building construction.

H.- The AMERICA TOWER, a 42-story, 620 ft. high rise composite building in Houston, Texas, features the closely spaced exterior composite columns and deep spandrel beams that form the basic lateral resisting framing system.

I.- The THREE HOUSTON CENTER GOLF TOWER, in Houston, Texas, is a 52-story tall building featuring an upper levels wind lateral bracing system consisting of

exterior composite columns interconnected with steel spandrel exterior beams.

J.- The MARATHON OIL TOWER, in Houston, Texas, is a 41-story tall building with two basement levels. It features a Wind Framing Resisting System consisting of an exterior tube with composite columns and long composite shear walls with concrete spandrel exterior beams. Some of the composite shear walls were fabricated by using steel plates to form the edges of the shear wall at the corners. The limitations in architectural dimensions required the engineer to design the structural steel shapes within the concrete shear walls.

K.- The 5956 SHERRY LANE OFFICE TOWER, in Dallas, Texas, is a 22-story office building, featuring a combination of steel, concrete, and mixed steel-concrete framing. The transition between the steel frame used in the upper levels and the concrete frame in the lower levels was achieved by using Composite Columns at one of the intermediate levels.

L.- The MERCANTILE FINANCIAL CENTER in Dallas, Texas, is a 60-story tower. Composite Columns were considered as part of the extensive value engineering studies to determine the most economical system for wind resistance.

## 1.3 Literature Review

The design of composite columns in Great Britain is covered in the 1959 edition of the British Standard BS 449, which allows some compressive stresses in the concrete encasement based on a modular ratio of 30, and the allowable stress in the steel using a larger radius of gyration. The British Standard limits the total axial load of the composite column to twice the axial load on the steel section alone, and the bending moments are to be carried only by the steel section. A straight line type

interaction formula is specified for combined axial load and bending moment with only the axial compressive load to be increased due to the encasement.

In mid-1960's, Stevens (195) in 1965 performed an experimental work on composite columns under eccentric loads, followed by theoretical work done by Bondale (34) in 1966 and Basu (22,23) in 1967 and 1969 respectively. They attempted to predict the actual strength of eccentrically loaded composite columns.

Based on the results of extensive tests on axially and eccentrically loaded encased steel columns conducted at the Building Research Station in London in 1965, where the primary variable was the slenderness radio, Stevens (195) in 1965 compared the column curve generated by these tests with those of reinforced concrete columns and concluded that due to the similarity of the behavior of the reinforced and encased columns, similar principles of design should govern both forms of columns.

In 1963 the ACI Building Code specified the use of an allowable axial load equation for structural steel encased in concrete based on the allowable stress in concrete with a corresponding equivalent modular ratio of 100. The bending moments were to be resisted by the structural steel section alone.

Stevens (195) in 1965 recommended an ultimate strength equation for short columns and a straight line type interaction formula for eccentrically loaded columns and suggested the use of the same reduction coefficients for long composite columns as those being used for long reinforced concrete columns to account for the slenderness effects.

Later in 1967 Basu (22) presented a theoretical approach to compute the failure load of eccentrically loaded composite columns. Their method is based on the

assumption that the deflected shape of the column is part of a cosine curve. From the previous theoretical approach, Basu and Sommerville (23) in 1969 presented an empirical method for predicting the failure loads of composite columns under axial load and different end eccentricities. This empirical method was derived from numerical results obtained from a generalized computer program for a large number of encased and filled rectangular tubular columns.

Basu and Hill (36) also reported analytical results obtained by the use of a new computer program that took into account the actual equilibrium shape of the deflected column rather than the previously assumed cosine deflected shape.

The British approach of the 1970's for the design of composite columns was based on the work of Basu and Sommerville (23) and Virdi and Dowling (218) respectively. The procedure made use of an idealized interaction diagram defined by coefficients k1, k2, and k3 and used an equivalent slenderness ratio parameter to account for the contribution of the concrete section to the strength and stability of the composite section. No minimum eccentricity requirement was imposed for the design of columns under axial loads alone, as required by the ACI-71. Long term loading effects and imperfections are handled by modification factors.

The British procedure consists of defining an idealized interaction diagram between the axial load and uniaxial moment that provides empirical coefficients k1, k2, and k3, which approximates the actual interaction diagram. Once the interaction diagram is determined, the strength of any column for a certain combination of axial load and moment can be checked. For biaxial moment conditions, Basu used the generalized Bresler's interaction equation.

The 1971 ACI Building Code provisions for analysis and design of composite

columns was based on the ultimate strength design concept and assumed the same design rules for composite columns as for reinforced concrete columns. The 1971 ACI Code specified a minimum eccentricity and a moment magnification factor to account for the slenderness effects.

Virdi and Dowling (222) in 1973, presented a method for computing the strength of a composite column under a combination of axial compressive load and Biaxial Bending moments, based on assuming a cosine type configuration of the deflected shape of the column under load, and which they compared with the test results of nine encased columns. In 1976, Virdi and Dowling (221) extended their study on composite columns and presented a general method for calculating the ultimate load of biaxially restrained composite columns by applying a numerical integration scheme to determine the exact configuration of deflected column shape.

A very valuable source of information on typical joint and fabrication details and fire protection specifications and concrete placement and compaction on concrete-filled hollow steel sections is available from CIDECT (46).

The topic of composite columns is covered very briefly in most textbooks of reinforced concrete and structural steel design. Even though some selected references and building codes are given on those textbooks, a lack of basic design examples and guidelines discourage the novice practicing structural design engineer to design the composite columns in an actual building project.

In the U.S. Furlong (65,66,67,68,74) have conducted a great amount of research work on composite columns in the past two decades. His findings, comparisons, and proposed design methods have formed the basis for the ACI and AISC recommended and current design approaches for short and slender steel-

encased and concrete-encased composite columns.

The ultimate strength of short composite columns was numerically studied by Brettle (37) and Lachance (129) among others. Lachance (129) developed a theoretical analysis to study the non-linear and linear behavior of composite sections of arbitrary shape subjected to biaxial loading. He compared the results with those obtained by other authors. Lachance (129) showed that the factor which most influences on the behavior of ultimate strength and curvature of biaxially loaded composite columns was the allowable concrete compressive strain and the shape of the concrete stress distribution had little influence on the cross sectional behavior.

Viest (220) in 1974 presented a report containing the state-of-the-art on Composite Steel-Concrete Construction. In this report, Viest highlighted the major subjects discussed in the 1972 Congress of the International Association for Bridge and Structural Engineering. Viest reported that Composite Steel-Concrete Construction has been widely used throughout the world and that a substantial progress on this field was achieved in 1960's and 1970's. Among other topics covered in this report, one can find a section on Steel-Concrete Composite Columns with pertinent references and bibliography.

In Japan, the design of composite columns in the Steel Reinforced Construction Industry is based on a simple method of superposition that uses the allowable stresses of the materials or the working stress method.

Roderick and Rogers (175) in 1969 performed experimental tests on simple composite columns. Knowles and Park (116) in 1970 also conducted tests on concrete filled steel tubes. A brief review of the current design methods on composite columns is presented in the Building Structural Design Handbook (102) published in 1987.

The ACI-UBC and the AISC-SSRC methods are also discussed in the Handbook mentioned above.

Furlong (69) in 1976 published rules for composite column design based on the AISC column design method. He compared the design provisions given by the ACI code with the test results and the AISC design method. In 1977, Furlong (74) proposed equations for the evaluation of allowable service loads on composite columns. He attempted to provide for a continuous transition between the existing AISC design provisions applicable to the structural steel and the existing ones recommended by the ACI Building Code for reinforced concrete. Later Furlong (70) in 1978 proposed interaction design equations for composite columns.

In 1980, Johnson and Smith (110) at the University of Warwick in England, presented a Design method and a set of recommendations in Code format for Composite Columns. A comparison with other design methods and worked examples were also given and discussed.

Roik and Bergmann (181) in 1982 proposed a design method of biaxially loaded composite columns based on the strength interaction curves for a uniaxial bending.

Bergmann (27) at the University of Ruhr, Bochum, in Germany (1981), presented a comprehensive calculation program to determine the strength of composite columns by taking into account their non-linear geometrical and physical characteristics.

Yee, Shakir-Khalil, and Taylor (238) in 1982 suggested the use of a new type of composite column for use in multi-story Buildings. The proposed new type of composite column consisted of battened steel channels with in-filled concrete. They

presented a set of design expressions to calculate the strength of the new type of composite column to be in accordance with the current U.K. Bridge Code. The method showed simple expressions for the calculation of ultimate loads. Later in 1983, Taylor et al. (217) presented the results of experimental tests done on nine large-scale composite columns of the type described in their early theoretical work (238).

The Structural Specifications Liaison Committee (SSLC) and the Structural Stability Research Council (SSRC) in 1979 published a design proposal that is based on ultimate strength concepts, however all the design formulations were expressed in the allowable stress terms, similar to the formats used by the AISC Specification.

The slenderness effects on composite columns corresponding to the reinforced concrete, and steel sections alone were discussed by Smith (198), with emphasis on the discrepancies between the reinforced concrete and composite designs.

Roberts (178) with the Department of Environment, Building Research Establishment in England in 1983 presented various methods for the design of short and slender pin-ended composite steel-concrete columns subjected to axial load alone and to axial load with uniaxial and biaxial bending.

Kennedy and MacGregor (122) discussed the type of shear transfer mechanism at the end connections where the load was introduced into the composite column. They used the references to the tests conducted during the previous thirty years and current Codes Standards, and to multi-story building construction practices.

Zhong and Miao (241) at the Harbin Architectural & Civil Engineering Institute of China in 1984, presented a load-strain relation curve of concrete-filled steel tubular short columns subjected to axial compressive loading. They carried out

a large number of experimental results. They also derived formulas for computing the bearing capacity of short columns, by means of the strength and plastic theories.

Moore and Gosain (146) in 1984, presented a technical paper in which they compared the composite column load capacities calculated by using ACI Code Procedure and the semi-empirical formulas previously published by others. Moore and Gosain (146) pointed out that the ACI Code requirements for designing composite columns were not complete at that time and that many areas of the column composite design were very questionable. The design might give a unsatisfactory design.

The ACI 318-83 Building Code specified that the strength of a composite column should be calculated for the same basic assumptions and limiting conditions applicable to normal reinforced concrete columns. Based on that principle, Moore and Gosain (146) developed a computer program which provided the axial load-moment interaction curves for circular, rectangular, and general shaped composite columns for any combination of reinforcing bars and embedded steel shapes. Bending about the major and minor axis were considered as well as asymmetrical layout of reinforcement.

Lu and Kato (133) presented a summary of the papers presented at the Composite and Mixed Construction published in the Proceedings of the U.S./Japan Joint Seminar in 1984. Two papers were presented reporting research done on concrete-encased steel columns. Moore and Gosain (146) discussed the interaction diagrams to estimate the strength of cross sections under axial load and uniaxial bending.

Morino, Matsui, and Watanabe (147) presented the results of an experimental

study on the elasto-plastic behavior of short and slender Steel Reinforced Concrete (SRC) composite columns under biaxial bending and axial compressive loads. They also discussed the effects of experimental parameters such as eccentricity and slenderness ratio on the composite column behavior.

Pham (168) presented a reliability analysis of concentrically loaded reinforced concrete and composite (cased) column sections under concentric loading. The test specimens were designed in accordance with the Australian Standards, AS 1480-1982 and AS 1250-1981, respectively.

Wakabayashi, et al. (232,235) published a new formula to design the SRC long composite columns. The AIJ (Architectural Institute of Japan) adopted this design formula for concrete filled steel tubular columns. An experimental investigation on SRC concentrically loaded composite columns and beam-columns containing steel H-shape sections was carried out at a later date to verify the accuracy of the new design formula.

Zhong (242) discussed the concept of equivalent confining force for concrete filled steel tubular columns subjected to axial compressive load and bending. The proposed design formulas were verified by a considerable number of test results and they were adaptable to members with arbitrary eccentricity and slenderness ratios.

In Germany, Bossart (33) in 1985 presented the idea of composite columns that used a core of massive steel, a liner formed by a steel tube and concrete as filling material. These composite columns combined the high steel and concrete strength with high fire resistance. He emphasized on the possibility of changing the fire resistance from a disadvantage to a very positive and beneficial structural component for Building Construction.

Nakai, Kitada, and Yoshikawa (158) studied the ultimate strength of steel plate elements in the concrete-filled square steel tubular column by using the Finite Element Method and the elastoplastic and large displacement theory. They proposed a tentative design method by adopting a simplified ultimate strength curve and a column model approach.

The present study intends to review the current design methods available in the United States for the analysis and design of composite columns. Also, an experimental testing program will provide the basis to understand the basic behavior of short and slender composite columns under axial compressive load and biaxial bending. An attempt will be made to develop a new mathematical design interaction equation; a computer model will also be presented to study the complete load-deformation behavior of reinforced concrete-encased structural steel columns under axial load and biaxial bending.

The test results of the present research and the ones presented by other researches are to be compared with the theoretical and analytical values obtained from the proposed mathematical design interaction equation and computer analysis program.

Two basic design methods for the analysis and design of composite columns are currently available in the U.S. They are both presented in the completely different format and by two entirely independent engineering institutions; These two institutions are dedicated to the research, development, building code recommendations, standardization and design guidelines for the two most widely used materials in the building construction industry: reinforced concrete and structural steel. These two institutions are: the ACI, American Concrete Institute and the AISC,

American Institute of Steel Construction.

The recommended design methods are contained in the following publications: The ACI 318-89 (1) "Building Code Requirements for Reinforced Concrete" (1989), and the LRFD (13) "Manual of Steel Construction", Latest Edition, (1990).

The Structural Stability Research Council (formerly the Column Research Council) SSRC, is another institution which is dedicated to provide guidance to practicing engineers and writers of codes, specifications and standards related to design procedures of metal structures, stability in general and composite members.

Having those two major design methods as a common ground, it is the intention of the present research to review the basic and fundamental principles of the behavior of short and slender composite columns under the combined action of biaxial bending and axial compressive loads.

### 1.3.1 Research on Structural Steel Shapes Encased in Concrete

In New York, United States, Burr (35) in 1908, performed a series of tests on encased latticed (built-up) steel sections, and observed that the concrete encasement provided a considerable increase in strength. Laredo and Bard (131), summarized the work done by Burr and others on built-up steel sections. Bondale (34a), in 1966 presented a Column Theory and results of tests on encased built up composite sections under eccentric loading.

In England, Faber (71) in 1955 reported tests on 16 axially loaded encased steel shapes specimens, which drew some attention to the advantage of using fireproofing concrete to help carry some axial loads and contribute to the strength capacity of the section.

Rizk and Jones (107) in 1963, reported tests on beam-column composite specimens that showed that the load capacity for the composite specimens was much higher than those of the steel section alone. They also noted that the concrete not only sustained its share of the load but also stiffened the steel shape. Varghese (219) on his tests noted that the composite column specimens tested showed a significant reserve in axial load capacity even after the first crushing of concrete had occurred.

Stevens (195) in 1965 tested 24 eccentrically loaded encased columns, with bending about the minor axis, he reported that the behavior and mode of failure of these columns were observed to be similar to those of reinforced concrete columns.

Bondale (25) proposed an analytical method for the design of axially-loaded concrete-encased steel columns.

Watanabe (234) in 1966, presented a study regarding the bond behavior between steel and concrete, and found that bond strength in short encased columns is not a problem.

Bridge and Roderick (29) performed a series of tests to investigate the behavior of pin-ended build-up composite columns (two steel channels with and without battens encased in unreinforced concrete). They developed an iterative inelastic analysis to predict the behavior from zero load up to collapse loading. They concluded that the absence of battens did not affect the load-carrying of the build-up composite column.

Bridge (31) presented the results of an experimental investigation of composite steel-concrete columns containing cracks prior to the application of the load. He found that in addition to reducing the stiffness of the column, pre-cracking could reduce the ultimate load capacity well below that for similar columns that were not

cracked before the application of the load. It was also found that the influence of pre-cracking can be accounted for in terms of an additional eccentricity of the loading.

Basu (32) at the Indian Institute of Technology, New Delhi, India in 1982, presented a study of the strength and behavior of 250 encased I-section composite columns, braced against sidesway and under uniaxial bending. The different parameters considered in this study include: end eccentricities, stiffness of column ends, slenderness, concrete cover. The tests were done for different end eccentricities, end restraints and with bending about both major and minor axes.

In England, Taylor, Shakir-Khalil, and Yee (217) in 1983 presented the results of testing done on nine large-scale concrete encased battened steel channels composite columns. They compared their load carrying capacities with the ultimate loads predicted by some simple design expressions presented by them in a previous paper (238).

In West Germany, Roik and Hanswille (183) in 1984 based on their tests and analysis showed that the bearing capacity of headed studs may be calculated by means of results obtained from push-out tests for composite beams. They also found that in composite columns with concrete-encased I-sections, the ultimate limit state of load introduction at column sections was marked by failure of headed studs or stirrups or by exceeding the principal compression stress in concrete.

Suzuya and Kawana (199) at the Tohoku Institute of Technology, Japan in 1984 carried out a series of experimental testing on Steel Reinforced Concrete (SRC) Beam-Columns with full web type steel section. The Test Specimens were subjected to a constant axial load followed by a variable lateral load, the specimens consisted

of four different size Wide-Flange (H-shape) sections (two sections were rolled H-shape and the other two were built up sections).

Kato (125) in 1983, at the University of Tokyo, Japan, tested a number of SRC composite columns subjected to weak axis bending, SRC beam to column connections, and shear wall members using concrete filled steel plates.

Suzuki (203) at the Tokyo Institute of Technology, Japan, presented the results of an investigation of the effects of hoops in SRC members with steel sections only and hoops without longitudinal reinforcing bars. Suzuki concluded that the hoops were effective in providing an increased strength and ductility of composite columns, beams, beam-columns, and connections for cross sections with high-strength steel.

Yamada, et al. (239) at Kobe University, Japan, performed tests of composite columns under concentric axial load on short columns, beam-columns under constant axial load and uniaxial repeated bending, and framing systems to study the behavior of SRC composite columns and energy dissipation capacity.

Matsui, et al. (151) at Kyushu University, Japan, presented the results of an experimental and theoretical investigation on the restraining effects of the reinforced concrete portion on the local buckling of the plate elements of the steel H-section of SRC composite columns. They considered the different stress-strain relationships for the confined concrete inside steel flanges and concrete outside of the compression flanges.

Masuda, et al. (152) at Kyusyu Sangyo University, Japan, performed bending tests of SRC composite columns with a fixed end at the base. Other researchers in Japan, in cooperation with the Construction Industries and Institutes of Steel Manufacturers performed tests on SRC composite sections with H-shape steel

reinforcement to study the ductility and behavior of those sections under cyclic loads.

Roik, Diekmann, and Schwalbenhofer (184) presented the results of tests on steel-concrete-composite columns consisting of steel-fiber-concrete encased wide flange H-sections without additional reinforcement. The major parameters studied from the tests were the bonding between the concrete and the steel section and the influence of the concentrated loading on the fire resistance concrete cover.

Abel-Sayed and Chung (18) developed a new system of Composite Column, by using lipped cold-formed steel channels with embedments and cast-in-place concrete. They found that due to the combined action of the embossment and the channel lips, a very good bond between the steel and the concrete was achieved. It was also found that by replacing the standard longitudinal reinforcing bars by cold formed steel sections of equal area, the structural performance of the columns remain almost unchanged. They proposed a design approach based on the test results.

A compilation of the development in the design of composite columns has been presented in the third edition of the Guide to Stability Design Criteria for Metal Structures edited by Johnston (106).

Design Tables and Charts for regular cross sections presented by Furlong (67), Basu and Sommerville (23) and computer programs for irregular shaped sections by Basu and Hill (36) can be used for design purposes.

### 1.3.2 Research on Steel-Encased Concrete Columns

Hollow circular, square, and rectangular steel tubes filled with concrete are composite columns that derive their own load carrying capacity from the combined effects of an increased concrete strength due to the confinement of the concrete core (triaxial state

of stress) by the steel shape and the improved conditions of the hollow steel shape to sustain the effects of local buckling due to the presence of the concrete core filling the hollow section.

The most common concrete-filled steel sections used at the beginning of this century were made with circular steel tubes. Square and Rectangular Steel Tubes began to be used just in the past recent years.

In Germany, 1957, Klöppel and Goder (118) performed a comprehensive series of tests on steel-encased concrete columns with different slenderness ratio to study the upper and lower bounds of a strength formula for axially loaded columns. An upper limit expressed in terms of the steel and concrete stiffness of the composite section was given as a Euler-type formula, and a lower limit based on the steel buckling strength and the adjusted area of the composite section established the boundaries of the composite column behavior. Salani and Sims (202) performed tests which provided results that were used to support the implementation of the Tangent Modulus.

Kerensky and Dallard (124) in England 1969, reported the characteristics of some exploratory tests on large diameter concrete-filled tubular columns at the Building Research Station and Imperial College in London. Some other similar tests were conducted parallely in Japan and Belgium, as well as extensive computer models were implemented to attempt to predict the behavior of these composite columns.

Guiaux and Dehose (83) in 1968 at the University of Liege, Belgium, performed another series of tests on eccentrically loaded square and rectangular concrete-filled tubes. The triaxial stress effect of confined concrete has been studied at the Imperial college of London and it was found that substantial increase of

strength was observed in short circular concrete-filled tubes.

Furlong (65,66) measured surface strains on stub-column specimens under axial force and increasing bending moments, which led him to formulating a tangent-modulus theory to predict the axial load capacity of slender columns. A very extensive testing program of concrete-filled steel tubes of both circular and square cross section was carried out by Furlong at the University of Texas which resulted in the development of an interaction equation for combined axial load and bending moment.

Knowles and Park (117) performed experimental tests on 3.5" and 3.25" round, and 4" square filled tubular steel columns and compared the results with the available design rules of the 1963 ACI Code. They also provided an equation that set the limits of slenderness ratio above which no increase in concrete strength could be expected due to the confinement by the steel section. They also presented in 1970 a concise summary of the previous studies done on axially loaded concrete-filled round tubes.

Gardner and Jacobson (78,79) performed tests on tubular composite columns and presented comparative results with the 1963 ACI Code. The steel tubes were considered to contribute to both the strength capacity and confinement of the concrete in the composite section. They developed equations to predict the ultimate axial load-carrying capacity of short columns and used the Tangent Modulus to estimate the buckling load of long columns.

Neogi et al. (156) reported that the apparent increase in concrete strength due to the confinement by the steel section, was not that significant for specimens with high slenderness ratio and considerable eccentricities of the axial load.

The International Committee for the Development and Study of Tubular

Structures (CIDECT), published a design manual for concrete filled hollow section steel columns; Monograph No. 1, 1970, which was based on the research work done by Basu and Sommerville (23), Neogi, Sen, and Chapman (156), and the British Standards Institution.

Tomii, Matsui, and Sakino (215) reported tests on concrete-filled steel square tubes to study the ductile behavior of composite columns under seismic loads. In 1977, Tommi, Yoshimura, and Morishita (216) reported the tests of 270 stub columns under concentrically axial loads to study the effect of factors such as shape and size of the steel tube and material properties of the confined concrete on the load and deformation capacities, ductility and strength of concrete filled steel tubular stub columns.

D'Huart and Wuerker (53) presented a paper in which they discussed different design methods for concrete-filled hollow structural sections under short and long term loading. Shear forces, creep effects, local buckling of the steel tube walls, were some of the factors taken into account in this study. Some guidelines for the design of joints, details of fabrication, and concrete filling were also considered.

Roik, Bode, and Bergmann (182) tested several short and slender concrete-filled steel columns of round and square sections, with the special interest of studying the effects of creep and shrinkage of the concrete part. They compared the test results with the theoretical values based on the draft of the DIN 18 806, Part 1 and found that the proposed method gave a safe design.

Liu and Chen (130) reported a full-range synchronistical measurements of pipe columns filled with concrete. A deflection controlled experimental test setup was used to monitor the load near and beyond the maximum peak value.

Nakai and Yoshikawa (157) in 1984 at the Osaka City University in Japan, did an experimental research work on the static and dynamic behavior of concrete filled steel columns. A field test of a bridge pier made of concrete filled steel column was tested in order to study the bending, shear stresses, and the dynamic properties such as natural frequency and damping coefficients.

Cai and Jiao (43) at the China Academy of Building Research in 1984, presented the tests results of 57 concentrically-loaded short columns. A limited equilibrium method by A.A. Gvozdev was used to derive formulas for the ultimate strength of columns. The proposed formulas were verified by the tests done and other tests results available in the literature.

Juchniewicz and Gorak (111) performed tests on eccentrically loaded composite columns with the circular section filled with concrete. Displacements, Strains, and Load Capacity of the columns were measured and compared with theoretically predicted values.

Cai and Di (44) at the China Academy of Building Research in 1985 presented the test results of 51 eccentrically-loaded concrete-filled steel tubular columns with eccentricity ratios (e/r) varying from 0 to 1.3 and length over diameter ratio (L/D) from 4 to 22. The test results showed that the ultimate strength of the column decreased significantly as its slenderness ratio and eccentricity ratio increased. They proposed a formula based on limit analysis where the overall strength reduction factor of the column was expressed as the product of a reduction due to slenderness ratio $\phi_r$ and that due to eccentricity ratio $\phi_e$.

Cai and Gu (45) presented the test results of 26 concentrically loaded long concrete-filled tubular columns with length over diameter ratio (L/D) varying from

3 to 50. An empirical formula for the strength reduction coefficient based on the test data was proposed.

Dunberry, Le-blanc, and Redwood (54) at McGill University in Canada in 1987, described the tests performed on short, rectangular steel columns filled with concrete and loaded to failure under an axial load. In the columns tested, part of the load was applied at the beam-column connection, within the column length, and part was applied at the top to represent the loads from the upper stories of a building.

### 1.3.3 Research on Composite Columns under Fire Conditions

Special importance has been given to the structural behavior of composite columns when subjected to the external effects of Fire.

Malhortra and Stevens (150) in 1964, reported tests to study the Fire Resistance of concrete encased steel columns at high temperatures. Different amounts of concrete cover over the steel shape were considered in their work.

In Germany, Quast (169) in 1979, tested 16 composite columns. He discussed the behavior of sections with concrete filled hollow or C-section, and with rolled steel sections embedded in concrete. The buckling strength of the connections, the required reinforcement, and the anchoring dowels were also studied.

Grimault and Mouty (82) presented the results of 107 tests conducted for a period of ten years, on columns filled with concrete and without external protection, to study the behavior of composite columns under fire conditions.

Schleich (200) with the ARBED-Researchers, in Luxemburg in 1985, discussed the theoretical basis of the fire resistance calculations, their experimental data, and the available design tools available, for the four basic types of composite columns.

The Lally Column (132) a manufacturing company of concrete-filled pipe columns in United States, reported that the fire resistance of an unprotected steel tube filled with concrete is about three to four times higher than the steel tube alone. There are some indications that entrapped moisture in concrete-filled tubes during a fire can cause the steel shell to explode.

## 1.4 Review of Strength and Behavior of Biaxially Loaded short Composite Columns

A graphical representation of the overall range of allowable combinations of axial load and bending moments for a composite column is shown in Fig. 1.3, and is called a Failure Surface Diagram. Fig. 1.3 represents the ultimate strengths of a column section subjected to a combination of axial load and biaxial bending moments. It is considered to have adequate strength under the given design conditions if a point lies inside this failure surface.

### 1.4.1 Theory and Fundamental Equations

The ultimate strength of short composite columns can be expressed as the sum of the individual strength of each one of the materials that form the composite cross section within the limitations of maximum allowable stress and strain values. It has been described by Brettle (37), Lachance (129), Furlong (64-70), Basu (32), Emperger (58), Klöppel and Goder (118), Knowles and Park (116), and others.

The researchers mentioned above among others have also found that the basic principles for strength analysis of reinforced concrete members can be applied to composite columns.

Tests performed by Furlong (65,66) on short concrete-filled steel tube beam columns showed that the bond between steel and concrete was very weak at low longitudinal stresses. The flexural stiffness for a composite column could be estimated as the sum of the flexural stiffness of each component of the composite section. Based on the tests performed an effective radius of gyration for the composite section was not very sensitive to small variations in steel and concrete properties. Structural steel as a ductile material provides its ultimate strength with very low sensitivity to a limit strain value. Concrete on the other hand is much less ductile than steel, and its ultimate strength depends primarily on a relatively low strain limit value.

The general theory to determine the flexural strength of short composite column sections is based on the following basic assumptions :

a. Plane sections before bending remain plane after bending.

b. The stress-strain curves for the reinforcing steel bars and the structural steel shape are known.

c. The tensile strength of the concrete is so low compared to its compressive strength, that it may be neglected.

d. The stress-strain curve for the concrete that expresses the distribution and magnitude of compressive stresses is known.

A lower-bound compression strain limit value for concrete in flexure has been taken as 0.3% (ACI 1989, Rev 1992) and a reliable lower-bound strength of $0.85f'_c$ is adopted for the design strength of concrete in compression.

A composite column subjected to axial load and biaxial bending can be represented by an axial load applied at a point with eccentricities $e_x$ and $e_y$ from the plastic centroid about the y and x axes, as shown in Fig. 1.3 and such that:

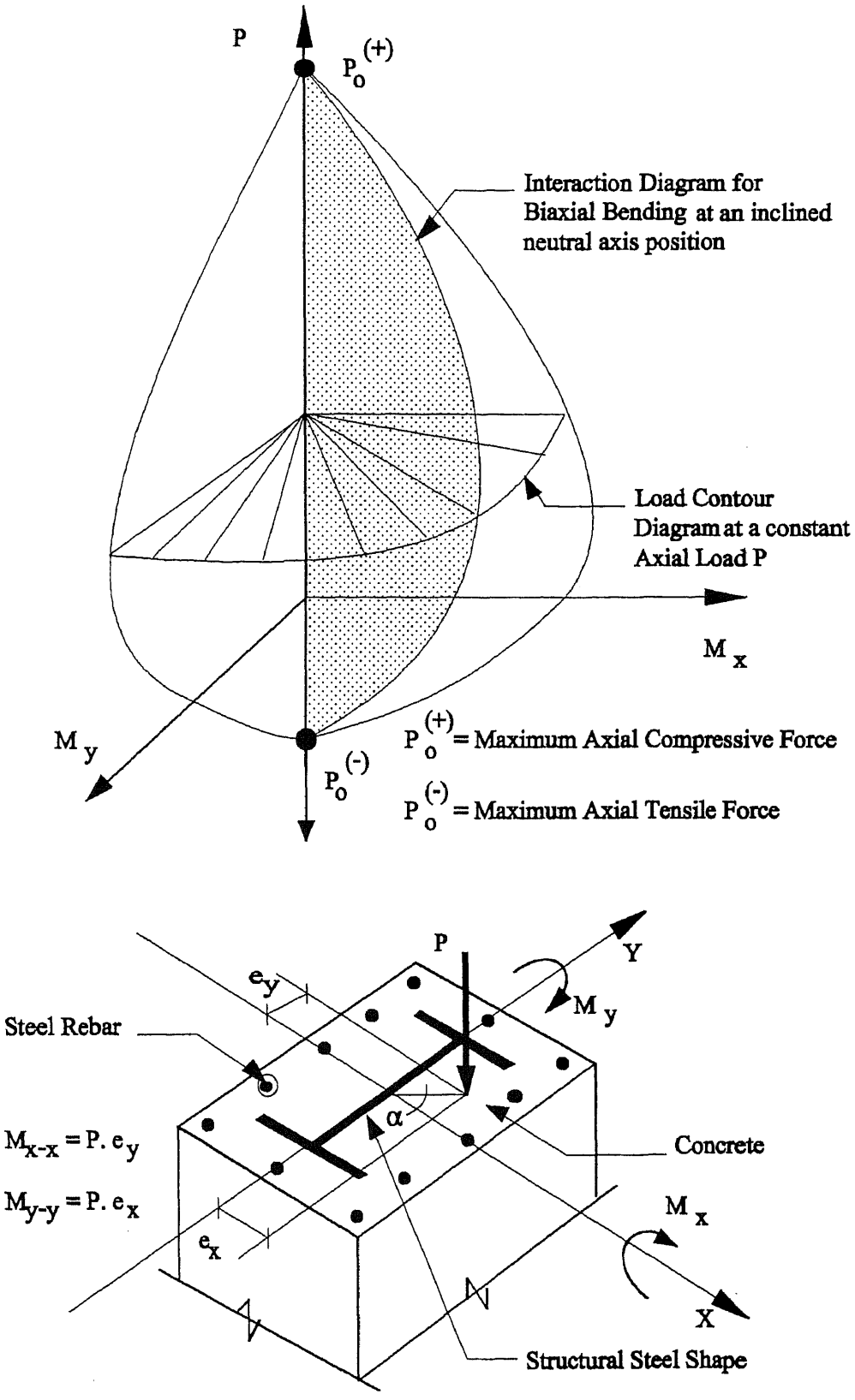


**Figure 1.3** Failure Surface Diagram and Composite Column cross section

$$e_x = \frac{M_y}{P} \quad ; \quad e_y = \frac{M_x}{P} \tag{1.1}$$

The inclination of the line of application of the eccentric resultant axial load P is given by the angle of eccentricity $\alpha$, as:

$$\alpha = \tan^{-1}\frac{e_y}{e_x} \tag{1.2}$$

The composite column under the action of the external biaxial bending moments and axial load will reach its flexural strength capacity that is defined by the combination of the nominal internal axial load $P_n$, and the bending moments $M_{nx}$, $M_{ny}$, at a position and inclination of the neutral axis.

The conditions of static equilibrium and strain compatibility given by the summation of the individual contributions of forces, stresses and strains of the concrete, reinforcing steel bars, and the structural steel shape, are satisfied on the entire cross section.

For a given position and inclination of the neutral axis, the following basic equations of equilibrium must be satisfied:

$$\sum F_z = 0, \quad F_z = \int_A \sigma dA \tag{1.3}$$

$$\sum M_X = 0, \quad M_X = \int_A y\sigma dA \tag{1.4}$$

$$\sum M_y = 0, \quad M_y = \int_a x\sigma dA \tag{1.5}$$

which in expanded and simplified form becomes:

$$P_n = C_c + \sum C_{si} - \sum T_{si} \tag{1.3a}$$

$$M_{nx} = P_n e_y = C_c y_c + \sum C_{si} y_{si} + \sum T_{si} y_{si} \tag{1.4a}$$

$$M_{ny} = P_n e_x = C_c x_c + \sum C_{si} x_{si} + \sum T_{si} x_{si} \tag{1.5a}$$

where

$C_c$ = Resultant Compressive Axial Strength by Concrete

$C_{si}, T_{si}$ = Compressive and Tensile Axial Strength by the ith reinforcing bar or the structural steel element respectively.

$x_{si}, y_{si}$ = x and y coordinates of the individual ith reinforcing bars and structural steel elements with respect to the plastic centroid.

$x_c, y_c$ = x and y coordinates of the point of application of the resultant compressive axial load with respect to the plastic centroid.

The strain compatibility must be satisfied and the appropriate stress-strain curves for concrete, reinforcing steel, and the structural steel shape are used to determine all the forces involved in the equations of static equilibrium. The basic assumptions presented at the beginning of this section are incorporated into the analysis of composite column section under biaxial bending moments and axial load which will lead to a solution of the triplet nominal strength of the cross section ($P_n$, $M_{nx}, M_{ny}$).

The mathematical solution of the equations presented above provides the most direct analytical approach for the analysis and design of composite columns and could be very well considered as the exact method of analysis.

Since a trial-and-error technique has to be used to determine the location and

the inclination of the neutral axis that satisfies a specific condition of external loads and equilibrium, this procedure is very lengthy and time consuming for hand calculations. A great number of design aids, computer programs and approximate methods of analysis and design have been developed over the past years to overcome these mathematical and numerical difficulties.

The Author has developed as part of this dissertation work, a computer method described below that is in complete accordance with the basic assumptions of the ultimate strength design method specified by the ACI Building Code (1), to study the strength of short concrete-encased steel composite columns under axial load and biaxial bending moments. The computational method is described in details in the next section.

### 1.4.2 Computational Method

A Computer program to meet the requirements of the equations of equilibrium and compatibility of strains for a uniaxially or biaxially loaded short composite column was developed by the Author and is presented in Appendix A. The computer program permits to study a wide range of square and rectangular composite column cross sections reinforced with or without longitudinal bars and structural steel shapes embedded or encased in concrete. This computer program addresses the need for a practical analytical tool to investigate into the behavior of composite columns with different proportions of steel rebars, different dimensions of I-shape and H-shape wide flange structural steel shapes and different aspect ratios of the rectangular sections. It can also be easily adapted to study the case of circular or square steel-encased concrete composite sections.

A description of the portion of the program to generate the uniaxial load-moment interaction diagram for both the weak and the strong axis of a composite column is presented in Chapter 2, section 2.4 of this dissertation.

In the following paragraphs, the Author will present the basic computational procedure to study the behavior of short composite sections under biaxial bending moments and axial loads.

A typical composite column cross section under biaxial bending moments and axial loads with the stress and strain distributions is shown in Fig. 1.4. When the section reaches its flexural strength one can obtain the summation of forces that provide force and moment equilibriums and strain compatibility over the entire section. At this point the neutral axis is inclined with respect to the horizontal axis an amount that depends on the ratio of the bending moments in the two directions and the section properties of all the materials part of the cross section.

The equivalent compressive stress block is assumed to have a depth of $\beta_1$ times the neutral axis depth c, and an average stress value of $0.85f_c'$. The equivalent stress block for an irregular compressed shape at an inclined position of the neutral axis, is not completely equal to the actual stress block but for practical and design purposes it is considered to be accurate enough.

Looking at Fig. 1.4, for a given position and inclination of the neutral axis, the flexural strength of the cross section can be found by considering first the strain compatibility that results from the similar triangle relationship of the strain diagram limited by the values of the maximum compressive strain of concrete of 0.3% and the maximum strain of the steel in tension. The steel stress values and all the compressive and tensile forces are then found from the stress-strain curve for the steel. Finally the

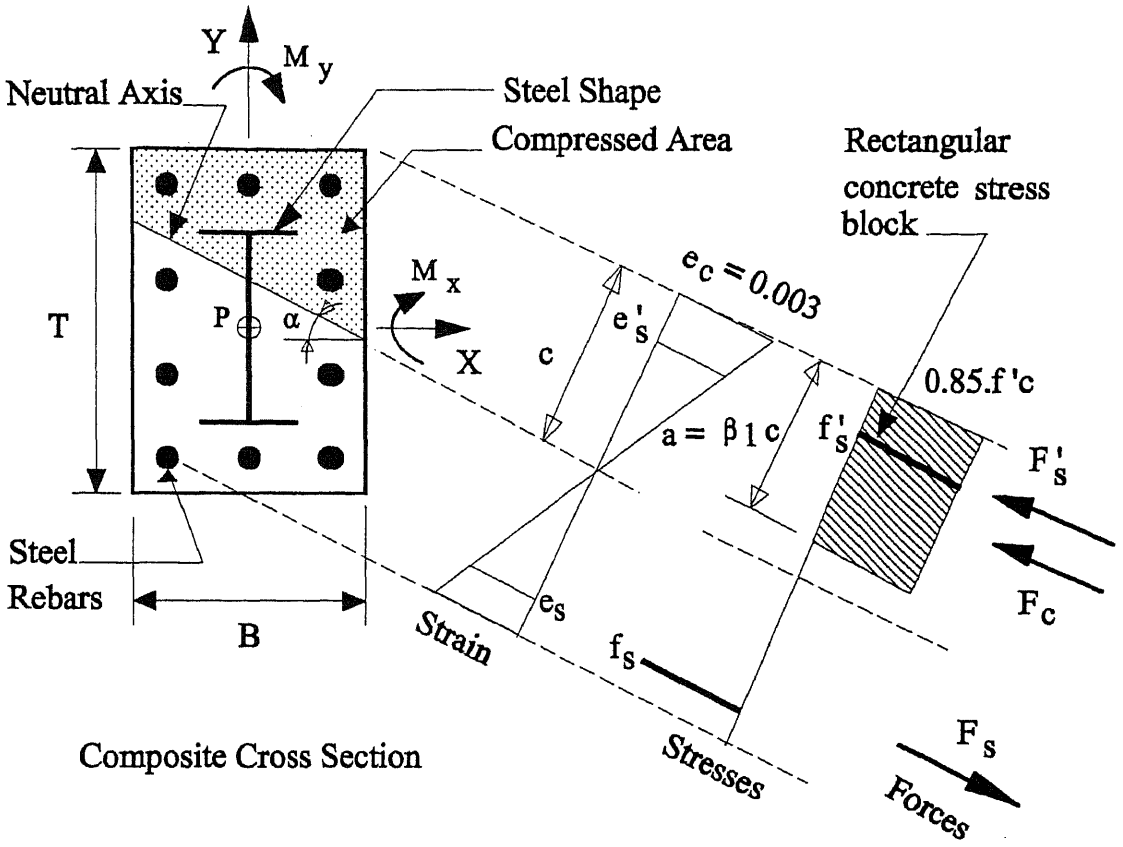


**Figure 1.4** Stress and Strain diagrams for a biaxially loaded composite section

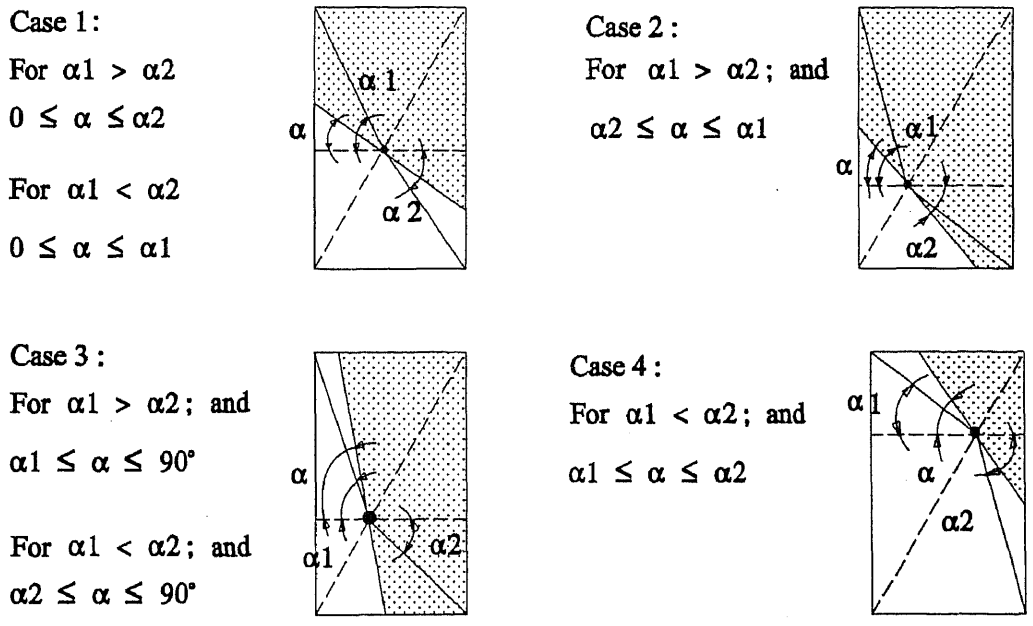


**Figure 1.5** Concrete stress block shapes for a biaxially loaded composite section

resultant compressive force in the concrete area and its position depends on the shape and total area of the equivalent stress block.

There are four possible shapes of the compressive stress block which are shown in Fig. 1.5 where $\alpha 1$ and $\alpha 2$ are angles that define the inclination of the point of location of the neutral axis with respect to the upper left hand corner and the lower right hand corner of the cross section respectively. Angle $\alpha$ is the angle of inclination of the neutral axis with respect to the horizontal x-axis.

The resultant compressive Force on the concrete section $F_c$ and the coordinates of location of the centroid of the compressive section $\overline{x}$ and $\overline{y}$ can be found for the four cases shown in Fig. 1.5 using the formulas given in Figs. 1.6 and 1.7 respectively.

The following basic equations of equilibrium must be satisfied in order to obtain the flexural strength of a given composite cross section:

$$\Sigma F = 0 \;\; ; \;\; \Sigma M_x = 0 \;\; ; \;\; \Sigma M_y = 0 \qquad (1.6)$$

From Fig. 1.4, the equilibrium of the resultant compressive and tensile forces is achieved for a position of the neutral axis such that the sum of the longitudinal forces is equal to zero.

The moments that correspond to the flexural strength of the cross section about the x and y axis are calculated by taking the bending moments of the compressive and tensile internal forces about the plastic centroid with the appropriate signs, positive for compression and negative for tension.

The composite cross section overall dimensions, size and coordinates of each one of the rebars around the sides of the cross section, steel shape size and thickness,

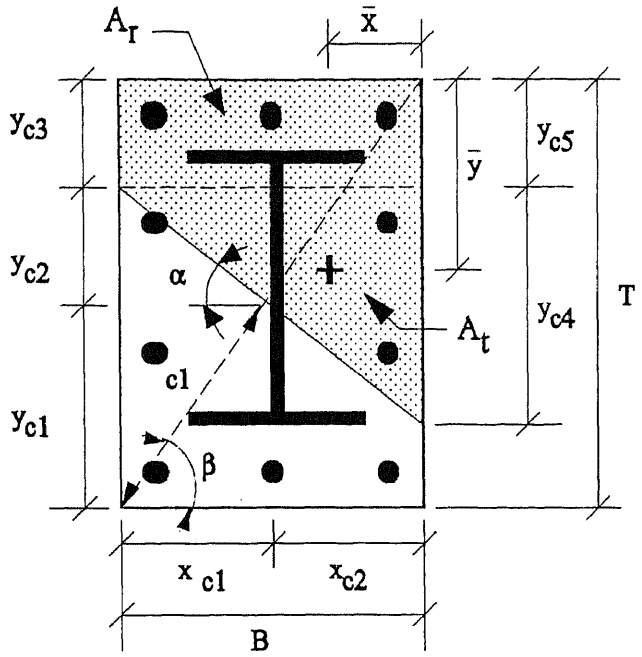


Case 1 :

Given : $c1, \alpha, \beta$

$x_{c1} = c1.\cos\beta$

$y_{c1} = c1.\sin\beta$

$y_{c2} = x_{c1}.\tan\alpha$

$y_{c3} = T-(y_{c1}+y_{c2})$

$x_{c2} = B-x_{c1}$

$y_{c4} = x_{c2}.\tan\alpha$

$A_r = B.y_{c3}$

$A_t = B.(y_{c2}+y_{c4})/2$

$A_{cs} = A_r + At$

$$\bar{x} = (A_r.B/2 + A_t.B/3)/A_{cs}$$

$$\bar{y} = (A_r.y_{c3}/2 + A_t.[(y_{c2}+y_{c4})/3 + y_{c3}])/A_{cs}$$

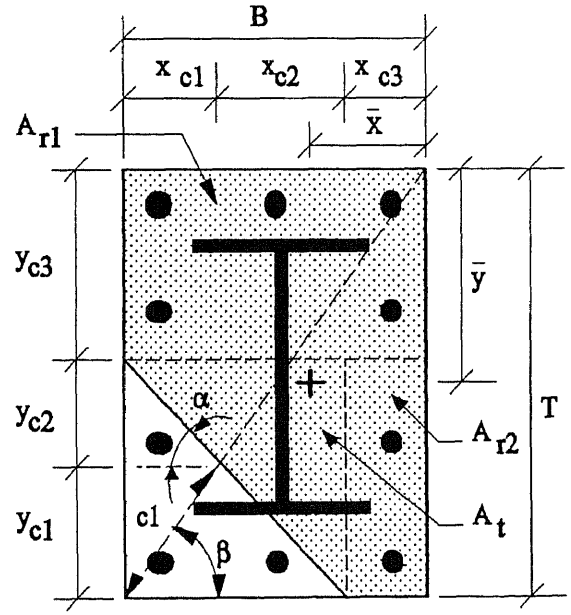


Case 2 :

Given : $c1, \alpha, \beta$

$x_{c1} = c1.\cos\beta$

$y_{c1} = c1.\sin\beta$ ; $x_{c2} = y_{c1}/\tan\alpha$

$y_{c2} = x_{c1}.\tan\alpha$

$y_{c3} = T-(y_{c1}+y_{c2})$

$x_{c3} = B-(x_{c1}+x_{c2})$

$A_{r1} = B.y_{c3}$

$A_{r2} = x_{c3}.(y_{c1}+y_{c2})$

$A_t = (x_{c1}+x_{c2}).(y_{c1}+y_{c2})/2$

$A_{cs} = A_{r1} + A_{r2} + A_t$

$$\bar{x} = (A_{r1}.B/2 + A_{r2}.x_{c3}/2 + A_t.[x_{c3} + (x_{c1}+x_{c2})/3])/A_{cs}$$

$$\bar{y} = (A_{r1}.y_{c3}/2 + A_{r2}.[y_{c3} + (y_{c1}+y_{c2})/2] + A_t.[y_{c3} + (y_{c1}+y_{c2})/3])/A_{cs}$$

**Figure 1.6** Compressive block geometry and center of gravity for cases 1 and 2

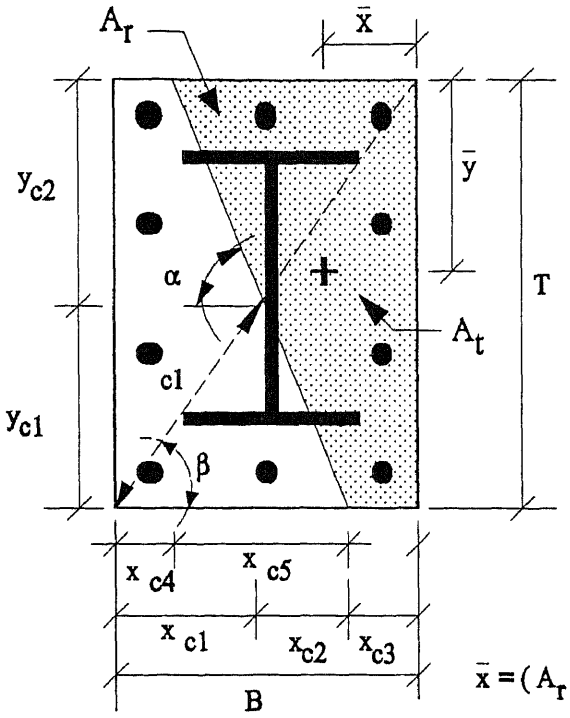


Case 3 :

Given : $c1, \alpha, \beta$

$x_{c1} = c1.\cos\beta$

$y_{c1} = c1.\sin\beta$

$x_{c2} = y_{c1}.\tan\alpha$

$x_{c3} = B - (x_{c1} + x_{c2})$

$x_{c5} = T / \tan\alpha$

$A_r = T.x_{c3}$

$A_t = T.x_{c5}/2$

$A_{cs} = A_r + At$

$\bar{x} = (A_r.x_{c3}/2 + A_t.(x_{c3} + x_{c5}/3))/A_{cs}$

$\bar{y} = (A_r.T/2 + A_t.T/3)/A_{cs}$

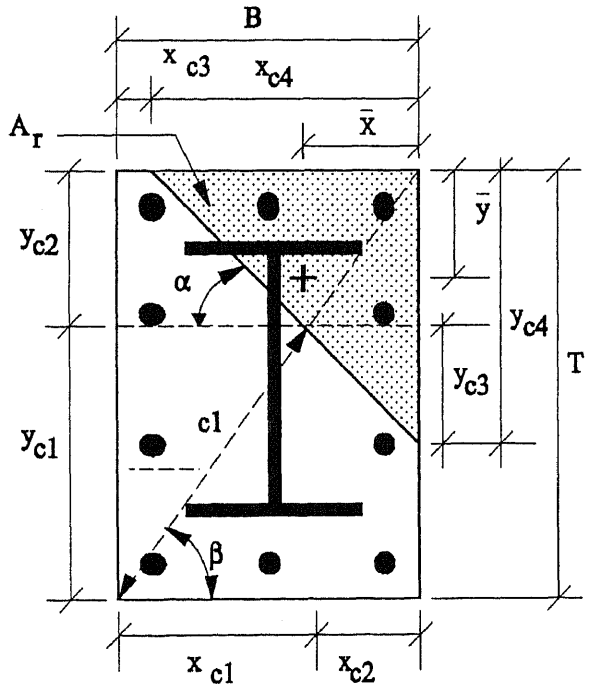


Case 4 :

Given : $c1, \alpha, \beta$

$x_{c1} = c1.\cos\beta$ ; $x_{c2} = B - x_{c1}$

$y_{c1} = c1.\sin\beta$ ; $y_{c2} = T - y_{c1}$

$y_{c3} = x_{c2}.\tan\alpha$

$y_{c4} = y_{c2} + y_{c3}$

$x_{c4} = y_{c4} / \tan\alpha$

$A_{cs} = x_{c4}.y_{c4}/2$

$\bar{x} = x_{c4}/3$

$\bar{y} = y_{c4}/3$

**Figure 1.7** Compressive block geometry and center of gravity for cases 3 and 4

clear cover of the rebars and steel shape, material properties for steel and concrete are the basic input parameters for the computer program to obtain the load-moment interaction diagrams about the principal axis of the cross section and the load-contour diagram for different values of the axial load.

The computer program generates the load-moment interaction diagram for any number of selected planes between the major and minor axis. Fig. 1.8 shows the geometric relationships required to locate each one of the steel rebars and steel elements of the structural steel shape (divided in a finite number of elements) with respect to the neutral axis location.

Finally, the computer program "INTRDIAG" presented in Appendix A, also generates a set of coefficients $\alpha$ and $\beta$ that would define a continuous mathematical function to represent the load-moment and the load-contour diagrams for a composite cross section under uniaxial or biaxial bending moment conditions with axial load. Details of a proposed mathematical function to represent the uniaxial load-moment interaction diagram are given in Chapter 2 together with the derivation of a generalized equation of failure surface that can be applicable to composite columns.

## 1.5 Review of Strength and Behavior of Biaxially Loaded slender Composite Columns

A slender column is defined as one in which the ultimate load capacity of the cross section is substantially reduced by the additional bending moment produced by the large lateral displacement of the line of application of the external axial load. In contrast to a short column that experiences very small lateral deflections under axial

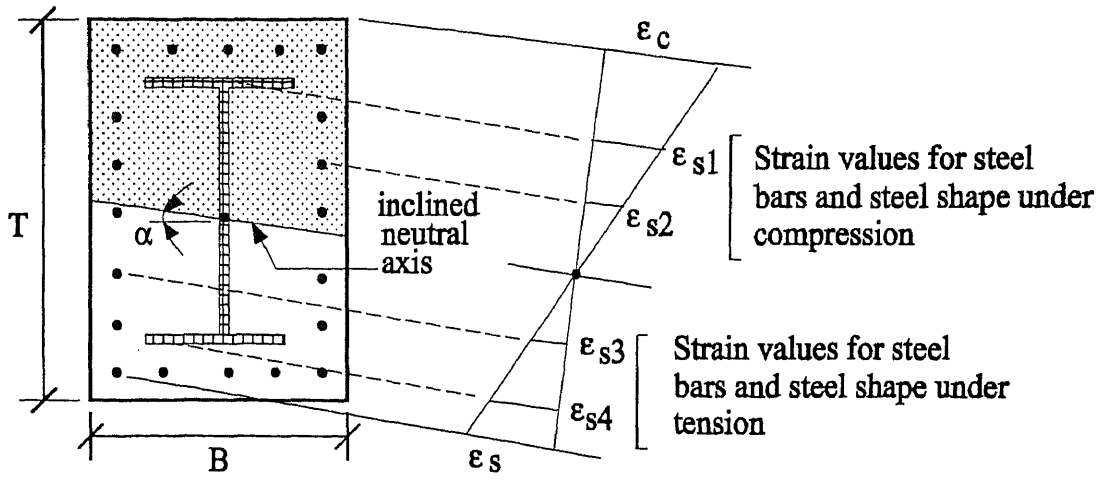


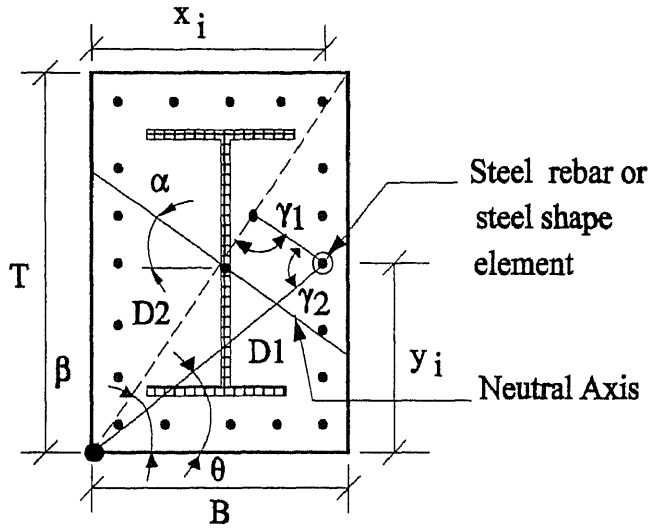


For $\theta < \beta$ :

$$D1 = \sqrt{x_i^2 + y_i^2}$$

$$\gamma 1 = 180 - (\beta + \alpha)$$

$$\gamma 2 = \alpha + \theta$$

$$D2 = D1 * \sin\gamma 2 / \sin\gamma 1$$

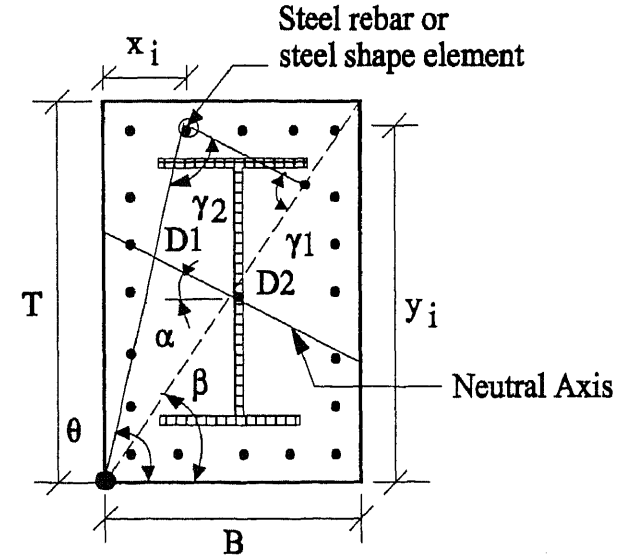


For $\theta > \beta$ :

$$D1 = \sqrt{x_i^2 + y_i^2}$$

$$\gamma 2 = 180 - (\beta + \theta)$$

$$\gamma 1 = \alpha + \beta$$

$$D2 = D1 * \sin\gamma 2 / \sin\gamma 1$$

**Figure 1.8** Geometrical location of steel rebars and steel shape elements

load and bending moments, a slender column will undergo a lateral displacement that when added to the original eccentricity of the applied axial load will generate a secondary or additional bending moment, commonly called the PΔ effect. This additional bending moment will cause the column to undergo an increased and larger lateral displacement that in turn generates an additional bending moment. The cycle will continue until the additional or secondary lateral displacement becomes so small as compared to the previous one. At this time, the effect of the secondary bending moment will be so small that the column will stabilize itself in its final deformed position with a total bending moment equal to the axial load times the sum of the eccentricity of the applied axial load plus the final lateral displacement of the center line of the column or P(e+Δ).

Fig. 1.9 shows a typical eccentrically loaded slender column with uniaxial bending in single curvature caused by the load P applied with equal eccentricity e at each end. The column has a lateral displacement Δ at the midheight of the column.

The parameter that measures the slenderness of a particular column is called the slenderness ratio, and is expressed as the ratio of the effective length of the column to the radius of gyration of the cross section or Kl/r.

The slenderness ratio of a composite column cross section depends on the effective length of the column kL and the radius of gyration r, which is a function of the Moment of Inertia I and the area A of the composite cross section. The flexural stiffness EI for a composite cross section is a very unpredictable parameter. The concrete portion of the composite section under the tensile flexural stresses develops a series of cracks that vary in length and width according to the material properties of the concrete and the level of combined stresses the cross section is being

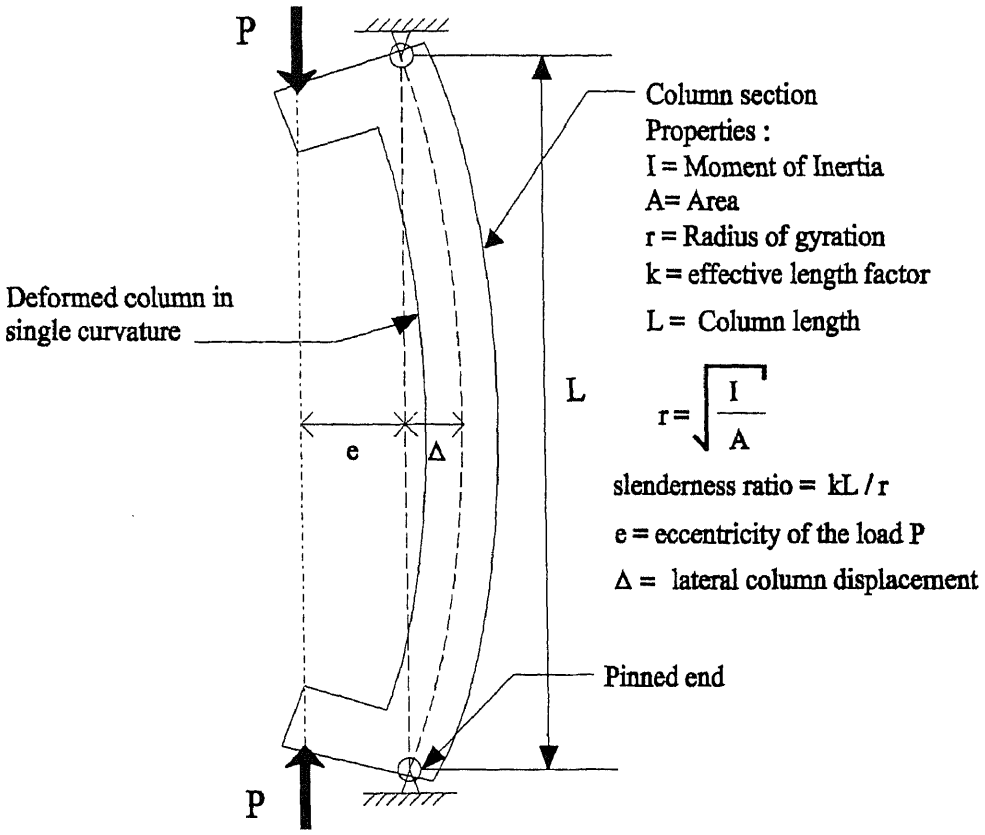


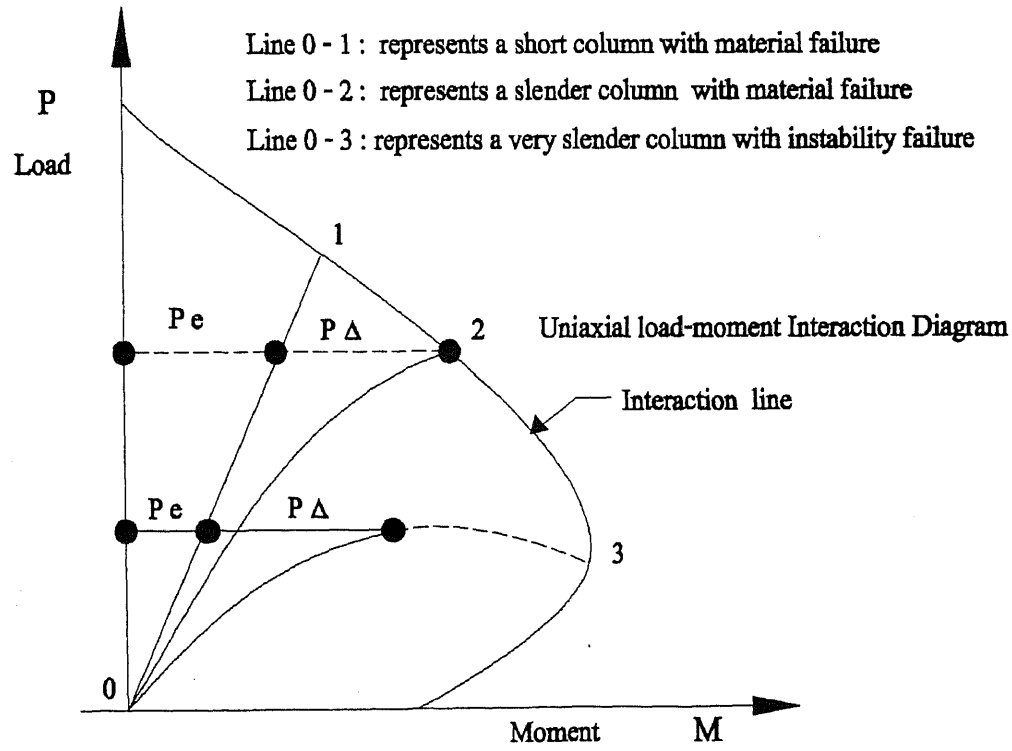


**Figure 1.9** Uniaxilly loaded slender column and interaction diagram

subjected. It is well known that concrete is less homogeneous than steel and that its modulus of Elasticity $E_c$ is very sensitive to sustained loads. The appropriate values of Modulus of Elasticity and Moment of Inertia used by the ACI and the AISC in their design methods for composite columns are presented in the following sections.

The behavior of slender composite columns under an increasing eccentrically applied axial load is illustrated by the schematic deflected shape of the column and the interaction diagram shown in Fig. 1.9. For a short column in uniaxial bending with a very small lateral displacement, the maximum bending moment M will be the P load times the eccentricity e or Pe at all load levels. In other words, the load versus moment interaction follows a linear relationship along the line 0-1 in Fig. 1.9 until the section reaches a material failure state at the intersection with the interaction line.

For the case of a slender composite column in uniaxial bending, the maximum bending moment M is $P(e+\Delta)$. Due to the larger lateral displacement of slender column and additional bending moments created by the $P\Delta$ effect, the load moment relationship becomes nonlinear and can be represented by the two curved lines 0-2 and 0-3 shown in Fig. 1.9.

The first line 0-2 of Fig. 1.9 represents the behavior of a slender column that becomes stable at the point of intersection with the interaction line but that reaches the material failure state. A typical case of intermediate slender columns are columns which form part of braced frames against sideways. The last line 0-3 represents a very slender column that becomes unstable without reaching the material failure state; the lateral displacement is too large and the column dimensions such as the axial load is controlled by the critical Euler load. This type of slender column is very often found in the buildings with very slender columns unbraced against sidesway.

It has been stated by different researchers, Dowling (221-223) among others, that slender composite columns behave very similar to reinforced concrete columns. However, the flexural stiffness of slender composite columns when loaded to the ultimate load levels can not be predicted with great accuracy. The value of flexural stiffness is believed to be the most dominant factor on the slenderness effects and the strength of the composite column cross section.

A brief summary of major variables that affect the strength of slender composite columns is herein presented as follows:

The ratio of unsupported height to cross section depth $l_u/h$, the ratio of end eccentricity to cross section depth e/h, the ratio of two end eccentricities, the degree of rotational end restraints and lateral restraint, the amount of structural steel and reinforcing steel rebars, the ultimate strengths of materials including the confined and unconfined conditions of the concrete part in composite section and duration of loading.

Fig. 1.10 illustrates the variation of the uniaxial load-moment interaction diagrams for different values of slenderness ratio. Note that the interaction line for the short column kL/r=0, provides the upper bound envelope of all the safe combinations of axial load and bending moment.

The design of slender composite columns can be approached with two different methods:

Firstly, the "Exact" design method which is based on actual bending moments and forces that are derived from a second order analysis of the structure. These include actual stiffness of the cross section, effect of lateral deflection on moments and forces, duration of loading and nonlinear characteristics of the material

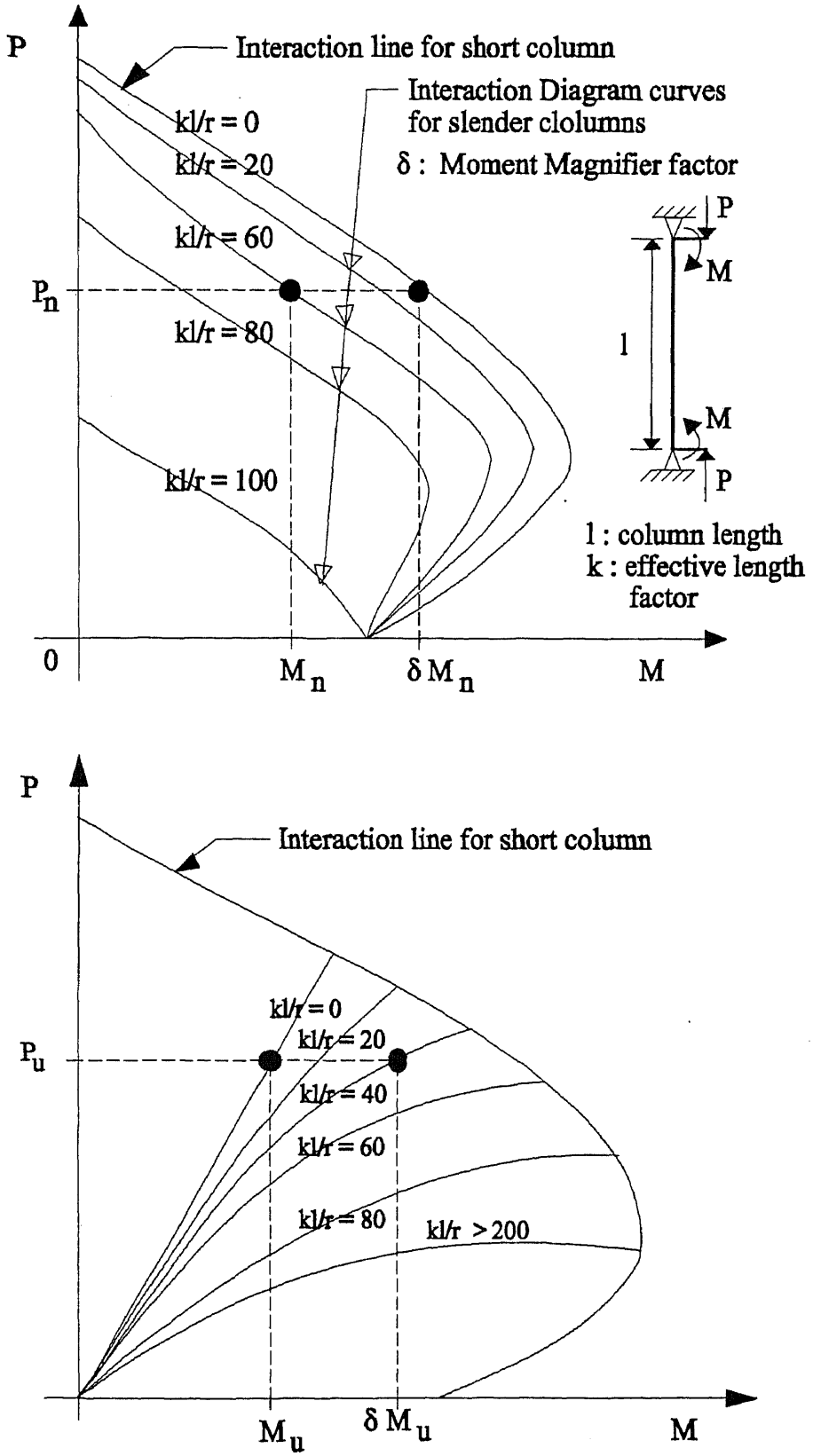


**Figure 1.10** Interaction Diagrams and Moment Magnifier Method

properties. The effect of column slenderness is already accounted for when the final member forces are found by this design method.

Reasonable assumptions regarding the stiffness parameters of beams and columns part of the structural framing have to be made in order to carry out the second order analysis. A single member can also be designed based on the ultimate strength of the cross section obtained by the second order analysis.

A computer program to study the complete load-deformation, moment-curvature behavior of slender composite columns under combined biaxial bending and axial load is presented in Chapter 3 of this dissertation.

The computer program provides the ultimate strengths of axial load and biaxial bending moments for a composite column in a single curvature and with pinned-ended conditions.

Secondly, the "Approximate" design approach for slender columns is called The Moment Magnifier Moment, which is given in the ACI 318-89 Rev. 1992 Building Code for Reinforced Concrete Buildings and in the AISC American institute of Steel Construction Specifications.

The method uses the first order analysis (analysis that ignores the influence of lateral deflections on final bending moments and forces) of structural members to find the moments and forces, then the bending moments are magnified to account for the second order effects of lateral displacement.

Fig. 1.10 shows a graphical representation of the moment magnifier method. The axial load and bending moment to be resisted by the column cross section, $P_u$ and $M_u=P_u e$, are determined from a first order elastic analysis, then the forces to be used in the final design of the cross section are taken as the same axial load $P_u$ and

a modified bending moment $\delta M_u$, where $\delta$ is the moment magnification factor, as a function of the slenderness of the column.

The equations for the moment magnification factor $\delta$ for composite columns are the same as the ones used for reinforced concrete design, as given in the ACI Building Code (1), and steel design, given in the LRFD Design Manual (13), with the appropriate modifications to account for the material properties and cross section geometry of the composite section.

## 1.6 Comparative Review of American Design Standards on Composite Columns

Two American Institutions, ACI (1) and AISC (12), have provided the Building Code Specifications, Regulations, Analysis and Design Guidelines for many decades. They promote the use of two most widely used materials in the Building Construction Industry, Reinforced Concrete and Structural Steel respectively.

Both ACI and AISC recognize the fact that regardless of the design method, large increases in Axial load and bending moment capacities can be obtained by embedding structural steel shapes in concrete. However neither one has yet adopted a unified and completely rational design procedures for composite columns.

The Structural Specifications Liaison Committee (SSLC) was formed in the United States in 1978 to evaluate the composite column design procedures that would be acceptable to both the ACI and the AISC.

The SSLC (196) published a report by the AISC describing the provisions on design of composite columns were compatible with the allowable stress design method of the AISC.

### 1.6.1 The ACI Design Method

The ACI design method for both short and slender composite columns is presented in chapter 10 of the ACI 318-89 Revised 1992 building code. In general the design approach and the strength calculations for a composite member shall be done for the same limiting conditions applicable to regular reinforced concrete columns. The resulting design interaction equations are based on ultimate strength forces and the concrete part of the composite section is considered to have reached a failure state when a strain value of 0.003 exists in the cross section.

The current ACI design methods for steel-encased concrete and pipes and tubes filled-in with concrete composite columns are based the theoretical and practical research work carried out by Furlong (64-70), the experimental work conducted by Roderick and Rogers (175) and Knowles and Park (116) among others.

The ACI specifies that every composite column either a concrete-encased steel section or steel-encased concrete, must be designed to adequately transfer the shear forces between concrete and steel. Also any axial load strength assigned to be carried by the concrete section must be transferred to concrete by direct bearing on the concrete by means of members or brackets. Any type of steel connectors such as plates, shear studs, lugs, or rebars welded to the steel shape before casting the concrete are suitable to transfer the force by direct bearing to the composite member concrete. All axial load and bending strength not assigned to the concrete part of the composite section shall be fully developed by direct connection to the structural steel member.

The maximum axial load allowed by the ACI for concentrically loaded short columns, when all parts of the section are subjected to a 0.3% strain can be written

in the following form:

$$P_o = A_s F_y + A_{sr} F_{yr} + 0.85 f'_c A_c \quad (1.7)$$

The ACI Building Code (1), does not allow the design of compression members with concentric axial force alone. All columns are to be considered to behave as beam-columns and a minimum eccentricity of the axial load must be included in the design.

The limit value of the axial force is taken as an upper limit of $0.8P_o$ for the encased shapes and $0.85P_o$ for the filled tubes, where $P_o$ is the ultimate axial strength of the column cross section.

The nominal strength values of axial load and bending moment must be reduced by capacity reduction factors $\phi$, according to the type of composite column and the specific region of axial load level and flexural condition.

The minimum nominal eccentricity specified by the ACI code must be 0.05 times the total thickness of the concrete-filled tubes, and 0.10 times the total thickness of the concrete-encased rolled steel shapes.

For the design of column cross sections subjected to axial load and bending moments, the ACI requires that an evaluation of material stresses, strains, and forces be integrated over the entire cross section to determine the combination of axial load $P_n$ and bending moment $M_n$ at the failure condition.

The maximum usable strain in any concrete part of the section is to be taken as 0.003, and all the compressive and tensile strain values calculated for steel and concrete are to be taken as being proportional to their distance to the neutral axis.

For the evaluation of slenderness effects and moment magnification factors to

be used in the calculations of the ultimate axial load capacity of the composite column, the ACI provides an equation to calculate the radius of gyration of a composite column section, which can be written in the following form:

$$r = \sqrt{\frac{(E_c I_g/5) + E_s I_t}{(E_c A_g/5) + E_s A_t}} \tag{1.8}$$

where: $E_c$ and $E_s$ are the modulus of elasticity of concrete and the structural steel shape, pipe or tubing, $I_g$ is the moment of inertia of the gross concrete section about centroidal axis neglecting reinforcement, $A_g$ is the gross area of the composite column section, $I_t$ is the moment of inertia of the structural steel shape, pipe, or tubing about the centroidal axis of the composite column cross section, and $A_t$ is the area of the structural steel shape, pipe or tubing of the composite column cross section.

Other provisions for minimum thickness of the structural steel shape encasing the concrete core, longitudinal bars within the encased concrete core, longitudinal and transversal spiral and lateral tie reinforcement around the structural steel core, minimum concrete compressive strength, minimum yield strength of the structural steel shape, size, spacing, and location of lateral ties and longitudinal reinforcement are given in sections 10.14.6 to 10.14.8.8 of the ACI Building Code.

The ACI provides an equation to calculate the stiffness factor EI as follows:

$$\max \quad EI = \frac{(E_c I_g/5)}{1 + \beta_d} + E_s I_t \tag{1.9}$$

The ACI does not specify an upper limit for the percentage of steel ratio to the total composite cross section.

### 1.6.2 The AISC-LRFD Design Method

The AISC, American Institute of Steel Construction, in his LRFD Manual of Steel Design (13), provides a design method for composite columns. The LRFD design method is based on the ultimate strength of the materials part of the cross section and takes into account the inelastic material properties with the required design loads as factored service loads.

The Load and Resistance Factor Design Method (LRFD) (13), contains the latest design approach of structural steel based on the ultimate strength concept. LRFD defines a composite column as a steel column fabricated from rolled or built-up steel shapes and encased in structural concrete or fabricated from steel pipe or tubing and filled with structural concrete.

The nominal strength of a cross section is calculated from the ultimate resistance to load, and reduction capacity factors related to material properties and characteristics of member failure are applied to the nominal strength of the cross section. The design recommendations of the SSLC Report (196) have strongly influenced the development of the interaction design expressions contained in the LRFD Specification for the analysis and design of composite columns.

Chapter I of the LRFD (12) includes the design provisions for composite members. Section I2 specifically presents the limitations that a composite member under compression have to meet in order to qualify as a composite column. A brief recount of these limitations is herein presented :

1.- The cross sectional area of the steel shape, pipe or tubing must comprise at least 4% of the total composite cross section.

2.- Concrete encasing the steel core shall have a certain minimum longitudinal

load carrying bars, longitudinal bars to restrain concrete and lateral ties. Layout requirements for longitudinal bars, minimum spacing of ties, and minimum clear cover of bars are also given in this section.

3.- Minimum compressive strength of concrete shall be 3,000 psi and maximum of 8,000 psi. for normal weight concrete, and minimum of 4,000 psi for light weight concrete.

4.- Minimum yield stress of steel shapes and reinforcing bars for calculating section strength shall not exceed 55 ksi.

5.- Minimum wall thicknesses of steel shape encasing concrete are given for structural steel pipe and for steel tubes filled with concrete.

The design strength of composite columns with axial load alone, $\phi_c P_n$ ($\phi_c$=0.85) can be calculated by use of the formulas E2-1 through E2-4 of the LRFD (12), and which are rewritten here as follows:

$$P_n = A_s F_{cr} \tag{1.10}$$

$$for \quad \lambda_c \leq 1.5; \quad F_{cr} = (0.658^{\lambda_c^2}) F_{my} \tag{1.11}$$

$$for \quad \lambda_c > 1.5; \quad F_{cr} = \left[\frac{0.877}{\lambda_c^2}\right] F_{my} \tag{1.12}$$

$$\lambda_c = \frac{Kl}{r_m \pi}\sqrt{\frac{F_{my}}{E_m}} \tag{1.13}$$

where $$F_{my} = F_y + c_1 F_{yr}(A_r/A_s) + c_2 f_c'(A_c/A_s), \tag{1.14}$$

$$E_m = E_s + c_3 E_c(A_c/A_s) \quad \text{and} \quad E_c = w^{1.5}\sqrt{f_c'} \tag{1.15}$$

$r_m$ = the radius of gyration of the steel shape, pipe or tubing except that for steel shapes it shall not be less than 0.3 times the overall width of the composite cross section in the plane about which buckling is being considered.

w = unit weight of concrete in lbs./cu.ft

Section I4 of the LRFD (12) covers the design of composite members with symmetric shape under the combined action of compression/tension and flexure with the following interaction equations:

$$for\ \frac{P_u}{\phi P_n} \geq 0.2;\ \frac{P_u}{\phi P_n} + \frac{8}{9}\left(\frac{M_{ux}}{\phi_b M_{nx}} + \frac{M_{uy}}{\phi_b M_{ny}}\right) \leq 1 \qquad (1.16)$$

$$for\ \frac{P_u}{\phi P_n} < 0.2;\ \frac{P_u}{2\phi P_n} + \left(\frac{M_{ux}}{\phi_b M_{nx}} + \frac{M_{uy}}{\phi_b M_{ny}}\right) \leq 1 \qquad (1.17)$$

$$M_u = B_1 M_{nt} + B_2 M_{lt} \qquad (1.18)$$

$$B_1 = \frac{C_m}{(1 - P_u/P_e)} \geq 1 \qquad (1.19)$$

$$C_m = 0.6 - 0.4(M_1/M_2) \qquad (1.20)$$

$$B_2 = \frac{1}{1 - \Sigma P_u \left(\frac{\Delta_{oh}}{\Sigma HL}\right)} \qquad (1.21)$$

$$B_2 = \frac{1}{\left(1 - \frac{\Sigma P_u}{\Sigma P_e}\right)} \qquad (1.22)$$

where

$P_u$ = required compression/tensile strength

$P_n$ = nominal compressive/tensile strength in accordance with Sect. E2 and D1

$M_u$ = required flexural strength

$M_n$ = nominal flexural strength determined from plastic stress distribution on the composite cross section with the noted exceptions noted in section I4

$\phi_{c,t}$ = resistance factors for compression and tension respectively,

$\phi_c$ = 0.85 for compression, and $\phi_t$ = 0.9 for tension

$\phi_b$ = resistance factor for flexure = 0.9

$M_{nt}$ = required flexural strength in the member assuming there is no lateral translation of the frame

$M_{lt}$ = required flexural strength in the member as a result of the lateral translation of the frame only

$P_e$ = $A_s F_{my} / \lambda_c^2$ is the elastic buckling load

Part 4 of the LRFD Steel Design Manual (13) presents load tables for composite columns reinforced with W shapes. $F_y$ ranges from 36 to 50 ksi and nominal depths of 8 in. up to 14 in. encased in square or rectangular normal weight concrete are also given. Concrete of $f_c'$ equal to 3.5, 5 and 8 ksi and Grade 60 reinforcing steel are used.

The Tables also shows structural pipes of 4 in. to 12 in. in nominal diameter and yield stress of $F_y$ equals to 36 ksi. They are filled with normal weight concrete of $f_c'$ at 3.5 and 5 ksi; Structural tubes of nominal side dimensions of 4 to 16 in. and yield stress of $F_y$ equal to 46 ksi filled with normal weight concrete of $f_c'$ equal to 3.5 and 5 ksi are also included in the Tables.

The tabulated loads were computed in accordance with Section I2.2 of the LRFD Specification (13) for axially loaded members. The axial design strengths are

given for members with effective lengths respect to the minor axis and with a Kl/r value of up to 200. For composite column sections under a combination of axial compressive or tensile load and bending moments, the design is done by successive approximations.

It is illustrated in Section I4 of the LRFD Specification, where the nominal flexural design strength $\phi_b M_n$ is calculated from formula C-I4-1 of the LRFD Commentary. The Elastic Buckling Load $P_e$ is also given in the composite column tables.

The ASD 9th Edition of the Steel Construction Manual, does not include any provisions for the design of composite columns.

**The SSLC Design Recommendations**

The AISC published a report (196), developed by the Structural Stability Liaison Committee (SSLC), which includes a design procedure for composite columns based on allowable stress limits under service load conditions identical to the ones given by the ASD (12) Design Manual of Steel Construction. Under the SSLC design procedure, composite cross sections are considered to be structurally adequate when the calculated stress values resulting from the action of the external loads never exceed the specific fractions of the allowable strength values of the different materials of the cross section. The SSLC design procedure for combined action of steel and concrete uses a modified yield stress $F_{my}$, a modified radius of gyration $r_m$, a modified modulus of elasticity $E_m$ and a modified section modulus $S_m$ to evaluate the axial load and bending moment capacity for composite columns.

The modified section modulus $E_m$ proposed by the SSLC is based on an estimate of the flexural strength capacity of the cross section in the absence of any

axial load and given as follows:

$$S_m = S_{sc} + 0.33A_{sr}(h_1 - 2c_r)\frac{F_{yr}}{F_y} + \left(\frac{h_2}{2} - \frac{A_w F_y}{1.7 f_c' h_1}\right)A_w \quad (1.23)$$

where

$A_w$ = area of the web of a rolled steel shape or zero for filled steel tubes or pipes.

$c_r$ = edge distance to centroid of reinforcing bars.

$h_1$ = thickness of cross section in the plane of bending.

$h_2$ = thickness of cross section perpendicular to the plane of bending.

$S_{sc}$ = elastic section modulus of the steel shape or tube.

The equation presented above was derived under the assumption that an equal amount of longitudinal rebars would be placed in each face of the cross section, that one third of the steel acts in tension for pure bending and that the web of the steel shape provides tensile reinforcement in the strength calculations for the cross section under bending about the strong axis. The SSLC recommends to incorporate the modified values of yield stress, radius of gyration, modulus of elasticity, and section modulus, into a parabolic type beam-column interaction equation that can be written in the following form:

$$\left(\frac{f_a}{0.6F_{my}}\right)^2 + \frac{f_b}{F_b} = 1 \quad (\textit{strength equation}) \quad (1.24)$$

$$\left(\frac{f_a}{F_a}\right)^2 + \frac{f_b}{F_b}\frac{C_m}{\left(1 - \frac{f_a}{F_e'}\right)} = 1 \quad (\textit{stability equation}) \quad (1.25)$$

where: $f_a$ = calculated axial stress; $F_a$ = allowable axial stress; $f_b$ = calculated

bending stress; $F_b$ = allowable bending stress; $F_e'$ = the reduced Euler buckling stress given by $(12/23)\pi^2 E_m/(kl/r_m)^2$; and $C_m$ is an end moment coefficient defined in Section H1 of the ASD 9th Edition Manual of Steel Design (12). The expressions for $F_{my}$ and $E_{my}$ for concrete filled tubes and concrete encased steel shapes are given in the SSLC Report (196) as a superposition of the corresponding contributions of the steel shape, reinforcing steel bars and concrete to the allowable stress and modulus of elasticity of the composite cross section.

The modified radius of gyration $r_m$ for a composite cross section should be taken as the radius of gyration for the steel section alone or for the concrete part alone, whichever is larger. The design equations presented by the SSLC provides a closed form analytic solution for the determination of the strength of short and slender composite columns.

### 1.6.3 Comparative Review of the ACI and AISC Design Methods

Structural Steel and Reinforced Concrete have their structural behavior represented by two separate design approaches. Steel is a ductile material and Concrete is brittle and has a very low resistance to tensile stresses. Structural Steel is produced, fabricated, and erected under well controlled conditions of dimensions and workmanship, while Reinforced Concrete is produced, cast, and cured under not totally controlled environments and many times under uncertain weather conditions that make quality control very difficult to predict. The Steel and Concrete Industry therefore have adopted different ratios of structural performance under service loads and ultimate load conditions for steel and concrete.

The two American Institutions, ACI (American Concrete Institute) and AISC

(American Institute of Steel Construction), both address the subject of design of composite columns, but each one with a different design philosophy. The ACI (1) and the LRFD (13) design equations for composite columns are expressed in terms of forces. The specified load factors given by the ACI and LRFD for the ultimate strength design of composite columns are very similar but are not completely equal.

Furlong (69,70,72,73,74), have presented an extensive and very well documented comparative study of the current ACI and AISC Standards on design of composite columns. He showed that from the basic equations of axial load, a transition function between the ACI and the AISC expressions would require a modified factor of safety to make both expressions comparable. In regard to the comparable flexural strength capacity, the AISC and the ACI analytical methods to calculate the allowable axial load on very slender columns tend to provide similar results. For low values of slenderness ratio the two design methods provide appreciable different results.

Additionally, Furlong (74), stressed the importance of the effective stiffness factor EI of composite columns, and pointed out that the creep effect and reduced stiffness of concrete has a strong influence in the evaluation of the radius of gyration of composite columns. Finally, Furlong (74), proposed an expression for the evaluation of the EI relationship of composite cross sections in the following form:

$$EI = E_s I_s + (1/3)E_c I_c \text{ ; where : } E_c = 33w^{1.5}(\phi f'_c)^{1/2} \qquad (1.26)$$

and w = density of concrete in lb/cu.ft.

Furlong also proposed a set of equations for the evaluation of the allowable loads under service conditions as functions of the EI and the kL parameters.

The AISC design equation for composite columns is presented as a linear

relationship between the allowable axial stress and the allowable flexural stress, Furlong (74), proposed a similar interaction equation to the AISC equation of axial load and bending moments. However in his formulation he expressed the participating terms in function of forces rather than stresses. Expressions for calculating the allowable flexural strength are given as a fraction of the plastic bending strength for concrete filled tubes and concrete encased steel shapes.

The interaction equation proposed by Furlong (74), is given as follows:

$$\frac{P}{P_a} + \frac{\delta M}{M_a} = 1 \qquad (1.27)$$

where $\delta$ is the slenderness magnification factor for composite columns.

According to the results obtained by using the equations presented by Furlong (74) composite columns that have a large percentage of steel section ratio to the total column section, would provide a design that is in close agreement with the provisions of the AISC specifications. On the other hand, composite columns that have larger concrete section ratio to the total section would provide a design closest to the ACI code rules.

One of the important differences between the ACI and the AISC design methods lies in the determination of the limiting values that distinguishes the short from the slender columns.

The ACI uses the same limiting values of $kl_u/r$ given in sections 10.11.4.1 and 10.11.4.2 for reinforced concrete columns to the case of composite columns with the adjusted radius of gyration r (ACI eq. 10-13) and stiffness factor EI for composite columns (ACI eq. 10-14) given in section 10.14.5. The minimum eccentricity specified by the ACI Building Code (1) for the design of compression members shows that a

typical concrete encased steel shape designed by the ACI method will carry less load than the same unencased steel shape alone designed by the AISC design method.

The AISC in his LRFD specifications (12) includes the slenderness parameter $\lambda_c$ as a function of KL/r, modified yield stress $F_{my}$, and the modified modulus of elasticity $E_m$, in the design formulas to calculate the axial load and bending moment capacity for composite sections.

A comparative review of Allowable Loads for two types of composite column cross sections: a) concrete encased steel wide flange shape with reinforcing steel bars, and b) concrete-filled steel pipe columns, was presented by Furlong (73). He reported numbers of figures illustrating the graphical representation of Load-Moment interaction and Load-Slenderness relationship of the above two types of composite cross sections. They are calculated based on the ACI, SSLC and the LRFD Design methods respectively. A summary of the findings highlighted by Furlong (73) are herein reproduced for illustrative purposes.

The ACI procedures for concrete filled pipe cross sections shows a greater flexural strength than does allow the LRFD and the SSLC rules for most of the axial load levels. The SSLC and the LRFD design procedures permit more axial load on filled tubes than does the ACI design method. From the figures presented for concrete filled pipes it is clearly shown that for relatively large Kl values of empty steel pipe columns designed by the AISC design method a higher allowable load than that allowed by the ACI design method for concrete-filled pipes is obtained.

The SSLC design procedure permits axial service loads somewhat higher than the LRFD design method for most of the bending moment and slenderness ratio values. It becomes more advantageous to use concrete-filled pipe columns and design

them by the ACI design method only for the case of relatively short columns subjected to minor bending moments.

From the figures presented by Furlong (73), for concrete encased steel wide flange shapes the followings are noted: a) the cross section containing a large structural shape as a core, approximately steel occupies 12% of the cross section, indicates that the ACI design procedure allows less load than either the LRFD and the SSLC design procedures. From both the strength and slenderness figures, the ACI design procedure for the composite section allows loads that are not much greater than the loads allowed by the AISC for the steel shape alone. b) the cross section containing a small structural shape as a core, approximately 4% of the cross section, makes it a cross section with a major portion being reinforced concrete. The ACI design procedure allows a larger load-moment combination for most of the axial load levels than that allowed by the AISC and the SSLC design procedures.

Again, for very long columns the LRFD allows loads significantly higher than that calculated by the ACI design method. From the latest figures for lightly reinforced composite columns, it is noted that the concrete encasement of a wide flange steel shape allows for a much higher allowable stress than that which could be allowed for the steel shape alone. A longer encased steel shape could be used in contrast to the steel shape alone.

The LRFD design procedure for slender composite columns allows the use of composite sections that would not be accepted by the ACI design rules. The ACI design procedures appear to be very conservative for the case of slender composite columns. The strength calculations are the most difficult to apply for the evaluation of nominal load-moment strength capacity.

The LRFD and SSLC design procedures would produce a better estimate of the actual beam-column behavior of composite sections. Specific equations for load-moment interaction and strength calculations are given and are applicable only to ordinary rectangular or circular composite cross sections but could be used for different slenderness ratios. LRFD provides the most appropriate design procedure for evaluating the load carrying capacity of slender composite columns.

### 1.7 Scope and Objectivity of Present Research

One of the main objectives of this study is an attempt to explore the possibility to incorporate the fundamental principles of the two current design methods of the ACI and the AISC into a unified approach that would satisfy the compatibility of deformation as well as the force and moment equilibrium conditions of the two materials which form part of the composite section.

It is true that depending on the proportions of each individual material with respect to the cross section of the structural element, the overall behavior would be controlled by either one of the two that would contribute the most to the load carrying capacity and structural stability of the whole section. However it is important to note that once different materials are put together into a composite element, the behavior of this new structural element is unique and therefore, there should be a unique and unified design approach that would control the behavior of this structural element.

An experimental project with a limited number of test specimens was carried out with the purpose of studying the complete load-deformation behavior of concrete-encased steel composite columns. This is one of the major contributions and

originality of present research. To perform a biaxial bending test that would include the ascending and descending branches of a composite column with considerable high slenderness ratio and within the limitations of the available testing equipment, it was decided to use the small scale specimens.

The analytical and theoretical part of this dissertation work will form the most important contribution of this study. A generalized analytical equation of failure surface is proposed herein to predict with reasonable accuracy the ultimate strength of composite columns under biaxial bending and axial loads. This analytical equation can be a preliminary or introductory equation that will form the basis for a unified design method of composite columns.

The present study ultimately is intended to comparatively review the current design methods available in the United States for the analysis and design of composite columns. Also, an experimental testing program will provide the basis to understand the basic behavior of short and slender composite columns under axial compressive load and biaxial bending. An attempt will be made to develop a new mathematical design interaction equation; a computer model will also be presented to study the complete load-deformation behavior of reinforced concrete-encased structural steel columns under axial load and biaxial bending. The test results of present research and others are to be compared with the theoretical and analytical values obtained from the proposed mathematical design interaction equation and computer analysis program.

# CHAPTER 2

# GENERALIZED INTERACTION EQUATION OF FAILURE SURFACE

## 2.1 General Theory

The Author will present the development of a generalized interaction equation of failure surface for the Analysis and Design of Composite Columns under biaxial bending moments and axial load. The proposed equation is based on a theoretical mathematical derivation that takes into account the uniaxial interaction diagrams about the two main perpendicular axes of bending and the load contour diagram at a constant axial load.

A general strength formula to predict the ultimate strength of biaxially loaded composite columns has not been thoroughly studied as it has been done for reinforced concrete columns. In the past years many investigators (4)(9)(16)(19) (38)(57)(64)(85)(86)(87)(88)(89)(90)(127), have presented their research work on the analysis, design and study of behavior of composite columns.

Roik and Bergman (181) in 1982, among others proposed a design method for biaxially loaded composite columns based on the strength interaction diagram in uniaxial bending.

The Author proposes herein a new equation of failure surface to study the behavior of short and slender composite columns under biaxial bending and axial loads. The proposed equation will incorporate a mathematical approach that is based on coefficients that represent both the uniaxial load-moment interaction diagram and the load contour diagram at a constant axial load for short columns.

Provisions also incorporate the moment magnification factor into the failure surface equation to account for the analysis and design of slender composite columns.

## 2.2 Three-Dimensional Failure Surface

The Three-Dimensional Failure Surface diagram as shown in Fig. 2.1 is basically a surface of revolution, composed of the interaction diagram lines for uniaxial bending about the major X-X and Y-Y axes and a series of interaction diagram lines at various angles to the major neutral axis of the section, obtained by changing the inclination and position of the neutral axis.

For a symmetrically reinforced composite column, the strength of a biaxially loaded cross section can be represented graphically by an interaction failure surface diagram as shown in Fig. 2.1, which includes the domain of biaxial bending, compression, and tension axial loads.

A typical rectangular composite column cross section under biaxial bending moments and axial load due to external actions is shown in Fig. 2.1.

The procedure to calculate every point of the interaction failure surface is based on the variation of: (1) the strain distribution across the column section, and (2) the position and inclination of the neutral axis with respect to the plastic centroid.

For a given point the conditions of strain compatibility and static equilibrium must be satisfied. It is not necessarily that the line of position of the neutral axis at the state of equilibrium must be perpendicular to the line of position of the resultant applied bending moments.

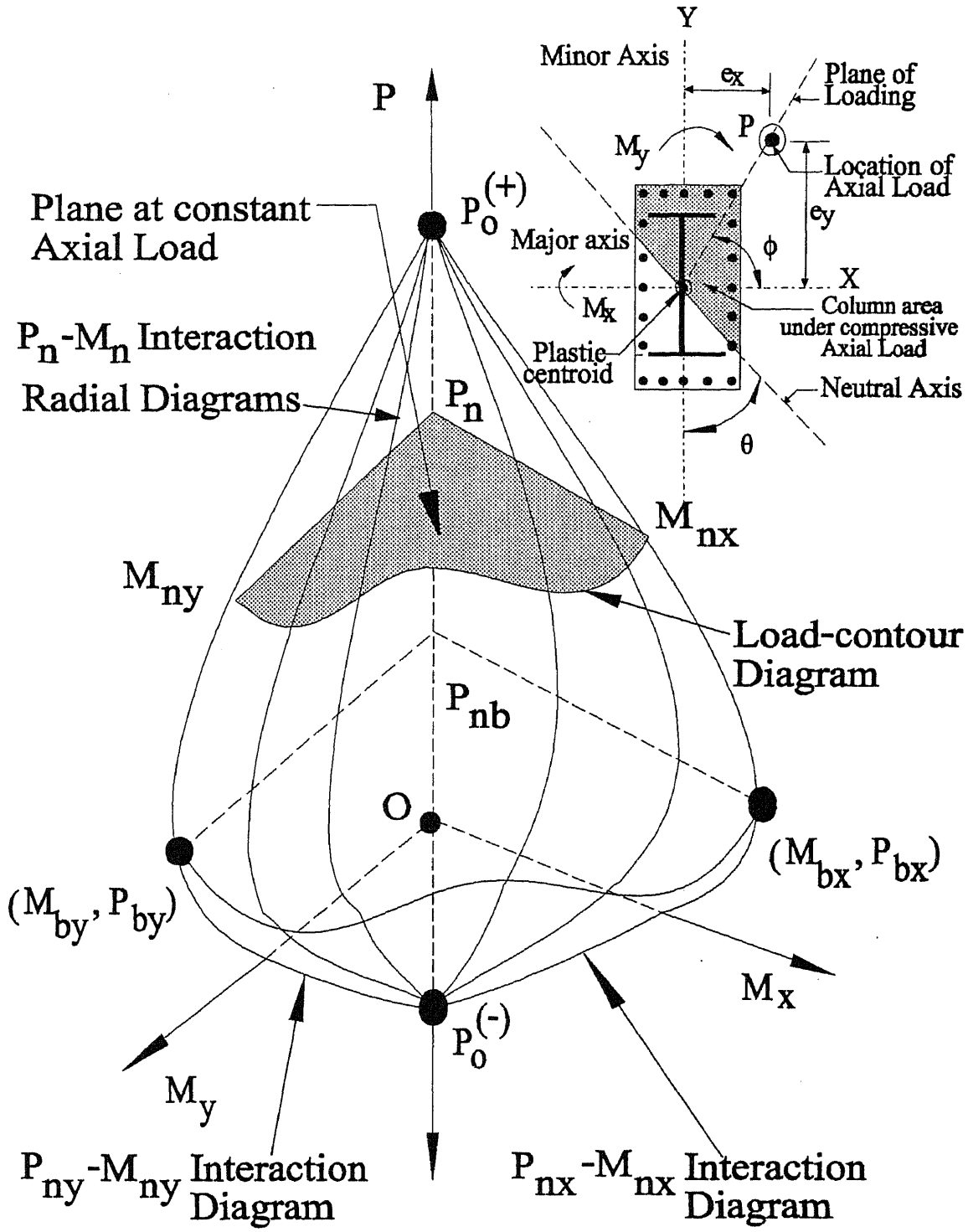


**Figure 2.1** Three-Dimensional Failure Surface

The basic assumptions and equations for the calculation of the uniaxial interaction diagrams and the load contour diagrams at a constant axial load for composite columns were presented in Chapter 1.

## 2.3 Load Contour Diagram

### 2.3.1 General

A load contour diagram is obtained by passing a horizontal plane parallel to the $M_x$ and $M_y$ axes through the interaction failure surface of Fig. 2.1 at a point of constant axial load P.

The shape of this load contour diagram for a given column cross section varies with the magnitude of the axial load, the material properties of concrete, steel shape and the steel reinforcing bars if any, the position and the amount of the steel reinforcement, structural steel area, and the column cross section geometry.

### 2.3.2 Load Contour Diagram Equation

The contour of the moment capacity for a given column cross section under biaxial bending and at a constant axial load value may be mathematically represented by a curve with the following equation:

$$\left(\frac{M_{nx}}{M_{ox}}\right)^{\beta} + \left(\frac{M_{ny}}{M_{oy}}\right)^{\beta} = 1 \qquad (2.1)$$

where the exponent $\beta$ defines the approximate shape of the curve depending on the level of the axial load and the geometry, concrete strength, size and layout of the steel reinforcement of the composite column cross section.

## 2.4 Uniaxial Load-Moment Interaction Diagram

### 2.4.1 General

A typical uniaxial load-moment interaction diagram plotted in the P-M plane is shown in Fig. 2.2. It represents the relationship between the ultimate axial load capacity and the ultimate bending moment capacity of a given column cross section.

The axial load and bending moment capacity at any load level can be computed by using the principles of static equilibrium and strain compatibility. The detailed procedures to obtain the nominal axial strength, $P_n$, and the nominal uniaxial bending strength, $M_n$, for an assumed position of the neutral axis for composite columns were presented in Chapter 1.

If a considerable number of neutral axis positions are processed, ranging from a compression failure under almost uniform concrete compression to a pure bending failure and beyond up to tensile failure, there will be enough points for the $P_n$ versus $M_n$ relationship that can be obtained and plotted to produce a load-moment interaction diagram.

The interaction diagram for a composite column with steel reinforcement in two opposite faces and a symmetrically placed structural steel shape, can be considered to be the sum of three components: (1) the load and moment strength provided by the concrete alone, (2) the load and moment strength provided by the steel rebars and the structural steel in the compression face, and (3) the load and moment strength provided by the steel rebars and the structural steel in the tensile face.

In general, the contribution of the concrete to the column strength is seen as a continuous curve, and the contribution of the steel rebars and the structural steel

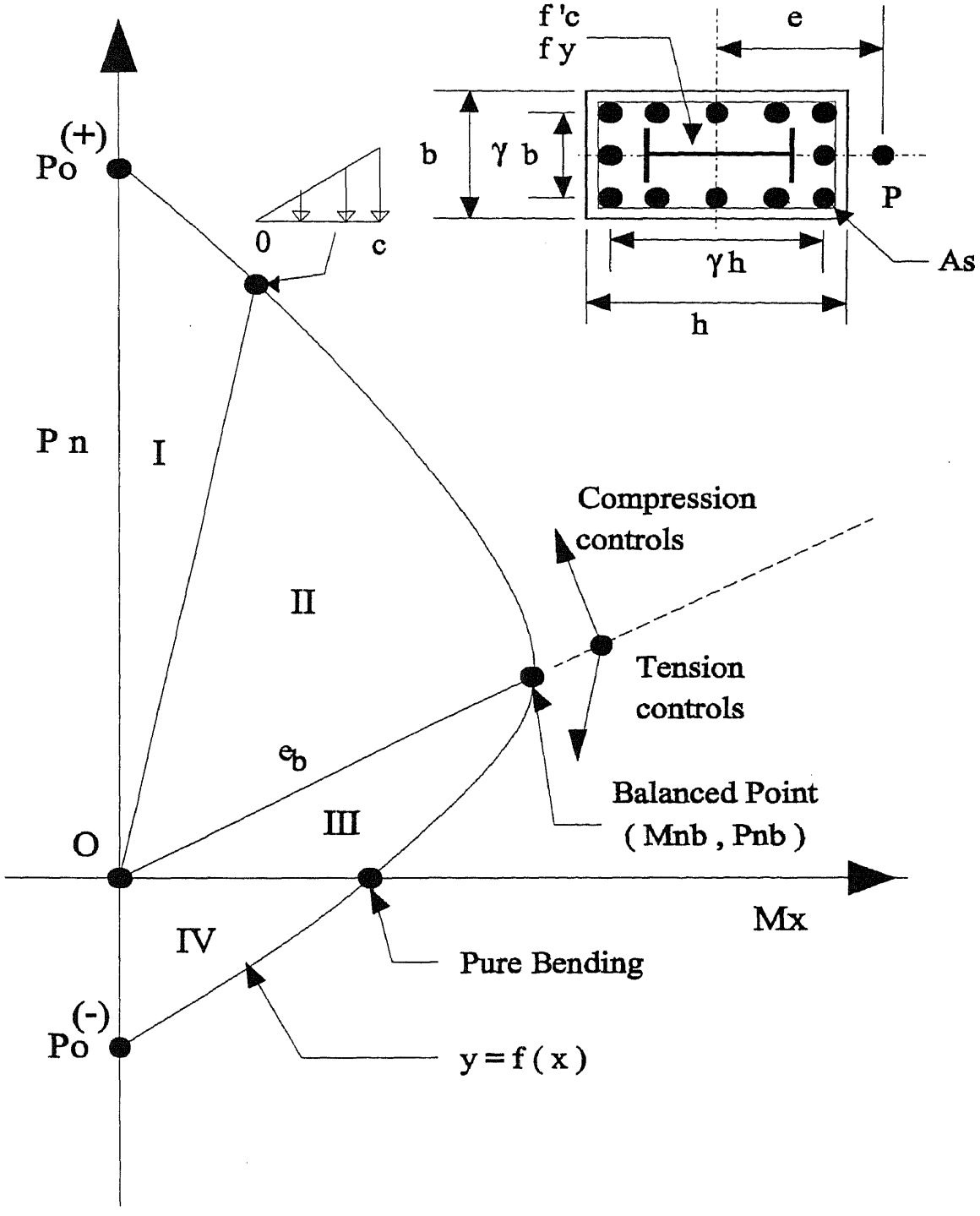


**Figure 2.2** A Typical Load-Moment Interaction Diagram for a composite column

in both faces as a curve with two branches relatively straight that intersect each other at a balanced point. In the case of columns with a high steel ratio, the shape of the interaction diagram becomes more linearized and in the case of low steel ratios, the interaction diagram is much more curved since the concrete part controls.

The Author developed a special-purpose computer program to study the shape of the interaction diagram for a composite column. The program is divided in two parts, the first part (Part I) is used to obtain the interaction diagram of rectangular composite columns for each of the two main axes of flexure, as described in the flowchart presented in Fig. 2.3. The second part of the program (Part II) is used to obtain the coefficients that best describe the shape of the interaction diagram and the load contour at different axial load levels. A listing of the computer program, "INTRDIAG", is presented in Appendix A, and a macro flowchart of the same is shown in Figs. 2.3 and 2.4.

The computer program computes the three basic points of the interaction diagram for the axial load and bending moments about X and Y axis as follows:

(1) the maximum axial compressive load,

(2) the balanced load and moment strength, and

(3) the maximum axial usable tensile load.

and it further computes additional points among the three key points.

The complete interaction diagram is basically divided in four regions: Regions I, II, III and IV. Region I covers the interaction points from the maximum axial compressive load up to a point where the cross section is at the limit of full axial compressive load. Region II covers the points from the previous limit up to the point of balanced condition. Region III covers the points from the balanced condition up

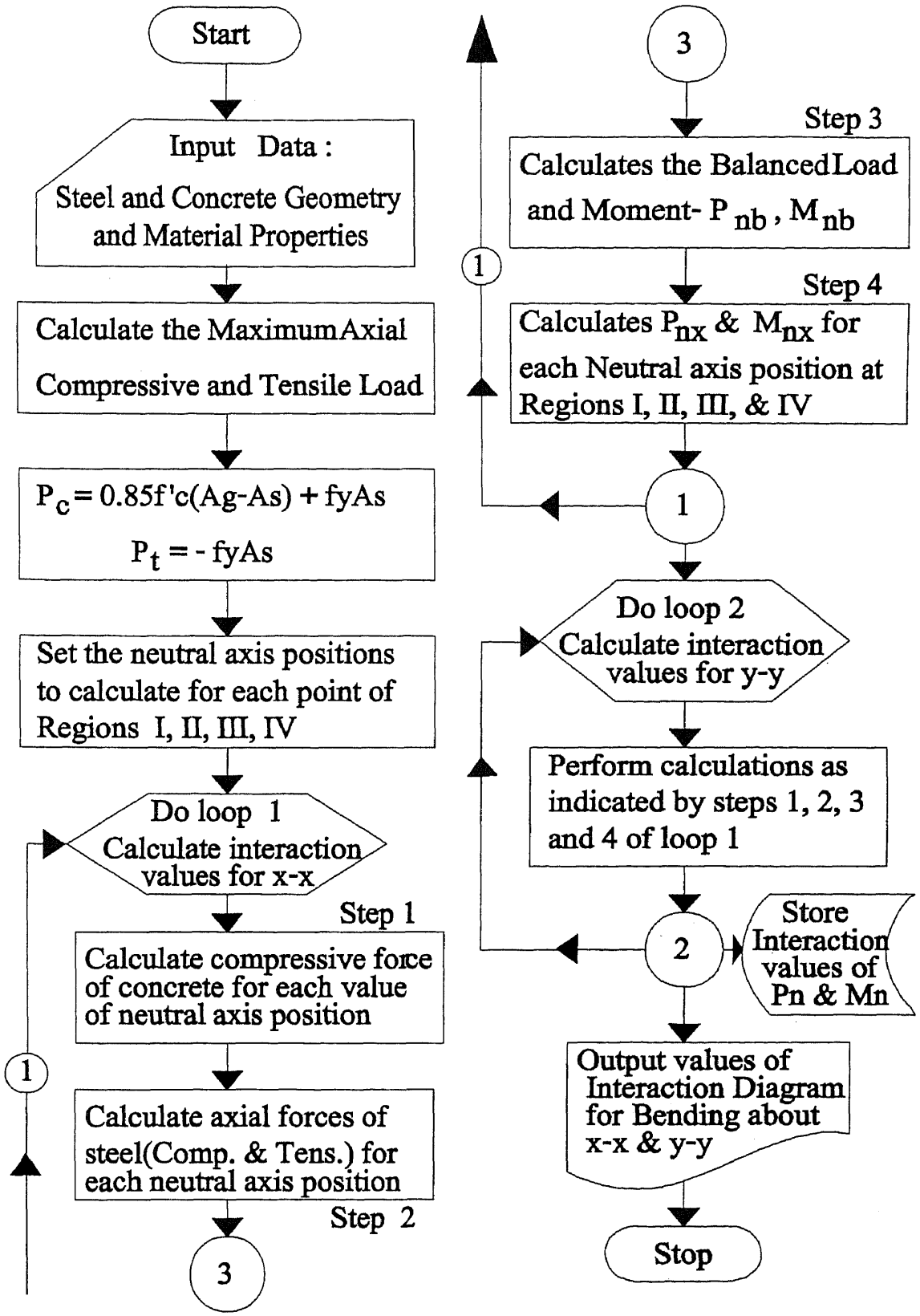


**Figure 2.3** Macro Flowchart of Computer Program "INTRDIAG" - Part I

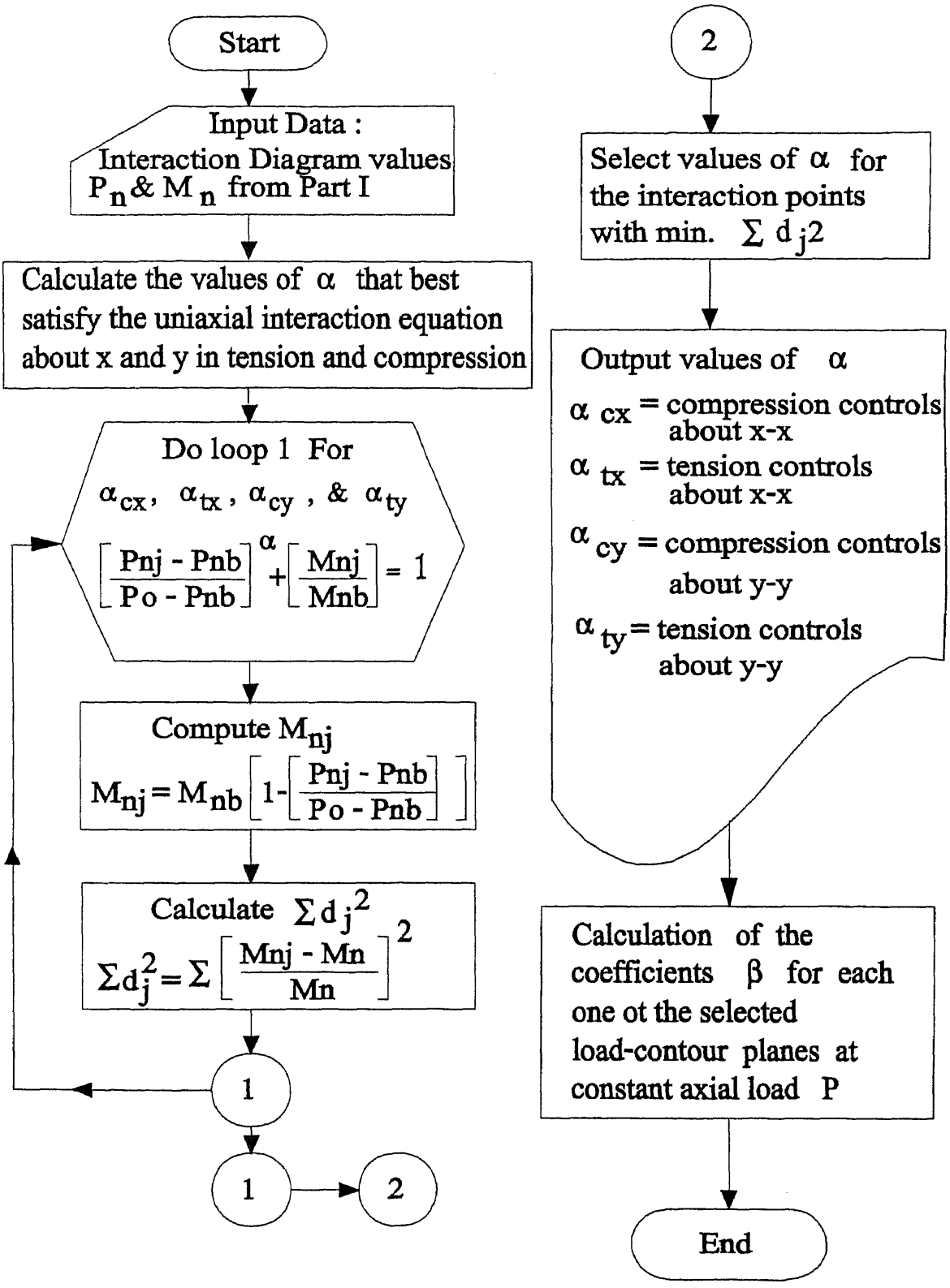


**Figure 2.4** Macro Flowchart of Computer Program "INTRDIAG", Part II

to the point of pure bending moment capacity of the column cross section. And finally, Region IV covers the points from the pure bending moment capacity up to the point of maximum axial tensile load. The design assumptions used in the program are consistent with the basic design criteria established in the ACI 318-89 Building Code (1), Section 10.2. For the Analysis and Design of Reinforced Concrete Members under Bending and Axial load. This provision is also recommended by the ACI to be used for the design of composite columns.

### 2.4.2 Uniaxial Load-Moment Interaction Diagram Equation

The uniaxial load-moment interaction diagram may be represented by a continuous mathematical function that best fits the complete range of bending moments and axial loads as shown schematically in Fig. 2.5.

Design interaction equations for beam-columns have been proposed in the past by several researchers for steel members and reinforced concrete. Chen (40), in 1989, published interactions equations for steel members (short and slender) under the uniaxial and biaxial bending moments about the strong and weak axis. For the case of uniaxial bending, Chen (40) proposed the following interaction equation for short steel beam-columns in bending about the strong axis:

$$\left(\frac{P}{P_n}\right)^{\alpha} + \frac{M_x}{M_{nx}} \leq 1.0 \qquad (2.2)$$

$$\alpha = 1.3 + 0.002\,\lambda_x \qquad (2.3)$$

where P, $M_x$ = Applied axial load and bending moment about x-x respectively.

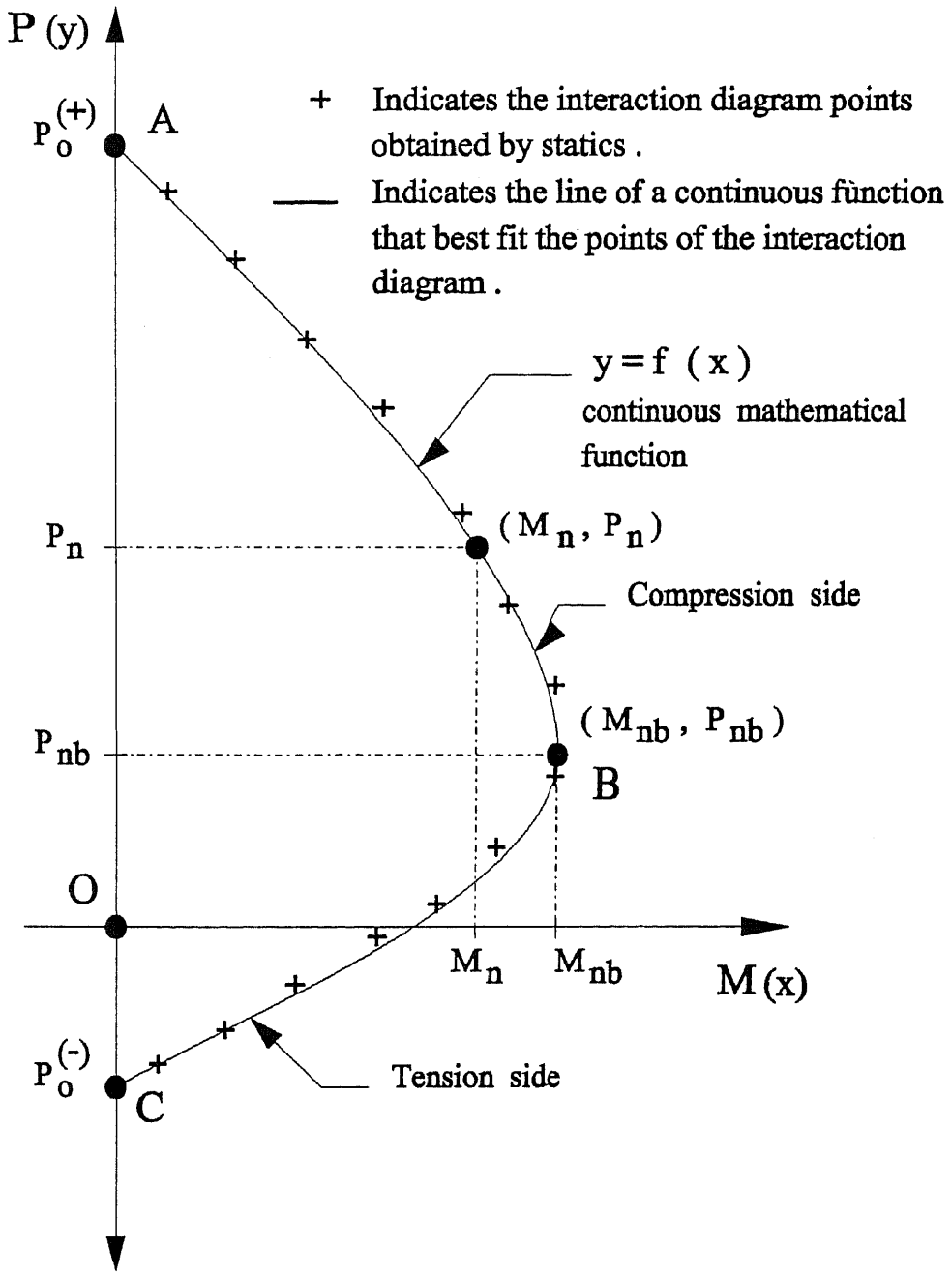


**Figure 2.5** A Typical Load-Moment Uniaxial Interaction Diagram

$P_n, M_{nx}$ = Nominal axial compressive strength and flexural strength about x-x respectively.

$\lambda_x$ = Effective slenderness ratio ($KL/r_x$).

Hsu (85) in 1988 proposed an interaction equation of failure surface for the analysis and design of square and rectangular reinforced concrete columns. The equation for combined biaxial bending and axial load case can be written as follows:

$$\left(\frac{P_n - P_{nb}}{P_o - P_{nb}}\right) + \left(\frac{M_{nx}}{M_{nbx}}\right)^{1.5} + \left(\frac{M_{ny}}{M_{nby}}\right)^{1.5} = 1.0 \qquad (2.4)$$

The above equation can also be used for the analysis and design of uniaxially loaded columns, by reducing the equation to include the terms in which the bending moments are being considered.

For uniaxially loaded columns with bending moments about X - Axis, the equation is written as follows:

$$\left(\frac{P_n - P_{nb}}{P_o - P_{nb}}\right) + \left(\frac{M_{nx}}{M_{nbx}}\right)^{1.5} = 1.0 \qquad (2.5)$$

For uniaxially loaded columns with bending moments about Y - Axis, the equation is written as follows:

$$\left(\frac{P_n - P_{nb}}{P_o - P_{nb}}\right) + \left(\frac{M_{ny}}{M_{nby}}\right)^{1.5} = 1.0 \qquad (2.6)$$

For composite columns, the Author have presented in Chapter 1 some of the most relevant information on the already published Analytical and Design Methods. Several different types of interaction equations were shown in Chapter 1.

In this chapter the Author will attempt to develop a mathematical equation that will represent the uniaxial load-moment interaction diagram of composite columns. Fig. 2.5 shows a typical load-moment interaction diagram of a column under axial load and uniaxial bending moment. For a given column cross section, position of longitudinal bars, steel ratio (including steel rebars and structural steel shape), and concrete and steel material properties, an interaction diagram following the points marked (+) in Fig. 2.5 can be generated.

A mathematical function that best fits the collection of interaction points for the compression and tension regions, can be used to represent an approximate closed-form solution of the load-moment uniaxial interaction diagram.

The Author developed an analytical technique to obtain the closest and most practical approximate mathematical function to represent the uniaxial interaction diagram and the load contour diagram.

The computer program "INTRDIAG" discussed in Chapter 1 and presented in Appendix A is proposed to obtain the interaction diagram for a composite column; It also includes a numerical technique based on the minimum least square error condensation procedure which provides not only the coefficient $\alpha$ for the interaction diagram but also the coefficient $\beta$ for the load contour diagram.

The mathematical function proposed by the Author can be written as follows:

$$\left(\frac{P_n - P_{nb}}{P_o - P_{nb}}\right)^{\alpha} + \left(\frac{M_n}{M_{nb}}\right)^{\beta} = 1 \qquad (2.7)$$

where the exponents $\alpha$ and $\beta$ are coefficients that vary according to the main parameters of the column cross section: column dimensions, material properties,

amount and location of reinforcement (steel rebars and structural steel shape), and clear cover. The coefficients $\alpha$ and $\beta$ are part of the generalized equation of failure surface and shown in Eq. 2.7. After an extensive study of different column cross sections and a vast combination of main column parameters, the Author found that the equation that best represents the interaction diagram of a square or rectangular composite column, uniformly and symmetrically reinforced along all sides, would be one with the exponents $\alpha$ and $\beta$ defined as follows: $\alpha$ varies, $1 \leq \alpha \leq 3$ and $\beta = 1$.

A computer program was developed as a part of this study, to estimate the values of the coefficient $\alpha$ based on the main column parameters. It is interesting to note that depending on these parameters, the overall interaction diagram can very well present different shapes for that portion of the values plotted above and below the balanced point.

For the special case of square composite column sections equally reinforced about the two main axis of bending, it is only necessary to estimate the coefficient $\alpha$ in one direction. For the typical square and rectangular composite column sections the overall interaction diagram may be represented by four different coefficients $\alpha$.

In summary, the "INTRDIAG" computer program is designed for the general case of a square or rectangular composite column section. The four different coefficients are defined as follows:

$\alpha_{cx}$ - define the compression-controlled region for bending about x - x.

$\alpha_{tx}$ - define the tension-controlled region for bending about x - x.

$\alpha_{cy}$ - define the compression-controlled region for bending about y - y.

$\alpha_{ty}$ - define the tension-controlled region for bending about y - y.

The Author's proposed equation for uniaxial bending and axial compressive load takes the following form:

$$\left(\frac{P_n - P_{nb}}{P_o - P_{nb}}\right)^{\alpha} + \left(\frac{M_n}{M_{nb}}\right) = 1 \qquad (2.8)$$

where $\alpha$ is the coefficient calculated by the computer program "INTRDIAG", for each particular column cross section under study. The other terms: $P_o$, $P_n$, $P_{nb}$, $M_n$, and $M_{nb}$ have been previously defined. A listing of the computer program "INTRDIAG" and a sample output showing the estimated values of $\alpha$ and $\beta$ are presented in Appendix A and B respectively. The special purpose computer program "INTRDIAG" is a very important tool that can be used to study a great number of composite cross sections.

## 2.5 Derivation of Generalized Interaction Equation of Failure Surface

A typical three dimensional failure surface of a rectangular composite column under axial load and biaxial bending is shown in Fig. 2.6, and the load contour diagram at a constant axial load is illustrated in Fig. 2.7. An expression to relate the relationship of the nominal bending moments $M_{nx}$ and $M_{ny}$ at a constant axial load $P_n$ has been presented by Bresler (19) and can be written as follows:

$$\left(\frac{M_{nx}}{M_{ox}}\right)^{\beta} + \left(\frac{M_{ny}}{M_{oy}}\right)^{\beta} = 1 \qquad (2.9)$$

For a rectangular composite column, one can find the interaction diagrams and the values of the balanced axial load and balanced bending moments for the two

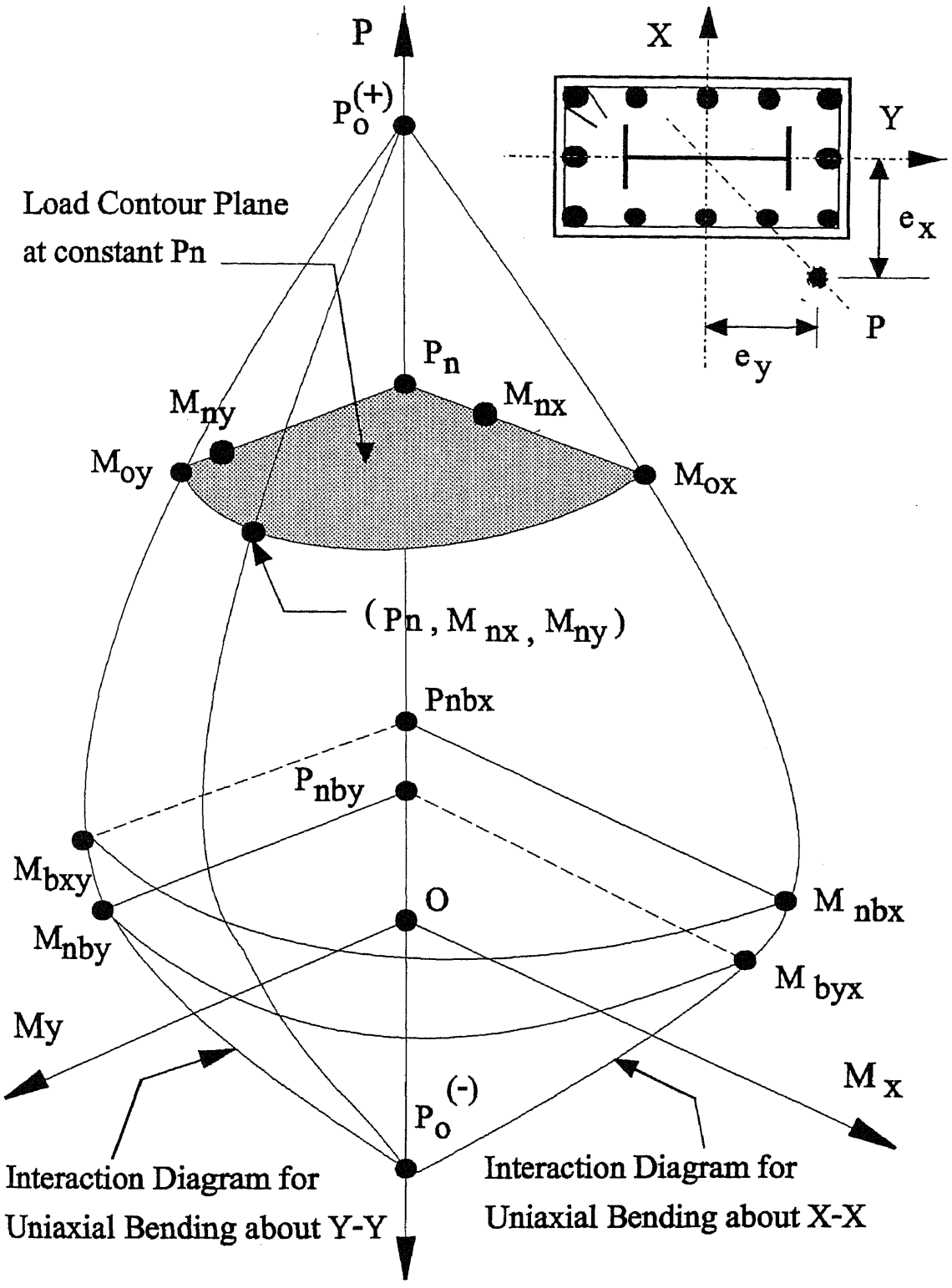


**Figure 2.6** Typical Three-Dimensional Failure Surface, P-Mx-My.

major axis. For a symmetrically reinforced composite column section, two cases may occur. Firstly $P_{nbx} > P_{nby}$, the balanced load for bending about X-X is greater than the balanced load for bending about Y-Y. Secondly, $P_{nby} > P_{nbx}$. The Author presents herein the analytical derivation of a generalized equation of failure surface for $P_{nbx} > P_{nby}$. From Fig. 2.7, the bending moments along the X axis are:

$$M_1 + M_2 = M_3 \tag{2.10}$$

From Fig. 2.7 the terms $M_1$, $M_2$, and $M_3$ are expressed in the following form:

$$M_{ox} + (M_{nbx} - M_{ox}) = M_{nbx} \tag{2.10a}$$

By dividing each term by $M_{nbx}$, one obtains;

$$\frac{M_{ox}}{M_{nbx}} + \left(\frac{M_{nbx} - M_{ox}}{M_{nbx}}\right) = 1 \tag{2.11}$$

which represents the basic identity equation in this derivation. From Fig. 2.8, for a given axial load $P_n$ and bending moment $M_{ox}$, the uniaxial interaction equation for bending about X axis proposed by the Author in Eq. 2.8 is used herein as follows:

$$\left(\frac{P_n - P_{nbx}}{P_o - P_{nbx}}\right)^{\alpha} + \frac{M_{ox}}{M_{nbx}} = 1 \tag{2.12}$$

Rearranging the terms above, one obtains;

$$\left(\frac{P_n - P_{nbx}}{P_o - P_{nbx}}\right)^{\alpha} = \left(\frac{M_{nbx} - M_{ox}}{M_{nbx}}\right) \tag{2.13}$$

The term on the right hand side of Eq. 2.13 is the same as the second term on the left side of Eq.2.11.

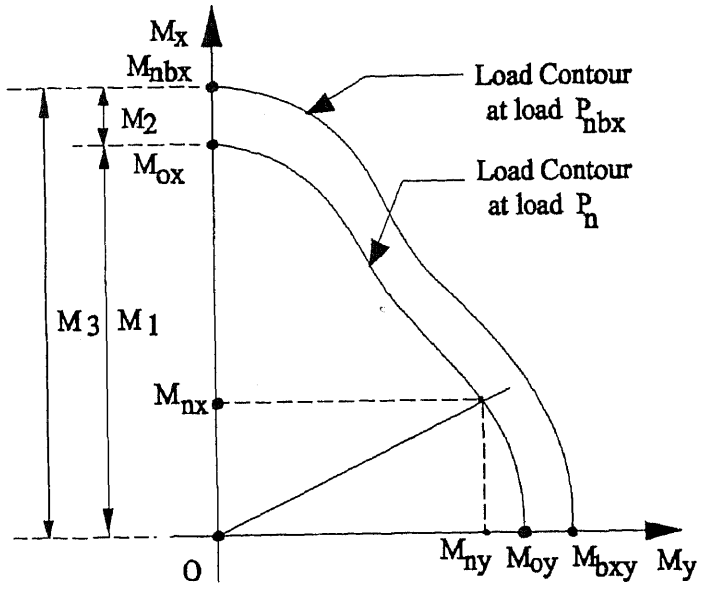


For : $P_{nbx} > P_{nby}$ and $P_n > P_{nbx}$

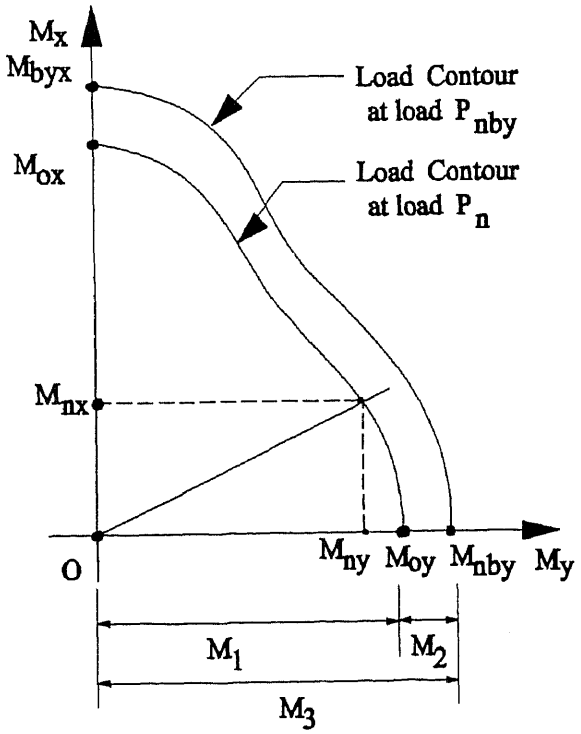


For : $P_{nby} > P_{nbx}$ and $P_n > P_{nby}$

**Figure 2.7** Typical Load-Contour Diagrams Mx - My at Axial Load $P_n$

Rewrite Eq. 2.11 as follows:

$$\left(\frac{M_{ox}}{M_{nbx}}\right) + \left(\frac{P_n - P_{nbx}}{P_o - P_{nbx}}\right)^{\alpha} = 1 \qquad (2.11a)$$

Next the Author expresses the first term on the left side of Eq. 2.11 in terms of the nominal bending moments $M_{nx}$ and $M_{ny}$.

Fig. 2.8 shows the uniaxial interaction diagrams for bending about X and Y, respectively. For a given axial load $P_n$, one can write two equations that represent the uniaxial load-bending moments relationship for the two major X and Y axis.

For uniaxial bending about X-X, the load-moment relationship is expressed in the following form:

$$\left(\frac{P_n - P_{nbx}}{P_o - P_{nbx}}\right)^{\alpha} + \left(\frac{M_{ox}}{M_{rx}}\right) = 1 \qquad (2.14)$$

and, for uniaxial bending about Y-Y, at the same value of the axial load $P_n$, the Author proposes the use of the following equation,

$$\left(\frac{P_n - P_{nbx}}{P_o - P_{nbx}}\right)^{\alpha} + \left(\frac{M_{oy}}{M_{ry}}\right) = 1 \qquad (2.15)$$

where $\alpha$ is the coefficient obtained from the uniaxial interaction diagram, and $M_{rx}$ and $M_{ry}$ are the reference nominal bending moments that take different values depending on the location of the nominal axial load $P_n$. They are written as follows:

For: $P_n > P_{nbx}$;

$$M_{rx} = M_{nbx}$$

$$M_{ry} = M_{bxy}$$

$$P_o = P_{o(+)}$$

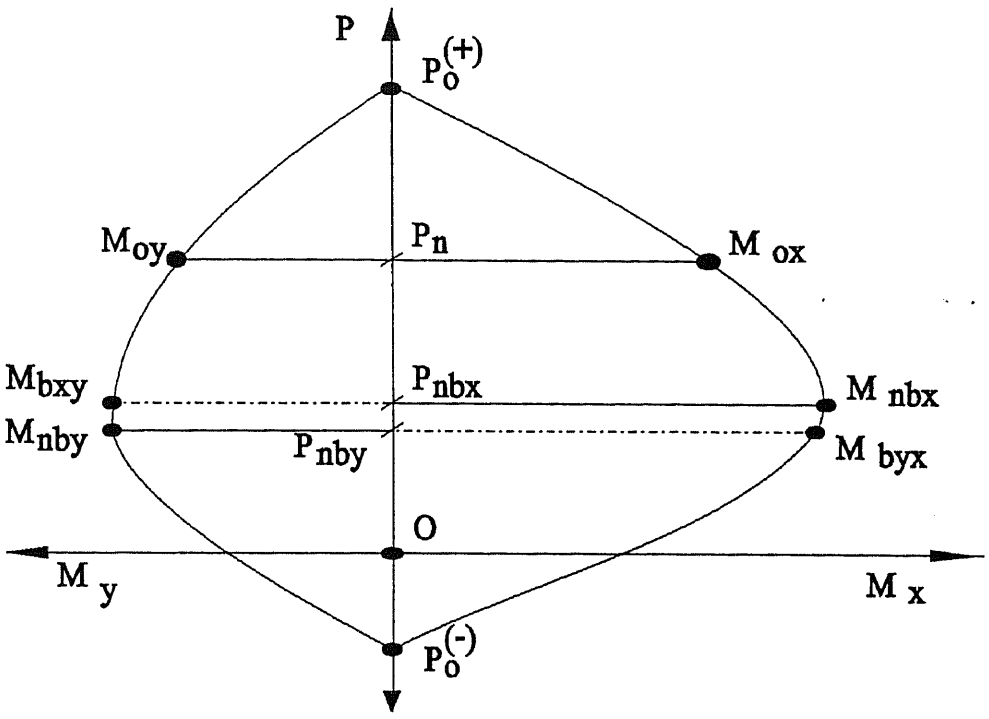


For $P_{nbx} > P_{nby}$ and $P_n > P_{nbx}$

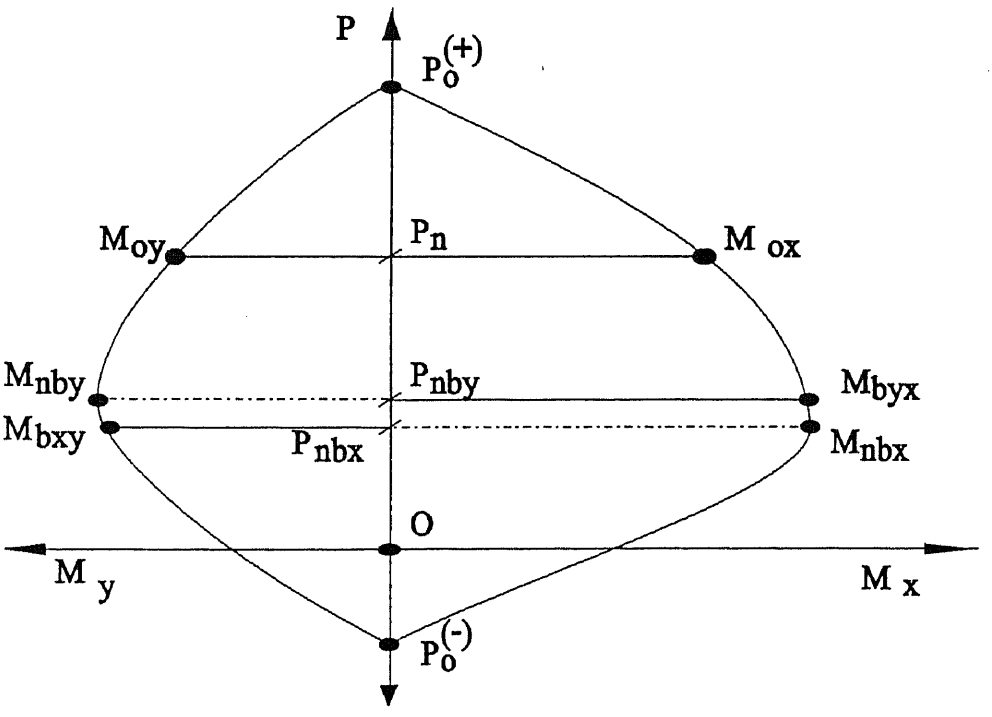


For $P_{nby} > P_{nbx}$ and $P_n > P_{nby}$

**Figure 2.8** Uniaxial P-Mx and P-My Interaction Diagrams

For: $P_{nby} \leq P_n \leq P_{nbx}$; $M_{rx} = M_{nbx}$

$M_{ry} = M_{nby}$

$P_o = P_{o(-)}$

For: $P_n < P_{nby}$; $M_{rx} = M_{byx}$

$M_{ry} = M_{nby}$

$P_o = P_{o(-)}$

By comparing Equations 2.14 and 2.15, the moment ratio equation is:

$$\left(\frac{M_{ox}}{M_{rx}}\right) = \left(\frac{M_{oy}}{M_{ry}}\right) \tag{2.16}$$

An extensive study of the moment ratio in Eq. 2.16 was carried out by the Author, the results showed that the proposed equation could be used with a very significant degree of accuracy. Eq. 2.16 can be rearranged as follows:

$$M_{oy} = M_{ry}\left(\frac{M_{ox}}{M_{rx}}\right) \tag{2.16a}$$

By substituting Eq. 2.16a into Eq. 2.9, one obtains;

$$\left(\frac{M_{nx}}{M_{ox}}\right)^{\beta} + \left(\frac{M_{ny}}{M_{ry}}\,\frac{M_{rx}}{M_{ox}}\right)^{\beta} = 1 \tag{2.17}$$

Rearranging, one obtains;

$$\left(\frac{M_{nx}}{M_{ox}}\right)^{\beta} + \left(\frac{1}{M_{ox}}\right)^{\beta}\left(\frac{M_{ny} \cdot M_{rx}}{M_{ry}}\right)^{\beta} = 1 \tag{2.17a}$$

$$(M_{nx})^{\beta} + \left(\frac{M_{ny}\ M_{rx}}{M_{ry}}\right)^{\beta} = (M_{ox})^{\beta} \tag{2.17b}$$

$$M_{ox} = \left[ (M_{nx})^{\beta} + \left(\frac{M_{ny}\ M_{rx}}{M_{ry}}\right)^{\beta} \right]^{1/\beta} \tag{2.17c}$$

Dividing each term of Eq. 2.17c by $M_{nbx}$, one obtains;

$$\left(\frac{M_{ox}}{M_{nbx}}\right) = \left[ \left(\frac{M_{nx}}{M_{nbx}}\right)^{\beta} + \left(\frac{M_{ny}}{M_{ry}}\ \frac{M_{rx}}{M_{nbx}}\right)^{\beta} \right]^{1/\beta} \tag{2.18}$$

by substituting the left term of Eq. 2.13 and the right term of Eq. 2.18 into Eq. 2.11, one finally obtains the desired equation of failure surface:

$$\left(\frac{P_n - P_{nbx}}{P_o - P_{nbx}}\right)^{\alpha} + \left[ \left(\frac{M_{nx}}{M_{nbx}}\right)^{\beta} + \left(\frac{M_{ny}}{M_{ry}}\ \frac{M_{rx}}{M_{nbx}}\right)^{\beta} \right]^{1/\beta} = 1 \tag{2.19}$$

A similar derivation can be done for the case when $P_{nby} > P_{nbx}$, and then one can obtain the following equation:

$$\left(\frac{P_n - P_{nby}}{P_o - P_{nby}}\right)^{\alpha} + \left[ \left(\frac{M_{nx}}{M_{rx}}\ \frac{M_{ry}}{M_{nby}}\right)^{\beta} + \left(\frac{M_{ny}}{M_{nby}}\right)^{\beta} \right]^{1/\beta} = 1 \tag{2.20}$$

For this case the following values of $M_{rx}$ and $M_{ry}$ are used:

For: $P_n > P_{nby}$;

$$M_{rx} = M_{byx}$$

$$M_{ry} = M_{nby}$$

$$P_o = P_{o(+)}$$

For: $P_{nbx} < P_n < P_{nby}$; $M_{rx} = M_{nbx}$

$M_{ry} = M_{nby}$

$P_o = P_{o(-)}$

For: $P_n < P_{nbx}$; $M_{rx} = M_{nbx}$

$M_{ry} = M_{bxy}$

$P_o = P_{o(-)}$

A generalized expression of the derived equations of failure surface can be written as follows:

$$\left(\frac{P_n - P_{nb}}{P_o - P_{nb}}\right)^{\alpha} + \left[\left(\frac{M_{nx}}{M_{nb}} M_{fx}\right)^{\beta} + \left(\frac{M_{ny}}{M_{nb}} M_{fy}\right)^{\beta}\right]^{1/\beta} = 1 \qquad (2.21)$$

where:

For: $P_{nbx} > P_{nby}$; $P_{nb} = P_{nbx}$

$M_{nb} = M_{nbx}$

$M_{fx} = 1$

$M_{fy} = M_{rx}/M_{ry}$

For: $P_{nby} > P_{nbx}$; $P_{nb} = P_{nby}$

$M_{nb} = M_{nby}$

$M_{fx} = M_{ry}/M_{rx}$

$M_{fy} = 1$

It is interesting to note that for a symmetrical square composite column equally reinforced about two major axes,

$P_{nb} = P_{nbx} = P_{nby}$; and $M_{rx} = M_{ry} = M_{nbx} = M_{nby}$

and Eq. 2.20 and 2.21 can be reduced to the following equation:

$$\left(\frac{P_n - P_{nb}}{P_o - P_{nb}}\right)^{\alpha} + \left[\left(\frac{M_{nx}}{M_{nbx}}\right)^{\beta} + \left(\frac{M_{ny}}{M_{nby}}\right)^{\beta}\right]^{1/\beta} = 1 \qquad (2.22)$$

The above equation can be further simplified to obtain the appropriate equation for the uniaxial bending case either about X-X or Y-Y, by dropping the proper term in the generalized equation. In which case one obtains the basic interaction equation for uniaxial bending, Eq. 2.8.

The Author proposes herein a single coefficient $\alpha$ in the proposed design equation for a composite column section by using the lowest of the two values defining the compression controlled or tension controlled regions. Depending on the location of the nominal axial load $P_n$, one uses a lower bound solution, which is conservative and practical to find.

For a given composite column under axial load and biaxial bending moments, the coefficient $\beta$ in the generalized Eq. 2.21 varies with the magnitude of the axial load $P_n$.

Several investigators have studied the variation of the coefficient $\beta$. Hsu (85) in his proposed equation of failure surface for reinforced concrete columns recommended a value of $\beta = 1.5$.

Amirthanandan and Rangan (4) discussed the strength of biaxially loaded reinforced concrete columns and presented an equation adopted by The British Standard BS8220 (21):

with $\beta$ ranging as follows: $1.0 < \beta < 2.0$

$$\beta = 0.7 + 1.7\left(\frac{P_n}{0.6\ P_o}\right) \tag{2.23}$$

An analytical formulation for $\beta$, was presented by Gowens (77), where the value of $\beta$ was taken as a function of the number of bars, the reinforcement index $q = A_{st}f_y/bhf'_c$ and the uniaxial load $P_n$.

Towfighi (209) developed a condensation procedure, that led to the tabulation of axial load, moment capacities and the $\beta$ values with minimum error. He used a regression analysis and the exact points of the load-contour plane and load-moment interaction diagrams.

The Author developed a computational technique similar to the one used by Towfighi (209) to obtain the appropriate value of the coefficient $\beta$ for a number of horizontal planes of load contour diagram at constant axial load $P_n$.

This computational technique was incorporated in the computer program "INTRDIAG". The computer program can evaluate the coefficient $\beta$, which has a significant variation, depending on the level of the axial load, the material properties and the ratio of steel reinforcement to the gross area of concrete.

The Author also used the proposed generalized equation of failure surface, Eq. 2.21, to study the analysis and design of reinforced concrete columns. The results are presented in details in Appendix D.

It can be found that the Author's proposed equation of failure surface provides very accurate results in predicting the failure load of uniaxially and biaxially loaded reinforced concrete columns with axial loads. The Author also studies herein the validity of Eq. 2.21 for the analysis and design of short and slender composite

columns under axial loads and in combination with uniaxial bending moments about the strong-axis, weak-axis or biaxial bending moments.

The results are presented and discussed in section 2.6, where an extensive verification of the Generalized interaction equation of failure surface is investigated. The values of the coefficients $\alpha$ and $\beta$ are calculated using of the Author's special-purpose computer program "INTRDIAG' which generates all the main column parameters required to process the generalized interaction equation of failure surface.

The Author also uses the MathCAD® software (138), to create a mathematical document to manipulate the variables involved in the calculations of the uniaxial and biaxial equations of failure surface.

A sample of the MathCAD documents used to calculate the uniaxial and biaxial interaction equations are presented in Appendix C.

In order to account for the effects of the slenderness of the columns under study, the Author makes use of the Moment Magnification Factor Method as it is outlined in the ACI Building Code ACI 318-89 Rev. 92 (1), Sections 10.11.5 to 10.11.7. Thus the proposed Generalized interaction Equation of Failure Surface Eq. 2.21. is modified in the following form:

$$\left(\frac{P_n - P_{nb}}{P_o - P_{nb}}\right)^{\alpha} + \left[\left(\delta_{mfx}\frac{M_{nx}}{M_{nb}}M_{fx}\right)^{\beta} + \left(\delta_{mfy}\frac{M_{ny}}{M_{nb}}M_{fy}\right)^{\beta}\right]^{1/\beta} = 1 \qquad (2.24)$$

$$\delta_{mfx} = \frac{C_{mx}}{\left(1 - \frac{P_n}{P_{crx}}\right)} \quad ; \quad \delta_{mfy} = \frac{C_{my}}{\left(1 - \frac{P_n}{P_{cry}}\right)} \qquad (2.25)$$

where $\delta_{mfx}$ and $\delta_{mfy}$ are the moment magnification factors with respect to the x and y axis, respectively. $P_{crx}$ and $P_{cry}$ are the critical Euler Loads about x and y axis.

## 2.6 Verification of Generalized Interaction Equation of Failure Surface

The analysis and design of composite columns under biaxial bending and axial loads can be approached by either one of the already described methods of the ACI and the AISC.

The proposed interaction equation of failure surface, Eq. 2.24 is herein used to study its applicability and accuracy in predicting the failure loads of short and slender composite columns in uniaxial and biaxial bending and axial loads.

Johnston (106) in Chapter Nineteen on Composite Columns of the 3rd Edition of the Guide to Stability Design Criteria for Metal Structures, discussed the design rules of the American Standards for composite columns.

There he presented design tables with the ultimate axial force for a 16-in. concrete-encased wide flange steel shape $F_y$=36 ksi under different values of eccentricity with the axial load applied at different points the composite cross section.

The strength interaction diagrams for different 12 in. steel shape sections encased in 3,000 psi, and 16x16 concrete section were also plotted to illustrate the variation of the shape of the interaction diagrams for different steel to concrete ratios.

The Author used the "INTRDIAG" computer program to generate the interaction diagrams about the x and y axis and obtained the design parameters required to solve the equation of failure surface for different eccentricities.

The calculated values of the Ultimate Axial Load using the Author's interaction equation, Eq. 2.8 (for short columns in combined uniaxial bending and axial load) are presented as $P_u$ (NJIT) in Tables 2.1 and 2.2.

The comparative ratio of the estimated axial load value using the ACI procedure and the Author's calculated value are presented in Tables 2.1 and 2.3 to illustrate the accuracy of the Author's proposed interaction equation.

It is noted that for low eccentricity values and for cross sections with lower steel to concrete ratio, the calculated ultimate axial loads from the two different procedures show very good agreement between each other.

Considerable differences are found for the composite sections under higher eccentricity values and higher steel to concrete ratio.

This difference can be attributed to the fact that the Author has modeled the steel shape section in a very large number of small elements, which provides a more accurate calculation of the contribution of the steel section to the stresses, strains, forces and moments used in the equilibrium equations for the different positions of the neutral axis.

Still for all practical purposes the obtained values of the ultimate axial load using the Author's interaction equation provides a very accurate way to predict the failure load of composite columns within acceptable limits of reliability.

The material properties of concrete and steel shape sections, the interaction diagram, coefficients $\alpha$, axial load and bending moment parameters for two major axes of bending for the composite columns studied by Johnston (106) and labeled SSLC1 to SSLC13 are presented in Tables 2.3 and 2.4.

**Table 2.1** Design Table for 16-in. composite column with bending about strong-axis

| Col. No. (bxd) | Steel Shape ρ % | Axial Forces; Pu (kips); Pu(ACI) Pu(NJIT) Pu(ACI)/Pu(NJIT) | | | | | | |
|---|---|---|---|---|---|---|---|---|
| | | Strong-axisbending; eccentricity $e_y$ (inches) | | | | | | |
| in.xin. | $A_s/A_g$ | 1.4 | 2.0 | 4.0 | 6.0 | 8.0 | 10.0 | 20.0 |
| SSLC1 | W12x27 | 530 | 482 | 353 | 269 | 209 | 170 | 87 |
| 16x16 | 2.9 | 515.9 | 473.3 | 360.3 | 280.5 | 221.9 | 173 | 81.6 |
| | | 1.027 | 1.018 | 0.979 | 0.959 | 0.942 | 0.983 | 1.066 |
| SSLC2 | W12x31 | 553 | 504 | 370 | 284 | 222 | 181 | 93 |
| 16x16 | 3.4 | 539.5 | 495.7 | 379.5 | 297.4 | 237.7 | 189.7 | 91.6 |
| | | 1.025 | 1.017 | 0.975 | 0.955 | 0.934 | 0.954 | 1.015 |
| SSLC3 | W12x36 | 582 | 531 | 392 | 303 | 239 | 196 | 102 |
| 16x16 | 4.0 | 568.2 | 522.3 | 402.1 | 318.0 | 257.3 | 210.3 | 104.8 |
| | | 1.024 | 1.017 | 0.975 | 0.953 | 0.929 | 0.932 | 0.973 |
| SSLC4 | W12x40 | 587 | 536 | 397 | 308 | 244 | 200 | 103 |
| 16x16 | 4.6 | 587.9 | 539.9 | 415.8 | 330.25 | 268.9 | 222.9 | 101.8 |
| | | 0.998 | 0.993 | 0.955 | 0.933 | 0.907 | 0.897 | 1.012 |
| SSLC5 | W12x45 | 616 | 562 | 418 | 326 | 261 | 214 | 111 |
| 16x16 | 5.2 | 615.2 | 564.9 | 434.7 | 345.4 | 282.1 | 235.6 | 113.4 |
| | | 1.001 | 0.995 | 0.962 | 0.944 | 0.925 | 0.908 | 0.979 |
| SSLC6 | W12x50 | 644 | 588 | 439 | 343 | 277 | 228 | 119 |
| 16x16 | 5.7 | 644.9 | 592.8 | 457.9 | 365.2 | 299.4 | 250.9 | 124.1 |
| | | 0.999 | 0.992 | 0.959 | 0.939 | 0.925 | 0.909 | 0.959 |
| SSLC7 | W12x53 | 647 | 591 | 444 | 349 | 284 | 234 | 122 |
| 16x16 | 6.1 | 660.2 | 606.9 | 469.9 | 376.4 | 310.0 | 261.2 | 131.4 |
| | | 0.98 | 0.973 | 0.945 | 0.927 | 0.916 | 0.896 | 0.928 |
| SSLC8 | W12x58 | 669 | 612 | 460 | 362 | 296 | 244 | 128 |
| 16x16 | 6.6 | 686.8 | 631.3 | 489.9 | 394.1 | 326.2 | 276.1 | 142.5 |
| | | 0.975 | 0.969 | 0.939 | 0.919 | 0.907 | 0.884 | 0.898 |

**Table 2.1** Design Table for 16-in. composite column with bending about strong-axis

| Col. No. (bxd) | Steel Shape ρ % | Axial Forces; Pu (kips); Pu(ACI) Pu(NJIT) Pu(ACI)/Pu(NJIT) | | | | | | |
|---|---|---|---|---|---|---|---|---|
| | | Strong-axis bending; eccentricity $e_y$ (inches) | | | | | | |
| in.xin. | $A_s/A_g$ | 1.4 | 2.0 | 4.0 | 6.0 | 8.0 | 10.0 | 20.0 |
| SSLC9 | W12x65 | 702 | 645 | 489 | 388 | 320 | 269 | 140 |
| | | 726.9 | 668.9 | 520.7 | 419.9 | 348.4 | 295.7 | 156.8 |
| 16x16 | 7.5 | 0.966 | 0.964 | 0.939 | 0.924 | 0.918 | 0.91 | 0.893 |
| SSLC10 | W12x72 | 737 | 678 | 516 | 411 | 340 | 287 | 151 |
| | | 763.3 | 702.0 | 547.0 | 442.5 | 368.5 | 313.9 | 171.2 |
| 16x16 | 8.2 | 0.966 | 0.966 | 0.943 | 0.929 | 0.923 | 0.914 | 0.882 |
| SSLC11 | W12x79 | 773 | 712 | 544 | 434 | 359 | 305 | 162 |
| | | 804.2 | 740.3 | 578.4 | 468.9 | 391.3 | 333.9 | 185.4 |
| 16x16 | 9.1 | 0.961 | 0.962 | 0.941 | 0.926 | 0.917 | 0.915 | 0.874 |
| SSLC12 | W12x85 | 801 | 738 | 565 | 451 | 374 | 319 | 170 |
| | | 851.4 | 784.6 | 614.8 | 499.6 | 417.7 | 357.1 | 200.3 |
| 16x16 | 10.0 | 0.941 | 0.941 | 0.919 | 0.903 | 0.895 | 0.893 | 0.845 |
| SSLC13 | W12x92 | 840 | 776 | 596 | 477 | 397 | 339 | 182 |
| | | 898.7 | 827.8 | 649.3 | 529.1 | 443.7 | 380.5 | 216.6 |
| 16x16 | 11.0 | 0.935 | 0.937 | 0.918 | 0.902 | 0.895 | 0.891 | 0.890 |

Fig. 2.9 presents a plot of all the interaction diagrams obtained using the "INTRDIAG" computer program for the composite sections studied by Johnston (106). Another composite column section used by the Author for verification, is an 18"x18" concrete section reinforced with a W12x120 steel shape and 8 reinforcing steel bars (6-#4 and 2-#9). This composite column was studied by Roik and Bergman (176) and is labeled "RKBG" in Tables 2.3 and 2.4. The composite section studied by Roik and Bergman (176) was presented in Chapter Ten on Composite Columns of the 4th edition of the Guide to Stability Design Criteria for Metal Structures, Edited by Galambos (80).

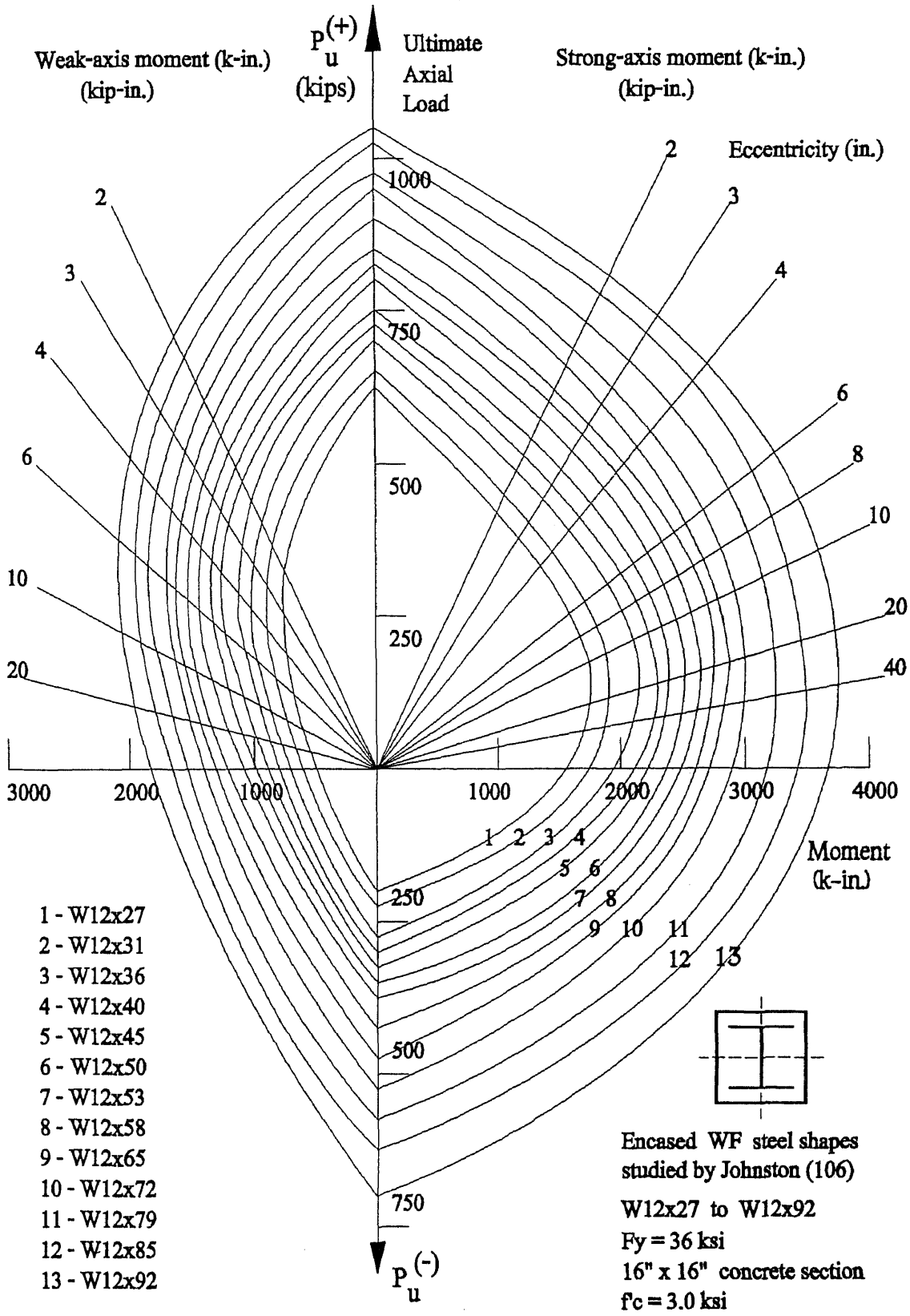


**Figure 2.9** Strength interaction diagrams for concrete-encased 12WF's shapes

**Table 2.2** Design Table for 16-in. composite column with bending about weak axis

| Col. No. (bxd) | Steel Shape ρ % | Axial Forces; Pu (kips); Pu(ACI) Pu(NJIT) Pu(ACI)/Pu(NJIT) | | | | | | |
|---|---|---|---|---|---|---|---|---|
| | | Weak-axis bending; eccentricity $e_x$ (inches) | | | | | | |
| in.xin. | $A_s/A_g$ | 1.4 | 2.0 | 4.0 | 6.0 | 8.0 | 10.0 | 20.0 |
| SSLC1 | W12x27 | 520 | 442 | 246 | 161 | 118 | 93 | 45 |
| | | 506.2 | 443.0 | 255.7 | 169.0 | 124.3 | 97.5 | 45.6 |
| 16x16 | 2.9 | 1.027 | 0.998 | 0.962 | 0.953 | 0.949 | 0.954 | 0.987 |
| SSLC2 | W12x31 | 541 | 452 | 248 | 163 | 120 | 95 | 46 |
| | | 510.5 | 441.7 | 259.8 | 173.8 | 129.9 | 103.3 | 50.1 |
| 16x16 | 3.4 | 1.059 | 1.023 | 0.955 | 0.938 | 0.924 | 0.920 | 0.918 |
| SSLC3 | W12x36 | 562 | 464 | 252 | 166 | 123 | 97 | 47 |
| | | 531.7 | 457.3 | 267.2 | 178.8 | 133.8 | 106.6 | 52.15 |
| 16x16 | 4.0 | 1.057 | 1.015 | 0.943 | 0.928 | 0.919 | 0.910 | 0.901 |
| SSLC4 | W12x40 | 570 | 476 | 268 | 179 | 132 | 104 | 50 |
| | | 563.8 | 491.5 | 297.5 | 200.1 | 150.0 | 119.7 | 58.73 |
| 16x16 | 4.6 | 1.011 | 0.968 | 0.9 | 0.895 | 0.88 | 0.869 | 0.851 |
| SSLC5 | W12x45 | 591 | 489 | 275 | 184 | 136 | 108 | 52 |
| | | 585.9 | 509.2 | 307.3 | 206.9 | 155.1 | 123.9 | 61.2 |
| 16x16 | 5.2 | 1.009 | 0.96 | 0.895 | 0.889 | 0.877 | 0.872 | 0.85 |
| SSLC6 | W12x50 | 611 | 502 | 281 | 188 | 140 | 111 | 54 |
| | | 608.6 | 527.7 | 317.8 | 214.1 | 160.6 | 128.3 | 63.56 |
| 16x16 | 5.7 | 1.004 | 0.951 | 0.885 | 0.878 | 0.872 | 0.865 | 0.849 |
| SSLC7 | W12x53 | 624 | 524 | 311 | 213 | 159 | 126 | 62 |
| | | 634.4 | 559.7 | 359.8 | 247.3 | 185.9 | 148.6 | 73.47 |
| 16x16 | 6.1 | 0.984 | 0.936 | 0.865 | 0.853 | 0.845 | 0.835 | 0.83 |
| SSLC8 | W12x58 | 641 | 535 | 315 | 213 | 159 | 126 | 62 |
| | | 658.1 | 580.3 | 374.6 | 258.5 | 194.5 | 155.6 | 77.05 |
| 16x16 | 6.6 | 0.974 | 0.922 | 0.841 | 0.824 | 0.815 | 0.810 | 0.805 |

**Table 2.2** Design Table for 16-in. composite column with bending about weak-axis

| Col. No. (bxd) | Steel Shape ρ % | Axial Forces; Pu (kips); Pu(ACI) Pu(NJIT) Pu(ACI)/Pu(NJIT) | | | | | | |
|---|---|---|---|---|---|---|---|---|
| | | Weak-axis bending; eccentricity $e_x$ (inches) | | | | | | |
| in.xin. | $A_s/A_g$ | 1.4 | 2.0 | 4.0 | 6.0 | 8.0 | 10.0 | 20.0 |
| SSLC9 | W12x65 | 684 | 586 | 367 | 254 | 191 | 152 | 74 |
| | | 700.3 | 624.6 | 425.2 | 303.2 | 230.6 | 184.9 | 91.6 |
| 16x16 | 7.5 | 0.977 | 0.938 | 0.863 | 0.838 | 0.828 | 0.822 | 0.808 |
| SSLC10 | W12x72 | 716 | 610 | 382 | 265 | 200 | 159 | 78 |
| | | 736.7 | 656.9 | 448.1 | 320.3 | 244.1 | 195.8 | 97.53 |
| 16x16 | 8.2 | 0.972 | 0.929 | 0.852 | 0.827 | 0.819 | 0.812 | 0.799 |
| SSLC11 | W12x79 | 748 | 636 | 397 | 277 | 209 | 167 | 82 |
| | | 770.4 | 686.4 | 469.3 | 337.1 | 257.6 | 206.9 | 103.3 |
| 16x16 | 9.1 | 0.971 | 0.927 | 0.846 | 0.822 | 0.795 | 0.783 | 0.778 |
| SSLC12 | W12x85 | 772 | 654 | 408 | 284 | 214 | 171 | 85 |
| | | 812.7 | 724 | 495.9 | 357.1 | 273.4 | 219.9 | 109.9 |
| 16x16 | 10.0 | 0.949 | 0.903 | 0.822 | 0.795 | 0.783 | 0.778 | 0.773 |
| SSLC13 | W12x92 | 807 | 683 | 427 | 298 | 226 | 181 | 89 |
| | | 857.0 | 763.4 | 524.7 | 379.8 | 291.8 | 235.1 | 117.7 |
| 16x16 | 11.0 | 0.942 | 0.895 | 0.814 | 0.785 | 0.775 | 0.77 | 0.76 |

Roik and Bergman (80) calculated the points to plot the simplified strength interaction diagram for the composite section as described in the reference above. He assumed a plastic stress distribution for both concrete and steel, which obviously produced the values of axial load and bending moments higher than the ones calculated by the ACI.

Tables 2.3 and 2.4 present some of the composite column cross sections selected by the Author to verify the equation of failure surface.

The column parameters, material properties and calculated interaction diagram coefficients $\alpha$ for Roik and Bergman composite column section labeled "RKBG" are presented in Tables 2.3 and 2.4.

Fig. 2.10 shows the plot of the interaction diagram obtained using the "INTRDIAG" computer program and the proposed uniaxial interaction equation Eq. 2.8. The plot of Fig. 2.10 is presented together with interaction diagram lines obtained by four other different methods.

Stevens (195) conducted tests on concrete-encased composite columns reinforced with a British Standard Universal steel I-beam. They were 180 inches long with various eccentricities about the weak axis, ranging from 0 to 8 inches. The composite column specimen was labeled "STV" in Tables 2.3 and 2.4.

The Author modeled the Stevens's type of composite column described above by using the "INTRDIAG" computer program. The design column parameters and coefficients required were attained to process the uniaxial interaction equation Eq. 2.8. The values are shown in Tables 2.3 and 2.4. The composite cross section, input parameters and sample calculations done with the MathCad software are presented in Fig. 2.11.

The Author used a modified form of the ACI 10-4 equation to calculate the value of stiffness parameter $EI_m$ for the composite cross section and in turn the critical axial load $P_{cr}$. Details of the calculations are presented in Fig. 2.11.

A coefficient of 3.75 was used to determine the $EI_c$ value in the calculation of the total cross section moment of inertia. This value was found to provide the most approximate ultimate load to the experimental failure load for the specimens tested by Stevens.

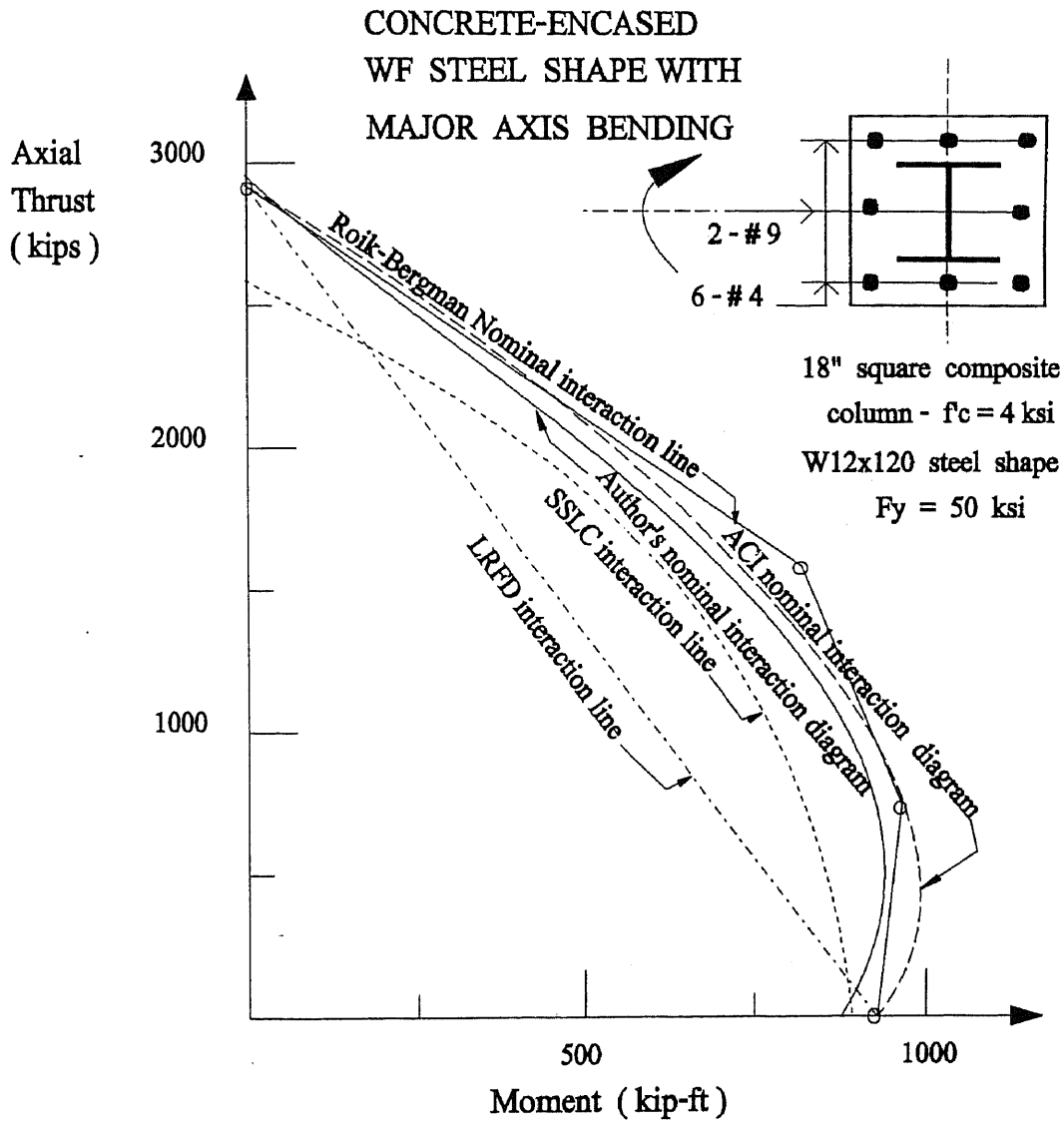


**Figure 2.10** Comparative strength interaction diagrams for 18x18 composite column

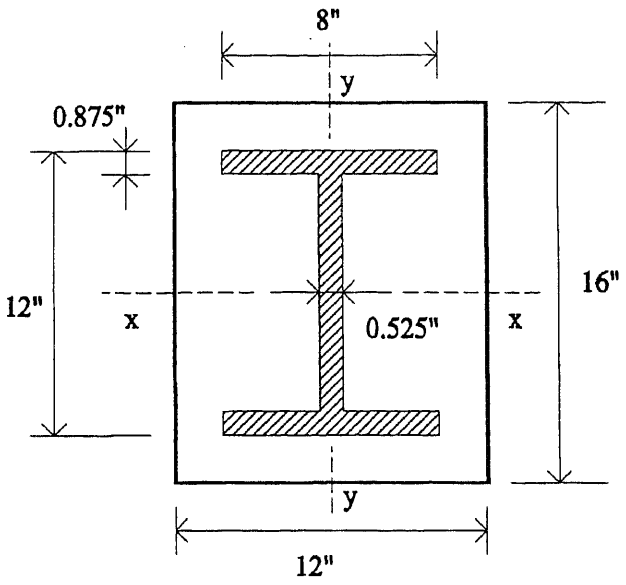


Concrete-encased British Standard 65 lb. Universal I-beam with bending about the weak-axis

MATHCAD FILENAME : COMPEQ.MCD

$\alpha := 2.75$ $\quad M_{nb} := 1559.476$

$e := 8$ $\quad P_{cr} := 1537.145$

$P_o := 1139.052$ $\quad P_n := 1$

$P_{nb} := 122.948$

GIVEN :

$$\left[\frac{P_n - P_{nb}}{P_o - P_{nb}}\right]^{\alpha} + \frac{e P_n P_{cr}}{M_{nb}(P_{cr} - P_n)} = 1$$

$P_n := \text{Find}(P_n)$

$P_n = 168.52$

Column Length = 180 "

f 'c = 3,000 psi

$Po^{(+)} = 1139.052$ kips

$Po^{(-)} = -698.925$ kips

Pnbx = 209.31 kips

Mnbx = 4074.593 kip-inch.

enby = 19.467 inch.

Pnby = 122.948 kips

Mnby = 1559.476 kip-inch.

enbx = 12.684 inch.

$\alpha_{cx} = 1.35$ $\quad \alpha_{cy} = 2.75$

$\alpha_{tx} = 1.55$ $\quad \alpha_{ty} = 2.65$

$A_t = 19.38\ in^2$ $\quad \rho = 10.1\ \%$

$A_g = 192\ in^2$ $\quad \beta_d = 0$

$E_c = 57{,}000\,(f'c)^{1/2} = 3.122 \times 10^6$ psi

$I_g = 2304\ in^4$

$E_s = 29 \times 10^6$ psi

$I_t = 74.79\ in^4$

$r_m = 2.3$ (weak-axis); ACI Eq. 10-13

$$EI_m = \frac{Ec\,Ig / \alpha_{EI}}{(1+\beta_d)} + E_s I_t$$

$\alpha_{EI} = 3.75$

$EI_m = 4087.067\ kip\text{-}in^2$

$P_{cr} = \pi^2 EI_m / (kl)^2 = 1244.992$ kips

**Figure 2.11** Steven's composite column dimensions and design parameters

**Table 2.3** Composite section Material Properties and Interaction Coefficients $\alpha$

| Col. No. | Steel Shape | $\rho$ % | $F_y$ (ksi) | $f_c'$ (ksi) | $\alpha_{cx}$ | $\alpha_{tx}$ | $\alpha_{cy}$ | $\alpha_{ty}$ |
|---|---|---|---|---|---|---|---|---|
| SSLC1 | W12x27 | 2.9 | 36 | 3 | 1.55 | 1.7 | 2.8 | 3.0 |
| SSLC2 | W12x31 | 3.4 | 36 | 3 | 1.55 | 1.7 | 3.0 | 3.0 |
| SSLC3 | W12x36 | 4.0 | 36 | 3 | 1.5 | 1.7 | 3.0 | 3.0 |
| SSLC4 | W12x40 | 4.6 | 36 | 3 | 1.45 | 1.65 | 3.0 | 2.9 |
| SSLC5 | W12x45 | 5.2 | 36 | 3 | 1.5 | 1.55 | 3.0 | 3.0 |
| SSLC6 | W12x50 | 5.7 | 36 | 3 | 1.5 | 1.55 | 3.0 | 3.0 |
| SSLC7 | W12x53 | 6.1 | 36 | 3 | 1.45 | 1.5 | 2.7 | 2.7 |
| SSLC8 | W12x58 | 6.6 | 36 | 3 | 1.4 | 1.45 | 2.65 | 2.7 |
| SSLC9 | W12x65 | 7.5 | 36 | 3 | 1.4 | 1.45 | 2.35 | 2.35 |
| SSLC10 | W12x72 | 8.2 | 36 | 3 | 1.35 | 1.45 | 2.35 | 2.55 |
| SSLC11 | W12x79 | 9.1 | 36 | 3 | 1.35 | 1.45 | 2.3 | 2.6 |
| SSLC12 | W12x85 | 10.0 | 36 | 3 | 1.35 | 1.45 | 2.3 | 2.6 |
| SSLC13 | W12x92 | 11.0 | 36 | 3 | 1.3 | 1.45 | 2.25 | 2.6 |
| RKBG | W12X12 | 11.9 | 50 | 4 | 1.25 | 1.55 | 2.2 | 2.3 |
| STV | I-65 lbs | 10.1 | 36 | 3 | 1.35 | 1.55 | 2.75 | 2.65 |
| AISC1 | W10X54 | 4.88 | 36 | 8 | 1.9 | 1.3 | 2.1 | 2.35 |
| AISC3 | W8X48 | 5.51 | 50 | 3.5 | 1.7 | 1.4 | 2.5 | 2.35 |
| AISC4 | W10X77 | 6.98 | 50 | 5 | 1.6 | 1.35 | 2.65 | 2.3 |
| A | W6X15 | 5.23 | 33 | 5.75 | 1.65 | 1.45 | 2.25 | 2.05 |
| B | W6X15 | 5.23 | 33 | 5.50 | 1.6 | 1.45 | 2.20 | 2.10 |
| C | W6X15 | 5.23 | 33 | 5.75 | 1.65 | 1.45 | 2.25 | 2.05 |
| D | W6X15 | 5.23 | 33 | 6.1 | 1.7 | 1.45 | 2.35 | 2.05 |
| E | W6X15 | 5.23 | 33 | 5.75 | 1.65 | 1.45 | 2.25 | 2.05 |
| F | W6X15 | 5.23 | 33 | 6.1 | 1.7 | 1.45 | 2.35 | 2.05 |
| G | W6X15 | 5.23 | 33 | 5.3 | 1.6 | 1.5 | 2.20 | 2.10 |
| H | W6X15 | 5.23 | 33 | 5.75 | 1.65 | 1.45 | 2.25 | 2.05 |
| I | W6X15 | 5.23 | 33 | 6.26 | 1.7 | 1.45 | 2.4 | 2.0 |
| MC1 | WF1X1 | 2.89 | 50 | 5.33 | 1.9 | 1.75 | 2.0 | 2.1 |
| MC2 | WF1X1 | 2.89 | 50 | 4.49 | 1.75 | 1.75 | 1.85 | 2.15 |
| MC3 | WF1X1 | 2.89 | 50 | 3.75 | 1.85 | 1.55 | 1.75 | 2.15 |
| MC4 | WF1X1 | 2.89 | 50 | 3.99 | 1.85 | 1.55 | 1.75 | 2.15 |

**Table 2.4** Composite section Axial Load and Bending Moment parameters

| Col. No. | L (in) | Sect. (bxd) | $P_o^{(+)}$ (kips) | $P_o^{(-)}$ (kips) | $P_{nbx}$ (kips) | $M_{nbx}$ (k-in) | $P_{nby}$ (kips) | $M_{nby}$ (k-in) |
|---|---|---|---|---|---|---|---|---|
| SSLC1 | 0 | 16x16 | 907.11 | -273.7 | 312.0 | 2537.1 | 372.3 | 1461.1 |
| SSLC2 | 0 | 16x16 | 945.54 | -315.0 | 312.4 | 2737.1 | 269.4 | 1489.7 |
| SSLC3 | 0 | 16x16 | 997.16 | -370.6 | 312.9 | 3008.6 | 268.1 | 1532.7 |
| SSLC4 | 0 | 16x16 | 1037.2 | -413.7 | 311.3 | 3188.1 | 265.3 | 1715.3 |
| SSLC5 | 0 | 16x16 | 1085.7 | -465.8 | 278.3 | 3432.9 | 263.9 | 1773.3 |
| SSLC6 | 0 | 16x16 | 1134.9 | -518.9 | 277.2 | 3693.2 | 262.5 | 1835.4 |
| SSLC7 | 0 | 16x16 | 1164.4 | -550.5 | 275.5 | 3889.0 | 261.9 | 2124. |
| SSLC8 | 0 | 16x16 | 1213.9 | -603.9 | 273.9 | 4179.7 | 260.4 | 2222.9 |
| SSLC9 | 0 | 16x16 | 1281.9 | -677.1 | 272.0 | 4539.9 | 258.4 | 2640.7 |
| SSLC10 | 0 | 16x16 | 1350.9 | -750.9 | 270.3 | 4916.1 | 256.6 | 2798.3 |
| SSLC11 | 0 | 16x16 | 1419.5 | -825.1 | 268.5 | 5298.2 | 254.8 | 2958.1 |
| SSLC12 | 0 | 16x16 | 1498.9 | -910.6 | 266.5 | 5744.7 | 252.8 | 3144.9 |
| SSLC13 | 0 | 16x16 | 1586.8 | -1005.2 | 263.9 | 6266.9 | 250.4 | 3365.7 |
| RKBG | 0 | 18X18 | 2907.1 | -1934.9 | 476.9 | 11379.4 | 102.9 | 6416.1 |
| STV | 180 | 12x16 | 1139.1 | -698.9 | 209.3 | 4074.6 | 122.9 | 1559.5 |
| AISC1 | 372 | 18X18 | 2827.3 | -751.7 | 723.1 | 7288.4 | 1104.1 | 6068.9 |
| AISC3 | 144 | 16x16 | 1555.1 | -842.1 | 217.7 | 4177.4 | 139.5 | 2823.2 |
| AISC4 | 132 | 18X18 | 2192.3 | -1310.9 | 424.6 | 8216.8 | 290.2 | 5408.9 |
| A | 72 | 10X10 | 623.0 | -192.4 | 204.2 | 1007.2 | 214.9 | 807.8 |
| B | 72 | 10X10 | 604.9 | -192.4 | 199.0 | 985.1 | 209.6 | 785.6 |
| C | 72 | 10X10 | 623.0 | -192.4 | 204.2 | 1007.2 | 214.9 | 807.8 |
| D | 144 | 10X10 | 554.3 | -192.4 | 211.1 | 1037.3 | 221.8 | 838.1 |
| E | 144 | 10X10 | 535.1 | -192.4 | 204.2 | 1007.2 | 214.9 | 807.8 |
| F | 144 | 10X10 | 554.3 | -192.4 | 211.1 | 1037.3 | 221.8 | 838.1 |
| G | 288 | 10X10 | 282.1 | -192.4 | 194.6 | 967.1 | 205.1 | 767.5 |
| H | 288 | 10X10 | 290.6 | -192.4 | 204.2 | 1007.2 | 214.9 | 807.8 |
| I | 288 | 10X10 | 299.1 | -192.4 | 214.0 | 1050.8 | 224.8 | 851.6 |
| MC1 | 32 | 2.5X2.5 | 46.6 | -29.2 | 9.57 | 18.14 | 9.51 | 16.14 |
| MC2 | 48 | 2.5X2.5 | 35.6 | -29.2 | 8.46 | 17.02 | 8.30 | 14.98 |
| MC3 | 48 | 2.5X2.5 | 33.6 | -29.2 | 4.33 | 15.97 | 7.03 | 13.90 |
| MC4 | 48 | 2.5X2.5 | 36.4 | -29.2 | 4.80 | 16.33 | 7.54 | 14.27 |

The comparative values of the ultimate loads for the Stevens's test specimens calculated by different design methods, including the interaction equation proposed by the Author, are presented in Table 2.5. It is noted from the results obtained by the Author's proposed equation of failure surface of axial load and uniaxial bending moments predict well the experimental ultimate load for these composite columns.

**Table 2.5** Comparative Ultimate Loads for column specimens tested by Stevens

| Test No. | $e_x$ inch. | $P_t$ Test Load (kips) | ACI-71 Ultimate Load (kips) | Ultimate Load by Basu (kips) | $P_{NJIT}$ Load by Eq. 2.8 (kips) | $P_t/P_{NJIT}$ |
|---|---|---|---|---|---|---|
| FE1 | 0 | 986 | 1007 | 922 | 1052.0 | 0.9373 |
| FE2 | 0 | 1055 | 1045 | 943 | 1052.0 | 1.0029 |
| FE3 | 1 | 672 | 556 | 545 | 639.0 | 1.0516 |
| FE4 | 2 | 486 | 393 | 386 | 464.4 | 1.0465 |
| FE5 | 2 | 515 | 435 | 420 | 464.4 | 1.1089 |
| FE6 | 3 | 361 | 331 | 321 | 361.86 | 0.9976 |
| FE7 | 4 | 296 | 272 | 265 | 295.18 | 1.0028 |
| FE8 | 5 | 262 | 235 | 230 | 248.77 | 1.0532 |
| FE9 | 6 | 231 | 200 | 198 | 214.78 | 1.0755 |
| FE10 | 7 | 199 | 187 | 183 | 188.88 | 1.0536 |
| FE11 | 8 | 168 | 167 | 162 | 168.52 | 0.9969 |
| $P_t / P_{NJIT}$ (average) = 1.0297 | | | | | | |

The proposed Equation of Failure Surface, Eq. 2.21 is also applicable to the case of axial load alone. In this case two terms that include the bending moments can be eliminated, and the equation becomes $P_n = P_o$, where $P_o$ is the axial load capacity of the composite column. The $P_o$ value varies according to the slenderness ratio, the lateral bracing conditions, the end conditions, and the material properties of the cross section.

As it was noted earlier in Chapter 1, the ACI provisions do not provide an equation to calculate directly the allowable axial load capacity of a composite column

as a function of its length and cross sectional dimensions. The LRFD Steel Design Manual, First Edition (13) does provide a set of equations that allows one to investigate into the axial load capacity of composite columns. In the following the Author utilizes of the LRFD equations (E2-1 to E2-4, I2-1 and I2-2) to verify the results obtained for some of the examples presented herein. The Author also explores the possibility to incorporate a set of applicable equations into a format that is satisfactory to the ACI design requirements for composite columns.

Example 1 on page 4-56 of the LRFD (13) presents the tabulated value of $\phi P_n$=1,033 kips axial load capacity for a composite section of a W10x54 steel shape encased in an 18in.x18in. concrete section reinforced with 4-#8 longitudinal rebars. The composite column section under study has a wide flange steel shape of $F_y$=36 ksi, concrete of $f_c'$= 8 ksi and rebar Grade 60 with an effective length with respect to its minor axis of 16 ft and 31 ft with respect to its major axis.

The following calculations based on the LRFD equations are presented as below: $P_d$ = Design strength of an axially loaded composite column = $\phi_c P_n$

$$\phi = 0.85 \; ; \; P_n = A_s F_{cr} \text{ LRFD Eq. E2-1}$$

$\lambda_c = (Kl/r_m\pi)(F_{my}/E_m)^{1/2}$; K = 1, l = 31'x12 = 372", $A_g$ = 18x18 = 324 $in^2$

$r_m$ = 0.3x18 = 5.4" ; $F_{my} = F_y + c_1F_{yr}(A_r/A_s) + c_2f_c'(A_c/A_s)$; $c_1$ = 0.7, $c_2$ = 0.6

$F_y$ = 36 ksi; $F_{yr}$ = 60 ksi; $f_c'$ = 8 ksi; $A_r$ = 3.16 $in^2$; $A_s$ = 15.8 $in^2$

$A_c = A_g - A_s - A_{sr}$ = 18x18 - 15.8 - 3.16 = 305.04 $in^2$

$F_{my}$ = 36 + 0.7x60x(3.16/15.8) + 0.6x8x(305.04/15.8) = 137.07 ksi

$E_m = E_s + c_3E_c(A_c/A_s)$; $c_3$ = 0.2, $E_s$ = 29,000 ksi, $E_c = 57{,}000(f_c')^{1/2}$ = 5098.24 ksi

$E_m$ = 29000 + 0.2x5098.24x(307.04/15.8) = 48,838.61 ksi

$\lambda_m = (1.0x372/5.4x\pi)(137.07/48{,}685)^{1/2} = 1.17 < 1.5$; $\lambda m = \lambda_c^2$

$F_{cr} = (0.658^{\lambda m})F_{my} = (0.658^{1.37})$x137.07 = 77.25 ksi; $P_n$ = 15.8x77.25 kips

$P_n$ = 1220.55 kips; $\phi_c P_n$ = 0.85x1220.55 = 1,037 kips as compared to 1,033 kips, OK.

The following equations to calculate the design axial load strength $\phi P_n$ of composite columns under compression are proposed by the Author:

$$P_d = \phi P_n \quad ; \quad P_n = A_g F_{mcr} \tag{2.26}$$

$$for \ \lambda_{mc} \le 1.5 \ ; \ F_{mcr} = \left( 0.658^{\lambda_{mc}^2} \right) F_{mc} \tag{2.27}$$

$$for \ \lambda_{mc} > 1.5 \ ; \ F_{mcr} = \left[ \frac{0.877}{\lambda_{mc}^2} \right] F_{mc} \tag{2.28}$$

$$F_{mc} = k_1 f_c' (A_c / A_g) + k_2 F_{yr} (A_{sr} / A_g) + k_3 F_y (A_s / A_g) \tag{2.29}$$

$$E_{mc} = E_{sr} ( A_{sr} / A_g ) + E_s ( A_s / A_g ) + k_4 E_c ( A_c / A_g ) \tag{2.30}$$

$$\lambda_{mc} = \frac{K l}{r_{mc} \pi} \sqrt{\frac{F_{mc}}{E_{mc}}} \tag{2.31}$$

$$r_{mc} = \sqrt{\frac{E_c I_g / 2.5 + E_s I_t + E_{sr} I_{sr}}{E_c A_g / 2.5 + E_s A_t + E_{sr} A_{sr}}} \quad ; \quad r_{mc} \le 0.3 \ b \tag{2.32}$$

where b = the least dimension of the column cross section, and

$k_1$ = 0.60, $k_2$ = 0.80, $k_3$ = 0.80 and $k_4$ = 1/5.

The Author incorporates the concept used by the LRFD into an ACI format to estimate the design axial strength of a compressively loaded composite column. The idea is to develop a compatible common ground between the AISC and the ACI design procedures for composite columns.

Calculations:

$I_g = 18x18^3/12 = 8748$ in.$^4$, $I_{sr} = 4x0.05 + 4x0.79x7^2 = 155.04$ in.$^4$

$$r_{mc} = \sqrt{\frac{5.0982x10^6x8748/2.5 + 29x10^6x303 + 30x10^6x155.04}{5.0982x10^6x324/2.5 + 29x10^6x15.8 + 30x10^6x3.16}} = 5.076'' < 5.4''$$

$F_{mc} = 0.60x8x(305.04/324) + 0.80x60x(3.16/324) + 0.80x36x(15.8/324)$

$F_{mc} = 4.5191 + 0.46815 + 1.4045 = 6.3918$ ksi

$E_{mc} = 29{,}000x3.16/324+29{,}000x15.8/324+0.2x5{,}098.24x(305.04/324) = 2{,}657$ ksi

$\lambda_{mc} = (1.0x31x12)/(5.076x\pi)x(6.3918/2{,}657)^{1/2} = 1.144 < 1.5$

$F_{mcr} = (0.658^{1.3087})x6.3918 = 3.6955$ ksi, $P_{nc} = 324x3.6955 = 1{,}197.33$ kips

$\phi P_{nc} = 0.85x1{,}197.33 = 1{,}017.73$ kips as compared to 1,033 kips by LRFD.

The tabulated value by the LRFD, Example 1 page 4-56, for the axial design strength of the composite section studied above is $\phi P_n = 1{,}033$ kips. Note that the excellent result is attained using the proposed equations.

The Author has found that a reasonable formula to calculate the allowable axial load capacity for a slender composite column can be found in the main design parameters of the ACI Building Code. The results obtained by the equation presented above agree very well with the ones obtained by the similar LRFD equations. They also compare very well with the tabulated values of the axial design strength for the composite columns given in Chapter 4 of the LRFD (13).

To verify the validity of the interaction equation of failure surface for the case of combined axial compression and uniaxial bending, the Author performs the calculations for the composite section presented in Example No. 3 of the LRFD (13), page 4-57 and labeled "AISC3" in Tables 2.3 and 2.4.

It is required to design a composite encased W shape column to resist a factored axial load $P_u$ of 200 kips and a factored moment $M_u$ about the X-X axis of 240 kip-ft. The unsupported length of the column is 12 ft., $F_y$ = 50 ksi, $f_c'$ = 3.5 ksi and $C_m$ = 1.0. The loads are of a first order analysis and there is no lateral translation of column ends. A composite column with a W8x48, 4-#7 and 16in.x16in. concrete encasement is selected for design check purposes.

To determine the slenderness ratio, $kl/r_m$, a modified ACI Eq. 10-11 is used:

$EI_m = E_c I_g/2.5 + E_s I_t + E_{sr} I_{sr}$

$E_c = 57{,}000(3{,}500)^{1/2} = 3.3722\text{x}10^6$ psi; $E_s$ = 29,000 ksi; $E_{sr}$ = 30,000 ksi

$I_g = 16\text{x}16^3/12 = 5461.33$ in.$^4$; $I_{t(x\text{-}x)} = 184$ in.$^4$; $I_{sr} = 86.515$ in.$^4$

$EI_m = 3.3722\text{x}10^6\text{x}5461.33/2.5 + 29\text{x}10^6\text{x}184 + 30\text{x}10^6\text{x}86.515 = 1.5298\text{x}10^{10}$ lb-in$^2$

The above calculated value of $EI_m$ includes the steel reinforcing bars. The following $EI_m$ is calculated without including the steel bars.

$EI_m = 3.3722\text{x}10^6\text{x}5461.33/2.5 + 29\text{x}10^6\text{x}184 = 1.27027\text{x}10^{10}$ lb-in$^2$

$P_{mcr} = \pi^2 EI_m/L^2 = \pi^2\text{x}1.27027\text{x}10^{10}/(12\text{x}12)^2 = 6{,}046$ kips

The column parameters obtained from the "INTRDIAG" computer program are presented in Tables 2.3 and 2.4. The Author's proposed uniaxial interaction equation of failure surface is solved by using the MathCad Software.

$$\left(\frac{P_n - 217.71}{1555.06 - 217.71}\right)^{1.7} + \frac{(14.4)\ P_n\ (6{,}046)}{(\ 6{,}046 - P_n\ )} = 1$$

The nominal axial load value obtained from the above equation is $P_n$ = 275.547 kips, which can be expressed in terms of ultimate load by using the resistance factor of the ACI for columns, $\phi$ = 0.7.

Thus the ultimate axial load and bending moment values obtained for the composite column of the Example No. 3 of the AISC are:

$P_u$ = 0.7x275.547 = 192.88 kips and $M_u$ = 192.88x14.4=2,777.5 kip-in.= 231.5 kip-ft.

Note that the values given by the AISC are $P_u$ = 200 kips and $M_u$ = 248 kip-ft.

Therefore the solution obtained by the Author is very accurate and still conservative.

Example No. 4 of the LRFD (13) on page 4-58 presents the calculations for a short composite column with a large axial load in relation to the uniaxial bending moment about the strong axis.

It is required to calculate a composite encased wide flange shape column to resist a factored axial load of 1,100 kips and factored moment of 200 kip-ft.

The column has un unsupported length of 11 ft. and Cm =0.85 and sidesway is prevented. The column parameters calculated using the "INTRDIAG" computer program and the Author's equation are shown in Tables 2.3 and 2.4.

The calculated $P_{cr}$ = 15,462.9 kips.

The LRFD (13) suggests to try a W10x77 W-shape $F_y$ = 50 ksi and encased in an 18in.x18in. concrete section $f_c'$ = 5 ksi and reinforced with 4-#8 reinforcing bars Grade 60.

By using the Author's proposed uniaxial interaction equation of failure surface and solving for the nominal axial load we obtain:

$$\left(\frac{P_n - 424.62}{2192.3 - 424.62}\right)^{1.6} + \frac{(0.85)\ (2.182)\ P_n\ (15{,}462.9)}{8216.85\ (15{,}462.9 - P_n)} \approx 1$$

which yields $P_n$ = 1,605 kips.

The ultimate design strength axial load is thus,

$P_u = \phi P_n$ = 0.7x1,605 = 1,123.5 kips. Compared to the required factored axial load of 1,100 kips by the LRFD, the Author's method achieves a very acceptable result.

Next, the proposed equation of Failure Surface, Eq. 2.21, is used to calculate the ultimate strength of nine pin-ended composite columns in biaxial bending. The columns were tested and reported by Virdi and Dowling (222) and are labeled "A" to "I" in Tables 2.3 to 2.7.

The four pinned-ended composite sections in biaxial bending were tested by the Author at NJIT as part of his experimental work for this dissertation.

The composite column specimens dimensions, material properties and design parameters for the columns described above are presented in Tables 2.3, 2.4 and 2.6. The calculated failure loads and the comparative ratio of test load to calculated load for the same column specimens are presented in Table 2.7.

The purpose of the calculations presented herein is to prove the validity of the Author's proposed equation of Failure Surface in predicting the ultimate strength of biaxially loaded composite columns with axial compressive loads. Appropriate load and materials factors can be incorporated to obtain a reasonable design equation.

The results presented show an excellent agreement of the predicted ultimate loads using the Author's proposed equation of failure surface with the failure loads obtained by experimental testings of composite columns.

The composite column specimens tested by Virdi and Dowling (222) and by the Author at NJIT are modeled and processed using the computational method presented in Chapter 3. The results show the validity of the computational method in predicting the failure loads.

**Table 2.6** Virdi-Dowling and NJIT eccentricities and column design parameters

| Col. | $e_x$ (in.) | $e_y$ (in.) | $M_{byx}$ k-in | $M_{bxy}$ k-in | $e_{byx}$ in. | $e_{bxy}$ in. |
|---|---|---|---|---|---|---|
| A | 2.5 | 1.45 | 1005.12 | 803.73 | 4.677 | 3.935 |
| B | 5.0 | 2.9 | 982.54 | 781.59 | 4.688 | 3.928 |
| C | 7.5 | 4.35 | 1005.12 | 803.73 | 4.677 | 3.935 |
| D | 2.5 | 1.45 | 1035.68 | 833.91 | 4.669 | 3.951 |
| E | 5.0 | 2.9 | 1005.12 | 803.73 | 4.677 | 3.935 |
| F | 7.5 | 4.35 | 1035.68 | 833.91 | 4.669 | 3.951 |
| G | 2.5 | 1.45 | 964.50 | 764.21 | 4.701 | 3.927 |
| H | 5.0 | 2.9 | 1005.12 | 803.73 | 4.677 | 3.935 |
| I | 7.5 | 4.35 | 1049.16 | 847.37 | 4.667 | 3.959 |
| MC1 | 1.5 | 1.5 | 18.14 | 16.14 | 1.907 | 1.687 |
| MC2 | 1.25 | 1.25 | 17.01 | 14.98 | 2.051 | 1.77 |
| MC3 | 1 | 1 | 15.87 | 13.65 | 3.151 | 2.257 |
| MC4 | 1.5 | 1.5 | 16.23 | 14.02 | 2.924 | 2.152 |

Other important information related to the overall behavior of slender composite columns, such as lateral column displacements, stresses, strains, forces, cracking, nonlinear behavior and stability of the composite column are undertaken in Chapters 3 and 4.

Morino, Matsui and Watanabe (147) tested some 40 composite column specimens in biaxial bending and compression. The Author investigated and examined the applicability of the proposed equation of failure surface to predict the failure load of these column specimens.

The composite column specimens dimensions, material properties and design parameters for the Morino et al. specimens are labeled "A4" to "D4" and "A8" to "D8" in Tables 2.8, 2.9 and 2.10 and their details are shown schematically in Fig. 2.12.

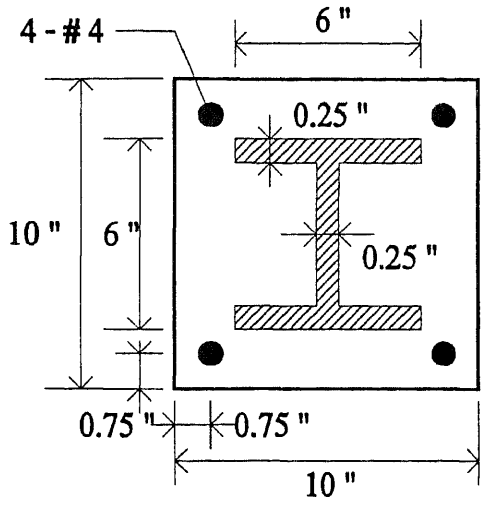


Virdi and Dowling Composite Section

W 6 x 15 Steel shape

$F_y$ = 33 ksi

$f_y$ = 60 ksi

$f'_c$ = 6.26 ksi (max.)

$E_s$ = 29,000 ksi

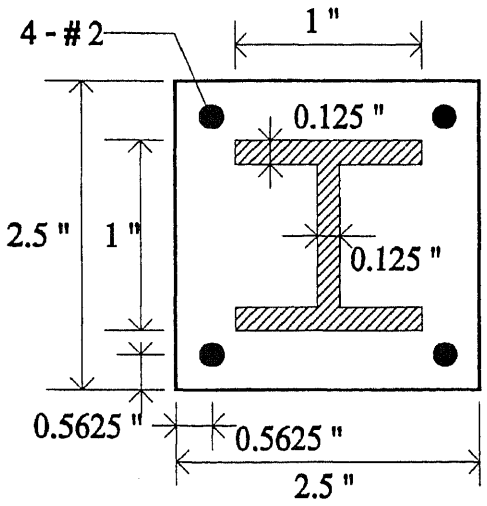


NJIT Composite section

WF 1 x 1 Steel shape

$F_y$ = 50 ksi

$f_y$ = 60 ksi

$f'_c$ = 5.33 ksi (max.)

$E_s$ = 29,000 ksi

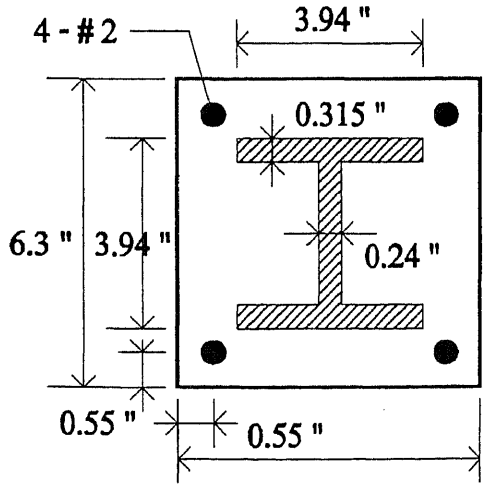


Morino, Matsui and Watanabe Composite section

WF 4 x 4 Steel shape

$F_y$ = 50 ksi

$f_y$ = 60 ksi

$f'_c$ = 4.874 ksi (max.)

$E_s$ = 29,000 ksi

**Figure 2.12** Composite section dimensions and properties for testing specimens

The computer program "INTRDIAG" was used to calculate the coefficients $\alpha_{cx}$, $\alpha_{tx}$, $\alpha_{cy}$ and $\alpha_{ty}$. The values are presented in Table 2.8.

The column parameters of axial load, bending moment and eccentricity values at the balanced point were also calculated using the "INTRDIAG" computer program and their values are presented in Tables 2.9 and 2.10.

**Table 2.7** Virdi-Dowling and NJIT composite column section comparative results

| Col. | $\alpha$ | $\beta$ | $P_{cr}$ | $P_{test}$ | $P_{NJIT}$ | $P_t/P_{NJIT}$ | $P_{anal.}$ |
|---|---|---|---|---|---|---|---|
| A | 2.25 | 1.75 | 4083 | 282.25 | 279.07 | 1.011 | 298.64 |
| B | 2.15 | 1.95 | 4023 | 145.61 | 138.7 | 1.049 | 153.78 |
| C | 2.05 | 2 | 4083 | 106.4 | 88.95 | 1.196 | 103.06 |
| D | 1.75 | 2.1 | 1041 | 208.33 | 196.55 | 1.059 | 240.57 |
| E | 2.05 | 2.5 | 1021 | 128.81 | 128.2 | 1.005 | 130.46 |
| F | 2.05 | 2.5 | 1041 | 94.08 | 87.2 | 1.078 | 91.14 |
| G | 2.1 | 2 | 248.1 | 150.09 | 148.70 | 1.009 | 118.36 |
| H | 1.65 | 1.6 | 255.2 | 79.52 | 79.42 | 1.001 | 84.58 |
| I | 1.85 | 2 | 262.7 | 66.08 | 64.4 | 1.026 | 64.36 |
| MC1 | 1.8 | 1.35 | 88.97 | 6.33 | 6.26 | 1.011 | 6.8 |
| MC2 | 1.6 | 1.2 | 37.63 | 5.59 | 5.94 | 0.941 | 6.154 |
| MC3 | 1.6 | 1.2 | 35.78 | 6.53 | 6.74 | 0.969 | 6.706 |
| MC4 | 1.6 | 1.2 | 36.41 | 4.05 | 4.85 | 0.835 | 4.829 |

$P_{anal.}$ = Analytical load computed by Virdi and Dowling (222).
Average $P_{test}/P_{NJIT}$ = 1.015
StandardDeviation = 0.0786

Again, the Author used the MathCad software to process the Equation of Failure Surface, Eq. 2.24. All the previous column parameters calculated by the "INTRDIAG" computer program are incorporated into the interaction equation together with the applied eccentricities of the axial load.

**Table 2.8** Morino et al. specimens dimensions, material properties and parameters

| Col. No. | Steel Shape | ρ % | $F_y$ (ksi) | $f_c'$ (ksi) | $\alpha_{cx}$ | $\alpha_{tx}$ | $\alpha_{cy}$ | $\alpha_{ty}$ |
|---|---|---|---|---|---|---|---|---|
| A4 | WF4X4 | 10.28 | 50 | 3.06 | 1.35 | 1.4 | 2.3 | 2.7 |
| B4 | WF4X4 | 10.28 | 50 | 3.39 | 1.35 | 1.4 | 2.3 | 2.65 |
| C4 | WF4X4 | 10.28 | 50 | 3.38 | 1.35 | 1.4 | 2.3 | 2.65 |
| D4 | WF4X4 | 10.28 | 50 | 3.08 | 1.35 | 1.4 | 2.3 | 2.7 |
| A8 | WF4X4 | 10.28 | 50 | 4.87 | 1.45 | 1.4 | 2.55 | 2.5 |
| B8 | WF4X4 | 10.28 | 50 | 4.83 | 1.45 | 1.4 | 2.55 | 2.5 |
| C8 | WF4X4 | 10.28 | 50 | 3.57 | 1.35 | 1.4 | 2.3 | 2.65 |
| D8 | WF4X4 | 10.28 | 50 | 3.32 | 1.35 | 1.4 | 2.3 | 2.65 |

**Table 2.9** Morino et al. specimens axial load and bending moment parameters

| Col. No. | L (in.) | Sect. (bxd) | $P_o^{(+)}$ (kips) | $P_o^{(-)}$ (kips) | $P_{nbx}$ (kips) | $M_{nbx}$ (k-in) | $P_{nby}$ (kips) | $M_{nby}$ (k-in) |
|---|---|---|---|---|---|---|---|---|
| A4 | 37.8 | 6.3X6.3 | 261.88 | -175.83 | 37.75 | 342.05 | 19.43 | 190.74 |
| B4 | 94.5 | 6.3x6.3 | 229.79 | -175.83 | 42.02 | 349.90 | 23.61 | 198.83 |
| C4 | 141.75 | 6.3X6.3 | 178.92 | -175.83 | 41.84 | 349.57 | 23.43 | 198.49 |
| D4 | 189 | 6.3x6.3 | 123.90 | -175.83 | 37.94 | 342.41 | 19.62 | 191.10 |
| A8 | 37.8 | 6.3x6.3 | 314.85 | -175.83 | 57.70 | 382.83 | 39.78 | 232.96 |
| B8 | 94.5 | 6.3x6.3 | 261.29 | -175.83 | 57.34 | 381.92 | 39.41 | 232.04 |
| C8 | 141.75 | 6.3x6.3 | 181.66 | -175.83 | 44.24 | 353.99 | 25.78 | 203.05 |
| D8 | 189 | 6.3x6.3 | 125.84 | -175.83 | 41.10 | 348.21 | 22.71 | 197.08 |

The MathCad document developed to solve the interaction equation of failure surface for uniaxial bending and biaxial bending in combination with axial compressive or tensile loads is presented in Appendix C.

**Table 2.10** Morino et al. critical load, moments and eccentricities design parameters

| Col. | $P_{cr}$(kips) | $M_{byx}$k-in | $M_{bxy}$k-in | $e_{byx}$in. | $e_{bxy}$in. |
|---|---|---|---|---|---|
| A4 | 2068 | 331.07 | 185.16 | 17.039 | 4.905 |
| B4 | 340.58 | 338.89 | 193.16 | 14.357 | 4.597 |
| C4 | 151.19 | 338.57 | 192.82 | 14.45 | 4.609 |
| D4 | 82.83 | 331.42 | 185.51 | 16.895 | 4.890 |
| A8 | 2368 | 372.31 | 228.76 | 9.359 | 3.965 |
| B8 | 377.76 | 371.40 | 227.83 | 9.423 | 3.973 |
| C8 | 153.54 | 342.97 | 197.33 | 13.303 | 4.461 |
| D8 | 84.63 | 337.21 | 191.43 | 14.852 | 4.658 |

The slender coefficients to account for the second order effects, the stiffness parameters to define the end column boundary conditions and the effective column length along each major axis of bending to calculate the nominal ultimate axial load capacity of the composite column are also considered. The coefficient $\beta$ that defines the shape of the load contour diagram at each axial load level is also calculated by the "INTRDIAG" computer program and is found to be a nonlinear function of the ratio of ultimate load to axial controlling load.

The calculated failure loads, the applicable interaction coefficients $\alpha$ and $\beta$ and the comparative ratio of the test load to the calculated load by the Author's proposed equation of failure surface for the column specimens tested by Morino, Matsui and Watanabe are presented in Table 2.11. The computer program "INTRDIAG" provides for every cross section under study a tabulation of the approximate values of coefficient $\beta$ that defines the shape of the load-contour diagram at a constant value of the axial load $P_n$.

The coefficient β is found to be the value that best fits the correlation of the calculated nominal biaxial bending moments at different inclined planes to the neutral axis and at a given value of the nominal axial load.

**Table 2.11** Morino et al. specimens eccentricities and comparative failure loads

| Col. | α | β | $e_x$ in. | $e_y$ in. | $P_{test}$ | $P_{NJIT}$ | $P_t/P_{NJIT}$ |
|---|---|---|---|---|---|---|---|
| A4-00 | 2.3 | - | 1.5748 | 0 | 112.34 | 104.61 | 1.074 |
| A4-30 | 2.05 | 1.5 | 1.3638 | 0.7874 | 115.38 | 105.69 | 1.092 |
| A4-45 | 1.85 | 1.5 | 1.1136 | 1.1136 | 116.59 | 110.27 | 1.057 |
| A4-60 | 1.6 | 1.5 | 0.7874 | 1.3638 | 117.81 | 117.48 | 1.003 |
| A4-90 | 1.35 | - | 0 | 1.5748 | 166.39 | 136.15 | 1.222 |
| B4-00 | 2.3 | - | 1.5748 | 0 | 83.38 | 87.49 | 0.953 |
| B4-30 | 2.05 | 1.45 | 1.3638 | 0.7874 | 88.23 | 87.96 | 1.003 |
| B4-45 | 1.85 | 1.45 | 1.1136 | 1.1136 | 87.56 | 91.23 | 0.960 |
| B4-60 | 1.6 | 1.45 | 0.7874 | 1.3638 | 98.07 | 96.25 | 1.019 |
| B4-90 | 1.35 | - | 0 | 1.5748 | 113.16 | 111.01 | 1.019 |
| C4-00 | 2.3 | - | 1.5748 | 0 | 61.71 | 66.71 | 0.925 |
| C4-30 | 2.05 | 1.45 | 1.3638 | 0.7874 | 63.72 | 67.33 | 0.946 |
| C4-45 | 1.85 | 1.45 | 1.1136 | 1.1136 | 68.42 | 69.54 | 0.984 |
| C4-60 | 1.6 | 1.45 | 0.7874 | 1.3638 | 76.47 | 72.91 | 1.049 |
| C4-90 | 1.35 | - | 0 | 1.5748 | 92.57 | 82.08 | 1.128 |
| D4-00 | 2.3 | - | 1.5748 | 0 | 46.38 | 46.25 | 1.003 |
| D4-30 | 2.05 | 1.45 | 1.3638 | 0.7874 | 45.16 | 48.87 | 0.924 |
| D4-45 | 1.85 | 1.45 | 1.1136 | 1.1136 | 46.99 | 50.25 | 0.935 |
| D4-60 | 1.6 | 1.45 | 0.7874 | 1.3638 | 49.43 | 52.32 | 0.945 |
| D4-90 | 1.35 | - | 0 | 1.5748 | 64.69 | 57.5 | 1.125 |
| A8-00 | 2.55 | - | 2.9528 | 0 | 77.38 | 75.95 | 1.019 |
| A8-30 | 2.35 | 2 | 2.5572 | 1.4764 | 84.73 | 81.36 | 1.041 |
| A8-45 | 2 | 2 | 2.0879 | 2.0879 | 85.12 | 85.08 | 1.001 |
| A8-60 | 1.7 | 2 | 1.4764 | 2.5572 | 100.6 | 98.64 | 1.019 |
| A8-90 | 1.45 | - | 0 | 2.9528 | 117.04 | 110.97 | 1.055 |

A few results of Table 2.11 are not as good as other results obtained by others.

**Table 2.11** cont. Morino et al. specimens eccentricities and comparative failure loads

| Col. | $\alpha$ | $\beta$ | $e_x$ in. | $e_y$ in. | $P_{test}$ | $P_{NJIT}$ | $P_t/P_{NJIT}$ |
|---|---|---|---|---|---|---|---|
| B8-00 | 2.55 | - | 2.9528 | 0 | 58.47 | 53.87 | 1.085 |
| B8-30 | 2.35 | 1.85 | 2.5572 | 1.4764 | 59.24 | 58.39 | 1.015 |
| B8-45 | 2 | 1.85 | 2.0879 | 2.0879 | 66.14 | 64.80 | 1.021 |
| B8-60 | 1.7 | 1.85 | 1.4764 | 2.5572 | 73.81 | 74.11 | 0.996 |
| B8-90 | 1.45 | - | 0 | 2.9528 | 93.94 | 90.99 | 1.032 |
| C8-00 | 2.3 | - | 2.9528 | 0 | 40.36 | 47.15 | 0.856 |
| C8-30 | 2.05 | 1.45 | 2.5572 | 1.4764 | 39.66 | 47.27 | 0.805 |
| C8-45 | 1.85 | 1.45 | 2.0879 | 2.0879 | 43.9 | 49.8 | 0.882 |
| C8-60 | 1.6 | 1.45 | 1.4764 | 2.5572 | 43.62 | 53.92 | 0.809 |
| C8-90 | 1.35 | - | 0 | 2.9528 | 66.56 | 64.39 | 1.034 |
| D8-00 | 2.3 | - | 2.9528 | 0 | 31.38 | 36.69 | 0.856 |
| D8-30 | 2.05 | 1.45 | 2.5572 | 1.4764 | 26.37 | 37.18 | 0.71 |
| D8-45 | 1.85 | 1.45 | 2.0879 | 2.0879 | 32.96 | 38.88 | 0.848 |
| D8-60 | 1.6 | 1.45 | 1.4764 | 2.5572 | 35.6 | 41.73 | 0.853 |
| D8-90 | 1.35 | - | 0 | 2.9528 | 49.85 | 48.50 | 1.028 |
| Average $P_{test}/P_{NJIT}$ = 0.9833<br>Standarddeviation = 0.099 | | | | | | | |

The Author notes that coefficient $\beta$ presents a variation with respect to the ratio of the nominal axial load to the maximum controlling axial load ($P_n/P_o$). There is a discontinuity at a value of axial load at the balanced point which divides the compression controlled region to the tensile controlled region.

The variation of coefficient $\beta$ may be expressed in terms of two linear relationships, one for the values of $P_n$ above the balanced load and the other for those values below the same balanced load.

It has been found that the important parameters that define the linear relationship are the ratio of depth of steel shape to the depth of the composite member (d/t), the ratio of the width of the steel shape to the width of the composite section ($b_f/b$), the percentage of steel $\rho$, and the ultimate compressive strength of concrete.

Table 2.12 presents a tabulation of the different composite columns studied by the Author with the estimated coefficients $c_1^c$, $c_2^c$, $c_1^t$ and $c_2^t$ for calculating the coefficient $\beta$ for each one of the cross sections.

The composite cross sections show variations in values of $f'_c$, $F_y$, $\rho$, b/t, $b_f/b$, d/t and other cross section material properties and dimensional parameters.

The last set of composite column specimens used by the Author for verification of the proposed Equation of Failure Surface are the specimens tested by Roik and Schwalbenhofer (180) in Germany. Some 27 pin-ended concrete-encased composite columns were tested in uniaxial and biaxial bending with axial compressive load.

All the 27 composite column specimens tested and reported by Roik and Schwalbenhofer had a 11"x11" (28 cm x 28 cm) cross section dimension and a length of 118.11" (3.0 m) and where longitudinally reinforced with 4 corner reinforcing bars in addition to the steel shape. The typical composite cross section dimensions and details are shown in Fig. 2.13

The composite column specimens dimensions, material properties, reinforcement and parameters required to process the equation of failure surface are labeled as V11 to V123 and they are shown in Tables 2.13, 2.14 and 2.15.

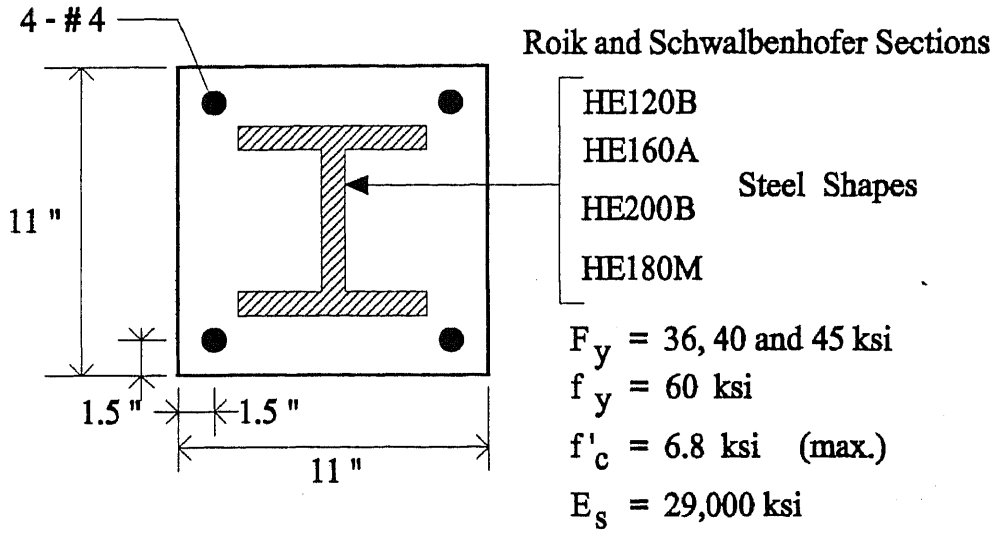


**Figure 2.13** Roik and Schwalbenhofer composite column specimens

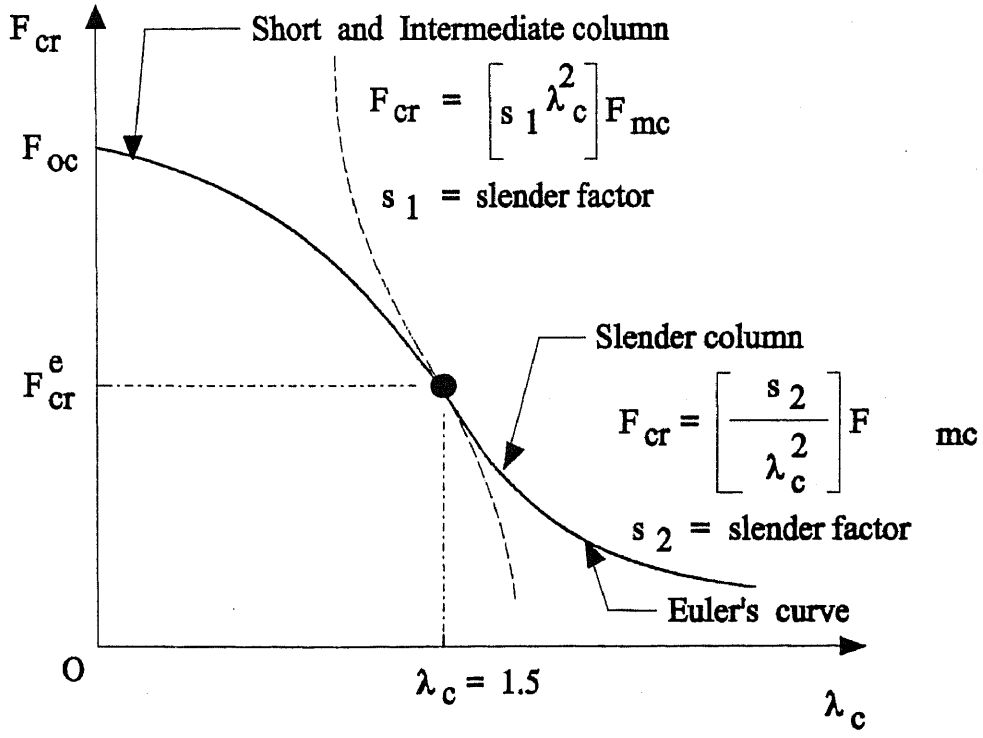


**Figure 2.14** Graphical curve of slenderness ratio versus composite stress

**Table 2.12** Composite column coefficients to define load-contour exponent β

| Col. | b/t | $f'_c$ | $F_y$ | ρ | $b_f/b$ | d/t | $c_1^c$ | $c_2^c$ | $c_1^t$ | $c_2^t$ |
|---|---|---|---|---|---|---|---|---|---|---|
| A | 1 | 5.75 | 33 | 5.23 | 0.6 | 0.6 | 1.361 | 0.76 | 2.118 | 0.694 |
| B | 1 | 5.5 | 33 | 5.23 | 0.6 | 0.6 | 1.349 | 0.789 | 2.144 | 0.739 |
| D | 1 | 6.1 | 33 | 5.23 | 0.6 | 0.6 | 1.347 | 0.771 | 2.098 | 0.637 |
| G | 1 | 5.3 | 33 | 5.23 | 0.6 | 0.6 | 1.424 | 0.694 | 2.154 | 0.756 |
| I | 1 | 6.26 | 33 | 5.23 | 0.6 | 0.6 | 1.311 | 0.817 | 2.082 | 0.613 |
| A4 | 1 | 3.06 | 50 | 10.28 | 0.635 | 0.635 | 1.33 | 0.919 | 1.797 | 0.605 |
| A8 | 1 | 4.87 | 50 | 10.28 | 0.635 | 0.635 | 1.234 | 0.971 | 1.694 | 2.159 |
| B4 | 1 | 3.39 | 50 | 10.28 | 0.635 | 0.635 | 1.329 | 0.876 | 1.793 | 0.608 |
| B8 | 1 | 4.83 | 50 | 10.28 | 0.635 | 0.635 | 1.235 | 0.969 | 1.702 | 2.04 |
| C4 | 1 | 3.38 | 50 | 10.28 | 0.635 | 0.635 | 1.333 | 0.874 | 1.793 | 0.609 |
| C8 | 1 | 3.57 | 50 | 10.28 | 0.635 | 0.635 | 1.316 | 0.887 | 1.794 | 0.604 |
| D4 | 1 | 3.08 | 50 | 10.28 | 0.635 | 0.635 | 1.33 | 0.919 | 1.792 | 0.606 |
| D8 | 1 | 3.32 | 50 | 10.28 | 0.635 | 0.635 | 1.336 | 0.874 | 1.797 | 0.603 |
| AISC1 | 1 | 8 | 36 | 10.1 | 0.561 | 0.555 | 1.138 | 1.023 | 1.758 | 0.356 |
| AISC3 | 1 | 3.5 | 50 | 5.51 | 0.531 | 0.507 | 1.16 | 0.854 | 1.57 | 1.394 |
| AISC4 | 1 | 5 | 50 | 6.98 | 0.589 | 0.566 | 1.117 | 1.082 | 1.667 | 0.838 |
| RKBG | 1 | 4 | 50 | 11.9 | 0.667 | 0.667 | 1.598 | 0.734 | 1.896 | 0.832 |
| SSLC1 | 1 | 3 | 36 | 2.9 | 0.764 | 0.406 | 2.732 | -0.931 | 2.242 | -0.44 |
| SSLC2 | 1 | 3 | 36 | 3.4 | 0.771 | 0.408 | 3.007 | -1.26 | 2.372 | -0.61 |
| SSLC3 | 1 | 3 | 36 | 4.0 | 0.781 | 0.41 | 3.333 | -1.616 | 2.577 | -0.85 |
| SSLC4 | 1 | 3 | 36 | 4.6 | 0.746 | 0.50 | 2.931 | -1.074 | 2.537 | -0.48 |
| SSLC5 | 1 | 3 | 36 | 5.2 | 0.825 | 0.503 | 3.219 | -1.422 | 2.685 | -0.69 |
| SSLC6 | 1 | 3 | 36 | 5.7 | 0.918 | 0.505 | 3.419 | -1.626 | 2.837 | -0.87 |
| SSLC7 | 1 | 3 | 36 | 6.1 | 0.754 | 0.625 | 2.769 | -0.776 | 2.619 | 0.018 |
| SSLC8 | 1 | 3 | 36 | 6.6 | 0.762 | 0.626 | 2.915 | -0.914 | 2.715 | -0.11 |
| SSLC9 | 1 | 3 | 36 | 7.5 | 0.758 | 0.75 | 2.394 | -0.267 | 2.508 | 0.745 |
| SSLC10 | 1 | 3 | 36 | 8.2 | 0.766 | 0.753 | 2.492 | -0.356 | 2.523 | 0.479 |
| SSLC11 | 1 | 3 | 36 | 9.1 | 0.774 | 0.755 | 2.569 | -0.427 | 2.574 | 0.297 |
| SSLC12 | 1 | 3 | 36 | 10.0 | 0.783 | 0.757 | 2.643 | -0.478 | 2.63 | 0.113 |
| SSLC13 | 1 | 3 | 36 | 11.0 | 0.794 | 0.76 | 2.748 | -0.561 | 2.71 | -0.04 |
| STV | 0.75 | 3 | 36 | 10.1 | 0.65 | 0.842 | 2.796 | -0.395 | 2.759 | 0.333 |
| MC1 | 1 | 5.33 | 50 | 2.89 | 0.4 | 0.4 | 1.10 | 0.679 | 1.361 | 0.618 |
| MC2 | 1 | 4.49 | 50 | 2.89 | 0.4 | 0.4 | 1.148 | 0.489 | 1.356 | 0.773 |
| MC3 | 1 | 3.75 | 50 | 2.89 | 0.4 | 0.4 | 1.174 | 0.366 | 1.294 | 0.969 |
| MC4 | 1 | 3.99 | 50 | 2.89 | 0.4 | 0.4 | 1.188 | 0.45 | 1.32 | 0.935 |

**Table 2.13** Roik and Schwalbenhofer-Specimens dimensions and material properties

| Col No. | Steel Shape | ρ % | $F_y$ (ksi) | $f_c'$ (ksi) | $\alpha_{cx}$ | $\alpha_{tx}$ | $\alpha_{cy}$ | $\alpha_{ty}$ |
|---|---|---|---|---|---|---|---|---|
| V11 | HE120B | 5.0 | 36 | 6.353 | 2.35 | 1.50 | 2.4 | 2.5 |
| V12 | HE120B | 5.0 | 36 | 6.353 | 2.35 | 1.50 | 2.4 | 2.5 |
| V13 | HE120B | 5.0 | 36 | 6.788 | 2.15 | 1.75 | 2.05 | 2.75 |
| V21 | HE160A | 5.63 | 45 | 6.788 | 2.0 | 1.40 | 2.20 | 2.70 |
| V22 | HE160A | 5.63 | 45 | 5.367 | 1.80 | 1.40 | 2.30 | 2.55 |
| V23 | HE160A | 5.63 | 45 | 5.367 | 1.80 | 1.40 | 2.30 | 2.55 |
| V31 | HE200B | 10.7 | 36 | 5.904 | 1.30 | 1.45 | 2.25 | 2.25 |
| V32 | HE200B | 10.7 | 36 | 5.904 | 1.30 | 1.45 | 2.25 | 2.25 |
| V33 | HE200B | 10.7 | 36 | 5.70 | 1.30 | 1.45 | 2.2 | 2.25 |
| V41 | HE180M | 13.1 | 40 | 5.70 | 1.30 | 1.45 | 2.40 | 2.45 |
| V42 | HE180M | 13.1 | 40 | 6.121 | 1.35 | 1.40 | 2.5 | 2.45 |
| V43 | HE180M | 13.1 | 40 | 6.121 | 1.35 | 1.40 | 2.5 | 2.45 |
| V81 | HE200B | 10.7 | 36 | 4.555 | 1.30 | 1.40 | 2.1 | 2.35 |
| V82 | HE200B | 10.7 | 36 | 4.555 | 1.30 | 1.40 | 2.1 | 2.35 |
| V83 | HE200B | 10.7 | 36 | 4.555 | 1.30 | 1.40 | 2.1 | 2.35 |
| V91 | HE160A | 5.63 | 40 | 5.120 | 1.75 | 1.40 | 2.55 | 2.15 |
| V92 | HE160A | 5.63 | 40 | 5.744 | 1.85 | 1.40 | 2.25 | 2.50 |
| V93 | HE160A | 5.63 | 40 | 5.744 | 1.85 | 1.40 | 2.25 | 2.50 |
| V101 | HE160A | 5.63 | 40 | 5.12 | 1.75 | 1.40 | 2.55 | 2.15 |
| V102 | HE160A | 5.63 | 40 | 5.744 | 1.85 | 1.40 | 2.25 | 2.50 |
| V103 | HE160A | 5.63 | 40 | 5.744 | 1.85 | 1.40 | 2.25 | 2.50 |
| V111 | HE160A | 8.28 | 40 | 5.817 | 1.45 | 1.20 | 1.50 | 1.95 |
| V112 | HE160A | 8.28 | 40 | 5.817 | 1.45 | 1.20 | 1.50 | 1.95 |
| V113 | HE160A | 8.28 | 40 | 5.817 | 1.45 | 1.20 | 1.50 | 1.95 |
| V121 | HE120B | 7.66 | 36 | 5.817 | 1.60 | 1.25 | 1.45 | 1.95 |
| V122 | HE120B | 7.66 | 36 | 5.817 | 1.60 | 1.25 | 1.45 | 1.95 |
| V123 | HE120B | 7.66 | 36 | 5.817 | 1.60 | 1.25 | 1.45 | 1.95 |

**Table 2.14** Roik and Schwalbenhofer-Specimens axial load and moment parameters

| Col. No. | $P_o^{(+)}$ (kips) | $P_o^{(-)}$ (kips) | $P_{nbx}$ (kips) | $M_{nbx}$ (k-in) | $P_{nby}$ (kips) | $M_{nby}$ (k-in) |
|---|---|---|---|---|---|---|
| V11 | 734.67 | -230.67 | 210.217 | 1237.45 | 321.955 | 1082.47 |
| V12 | 734.67 | -230.67 | 210.217 | 1237.45 | 321.955 | 1082.47 |
| V13 | 841.37 | -230.67 | 281.701 | 1282.44 | 394.698 | 1138.45 |
| V21 | 859.51 | -304.71 | 218.954 | 1579.48 | 357.798 | 1252.91 |
| V22 | 746.69 | -304.71 | 190.275 | 1435.59 | 253.034 | 1086.98 |
| V23 | 746.69 | -304.71 | 190.275 | 1435.59 | 253.034 | 1086.98 |
| V31 | 911.43 | -468.34 | 255.765 | 2168.69 | 232.433 | 1447.18 |
| V32 | 911.43 | -468.34 | 255.765 | 2168.69 | 232.433 | 1447.18 |
| V33 | 896.35 | -468.34 | 251.113 | 2146.25 | 227.978 | 1425.33 |
| V41 | 1050.0 | -649.19 | 223.808 | 2697.71 | 197.101 | 1544.53 |
| V42 | 1082.0 | -649.19 | 231.869 | 2738.85 | 205.843 | 1587.94 |
| V43 | 1082.0 | -649.19 | 231.869 | 2738.85 | 205.843 | 1587.94 |
| V81 | 824.22 | -468.34 | 196.292 | 2017.40 | 198.954 | 1295.14 |
| V82 | 824.22 | -468.34 | 196.292 | 2017.40 | 198.954 | 1295.14 |
| V83 | 824.22 | -468.34 | 196.292 | 2017.40 | 198.954 | 1295.14 |
| V91 | 703.03 | -276.184 | 188.109 | 1337.97 | 196.592 | 1032.52 |
| V92 | 753.29 | -276.184 | 202.416 | 1405.20 | 286.502 | 1105.74 |
| V93 | 753.29 | -276.184 | 202.416 | 1405.20 | 286.502 | 1105.74 |
| V101 | 703.03 | -276.184 | 188.109 | 1337.97 | 196.592 | 1032.52 |
| V102 | 753.29 | -276.184 | 202.416 | 1405.20 | 286.502 | 1105.74 |
| V103 | 753.29 | -276.184 | 202.416 | 1405.20 | 286.502 | 1105.74 |
| V111 | 917.76 | -468.184 | 196.051 | 1941.19 | 280.443 | 1642.88 |
| V112 | 917.76 | -468.184 | 196.051 | 1941.19 | 280.443 | 1642.88 |
| V113 | 917.76 | -468.184 | 196.051 | 1941.19 | 280.443 | 1642.88 |
| V121 | 876.15 | -422.669 | 191.556 | 1654.48 | 298.866 | 1488.01 |
| V122 | 876.15 | -422.669 | 191.556 | 1654.48 | 298.866 | 1488.01 |
| V123 | 876.15 | -422.669 | 191.556 | 1654.48 | 298.866 | 1488.01 |

**Table 2.15** Roik and Schwalbenhofer-Critical load, moment and design parameters

| Col. No. | $P_{cr}$ (kips) | $M_{byx}$ (k-in) | $M_{bxy}$ (k-in) | $e_{byx}$ (in) | $e_{bxy}$ (in) |
|---|---|---|---|---|---|
| V81 | 2645.0 | 2015.94 | 1294.576 | 10.133 | 6.595 |
| V82 | 2645.0 | 2015.94 | 1294.576 | 10.133 | 6.595 |
| V83 | 2645.0 | 2015.94 | 1294.576 | 10.133 | 6.595 |
| V91 | 2041.0 | 1337.16 | 1028.806 | 6.802 | 5.469 |
| V92 | 2124.0 | 1371.61 | 1028.493 | 4.787 | 5.0811 |
| V93 | 2124.0 | 1371.61 | 1028.493 | 4.787 | 5.0811 |
| V101 | 2041.0 | 1337.16 | 1028.806 | 6.802 | 5.469 |
| V102 | 2124.0 | 1371.61 | 1028.493 | 4.787 | 5.0811 |
| V103 | 2124.0 | 1371.61 | 1028.493 | 4.787 | 5.0811 |

The comparative results of failure load obtained by Roik and Schwalbenhofer to the loads obtained by the Author when using the proposed equation of failure surface are presented in Table 2.16.

A review of the failure loads obtained by the Author and presented in Table 2.16 indicates that excellent agreement is achieved in predicting the failure load of uniaxially and biaxially loaded concrete-encased composite columns.

The expressions that define the relationship of axial stress and slenderness ratio for short, intermediate and slender composite columns were slightly modified by the Author to account for a proportional ratio of each one of the components of the composite section to the gross column cross section.

An extensive verification of the modified equation of axial stress for composite sections reveals that excellent results in predicting the axial load of short and slender composite columns may be obtained by using the proposed modified equation of axial stress Eq. 2.26.

**Table 2.16** Roik and Schwalbenhofer-Eccentricities and comparative failure loads

| Col. No. | $\alpha$ | $\beta$ | $e_x$ (in) | $e_y$ (in) | $P_{test}$ (kips) | $P_{NJIT}$ (kips) | $P_t/P_{NJIT}$ |
|---|---|---|---|---|---|---|---|
| V11 | 1.5 | - | 0 | 6.3 | 171.54 | 167.86 | 1.022 |
| V12 | 2.35 | - | 0 | 2.36 | 366.01 | 365.82 | 1.001 |
| V13 | 2.15 | - | 0 | 3.937 | 322.62 | 303.67 | 1.062 |
| V21 | 2.0 | - | 0 | 3.937 | 337.91 | 331.59 | 1.019 |
| V22 | 1.80 | - | 0 | 6.30 | 213.58 | 205.05 | 1.042 |
| V23 | 1.80 | - | 0 | 2.36 | 436.83 | 403.15 | 1.084 |
| V31 | 1.30 | - | 0 | 3.937 | 383.77 | 390.17 | 0.984 |
| V32 | 1.30 | - | 0 | 2.36 | 506.52 | 501.75 | 1.010 |
| V33 | 1.30 | - | 0 | 6.3 | 294.06 | 289.43 | 1.016 |
| V41 | 1.30 | - | 0 | 3.937 | 477.30 | 460.57 | 1.036 |
| V42 | 1.35 | - | 0 | 6.3 | 344.65 | 353.67 | 0.975 |
| V43 | 1.35 | - | 0 | 2.36 | 614.45 | 609.29 | 1.008 |
| V81 | 1.95 | 1.75 | 2.95 | 2.36 | 463.81* | 326.85 | 1.419* |
| V82 | 1.90 | 2.15 | 1.57 | 1.18 | 497.53 | 481.25 | 1.034 |
| V83 | 1.35 | 1.80 | 0.591 | 2.36 | 443.57 | 453.255 | 0.979 |
| V91 | 2.35 | 2.25 | 2.36 | 0.591 | 406.47 | 393.816 | 1.032 |
| V92 | 1.95 | 2.25 | 1.18 | 2.36 | 396.81 | 361.21 | 1.099 |
| V93 | 2.15 | 2.0 | 2.36 | 1.57 | 339.03 | 354.90 | 0.955 |
| V101 | 1.80 | 2.15 | 1.18 | 2.36 | 317.67 | 317.117 | 1.002 |
| V102 | 1.4 | 2.0 | 0 | 3.937 | 252.02 | 241.70 | 1.043 |
| V103 | 2.0 | 2.0 | 1.18 | 1.57 | 360.39 | 358.44 | 1.005 |
| V111 | 1.45 | - | 0 | 3.937 | 394.56 | 390.631 | 1.01 |
| V112 | 1.45 | - | 0 | 2.36 | 565.42 | 516.99 | 1.094 |
| V113 | 1.45 | - | 0 | 0 | 1031.92 | 917.76 | 1.124 |
| V121 | 1.60 | - | 0 | 6.3 | 255.85 | 240.01 | 1.066 |
| V122 | 1.60 | - | 0 | 7.87 | 182.78 | 197.552 | 0.925 |
| V123 | 1.60 | - | 0 | 3.94 | 345.1 | 342.757 | 1.007 |

Average $P_{test}/P_{NJIT}$ = 1.024
StandardDeviation = 0.044

A graphical representation of the LRFD method to calculate the axial stress of a concentrically loaded short and slender composite section is presented in Fig. 2.14 to illustrate the concept of expressing the axial stress of a composite section as a function of the slenderness ratio.

It is important to note that the Author's proposed equations of Failure Surface, Eq. 2.21 and 2.24, can be used to predict the failure load of composite columns. They provide a solution that achieves an excellent agreement with already established methods of analysis, design and test results obtained for composite columns in uniaxial and biaxial bending conditions.

Therefore the Author recommends that with appropriate factors for load and strength of materials the proposed Generalized Equation of Failure Surface may be useful in the design of concrete-encased composite columns.

# CHAPTER 3

# COMPLETE LOAD-DEFORMATION COMPUTER ANALYSIS FOR BIAXIALLY LOADED COMPOSITE COLUMNS

## 3.1 Introduction

The Analysis of composite columns has been studied and developed throughout the past decades. Material Failure is the dominant factor for the strength of short or stocky columns while instability controls the capacity and failure load of slender members.

A computer method to study the ultimate strength of pinned-ended and end-restrained composite columns under combined biaxial bending and axial loads is presented herein. The analytical method is based on the numerical integration technique originally developed by Hsu (85). Extensive modifications and adaptations to the Hsu's analytical method were incorporated into a computer program by Wang and Hsu (226) in 1990, and Tsao (208) in 1991 at The New Jersey Institute of Technology, to study the behavior of short and slender reinforced concrete columns with pinned ends under biaxial bending and axial loads.

The Author has further extended the above analytical method to study the composite columns with both pinned and restrained ends under combined biaxial bending and axial loads. This numerical analysis is based on the Secant Modulus of Elasticity and a segmental subdivision of the column length is used to determine the complete load-moment-curvature-deflection (P-M-$\phi$-$\delta$) for both short and slender columns under combined biaxial bending and axial load.

The computer method accounts for inelastic action of the different materials in the composite section. The load-deformation behavior includes the ascending and descending branches of the column behavior under study. An incremental deflection control computational procedure is undertaken to achieve the complete load-deformation behavior of concrete-encased composite columns.

Bending of the composite column section is assumed to take place about the two principal axes of the cross section. The bending moments developed in the restrained ends of the column may be linear or non-linear functions of the column end rotations.

The column model under study, a symmetrically reinforced composite slender column laterally restrained against sidesway at both ends (top and bottom) is shown in Fig. 3.1. The column is idealized as a number of linear segments. Also the column cross section is discretized into a number of small square or rectangular areas for which the conditions of equilibrium and strain compatibility must satisfy at the nodal points.

The second-order effects due to the deformed shape of the composite column under load are included in the analysis. The numerical technique adopted in the computer method is based on the incremental deflection approach, where an assumed deflection value is specified at a selected joint in a specific direction. The corresponding equilibrium loads to the specified deflection are calculated and the conditions of strain compatibility and equilibrium are satisfied along the column length. The procedure successfully carries out the results when the assumed deflection values accurately match with the computed deflection values within certain allowable limits.

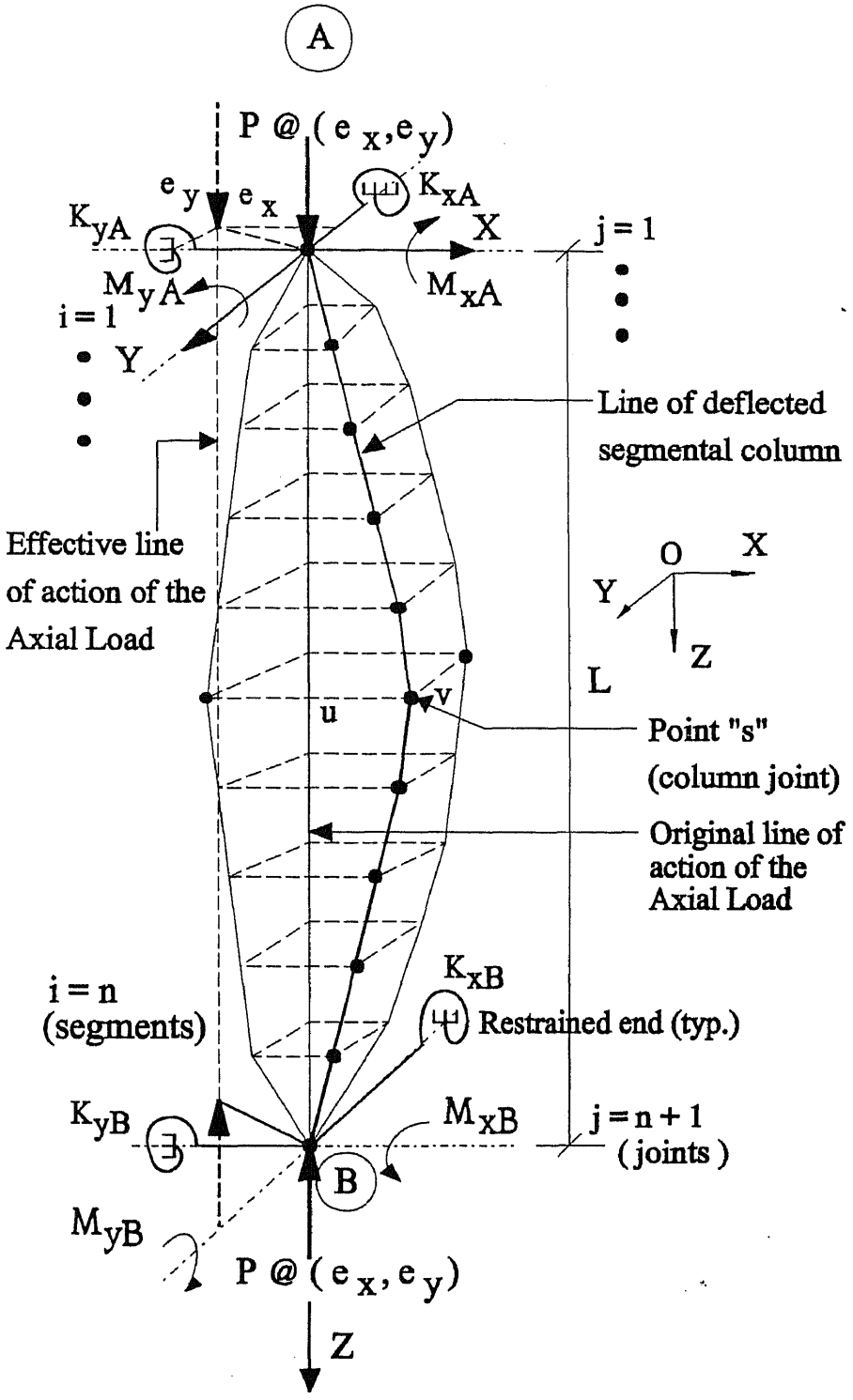


**Figure 3.1** Biaxially loaded segmented column with restrained ends

An iterative procedure to solve a system of non-linear equations is used to obtain the solution of the non-closed form of the second order equations generated by the Finite Difference Method with extremely rapid convergence.

This method can predict the failure load of a composite column with great accuracy provided the column cross section is subdivided into a sufficiently large numbers of elements and the column length is divided into several segments.

The iteration process achieves the maximum load in the ascending branch and proceeds with the descending branch up to failure.

The stress-strain curves for concrete accounts for unconfined, confined and highly confined type of concrete elements.

The stress-strain curve for the reinforcing steel is idealized as an elastic-inelastic piece-wise linear relationship.

The computer method is based on the concept of using the condition of very small column stiffness as the convergence criteria to achieve the ultimate load.

## 3.2 Basic Assumptions

The proposed numerical analysis used in the computer program is developed by Wang and Hsu (226) and Tsao (208). It is now extended by the Author. The computer Analysis is based on the following assumptions:

1. Plane sections remain plane during and after bending.
2. The stress-strain relationships for the composite column materials are known. The tensile strength of concrete as well as the confined, unconfined, and highly confined characteristics of the concrete zones are well defined. Strain

softening of concrete is considered and the reinforcement steel is being modeled as an elastic-inelastic material.

3. The effect of creep and any tensile stresses due to shrinkage are neglected.
4. Perfect bond exists between concrete and steel.
5. The twisting effects and the axial and shear deformations are considered to be negligible. The column does not buckle locally before the ultimate load is achieved.
6. The column segments are considered to be straight at zero loading and each segment curvature varies linearly along the segment under increasing loading conditions.
7. The member does not have any initial deflection or curvature.
8. The member is subjected to a monotonic loading condition. loading path.
9. The moment-rotation end conditions are known.
10. The effect of residual stresses in the structural steel section are not included.

### 3.3 Method of Analysis and Fundamental Equations

An approximate method of analysis for the calculation of pin-ended reinforced concrete columns in biaxial bending and axial compressive loads has been presented by Tsao (208).

The method is based on the assumption that the deflected shape of the column in each of the two bending planes is formed by a series of interconnected linear segments. The Author will include the effect of restrained rotations at both ends and they are about the two major axes directions of the biaxially loaded composite columns.

### 3.3.1 Moment-Curvature-Thrust Relationships

The procedure used to develop the moment-curvature-thrust relationship is based on the cross-sectional secant stiffness matrix approach for biaxial bending as it has been proposed by Wang and Hsu (226). For a biaxially loaded column section, one can define the generalized force (stress) vector, {F}, and the generalized deformation (strain) vector {D}, as follows:

$$\{F\} = \begin{Bmatrix} P \\ M_x \\ M_y \end{Bmatrix} \quad ; \quad \{D\} = \begin{Bmatrix} \epsilon_o \\ \phi_x \\ \phi_y \end{Bmatrix} \tag{3.1}$$

where P is the Axial Force on the cross section, $M_x$ and $M_y$ are the Bending Moments about the x and y coordinate axes respectively, $\epsilon_o$ is the centroidal axial strain, and $\phi_x$ and $\phi_y$ are the curvatures about the x and y coordinate axes respectively.

Consider a composite column of length L divided into a number of linear segments and the column is subjected to an axial compressive force P, and biaxial bending moments $M_x$ and $M_y$ with the X-Y axis as shown in Fig. 3.1. The column cross section is divided into a number of n small elements as presented in Fig. 3.2. The principal axes are labeled X and Y and the local coordinate origin O is located at the geometric and plastic centroid of the cross section.

The derivation of the fundamental Moment-Curvature-Thrust relationship of a slender composite column under a given combination of end bending moments and axial compressive load is based on the deflected shape and the changing curvatures along the length of the member. The varying curvatures of the column segments produces internal moments, which are in equilibrium with the internal forces. From

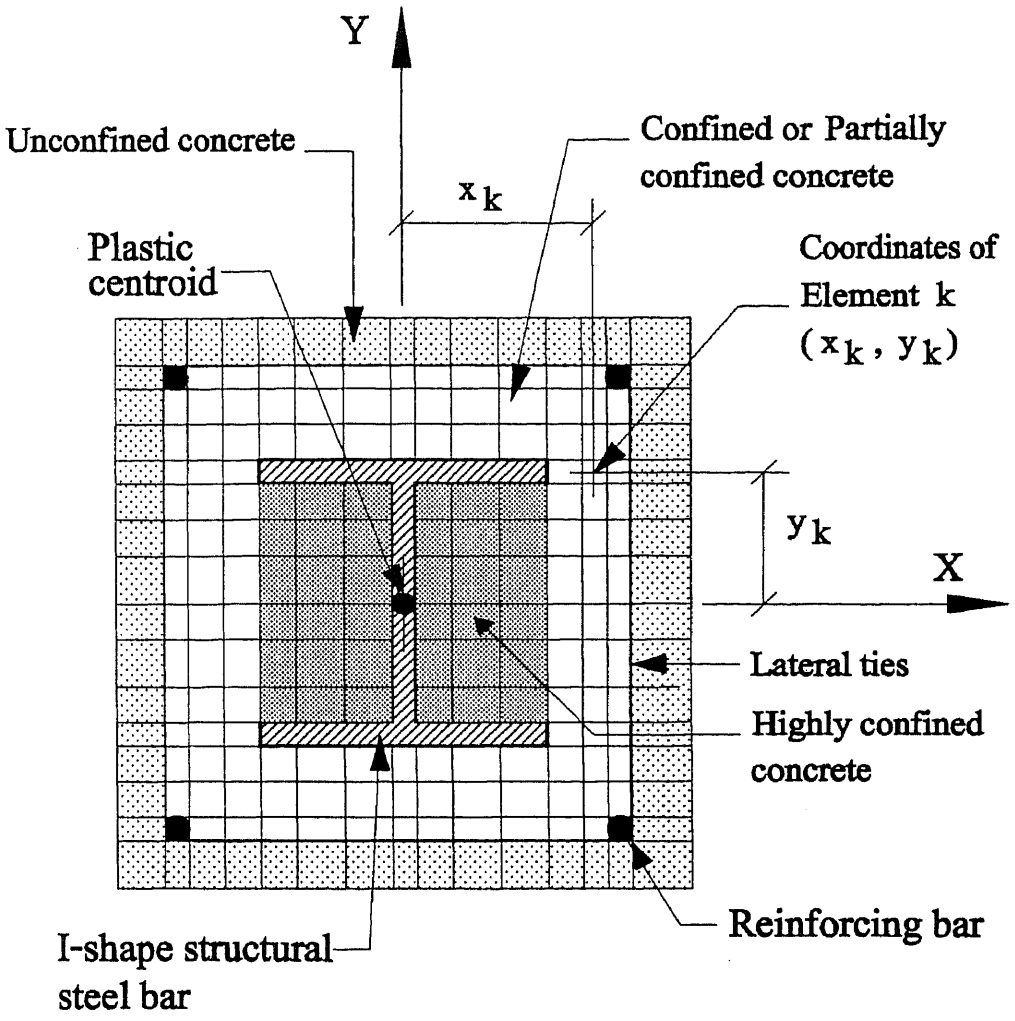


**Figure 3.2** Composite column cross section and local coordinate system

Fig. 3.1, for a given point "s" along the column length, the deflections of that point "s" along the X and Y axes are denoted by "u" and "v".

The externally applied eccentric axial load P, produces bending moments $M_x$ and $M_y$ at a given section along the column by the following equations:

$$M_x = P(e_y + v) \tag{3.2}$$

$$M_y = P(e_x + u) \tag{3.3}$$

where $e_x$ and $e_y$ are the eccentricities of the line of action of the axial load P measured with respect to the plastic centroid of the section in the undeformed original vertical position of the column.

The displacements of the column joints are assumed to be small, so that the total curvature in the two major bending planes labeled as $\phi_x$ and $\phi_y$, can be represented in the form of second derivatives of the displacements as follows:

$$\phi_x = -\partial^2 u/\partial x^2 \tag{3.4}$$

$$\phi_y = -\partial^2 v/\partial y^2 \tag{3.5}$$

For a position of the neutral axis at an angle $\theta$ with respect to the horizontal X axes, the curvatures $\phi_x$ and $\phi_y$ may be combined to obtain the principal curvature $\phi$, in the following form:

$$\phi = \sqrt{(\phi_x^2 + \phi_y^2)} \tag{3.6}$$

$$\theta = \tan^{-1}( \phi_y / \phi_x ) \tag{3.7}$$

The resultant strain distribution corresponding to the curvatures $\phi_x$, $\phi_y$ and the axial compressive strain $\epsilon_o$ is assumed to be uniformly distributed over each element "k" of the cross section and can be expressed in the following form:

$$\epsilon_k = \epsilon_o + \phi_x y + \phi_y x \tag{3.8}$$

where

$\epsilon_k$ = strain at the element "k" of the cross section

$\epsilon_o$ = centroidal strain at the plastic centroid

$\phi_x$ = curvature with respect to $M_x$. $\phi_x$ is positive when it can produce compressive strains in the positive y direction.

$\phi_y$ = curvature with respect to $M_y$. $\phi_y$ is positive when it can produce compressive strains in the positive x direction.

x, y = coordinates of the element "k" along the x and y axes respectively.

### 3.3.2 Stress-Strain relationships of materials

The resultant stress distribution at each element "k" is obtained by using the material properties of the corresponding element "k".

The idealized stress-strain curves and relationship for the reinforcement steel and concrete are given in Figs. 3.3 and 3.4 respectively, and are expressed in the following generalized form:

$$\sigma = f(\epsilon) \tag{3.9}$$

The composite column cross section consists of three materials: concrete, structural steel, and reinforcing steel. The effect of residual stresses is neglected in this method of analysis.

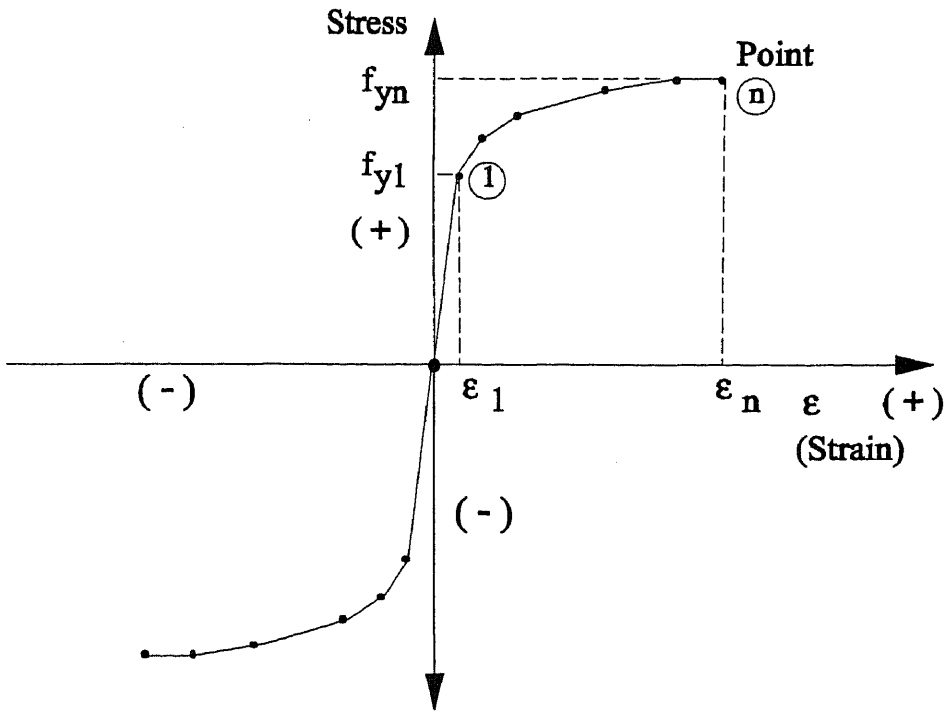


**Figure 3.3** Idealized Stress-Strain curve for steel rebar and steel shape

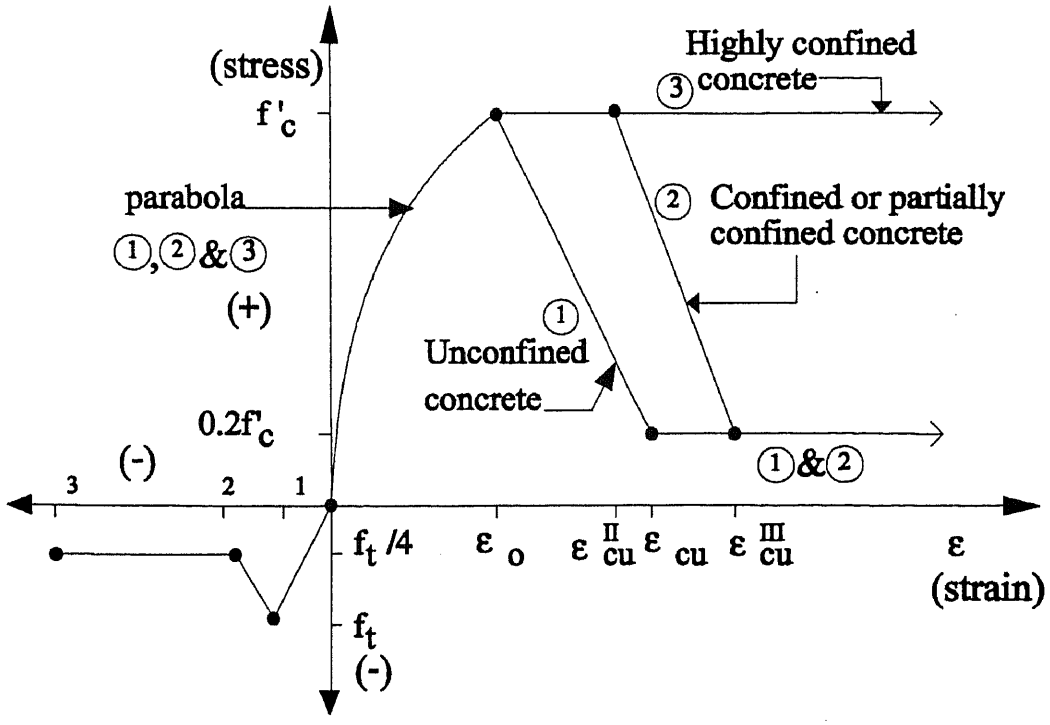


**Figure 3.4** Idealized Stress-Strain curve for concrete

**Stress-Strain relationship for concrete in compression**

The concrete has been subdivided into three types: the unconfined concrete elements outside the lateral ties, the confined or partially confined concrete elements inside the lateral ties but outside the boundaries of the structural steel shape, and the highly confined concrete elements inside the boundaries of the structural steel shape.

A combination of Hsu (96) and Park, et al. (167) stress-strain relationship has been used for concrete in compression, as shown in Fig. 3.4. The first part of the curve up to the maximum compressive strength is represented by a second order parabola and from this point the curve branches into three different lines according to the type of concrete being considered.

The first line defines the unconfined concrete with a descending slope down to a minimum value of concrete stress of $0.2\,f'_c$ and a strain value of $\epsilon_{cu}$. Then the curve remains horizontal for any increase in the strain level beyond the minimum concrete compressive strength.

The second line defines the confined or partially confined concrete with a short straight horizontal portion up to a strain value of $\epsilon_{cu}^{II}$, and then followed by a descending slope down to a value of concrete stress of $0.2\,f'_c$ and a strain value of $\epsilon_{cu}^{III}$. Again the curve remains a horizontal line at a constant minimum stress value of $0.2\,f'_c$.

The third line does not have any descending branch and it rather remains horizontal at a constant stress value of $f'_c$. For the confined and partially confined concretes, the slope of the descending branch depends on the concrete compressive strength and the degree of concrete confinement provided by the size and spacing of the lateral ties. For the highly confined concrete, the slope of the straight line can be

reasonably assumed to be zero due to the condition of confinement provided by the laterally confined concrete on one side and by the faces of the web and flanges of the structural steel shape on the others. A recent analytical model for the stress-strain relationship of confined concrete has been presented by Razvi and Saatcioglu (192). Based on their study the concrete confinement has been considered as a three-dimensional phenomenon.

In order to achieve a reasonable confinement condition for the concrete cross section inside the lateral ties, the ties have to be closely spaced and laterally supported by longitudinal reinforcing bars. Under this condition it is assumed that a uniform lateral pressure provides the desired confinement and that the vertical reinforcement bars will not buckle before the ultimate load is achieved.

The proposed stress-strain relationship for concrete proposed by Razvi and Saatcioglu (192), includes a peak value of the concrete compressive strength $f'_{cc}$, which is greater than the normal ultimate compressive strength for unconfined concrete $f'_c$. In the present computer model, the Author uses the same peak value of $f'_c$ for the highly confined, confined and unconfined concrete. This approach should lead to a conservative analysis result.

The stress-strain relationship curves for concrete shown in Fig. 3.4 have been used in the computer model to study the behavior of short and slender composite columns under biaxial bending and axial compressive loads.

The stress-strain curves for concrete in compression are defined as follows: The ascending part of the curves, common to the unconfined, confined and highly confined concrete is represented by a second-degree parabolic curve. It is expressed in the following mathematical form:

$$\sigma_c = f'_c \left[ \frac{2\varepsilon_c}{\varepsilon_o} - \left( \frac{\varepsilon_c}{\varepsilon_o} \right)^2 \right] , \quad \varepsilon_c \leq \varepsilon_o \tag{3.10}$$

The following parts of the curves beyond the ascending branch are defined as follows:

For unconfined concrete:

$$\sigma_c = 0.2 f'_c + \frac{0.8 f'_c(\varepsilon_c - \varepsilon_{cu})}{(\varepsilon_o - \varepsilon_{cu})} , \quad \varepsilon_o < \varepsilon_c \leq \varepsilon_{cu} \tag{3.11a}$$

$$\sigma_c = 0.2 f'_c , \quad \varepsilon_c > \varepsilon_{cu} \tag{3.11b}$$

For confined or partially confined concrete:

$$\sigma_c = f'_c , \quad \varepsilon_o < \varepsilon_c \leq \varepsilon_{cu}^{II} \tag{3.12a}$$

$$\sigma_c = 0.2 f'_c + \frac{0.8 f'_c(\varepsilon_{cu} - \varepsilon_{cu}^{III})}{(\varepsilon_{cu}^{II} - \varepsilon_{cu}^{III})} , \quad \varepsilon_{cu}^{II} \leq \varepsilon_c \leq \varepsilon_{cu}^{III} \tag{3.12b}$$

$$\sigma_c = 0.2 f'_c , \quad \varepsilon_c > \varepsilon_{cu}^{III} \tag{3.12c}$$

For highly confined concrete:

$$\sigma_c = f'_c , \quad \varepsilon_c > \varepsilon_o \tag{3.13}$$

The values of strain constants $\varepsilon_{cu}^{II}$ and $\varepsilon_{cu}^{III}$ are function of the confinement conditions provided by the size and spacing of the lateral ties as follows:

$$\epsilon_{cu}^{II} = \epsilon_o + (C_1)^{1/3} / 24.5 \tag{3.14}$$

$$\epsilon_{cu}^{III} = \epsilon_o + (C_1 + 0.05)^{1/3} / 24.5 \tag{3.15}$$

where $C_1$ may be expressed as a function of the lateral dimensions of the ties (B2 and D2), spacing of the ties (SP), and cross sectional area of each tie (AS2).

$$C_1 = \frac{.2(B2 + D2)AS2}{(B2)(D2)(SP)} \tag{3.16}$$

**Stress-Strain relationship for concrete in tension.**

The stress-strain relationship for the concrete in tension is defined as a type of "linear brittle" with the rupture tensile strain equal to $\epsilon_t = f_t / E_c$, where $f_t$ is the modulus of rupture for concrete and $E_c$ is the modulus of elasticity of the concrete.

The tensile part of the stress-strain curve of concrete as shown in Fig. 3.4 is divided in two branches. The first branch is a linear segment up to a value of $f_t$ and with a slope of $E_{t1}$. The second branch is a bilinear segment, with the first one having a slope $E_{t2}$ and the second one with a zero slope.

The value of $E_{ct}$ is chosen as $E_{ct} = 1{,}000\ f'_c$. For the computer analysis model, the value of $f_t$ and $E_c$ are chosen in accordance with the latest issue of the ACI Building Code, ACI-318-89 (1) and they are given by the following expressions:

$$f_t = 7.5\sqrt{f'_c} \tag{3.17}$$

$$E_c = 57{,}000\sqrt{f'_c} \tag{3.18}$$

The stress-strain equations for concrete in tension are defined as follows: where the values of $\epsilon_1$, and $\epsilon_2$ are:

$$\sigma_t = E_{t1}\,\epsilon_t\,, \qquad \epsilon_t \le \epsilon_1 \tag{3.19a}$$

$$\sigma_t = f_t + E_{t2}(\epsilon_t - 1)\,, \qquad \epsilon_1 \le \epsilon_t \le \epsilon_2 \tag{3.19b}$$

$$\sigma_t = f_t / 4 \qquad , \qquad \epsilon_t > \epsilon_2 \tag{3.19c}$$

$$E_{t1} = E_{ct} \tag{3.20a}$$

$$E_{t2} = (3/4)\ E_{t1}\ ; \quad E_{t3} = 0.0 \tag{3.20b}$$

$$\epsilon_1 = E_{ct} = f_t / E_{ct}\ ; \quad \epsilon_2 = 2\epsilon_{ct} \tag{3.21}$$

**Stress-Strain relationship for steel reinforcing bars and steel shapes**

The stress-strain relationship of structural steel and reinforcing steel rebar is assumed to be elastic-inelastic piece-wise linear relationship as shown in Fig. 3.3 in both compression and tension for purposes of the analysis.

### 3.4 Matrix Formulation of Analytical Method

The basic equations of equilibrium for the axial load P, and the biaxial bending moments $M_x$ and $M_y$ are given in terms of the stress resultants of all the elements:

$$P = \int_A \sigma\, dA \tag{3.22}$$

$$M_x = \int_A \sigma\, y\, dA \tag{3.23}$$

$$M_y = \int_A \sigma\, x\, dA \tag{3.24}$$

By using the secant modulus of elasticity $(E_s)_k = \sigma_k/\epsilon_k$ the above equations are:

$$P = \sum_{k=1}^{n} (E_s)_k \, \epsilon_k \, a_k \tag{3.22a}$$

$$M_x = \sum_{k=1}^{n} (E_s)_k \, \epsilon_k \, a_k \, y_k \tag{3.23a}$$

$$M_y = \sum_{k=1}^{n} (E_s)_k \, \epsilon_k \, a_k \, x_k \tag{3.24a}$$

The centroidal strain value at each small element of the cross-section $\epsilon_k$, can be expressed as a linear strain relationship based on the assumption that plane sections remain plane during biaxial bending.

The strain $\epsilon_k$ has been previously defined and may be rewritten here in the following form:

$$\epsilon_k = \epsilon_o + \phi_x y + \phi_y x \tag{3.25}$$

By substituting the value of $\epsilon_k$ into the basic equilibrium Equations (4.22a), (3.23a), and (3.24a) one obtains the following equation in a matrix form:

$$\begin{Bmatrix} P \\ M_x \\ M_y \end{Bmatrix} = \begin{bmatrix} S_{11} & S_{12} & S_{13} \\ S_{21} & S_{22} & S_{23} \\ S_{31} & S_{32} & S_{33} \end{bmatrix} \begin{bmatrix} \epsilon_o \\ \phi_x \\ \phi_y \end{bmatrix} \tag{3.26}$$

where:

$$S_{11} = \sum_{k=1}^{n} (E_s)_k \, a_k$$

$$S_{12} = S_{21} = \sum_{k=1}^{n} (E_s)_k \, a_k \, y_k$$

$$S_{13} = S_{31} = \sum_{k=1}^{n} (E_s)_k \, a_k \, x_k$$

(3.26a)

$$S_{22} = \sum_{k=1}^{n} (E_s)_k \, a_k \, y_k^2$$

$$S_{23} = S_{32} = \sum_{k=1}^{n} (E_s)_k \, a_k \, x_k \, y_k \qquad (3.26b)$$

$$S_{33} = \sum_{k=1}^{n} (E_s)_k \, a_k \, x_k^2$$

For a short column, the Moment-Curvature-Thrust relationship may be obtained directly from Eq. 3.26 and the second order effect of the lateral deflection of the column segments may be considered negligible.

For a slender column, the second-order effect and the material non-linearity become important factors in the overall behavior of the column. Therefore it is necessary to express the relationship between the generalized force (stress) vector and the generalized deformation (strain) vector in an incremental form.

For a given slender column with restrained ends under an applied axial load and biaxial bending moments at each column end, the bending moments at any certain location "s" along the column length with lateral deformations "u" and "v" along the x and y axes respectively are as shown in Fig. 3.1. They can be expressed as a function of the induced moments at the restrained ends and the load-deformation effect along the column.

For a deflected position of the column and for the given rotations at each end of the column $\theta_A$ and $\theta_B$, the induced moments at the restrained ends are given by $M_{RA}$ and $M_{RB}$, respectively. They can be found from the appropriate Moment-Rotation relationship of the restrained column ends. The relationship between the restraining moment and the end rotations may be assumed to be a linear or a non-linear curve. A typical representation of that Moment-Rotation curve is presented in

Fig. 3.5. The final moments at each end of the column can be expressed as a summation of the externally applied bending moment and the bending moment response from the restrained end. A set of equations for the column end A shown in Fig. 3.1 can be written in the following forms:

$$(M_{XA})_F = (M_{XA})_o + (M_{XA})_R \tag{3.27a}$$

$$(M_{YA})_F = (M_{YA})_o + (M_{YA})_R \tag{3.27b}$$

where $(M_{XA})_o = P\,(e_y)_A$; $(M_{YA})_o = P\,(e_x)_A$,

$(M_{XA})_R = K_{XA}\,\theta_{XA}$; $(M_{YA})_R = K_{YA}\,\theta_{YA}$

$K_{XA}$ and $K_{YA}$ are the coefficients that define the moment-rotation relationship about the x and y axes respectively.

$\theta_{XA}$ and $\theta_{YA}$ are the final slopes of the column end A about the X and Y axes respectively. The bending moments $M_{xj}$ and $M_{yj}$ at a point "s" along the column length are expressed in the following form:

$$M_{xj} = (M_{XA})_F - \frac{[(M_{XA})_F + (M_{XB})_F]\sum_{i=1}^{j} h_i}{L} + P\,v_j \tag{3.28a}$$

$$M_{yj} = (M_{YA})_F - \frac{[(M_{YA})_F + (M_{YB})_F]\sum_{i=1}^{j} h_i}{L} + P\,u_j \tag{3.28b}$$

where $(M_{XA})_F$ and $(M_{YA})_F$ are the final bending moments at end A about the X and Y axes respectively, $(M_{XB})_F$ and $(M_{YB})_F$ are the values for end B, $u_j$ and $v_j$ are the lateral deflections of the member at point j in the x and y directions respectively, $h_i$ is the length of column segment i, and L is the column length.

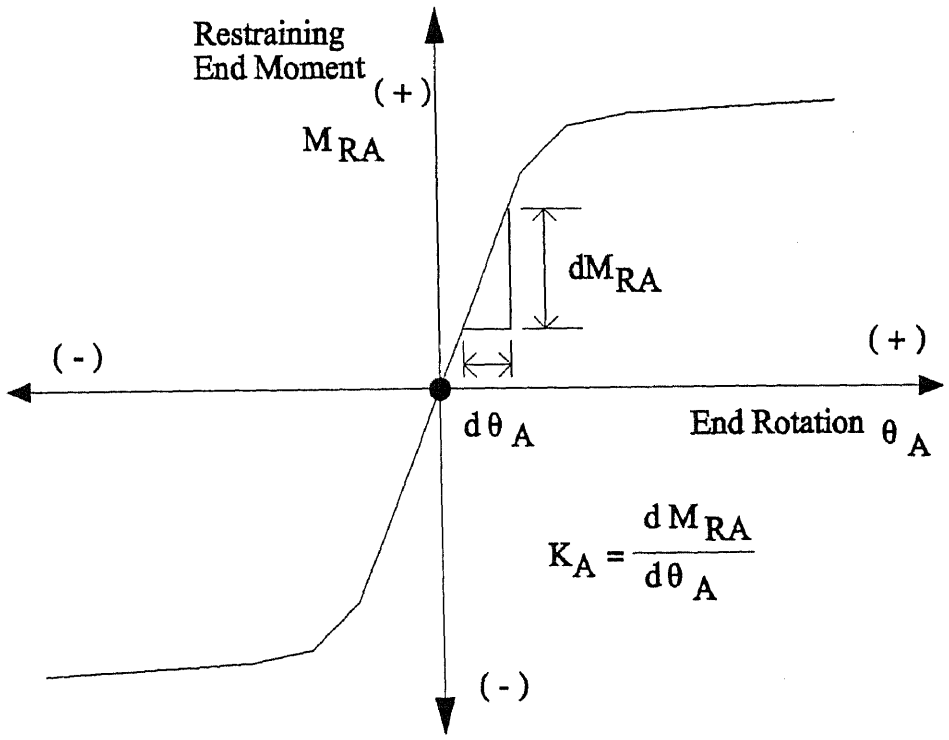


**Figure 3.5** Typical Moment-Rotation curve at column end

The system of equations is generated for a column with length "L". The column is divided into a number of "i" equal segments of length "h". An iterative technique is used which leads the second order non-linear equations to a solution within specified margins of tolerance and degree of accuracy.

The two equations presented above, Eq. (3.28a) and (3.28b), give the bending moment at any point "s" along the column length. The computed bending moments take into account the second-order effect and the restrained conditions at the column ends.

For a restrained column with similar and symmetrical conditions at each end A and B, the second term at the right hand side of equations (3.28a) and (3.28b) vanishes and the final bending moments at end A of the restrained column may be written in the following form:

$$M_x = P\,(e_y + v) + k_x\,\theta_x \tag{3.29a}$$

$$M_y = P\,(e_x + u) + k_y\,\theta_y \tag{3.29b}$$

For small rotations at the end of the column, the end slopes $\theta_x$ and $\theta_y$ may be expressed in terms of the lateral displacements of the end column segments are:

$$\theta_x = v/h \quad \text{and} \quad \theta_y = u/h \tag{3.30}$$

Finally, for a slender column with restrained ends and symmetrical end conditions, the moment-curvature-thrust relationship is expressed in matrix form as:

$$\begin{Bmatrix} P \\ P\,(e_y + v) + k_x\,v/h \\ P\,(e_x + u) + k_y\,u/h \end{Bmatrix} = \begin{bmatrix} S_{11} & S_{12} & S_{13} \\ S_{21} & S_{22} & S_{23} \\ S_{31} & S_{32} & S_{33} \end{bmatrix} \begin{Bmatrix} \epsilon_o \\ \phi_x \\ \phi_y \end{Bmatrix} \tag{3.31a}$$

The equation presented above includes the effect of restrained end conditions by incorporating the additional terms of $k_x$ v/h and $k_y$ u/h into the bending moment equilibrium equations.

The expanded matrix representation of the moment-curvature-thrust relationship for the overall column becomes a non-linear system of equations that requires an iterative procedure to obtain a solution of the final displacements and internal forces.

The second order partial derivatives of the joint displacements are expressed in terms of the finite difference operators and the curvatures of each column segment in equations (3.4) and (3.5). They are expressed as follows:

$$\phi_{x\,i} = -\frac{\partial^2 u_i}{\partial x_i^2} = \frac{1}{h^2}\,(-u_{i-1} + 2u_i - u_{i+1}) \qquad (3.32)$$

$$\phi_{yi} = -\frac{\partial^2 v_i}{\partial y_i^2} = \frac{1}{h^2}\,(-v_{i-1} + 2v_i - v_{i+1}) \qquad (3.33)$$

Appropriate boundary conditions are introduced to account for the end conditions and proper modifications for a symmetrical case reduce the size of the matrix solution.

The second order effects are taken into account by calculating the external bending moments as the product of the axial compressive load times the sum of the eccentricity of the load and the lateral displacement. The incremental displacement control procedure takes the central column joint as the basic point to generate the deflected shape of the overall column and increase the control joint displacements by a preset value at each iteration cycle.

Residual stresses have been found to have no significant influence on the ultimate strength capacity of composite columns as indicated by Lachance (129). Therefore they are not included in the computational method presented in this chapter.

For the case of columns with pinned ends, the values of the rotational stiffness at the column ends given by $k_x$ and $k_y$ become zero and the basic moment-curvature-thrust equations of equilibrium may be expressed in the following form:

$$\begin{Bmatrix} P \\ P\ (e_y + v) \\ P\ (e_x + u) \end{Bmatrix} = \begin{bmatrix} S_{11} & S_{12} & S_{13} \\ S_{21} & S_{22} & S_{23} \\ S_{31} & S_{32} & S_{33} \end{bmatrix} \begin{Bmatrix} e_o \\ \phi_x \\ \phi_y \end{Bmatrix} \qquad (3.31b)$$

In an expanded form the above equation becomes the set of equations presented by Tsao (208), and has been solved by using a computer program coded in FORTRAN.

This computer program provides the ultimate axial load and bending moments at each iteration cycle and the axial deformation and the lateral displacements at each joint of the segmented column for every load level. Here the Author has developed the Method of Analysis for composite columns with both restrained and pinned ends.

Material properties and column cross section properties are also part of the major changes incorporated by the Author into the original computer program presented by Tsao(208). These changes properly reflect the composite column behavior under study.

The modified computer program "PROCOMP" is also coded in FORTRAN and adapted to study the composite column cross sections of a great variety.

They can be of symmetrically placed steel rebars and structural steel shapes of different configurations (I-shape, H-shape, C-shape, L-shape, T-shape, and many other symmetrically placed steel reinforcement).

To generate the appropriate input file with the column dimensions, concrete and steel material properties, steel rebars and structural steel shapes layout, and other parameters necessary to model the column cross section, the Author developes a preprocessor program written in BASIC, "PRECOMP", that provides an interactive way to create, edit, screenview, copy, and save the input data files that may be in turn later processed by the FORTRAN program "PROCOMP". The Author has incorporated the appropriate stress-strain curves for concrete, reinforcing steel and structural steel to model the composite column cross sections MC1, MC2, MC3, and MC4, respectively.

They were tested at the Structures Laboratory of NJIT. The columns are modeled by dividing them into a number of segments and the input file is processed until a convergence of the ultimate load is obtained. The accuracy of the results and the convergence criteria depend mainly on the number of elements and segments in the column which has been divided. At the same time, however, the computation time increases as the number of elements and segments are increased.

The stress-strain curves for reinforcing steel and structural steel were obtained by performing a tensile test in the Strength of Materials Laboratory of NJIT.

The piecewise linear curve for each type of steel is incorporated into the computer model by providing the stress and strain values of a selected number of segments that best describes the tensile stress-strain relationship of the appropriate steel reinforcement.

The basic values of the tensile stress-strain piece-wise relationship for the different types of steel rebars and structural steel are presented in Tables 3.1, 3.2, 3.3 and 3.4, respectively.

**Table 3.1** Tensile stress-strain test values for smooth steel rebar

| Segment | Stress (psi) | Strain (in/in) |
|---|---|---|
| 1 | 83,180 | 0.003639 |
| 2 | 89,923 | 0.005558 |
| 3 | 97,177 | 0.016114 |
| 4 | 99,815 | 0.02915 |
| 5 | 100,939 | 0.042785 |
| 6 | 100,939 | 0.120 |

**Table 3.2** Tensile stress-strain test values for deformed steel rebar

| Segment | Stress (psi) | Strain (in/in) |
|---|---|---|
| 1 | 69,570 | 0.003379 |
| 2 | 74,539 | 0.005118 |
| 3 | 83,483 | 0.016154 |
| 4 | 88,453 | 0.026271 |
| 5 | 93,422 | 0.041305 |
| 6 | 97,894 | 0.060819 |
| 7 | 99,882 | 0.076813 |
| 8 | 101,621 | 0.124796 |
| 9 | 101,621 | 0.125 |

**Table 3.3** Tensile stress-strain test values for cold-rolled structural steel

| Segment | Stress (psi) | Strain (in/in) |
|---|---|---|
| 1 | 80,146 | 0.003267 |
| 2 | 89,305 | 0.005533 |
| 3 | 90,221 | 0.053333 |
| 4 | 90,221 | 0.120 |

**Table 3.4** Tensile stress-strain test values for hot-rolled structural steel

| Segment | Stress(psi) | Strain (in/in) |
|---|---|---|
| 1 | 43,750 | 0.0014 |
| 2 | 43,851 | 0.0154 |
| 3 | 54,957 | 0.040667 |
| 4 | 61,483 | 0.080 |
| 5 | 67,208 | 0.13333 |
| 6 | 68,353 | 0.186667 |
| 7 | 68,467 | 0.293333 |
| 8 | 68,467 | 0.30 |

### 3.5 Computer Model Analytical Study and Results

The four composite column specimens tested at the Structures Laboratory of NJIT are analytically modeled in accordance with the material properties obtained from the control cylinders of the concrete. The same concrete is used to cast the columns. The stress-strain recorded values of the steel reinforcement are presented in Tables 3.1, 3.2, 3.3, and 3.4. The column cross section is divided in small areas as shown in Fig. 3.14.

The analysis is performed using the computer program "PROCOMP" at the Mainframe VAX computer system of NJIT. The great speed of this computer system allows completing the analysis in a very short period of time and the results can be saved for a later postprocessing, comparative analysis, and plotting.

A summary of the analytical results obtained from the computer modelling of the four composite column cross sections, namely MC1, MC2, MC3, and MC4, are

presented in Table 3.5. The test failure loads are compared to the ultimate loads calculated by the computer model, and they show a very good agreement.

These comparative good results confirm the accuracy and validity of the proposed computer model to predict the ultimate load of pin-ended composite columns under biaxial bending and axial compressive loads.

Plots of the Load-Deflection and Moment-Curvature Analytical Results obtained from the Theoretical Computer Model for column specimens MC1, MC2, MC3, and MC4 are presented in Figs. 3.6 to 3.13 respectively.

**Table 3.5** Comparative Analytical and Experimental Results for Column Specimens MC1, MC2, MC3, and MC4

| Spec. No. | Length L (in) | Eccentricity at balanced condition | | Eccentricity of applied axial load | | Max. $P_t$ (Kips.) | Max. $P_a$ (Kips.) | $P_t/P_a$ |
|---|---|---|---|---|---|---|---|---|
| | | $e_{bx}$ | $e_{by}$ | $e_x$ | $e_y$ | | | |
| MC1 | 32 | 1.697 | 1.896 | 1.50 | 1.50 | 6.33 | 6.80 | 0.931 |
| MC2 | 48 | 1.805 | 2.012 | 1.25 | 1.25 | 5.95 | 6.154 | 0.967 |
| MC3 | 48 | 1.977 | 3.688 | 1.0 | 1.0 | 6.53 | 6.706 | 0.974 |
| MC4 | 48 | 1.893 | 3.402 | 1.50 | 1.50 | 4.95 | 4.829 | 1.025 |

* The dial gage readings for specimen MC2 measuring central displacements were not properly recorded.

Average of $(P_t/P_a)$ = 0.974

$P_t$: denotes Maximum Axial Experimental Load
$P_a$: denotes Maximum Axial Analytical Load

Virdi and Dowling (222) in 1973, presented the results of ultimate loads and lateral deflections of nine pinned-ended composite columns tested under axial loads and biaxial eccentricities in a single curvature. In 1976, Virdi and Dowling (221) presented a method to calculate ultimate loads of biaxially restrained columns.

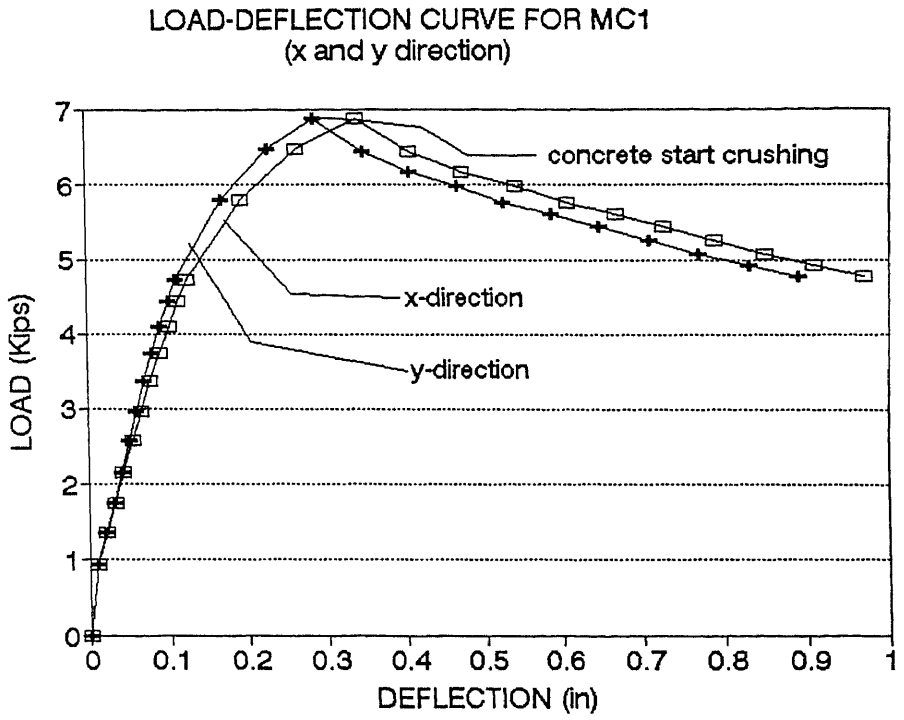


**Figure 3.6** Analytical Load-Deflection curves for column MC1

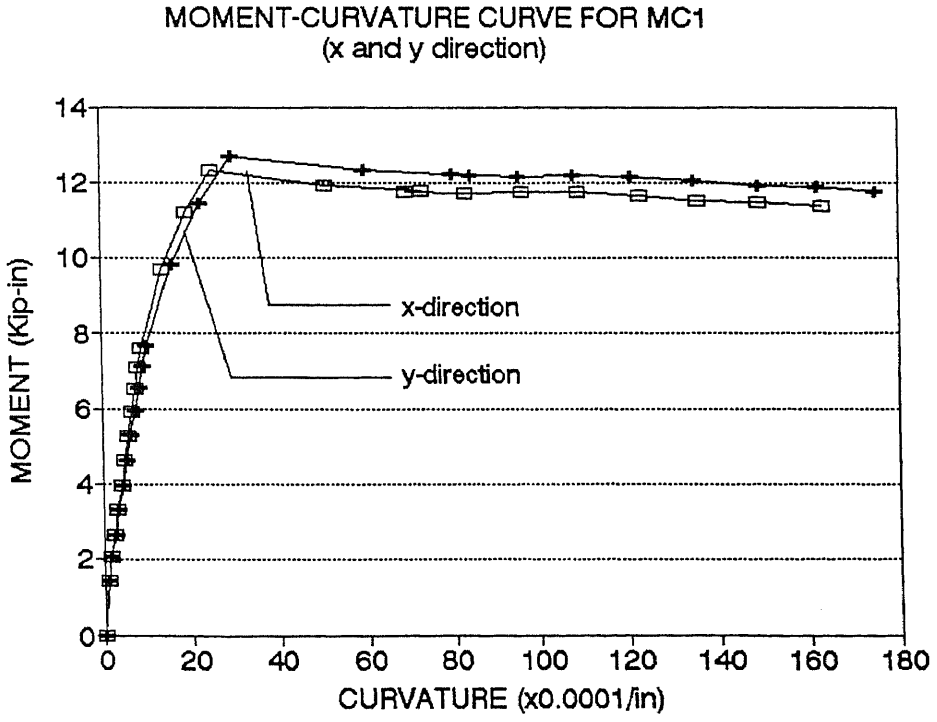


**Figure 3.7** Analytical Moment-Curvature curves for column MC1

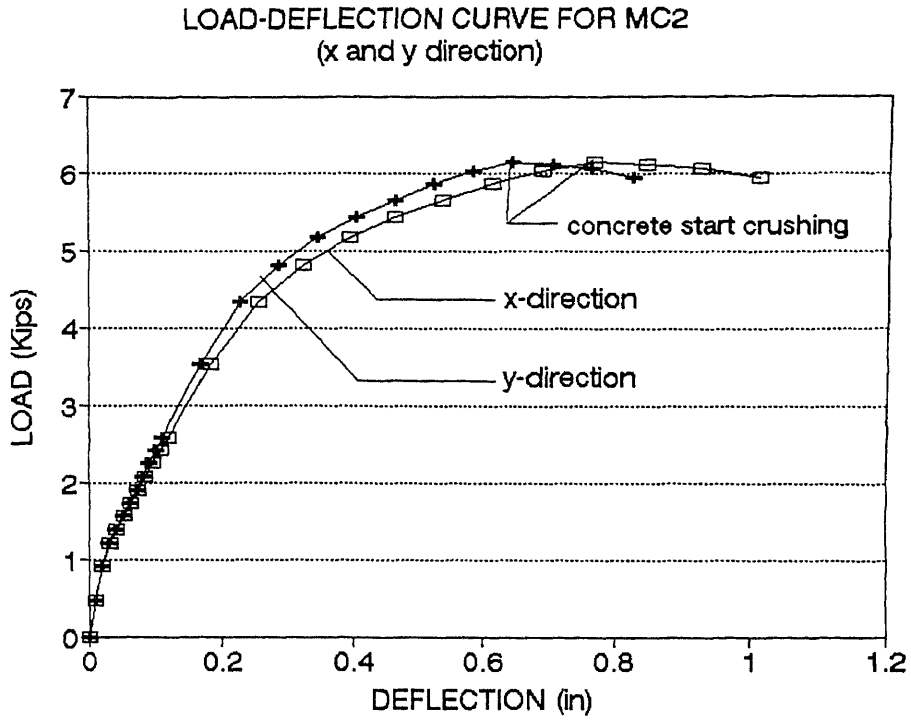


**Figure 3.8** Analytical Load-Deflection curves for column MC2

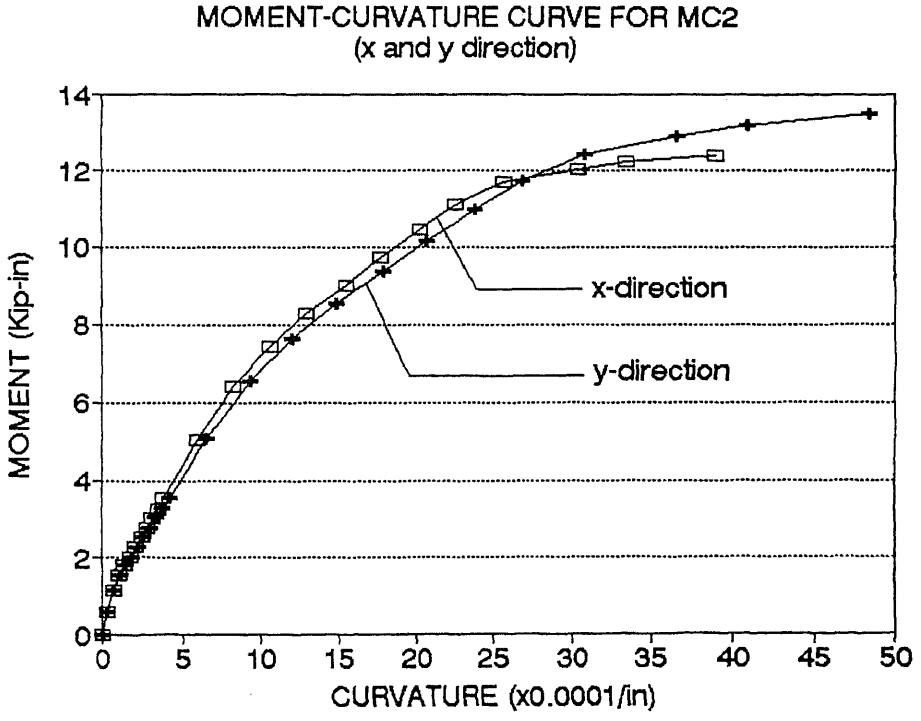


**Figure 3.9** Analytical Moment-Curvature curves for column MC2

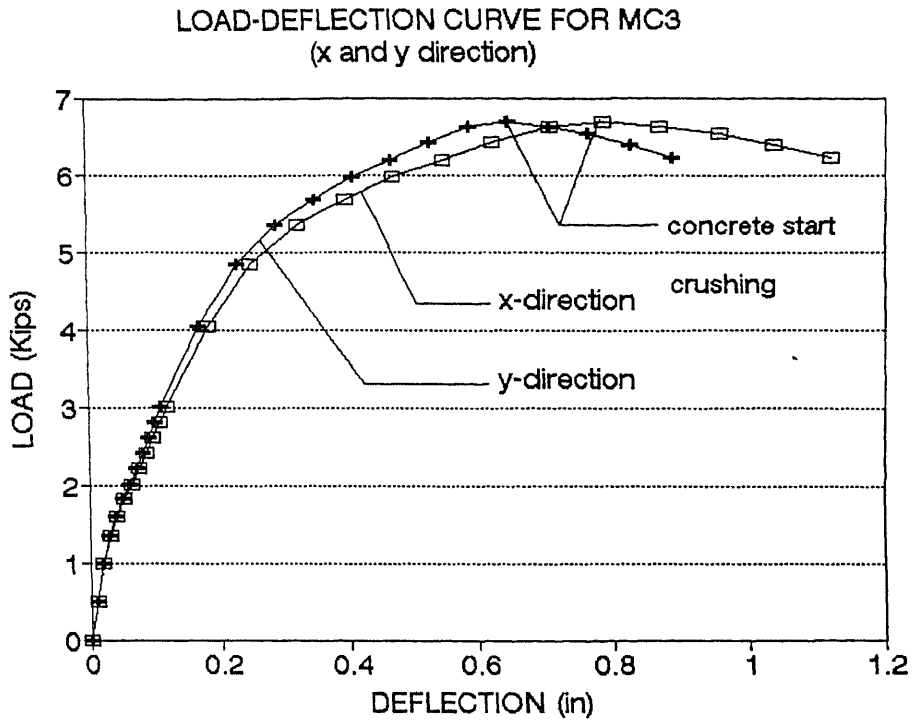


**Figure 3.10** Analytical Load-Deflection curves for column MC3

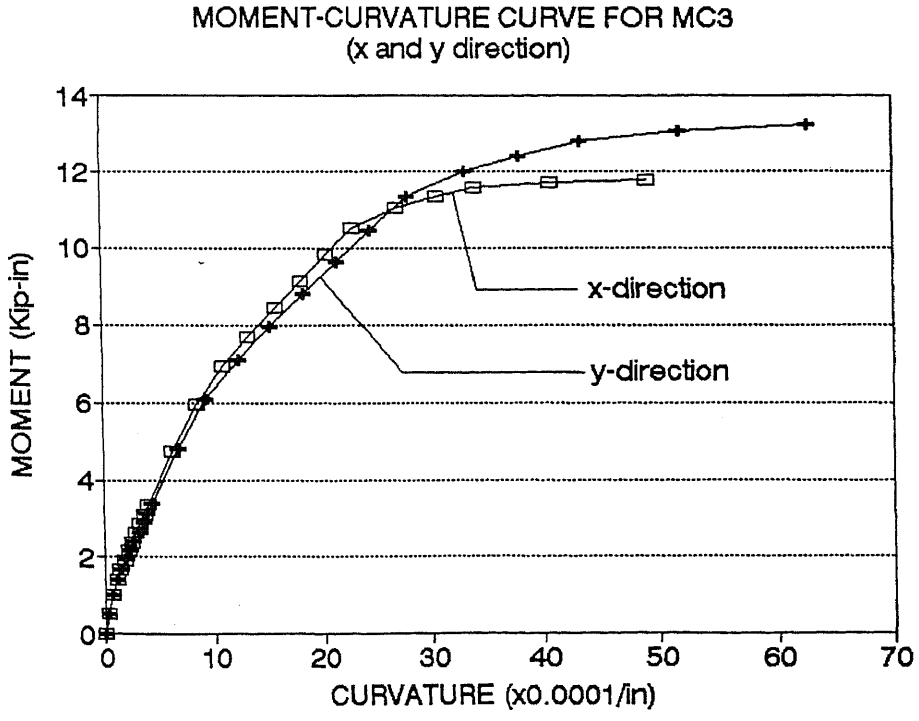


**Figure 3.11** Analytical Moment-Curvature curves for column MC3

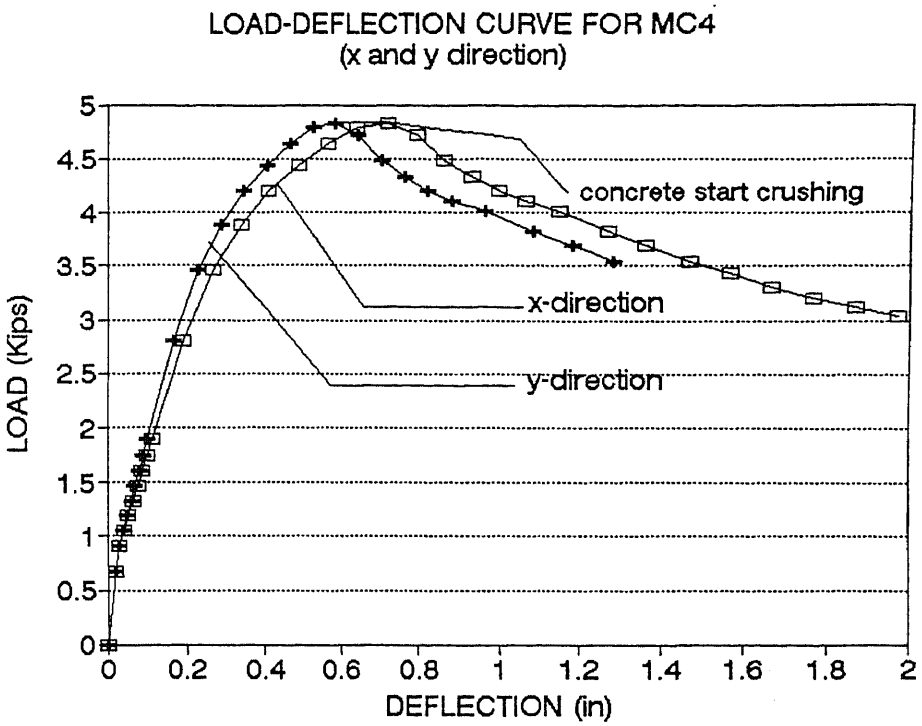


**Figure 3.12** Analytical Load-Deflection curves for column MC4

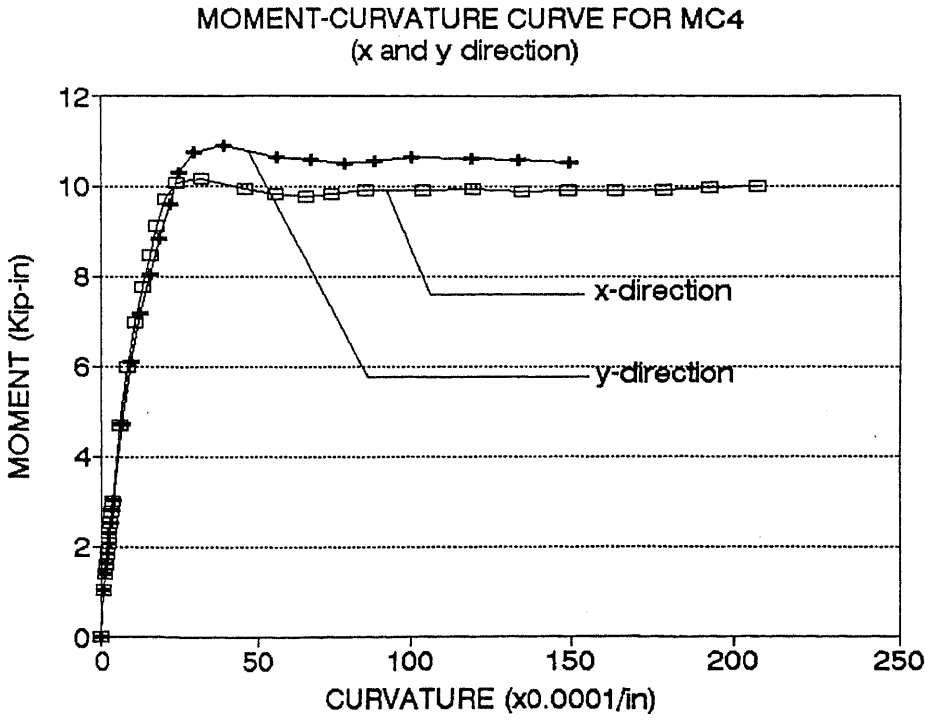


**Figure 3.13** Analytical Moment-Curvature curves for column MC4

The Author models the nine composite columns tested by Virdi and Dowling (222) by dividing the cross section of the column specimens into small elements as shown in Fig. 3.15. The input files are created and processed for the column specimens A to I using the FORTRAN computer program "PROCOMP. The length of the column specimens, eccentricity of the applied axial load, and the strength of the concrete for the nine columns A to I, are presented in Table 3.6. The value of the yield stress for the steel used here is $f_y$ = 33 ksi.

**Table 3.6** Dimensions and load eccentricities for tests on biaxially loaded composite columns by Virdi and Dowling

| Columns 10"x10" | L inch. | $e_x$ inch. | $e_y$ inch. | $\sigma_c$ tonf/sq.in. | $f'_c$ psi |
|---|---|---|---|---|---|
| A | 72 | 2.50 | 1.45 | 2.56514 | 5,746 |
| B | 72 | 5.00 | 2.90 | 2.45603 | 5,502 |
| C | 72 | 7.50 | 4.35 | 2.56514 | 5,746 |
| D | 144 | 2.50 | 1.45 | 2.71750 | 6,087 |
| E | 144 | 5.00 | 2.90 | 2.56514 | 5,746 |
| F | 144 | 7.50 | 4.35 | 2.71750 | 6,087 |
| G | 288 | 2.50 | 1.45 | 2.35809 | 5,282 |
| H | 288 | 5.00 | 2.90 | 2.57030 | 5,758 |
| I | 288 | 7.50 | 4.35 | 2.79453 | 6,260 |

Nine composite columns A to I, tested by Virdi and Dowling (222), have a typical square 10"x10" cross section reinforced with a 6"x6"x15.7 lbs/ft structural steel section encased in 2 inches of concrete and four 1/2" diameter rebars, one at each corner and with a 3/4" clear cover. The specimens were loaded in symmetrical biaxial bending and axial compressive load and in single curvature.

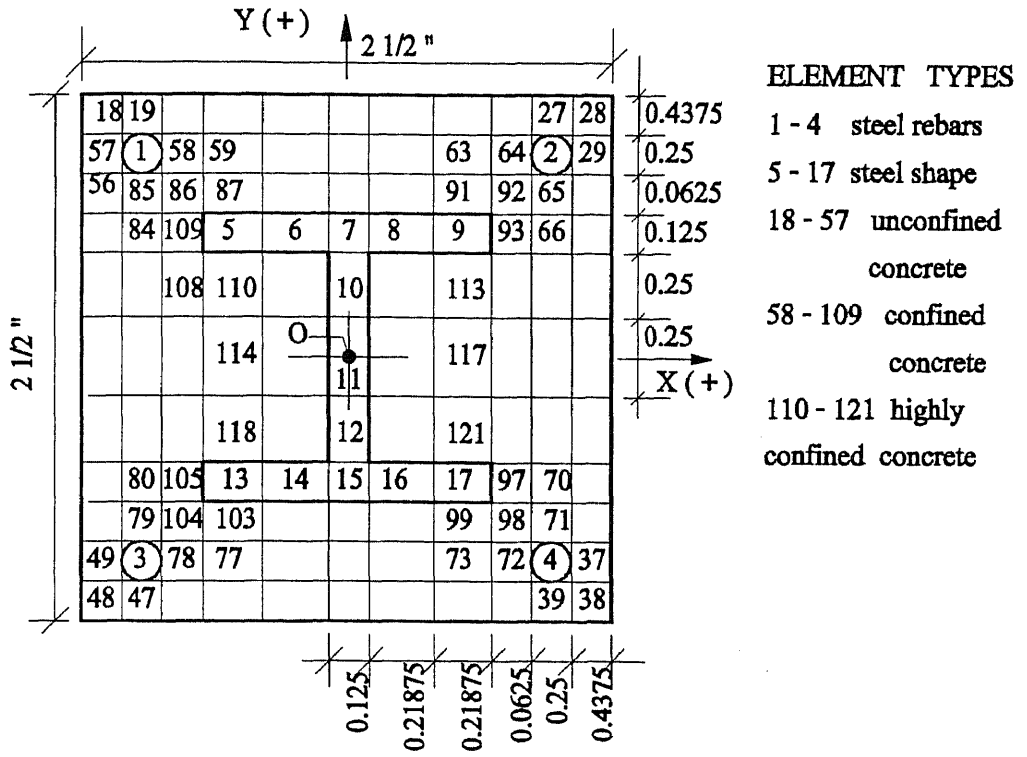


**Figure 3.14** Cross section model for Specimens MC1, MC2, MC3, and MC4

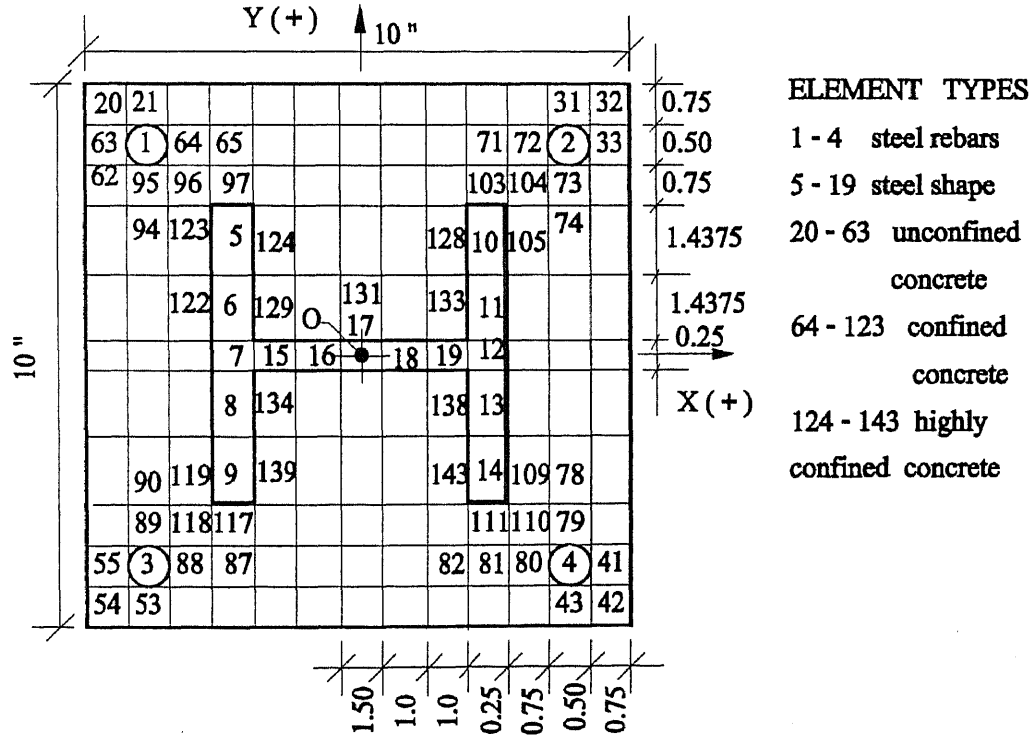


**Figure 3.15** Cross section model for Specimens CCA thru CCI

They reported to have obtained test results to be in good agreement with their analytical ultimate load and load-deflection curves. The Author models and analyzes the nine composite column specimens A to I by using the present computer program "PROCOMP". The results of the ultimate load obtained by the computer method described in this chapter are presented in Table 3.7. Morino, Matsui, and Watanabe (147), also presented the experimental results of biaxially loaded composite columns.

The concrete-encased wide flange steel sections were used. The column specimens had a 160x160 mm. concrete square cross section encasing a rolled steel H-section of 100x100x6x8 mm. and four corner deformed bars of 6 mm. diameter and rectangular ties of 4mm. diameter evenly spaced at a pitch of 150 mm.

The Author modeled the column specimens tested by Morino et al. (147) using the appropriate parameters of material properties, specimens dimensions, steel shape and rebars layout. The appropriate unit conversion factors to perform the computer analysis and compare and verify the validity of the computer method of analysis of biaxially loaded composite columns are also presented here. The Morino et al.(147) column specimens dimensions, slenderness ratio, and eccentricities of the applied axial load are shown in Table 3.8.

In Table 3.8, the $\lambda_g$ is the slenderness ratio of the concrete gross section of the composite column specimen, and $\theta$ is the angle of application of the axial compressive load measured from the major axis of the cross section. $\lambda_g = L/r = L/(0.3B)$, $e_x = e \cos \theta$ ; $e_y = e \sin \theta$. Table 3.9 shows the average values of the material properties from the tensile tests of the steel shape and rebar and the concrete cylinder compressive tests (in English units) that are used by the Author in the computer model.

The Author divides the composite column cross section tested by Morino et al. (147) into small elements as shown in Fig. 3.16 and the FORTRAN computer program "PROCOMP" is used to study the behavior of four types of column specimens: A4, A8, B4, B8, C4, C8, D4 and D8.

**Table 3.7** Comparative Analytical and Experimental results for biaxially loaded composite columns tested by Virdi and Dowling

| Column | $P_{test}$ tonf | $P_{xy}$ tonf | $P_{NJIT}$ tonf | $P_{test}/P_{xy}$ | $P_{test}/P_{NJIT}$ |
|---|---|---|---|---|---|
| A | 126 | 133.312 | 128.15 | 0.945146 | 0.9831 |
| B | 65 | 68.654 | 65.76 | 0.946775 | 0.9884 |
| C | 47.5 | 46.009 | 43.5 | 1.032408 | 1.0919 |
| D | 93 | 107.391 | 105.27 | 0.865994 | 0.8835 |
| E | 57.5 | 58.240 | 55.84 | 0.987293 | 1.0298 |
| F | 42 | 40.686 | 38.68 | 1.032283 | 1.0858 |
| G | 67 | 52.836 | 54.81 | 1.268081 | 1.2223 |
| H | 35.5 | 37.757 | 34.90 | 0.965802 | 1.0172 |
| I | 29.5 | 28.732 | 25.9 | 1.026731 | 1.1389 |
| $P_{test}$: Ultimate test load by Virdi and Dowling (222)<br>$P_{xy}$: Analytical ultimate load by Virdi and Dowling method (221)<br>$P_{NJIT}$: Analytical ultimate load by the "PROCOMP" computer<br>Conversion factor: 1 tonf = 2,240.1lbs | | | mean =<br>standard deviation = | 0.998097<br>0.094 | 1.04072<br>0.086 |

The Modulus of Elasticity of steel is $E_s = 29.879 \times 10^6$ psi. Three experimental parameters were varied for the tested column specimens: a) the slenderness ratio, b) the eccentricity of the applied axial compressive load, and c) the angle location of the applied load. The results of the maximum load carrying capacity obtained from the computer model presented by the Author and the experimental and theoretical values

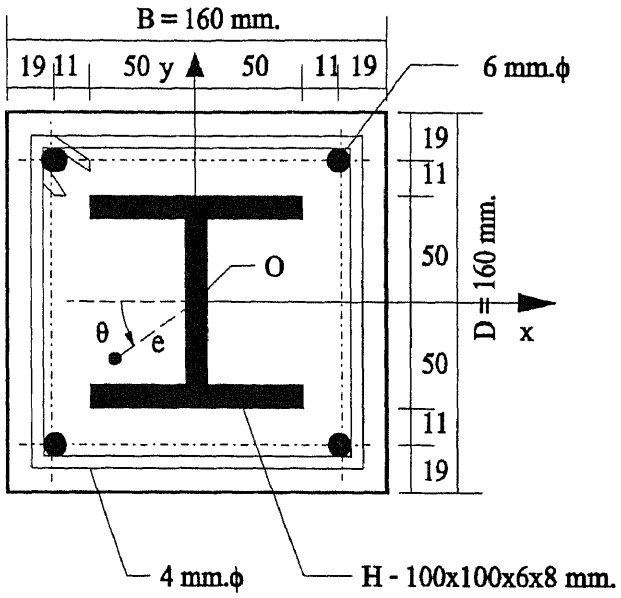


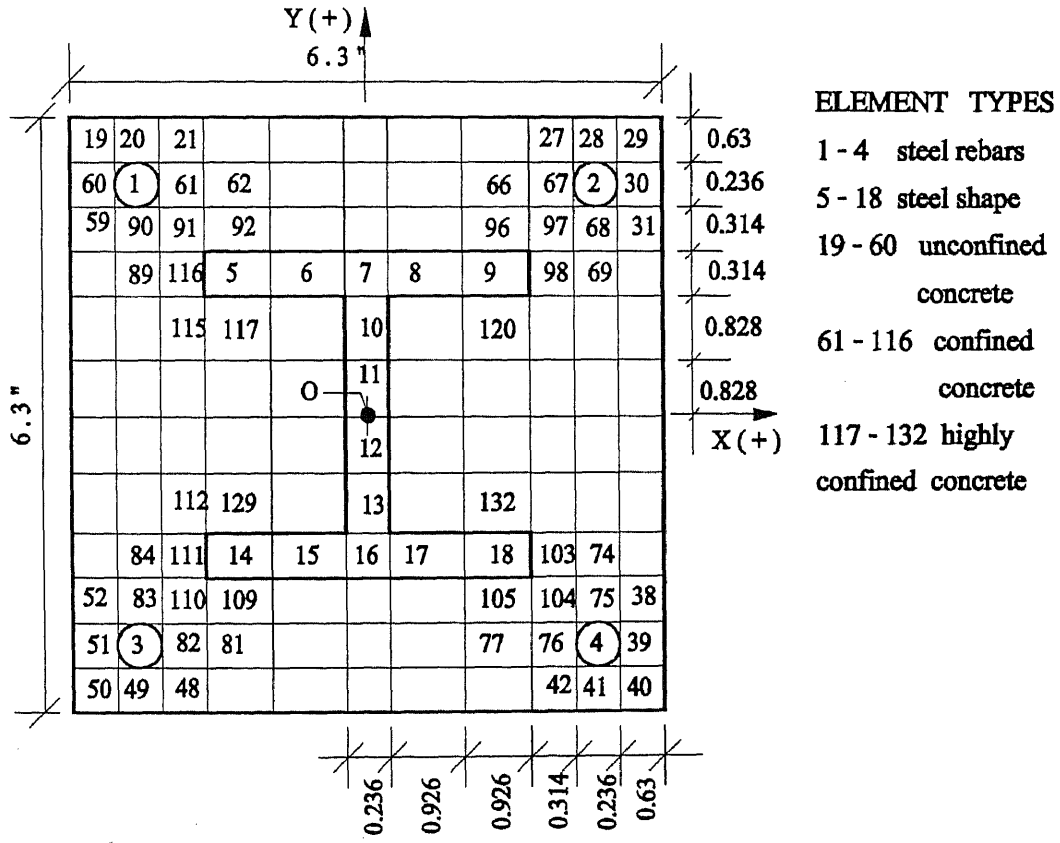


**Figure 3.16** Composite column model for specimens tested by Morino et al.

obtained by Morino, Matsui, and Watanabe (147) together with the comparative ratio of Analytical load to Test load are shown in Table 3.10. It can be seen that excellent agreement between theoretical and experimental ultimate load is obtained.

**Table 3.8** Dimensions and load eccentricities for biaxially loaded composite columns tested by Morino et al.

| Column | $\lambda_g$ = L/r r=0.3B | L inch. | θ (deg.) | e mm. | $e_x$ inch. | $e_y$ inch. |
|---|---|---|---|---|---|---|
| A4-00 | 20 | 37.8 | 0 | 40 | 1.5748 | 0 |
| A4-30 | 20 | 37.8 | 30 | 40 | 1.3638 | 0.7874 |
| A4-45 | 20 | 37.8 | 45 | 40 | 1.1136 | 1.1136 |
| A4-60 | 20 | 37.8 | 60 | 40 | 0.7874 | 1.3638 |
| A4-90 | 20 | 37.8 | 90 | 40 | 0 | 1.5748 |
| B4-00 | 50 | 94.5 | 0 | 40 | 1.5748 | 0 |
| B4-30 | 50 | 94.5 | 30 | 40 | 1.3638 | 0.7874 |
| B4-45 | 50 | 94.5 | 45 | 40 | 1.1136 | 1.1136 |
| B4-60 | 50 | 94.5 | 60 | 40 | 0.7874 | 1.3638 |
| B4-90 | 50 | 94.5 | 90 | 40 | 0 | 1.5748 |
| C4-00 | 75 | 141.75 | 0 | 40 | 1.5748 | 0 |
| C4-30 | 75 | 141.75 | 30 | 40 | 1.3638 | 0.7874 |
| C4-45 | 75 | 141.75 | 45 | 40 | 1.1136 | 1.1136 |
| C4-60 | 75 | 141.75 | 60 | 40 | 0.7874 | 1.3638 |
| C4-90 | 75 | 141.75 | 90 | 40 | 0 | 1.5748 |
| D4-00 | 100 | 189 | 0 | 40 | 1.5748 | 0 |
| D4-30 | 100 | 189 | 30 | 40 | 1.3638 | 0.7874 |
| D4-45 | 100 | 189 | 45 | 40 | 1.1136 | 1.1136 |
| D4-60 | 100 | 189 | 60 | 40 | 0.7874 | 1.3638 |
| D4-90 | 100 | 189 | 90 | 40 | 0 | 1.5748 |

The values of $\eta_{max}$ for each specimen were obtained from the tabulated values shown in Fig. 9 of Reference (147).

**Table 3.8** (cont.) Dimensions and load eccentricities for tests on biaxially loaded composite columns by Morino et al.

| Column | $\lambda_g$ = L/r r=0.3B | L inch. | θ (deg.) | e mm. | $e_x$ inch. | $e_y$ inch. |
|---|---|---|---|---|---|---|
| A8-00 | 20 | 37.8 | 0 | 75 | 2.9528 | 0 |
| A8-30 | 20 | 37.8 | 30 | 75 | 2.5572 | 1.4764 |
| A8-45 | 20 | 37.8 | 45 | 75 | 2.0879 | 2.0879 |
| A8-60 | 20 | 37.8 | 60 | 75 | 1.4764 | 2.5572 |
| A8-90 | 20 | 37.8 | 90 | 75 | 0 | 2.9528 |
| B8-00 | 50 | 94.5 | 0 | 75 | 2.9528 | 0 |
| B8-30 | 50 | 94.5 | 30 | 75 | 2.5572 | 1.4764 |
| B8-45 | 50 | 94.5 | 45 | 75 | 2.0879 | 2.0879 |
| B8-60 | 50 | 94.5 | 60 | 75 | 1.4764 | 2.5572 |
| B8-90 | 50 | 94.5 | 90 | 75 | 0 | 2.9528 |
| C8-00 | 75 | 141.75 | 0 | 75 | 2.9528 | 0 |
| C8-30 | 75 | 141.75 | 30 | 75 | 2.5572 | 1.4764 |
| C8-45 | 75 | 141.75 | 45 | 75 | 2.0879 | 2.0879 |
| C8-60 | 75 | 141.75 | 60 | 75 | 1.4764 | 2.5572 |
| C8-90 | 75 | 141.75 | 90 | 75 | 0 | 2.9528 |
| D8-00 | 100 | 189 | 0 | 75 | 2.9528 | 0 |
| D8-30 | 100 | 189 | 30 | 75 | 2.5572 | 1.4764 |
| D8-45 | 100 | 189 | 45 | 75 | 2.0879 | 2.0879 |
| D8-60 | 100 | 189 | 60 | 75 | 1.4764 | 2.5572 |
| D8-90 | 100 | 189 | 90 | 75 | 0 | 2.9528 |

The value of the maximum experimental load obtained by Morino et al.(147) was calculated by using the following expression:

$$\eta_{max} = N / f'_c B^2 ,$$

where $N = P_{exp.}$, $f'_c$ is the concrete compressive strength of specimen, and B is a column width. The Author also calculates the comparative values of mean and

standard deviations for each group of column specimens with the same slenderness ratio and the results are presented in Table 3.11.

**Table 3.9** Material properties for column specimens tested by Morino et al.

| Column specimen | $\sigma_y$ psi | $e_y$ | $\sigma_u$ psi | $e_u$ | $f'_c$ psi |
|---|---|---|---|---|---|
| A4 | 47,285 | 0.001583 | 63,602 | 0.2465 | 3,060 |
| A8 | 48,663 | 0.001629 | 63,892 | 0.2415 | 4,874 |
| B4 | 46,197 | 0.001546 | 63,602 | 0.2470 | 3,394 |
| B8 | 49,098 | 0.001643 | 64,473 | 0.19 | 4,830 |
| C4 | 45,182 | 0.001512 | 62,079 | 0.238 | 3,380 |
| C8 | 48,880 | 0.001636 | 63,892 | 0.239 | 3,568 |
| D4 | 47,285 | 0.001583 | 63,530 | 0.2535 | 3,075 |
| D8 | 48,590 | 0.001626 | 63,892 | 0.243 | 3,322 |
| SB | 56,132 | 0.001879 | 82,386 | 0.162 | --- |

It is noted that some of the calculated values of $P_{exp.}$ from the $\eta_{max}$ coefficients given by Morino et al. (147) in Fig. 9 show very abrupt variations. They are not reasonable correlated with the most logical and expected values of maximum axial compressive loads for an increasing variation of the angle of the biaxial load.

It can be concluded from the values of the maximum axial load obtained by the present computer method proposed by the Author that the ultimate strength or maximum capacity increases with the increase in the value of the angle $\theta$ of the biaxially loaded composite columns.

The Author has achieved a very good correlation between the experimental maximum load capacity for the column specimens tested by Morino et al. (147)

and the analytical values obtained by using the present computer method presented in this chapter.

**Table 3.10** Comparative Analytical and Experimental ultimate loads obtained by Morino et al. and Author's computer study

| Column | $\eta_{max}$ | $P_{exp.}$ (Kips) | $P_{NJIT}$ (Kips) | $P_{exp.}/P_{NJIT}$ | $P_{exp.}/P_{theo.}$ |
|---|---|---|---|---|---|
| A4-00 | 0.925 | 112.34 | 105.56 | 1.064 | 0.952 |
| A4-30 | 0.95 | 115.38 | 109.51 | 1.053 | 0.98 |
| A4-45 | 0.96 | 116.59 | 115.29 | 1.01 | 0.862 |
| A4-60 | 0.97 | 117.81 | 121.08 | 0.971 | 1.00 |
| A4-90 | 1.37 | 166.39 * | 128.8 | 1.299 | 0.833 |
| B4-00 | 0.619 | 83.38 | 76.41 | 1.092 | 0.99 |
| B4-30 | 0.655 | 88.23 | 80.88 | 1.091 | 0.944 |
| B4-45 | 0.65 | 87.56 | 85.66 | 1.022 | 1.00 |
| B4-60 | 0.728 | 98.07 | 92.88 | 1.056 | 0.971 |
| B4-90 | 0.84 | 113.16 | 111.49 | 1.015 | 0.98 |
| C4-00 | 0.46 | 61.71 * | 51.52 | 1.198 | 0.99 |
| C4-30 | 0.475 | 63.72 | 58.35 | 1.092 | 0.99 |
| C4-45 | 0.51 | 68.42 | 62.36 | 1.098 | 1.00 |
| C4-60 | 0.57 | 76.47 | 68.12 | 1.111 | 0.943 |
| C4-90 | 0.69 | 92.57 | 88.36 | 1.047 | 1.031 |
| D4-00 | 0.38 | 46.38 * | 37.65 | 1.232 | 0.935 |
| D4-30 | 0.37 | 45.16 | 40.36 | 1.111 | 1.01 |
| D4-45 | 0.385 | 46.99 | 43.00 | 1.093 | 0.943 |
| D4-60 | 0.405 | 49.43 | 47.2 | 1.047 | 0.971 |
| D4-90 | 0.53 | 64.69 | 61.82 | 1.046 | 1.01 |

$P_{exp}$ = the experimentalor testing ultimate load obtained by Morino et al.
$P_{NJIT}$= the analytical ultimate load obtained by the Author's equation of failure surface
$P_{theo}$ = is the theoretical ultimate load obtained by Morino et al.

Most of the computed loads are below the experimental maximum load give a lower bound solution for the biaxially loaded column specimens tested. From the practical point of view it is considered as conservative and safe for design purposes.

**Table 3.10** (cont.) Comparative Analytical and Experimental ultimate loads obtained by Morino et al. and Author's computer study

| Column | $\eta_{max}$ | $P_{exp.}$ (Kips) | $P_{NJIT}$ (Kips) | $P_{exp.}/P_{NJIT}$ | $P_{exp.}/P_{theo}$ |
|---|---|---|---|---|---|
| A8-00 | 0.40 | 77.38 | 73.94 | 1.046 | 1.042 |
| A8-30 | 0.438 | 84.73 | 78.94 | 1.073 | 0.98 |
| A8-45 | 0.44 | 85.12 | 82.65 | 1.030 | 0.99 |
| A8-60 | 0.52 | 100.60 * | 88.47 | 1.136 | 0.917 |
| A8-90 | 0.605 | 117.04 | 109.91 | 1.064 | 0.99 |
| B8-00 | 0.305 | 58.47 | 57.53 | 1.016 | 1.053 |
| B8-30 | 0.309 | 59.24 | 60.35 | 0.981 | 1.031 |
| B8-45 | 0.345 | 66.14 | 64.13 | 1.031 | 1.00 |
| B8-60 | 0.385 | 73.81 | 70.48 | 1.047 | 0.98 |
| B8-90 | 0.49 | 93.94 | 91.04 | 1.032 | 1.01 |
| C8-00 | 0.285 | 40.36 | 39.05 | 1.033 | 1.042 |
| C8-30 | 0.28 | 39.66 | 40.91 | 0.969 | 1.075 |
| C8-45 | 0.31 | 43.9 | 43.77 | 1.003 | 1.00 |
| C8-60 | 0.308 | 43.62 * | 48.44 | 0.901 | 1.099 |
| C8-90 | 0.47 | 66.56 | 65.77 | 1.012 | 1.053 |
| D8-00 | 0.238 | 31.38 | 29.36 | 1.068 | 1.042 |
| D8-30 | 0.20 | 26.37 * | 30.7 | 0.859 | 1.075 |
| D8-45 | 0.25 | 32.96 | 32.74 | 1.007 | 1.053 |
| D8-60 | 0.27 | 35.6 | 36.17 | 0.984 | 1.064 |
| D8-90 | 0.378 | 49.85 * | 43.52 | 1.145 | 1.075 |

The Author has also extended his study on the Behavior of Composite columns to the case of Built-Up Composite Columns. This type of composite columns has been used in the USA since the very early 1900's.

**Table 3.11** Comparative results of mean and standard deviations for column specimens studied by Morino et al. and Author

| Column | $\lambda_g$ = L/r r=0.3B | $P_{exp.}/P_{NJIT}$ | | $P_{exp.}/P_{theo.}$ | |
|---|---|---|---|---|---|
| | | mean | standard deviation | mean | standard deviation |
| All | ---- | 1.042 | 0.036 | 0.998 | 0.045 |
| A4 - A8 | 20 | 1.037 | 0.031 | 0.972 | 0.055 |
| B4 - B8 | 50 | 1.037 | 0.030 | 0.995 | 0.029 |
| C4 - C8 | 75 | 1.044 | 0.044 | 1.015 | 0.038 |
| D4 - D8 | 100 | 1.049 | 0.038 | 1.011 | 0.041 |

Experimental tests were carried out by some investigators such as Emperger (58), Burr (24), and Mensch (140) among others. These concentric and eccentrically loaded built-up sections consisted of two or more rolled steel sections or channels and angles latticed or battened together.

The computer method presented earlier in this chapter is used again to model and obtain the maximum axial load carrying capacity of uniaxially and biaxially loaded built-up composite columns.

Bridge and Roderick (29) in 1978 at the Sydney University, Australia, performed a series of tests on build-up composite columns. All the column specimens had the same cross section, consisting of two C3x5 steel channels encased in concrete as shown in Fig. 3.17. The material properties are as shown in Table 3.12.

The Author modeled the composite column specimens tested by Bridge and Roderick (29) by dividing the column cross section into small elements as shown in Fig. 3.17. Table 3.13 presents the column dimensions and eccentricity of the applied load and the obtained analytical maximum axial load carrying capacity values for each column together with the comparative results with the test loads.

**Table 3.12** Material properties for column specimens tested by Bridge and Roderick

| Column specimen | Steel | | Concrete | | |
|---|---|---|---|---|---|
| | $\sigma_y$ (psi) | $e_y$ | $f'_c$ (psi) | $e_{co}$ | $f_{ct}$ (psi) |
| CC1 | 40,300 | 0.00139 | 4,020 | 0.00139 | 450 |
| CC2 | 40,300 | 0.00139 | 4,370 | 0.00138 | 430 |
| CC3 | 44,200 | 0.00152 | 4,450 | 0.00137 | 480 |
| CC4 | 42,900 | 0.00148 | 3,960 | 0.00124 | 410 |
| CC5 | 40,600 | 0.0014 | 3,710 | 0.00126 | 440 |
| CC8 | 40,800 | 0.0014 | 3,680 | 0.001353 | 300 |
| CC9 | 40,700 | 0.0014 | 3,560 | 0.00123 | 350 |
| CC10 | 41,000 | 0.00141 | 3,430 | 0.00121 | 330 |

The Author has found a great discrepancy between the test and analytical maximum load for column specimen CC4 (marked with *).

It is interesting to note that column specimen CC8 was fabricated by using a set of two steel channels previously tested as bare steel columns under eccentrically applied compressive load and labeled as specimen CC6 by Bridge and Roderick (29).

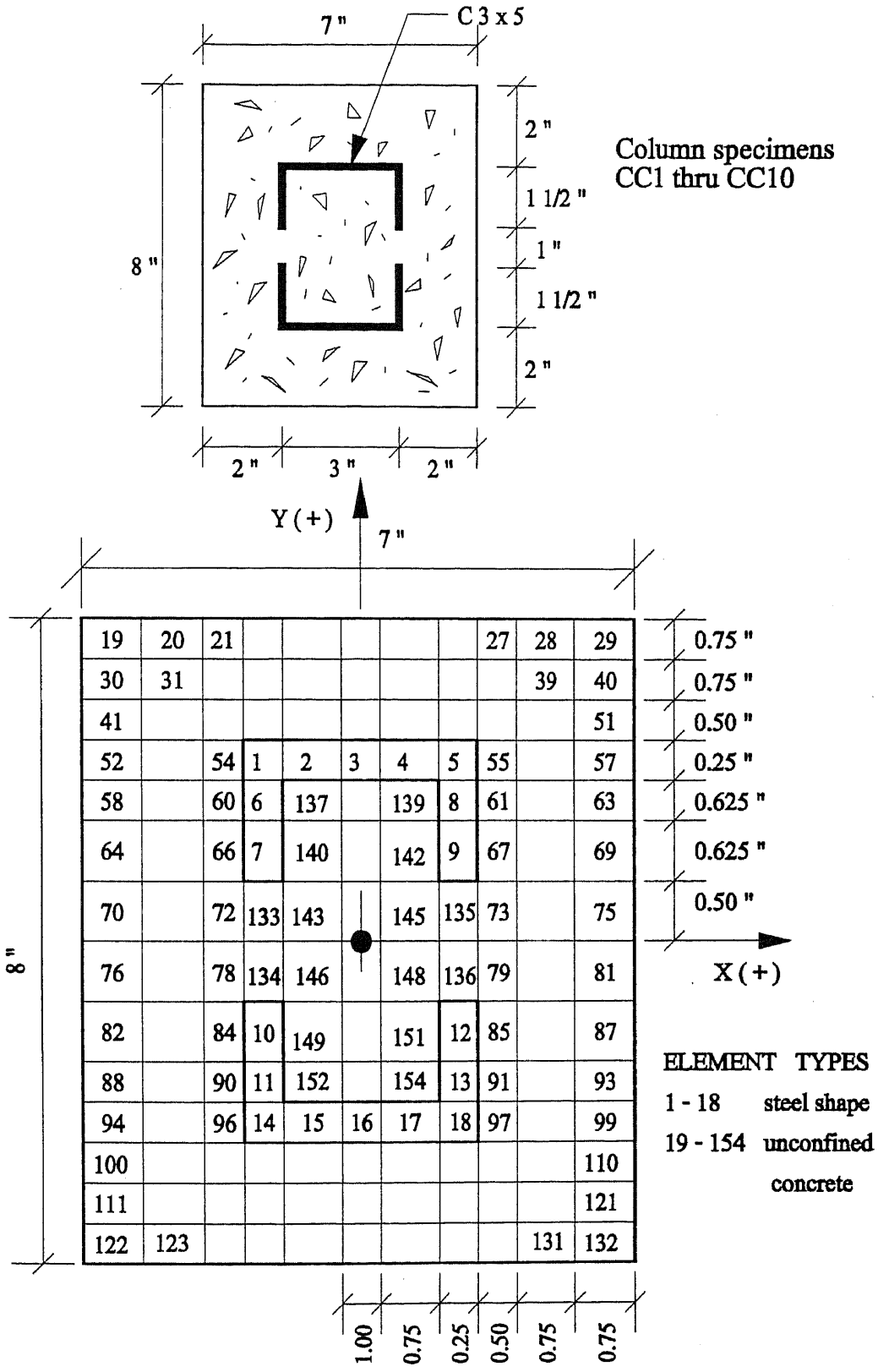


**Figure 3.17** Composite column model for specimens tested by Bridge and Roderick

The maximum reported test load for specimen CC8 (marked with **) clearly shows the influence of large negative residual stresses left in the steel section by a previous history of axial and bending stresses.

Taylor et al. (217) in 1983, presented the results of tests done on a new type of composite column subjected to concentric compressive load and to uniaxial bending and axial compressive loads. The new type of composite column proposed by Taylor et al. (217,238) is of an unusual cross section, consisting of two channels joined together using welded battens and filled with concrete to form a rectangular shaped cross section. Nine large-scale composite columns of the type described above were tested by Taylor et al. (217) at the University of Manchester, England in 1983. The specimen dimensions and material properties are given in Table 3.14.

**Table 3.13** Dimensions, load eccentricity and comparative ultimate loads for specimens tested by Bridge and Roderick

| Column | L inch. | $e_x$ inch. | $e_y$ inch. | $P_{test}$(29) (Kips) | $P_{NJIT}$ (Kips) | $P_{test}/P_{NJIT}$ |
|---|---|---|---|---|---|---|
| CC1 | 84 | 0.0 | 0.0 | 270 | 261.73 | 1.04 |
| CC2 | 84 | 0.0 | 0.8 | 196 | 207.15 | 0.95 |
| CC3 | 84 | 0.0 | 1.5 | 159 | 152.9 | 1.04 |
| CC4 | 84 | 1.5 | 0.0 | 117 * | 89.56 | 1.31 * |
| CC5 | 84 | 0.604 | 0.525 | 158 | 164.95 | 0.96 |
| CC8 | 120 | 0.0 | 0.8 | 147 ** | 169.56 | 0.87 ** |
| CC9 | 120 | 0.0 | 1.5 | 110 | 116.61 | 0.94 |
| CC10 | 120 | 0.0 | 0.8 | 150 | 159.52 | 0.94 |

mean = 0.976

standard deviation = 0.043

* and ** denotes values not included to calculate the mean and standard deviation above

The Author modeled the composite columns tested by Taylor et al. (217), according to the given dimensions and material properties presented in Taylor's experimental test report.

The new type of composite column specimens are analyzed by the Author using the FORTRAN computer program "PROCOMP". The overall column cross section dimensions and layout of the steel channels are shown in Fig. 3.18.

The cross section of each typical composite column specimen is divided into small elements as shown in Fig. 3.19 with the corresponding material properties assigned to the steel channel elements and to the unconfined concrete elements filling the space between the two steel channels.

**Table 3.14** Dimensions and Material Properties for column specimens tested by Taylor et al.

| Column | L (inch.) | Steel Shape | Steel | | Concrete | | |
|---|---|---|---|---|---|---|---|
| | | | $\sigma_y$ | $\varepsilon_y$ | $f'_c$ | $\varepsilon_{co}$ | $f_{ct}$ |
| CT1 | 106.3 | C6x13 | 38,727 | 0.0013 | 6,527 | 0.00196 | 650 |
| CT2 | 106.3 | C6x13 | 39,162 | 0.00132 | 5,367 | 0.00213 | 530 |
| CT3 | 106.3 | C6x13 | 38,872 | 0.00131 | 5,077 | 0.00211 | 500 |
| CT4 | 106.3 | C8x18 | 39,742 | 0.00134 | 5,947 | 0.00240 | 590 |
| CT5 | 106.3 | C8x18 | 40,468 | 0.00136 | 5,512 | 0.00350 | 680 |
| CT6 | 106.3 | C10x20 | 48,880 | 0.00164 | 5,947 | 0.0030 | 590 |
| CT7 | 106.3 | C10x20 | 48,300 | 0.00162 | 6,817 | 0.00267 | 680 |
| CT8 | 106.3 | C6x13 | 47,865 | 0.00161 | 5,657 | 0.0020 | 560 |

The columns were subjected to axial compressive load (CT1 and CT8) and to uniaxial bending about the minor axis (CT2, CT3, CT4, CT5, CT6, and CT7).

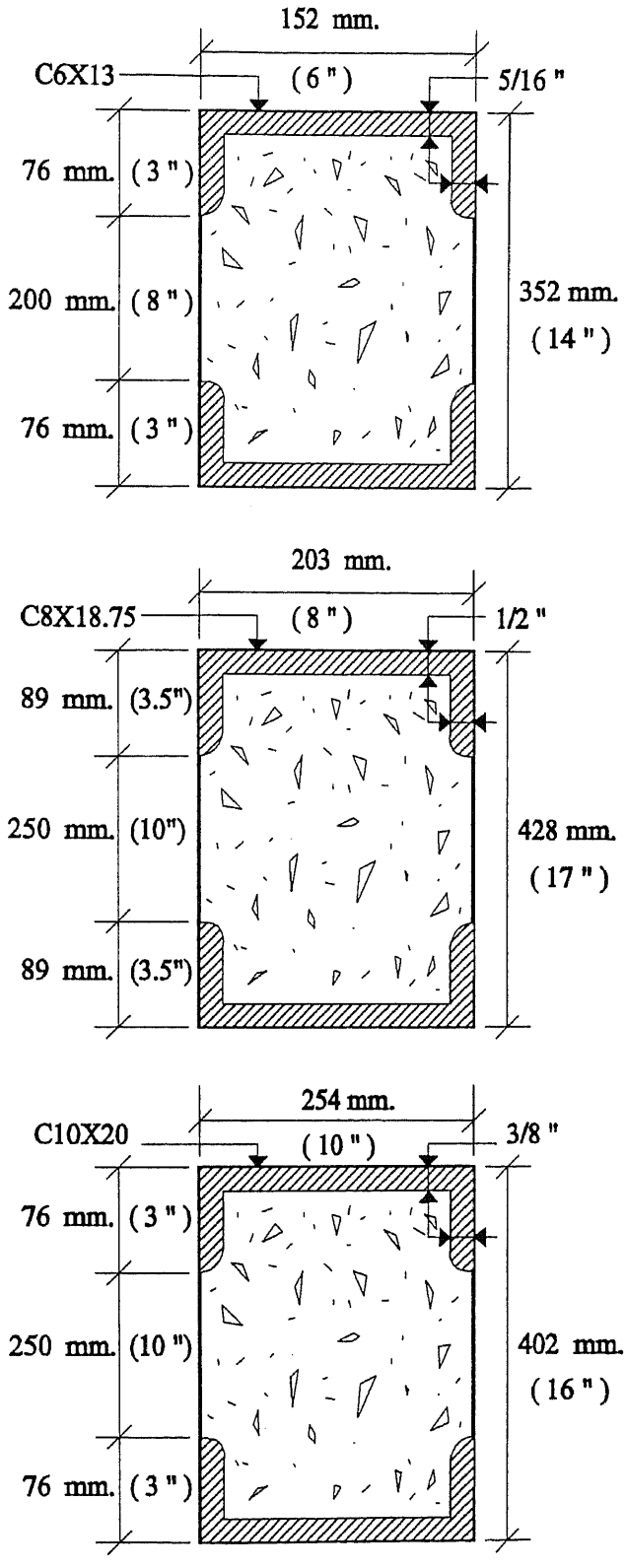


**Figure 3.18** Composite column section for specimens tested by Taylor et al.

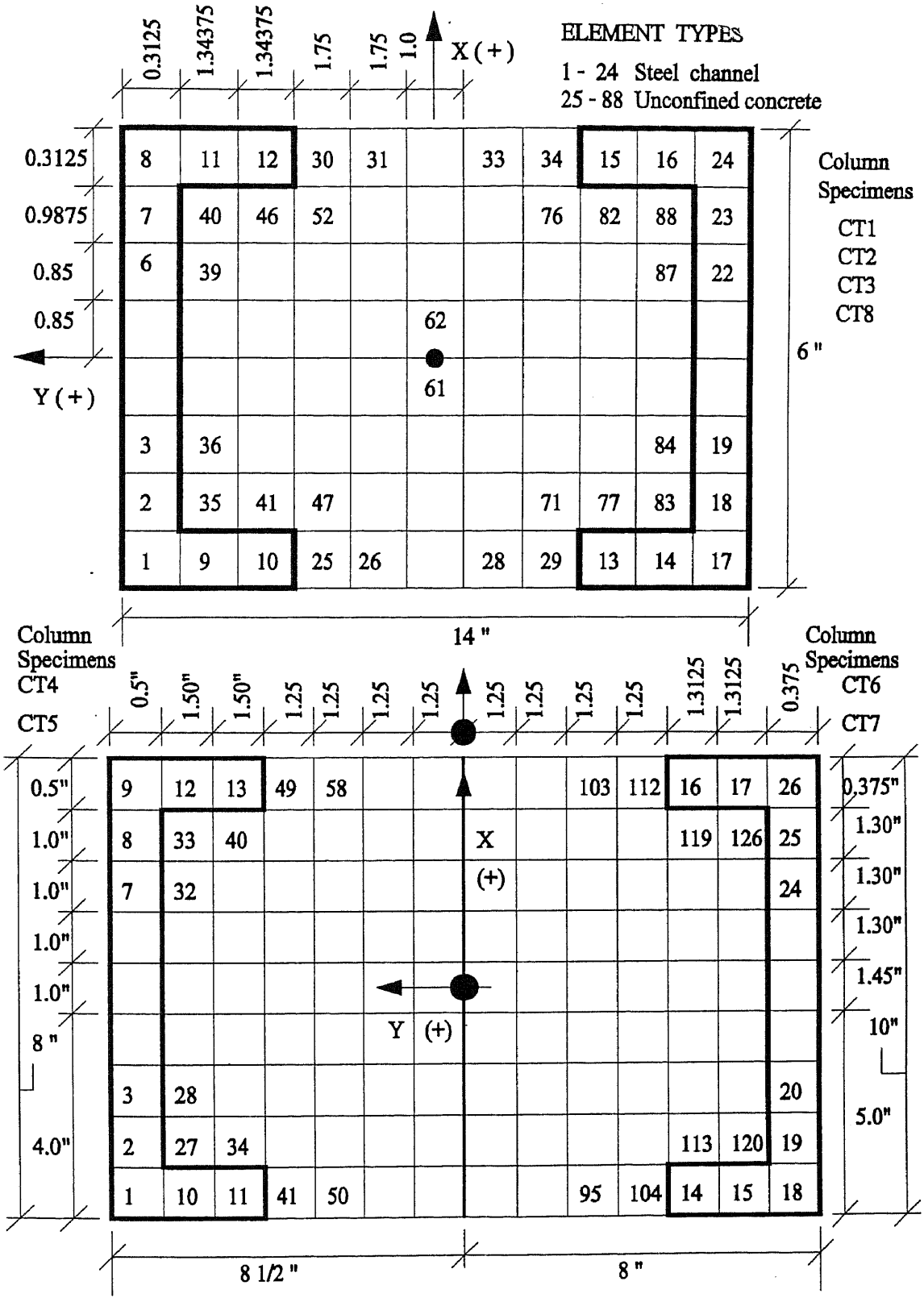


**Figure 3.19** Composite column model for specimens tested by Taylor et al.

The results (units converted from SI system to English units by the Author) of the ultimate experimental and theoretical calculated load obtained by Taylor et al. (217) and the ultimate load obtained by the Author using the computer method presented in this chapter are shown in Table 3.15.

It is important to note from the results presented in Table 3.15, that the calculated ultimate loads by Taylor et al. (217) $P_{theo.}$ show a very large conservative margin, while the ultimate loads predicted by the Author show an excellent degree of accuracy.

**Table 3.15** Eccentricity and Comparative Analytical and Experimental ultimate loads for column specimens tested by Taylor et al.

| Column | BxT in.xin. | $e_x$ (inch.) | $P_{test}$ (kips) | $P_{th}$ (kips) | $P_{NJIT}$ (kips) | $P_{test}/P_{th}$ | $P_{test}/P_{NJIT}$ |
|---|---|---|---|---|---|---|---|
| CT1 | 6x14 | 0 | 586.78 | 479.54 | 568.79 | 1.224 | 1.032 |
| CT2 | 6x14 | 0.315 | 514.84 | 342.63 | 503.83 | 1.502 | 1.021 |
| CT3 | 6x14 | 1.575 | 300.81 | 177.83 | 271.71 | 1.692 | 1.107 |
| CT4 | 8x17 | 0.394 | 955.49 | 637.59 | 961.67 | 1.499 | 0.993 |
| CT5 | 8x17 | 1.181 | 695.37 | 438.17 | 721.65 | 1.587 | 0.963 |
| CT6 | 10x16 | 0.4725 | 1138.26 | 830.49 | 1144.00 | 1.370 | 0.995 |
| CT7 | 10x16 | 0.9843 | 996.40 | 696.27 | 1004.0 | 1.431 | 0.993 |
| CT8 | 6x14 | 0 | 570.82 | 508.32 | 577.05 | 1.122 | 0.989 |
| mean | | | | | | 1.406 | 1.010 |
| standard deviation | | | | | | 0.0929 | 0.0382 |

Throughout the course of the computer study to determine the maximum load carrying capacity of the column specimens presented in this chapter, the Author has corroborated the theoretical findings stated by Lachance (129) in 1982. In his study of the ultimate strength of biaxially loaded composite columns, Lachance (129) shows the factors that influence the most the strength and

curvature of a particular column specimen are the ultimate compressive strength of concrete and its corresponding maximum compressive strain. The shape of the concrete stress distribution has minor effect on the ultimate strength and behavior of the column under study.

The Author has demonstrated the validity of the present computer method to study the composite columns of different cross sections. It can be applied to both short and slender columns and also to concentrically, uniaxially, and biaxially loaded composite columns. The Analysis can also be used to analyze a great variety of composite cross sections including circular, square and rectangular tubular cross sections filled with concrete.

From the computer analysis of the four column specimens MC1, MC2, MC3 and MC4 tested at NJIT it is noted that none of the column specimens had any steel elements yielding throughout the complete loading condition. Instead a concrete material failure occurred at loading level corresponding to the maximum axial load. At that point some of the unconfined concrete elements at the extreme side of the most compressed area of the cross section failed under compression.

The eccentricity values corresponding to the balanced condition were calculated by using the computer program "INTRDIAG" and they are shown in Table 3.5.

When comparing the eccentricity values of the applied axial load to the eccentricity at the balanced condition it can be clearly expected that the failure mode for the tested column specimens will be in the compression side.

# CHAPTER 4

# EXPERIMENTAL TESTS ON BIAXIALLY LOADED CONCRETE-ENCASED COMPOSITE COLUMNS

## 4.1 General

An experimental investigation of the behavior of composite columns under biaxial bending and axial loads is presented. The primary objective of this investigation is to examine and study the effect of a monotonically and eccentrically applied compressive short-time axial load on the ultimate strength, load-deflection response and moment-curvature relationship of four small scale models of concrete-encased I-shape steel columns.

The column specimens were tested in a vertical position and were deflected in a single curvature by an eccentrically applied axial load on the top of the specimens.

The main variables considered in the experimental investigation are:

a) the concrete compressive strength $f'_c$ ,

b) type of steel: structural steel, smooth and deformed reinforcing rods,

c) slenderness ratio, and

d) eccentricity of the applied load.

The columns were tested under a monotonically increasing axial load; midheight lateral displacements and surface axial deformations were measured at each loading step. During testing, the measurements were taken until evidence of concrete spall-off and/or buckling of reinforcing bars. At this time noticeable large

lateral midheight displacement was taking place at an increased rate of axial strain and decreasing readings of applied axial load. The test was then stopped and the specimen was removed from the testing machine to observe the tensile cracks and spalling of the concrete. The concrete spall-off is usually located near the mid-height of the column specimen.

The composite column specimens were fabricated and tested at the Structures and Concrete Laboratory of the New Jersey Institute of Technology in Newark, New Jersey, during the Summer of 1991 and Spring of 1992.

## 4.2 Test Specimens

The experimental program includes four symmetrically reinforced composite columns, Specimens MC1, MC2, MC3, and MC4. Specimen MC1 is a short column, and MC2, MC3 and MC4 are long column specimens. They were constructed and tested under biaxial bending and axial compressive load.

The specimens were built as a composite structural member by encasing a structural steel I-shaped section into the reinforced concrete. The column specimens had a square cross-section with nominal dimensions of 2 1/2 in. by 2 1/2 in. The overall length of the long and short columns was 48 in. and 32 in., respectively, which resulted in an approximate length over width ratio (L/b) of 64 for the long column and 42.7 for the short column.

All four columns were tested in a pinned-ended condition and were bent in a single curvature with respect to the major axis of biaxial bending.

The overall dimensions of the column specimens and the details of a typical cross-section are given in Fig. 4.1.

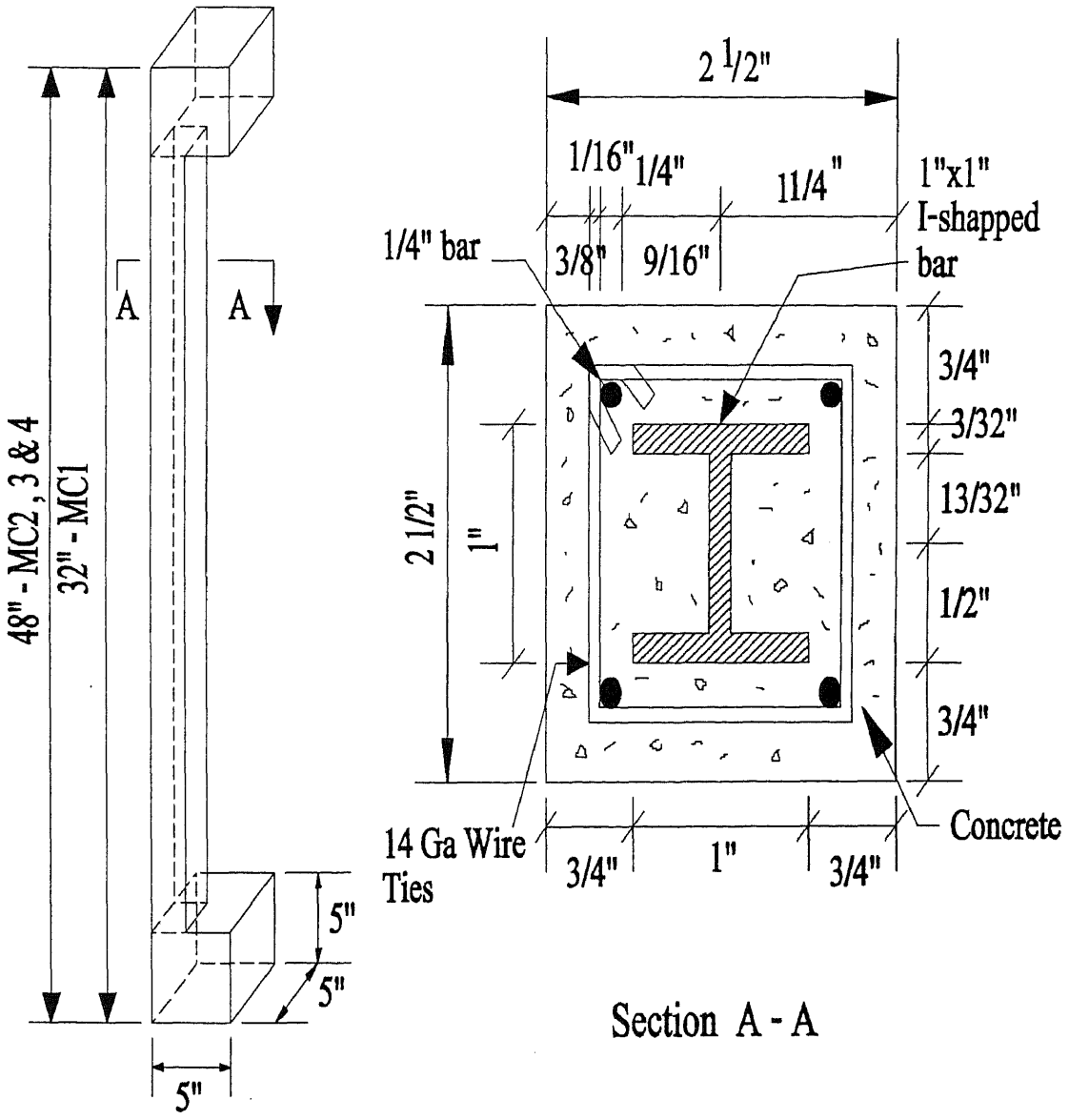


**Figure 4.1** Test specimen dimensions and composite column cross section

## 4.3 Materials and Specimen Fabrication

The basic materials used to build the composite column test specimens were:

a) Normal weight microconcrete.

b) Smooth and deformed reinforcing rods.

c.) Smooth structural steel I-shaped bar, and

d.) Smooth wires.

The column specimens were built in a small scale in order to take advantage of the available MTS testing machine in the Structures Laboratory and also to achieve the specimens with a reasonable high slenderness ratio.

A total of six specimens were originally planned to be tested, starting with two existing I-shaped structural bars that were being left unused at the Structures Laboratory of NJIT for a research project with minipiles.

Two column specimens, one 32 in. long and the other 48 in. long, were built and tested during the Summer of 1991. The results obtained from these two column tests were taken as the basic reference data for the remaining four tested specimens.

The experience gained from the fabrication of the two first column specimens allowed us to correct and improve the casting procedure, mix proportions and to adjust the size of the column specimen in order to provide proper concrete cover of the vertical reinforcing rods.

The most important data collected and observed during the testings of these two first column specimens were the maximum axial load carried by the specimens and the development of cracking and lateral displacements during the initial and different load increments. It was also noted that adjustments had to be made to the

ball and socket hinge devices at the top and bottom of the column specimen to allow for proper free moment rotation at both ends of the specimen.

After all the above improvements, the specimens were able to provide the complete load-deformation behavior, including the ascending and descending branches of the load-deformation and moment-curvature curves.

### 4.3.1 Formwork

The column specimens were cast horizontally inside a formwork made out of 3/4 in. precut pieces of plywood. They were put together and connected by black screws which allowed one to reuse the forms for the total number of tested specimens. The details of the formwork are given in Fig. 4.2.

### 4.3.2 Reinforcement

Four different types of high strength reinforcement were used to build the composite column specimens. No. 2 Smooth and deformed bars (1/4 in. diameter) were used as vertical reinforcing rods at the four corners of the column cross section.

Hot-rolled and cold-rolled structural steel 1 in. x 1 in. I-shaped bars were used as the main reinforcement of the composite column specimen at the center line of the cross section.

No. 2 deformed bars were available only in limited quantities at the Structures Laboratory of NJIT. Due to this shortage of rebars and the difficulty in obtaining them from the local suppliers, it was necessary to use smooth bars for some of the column specimens.

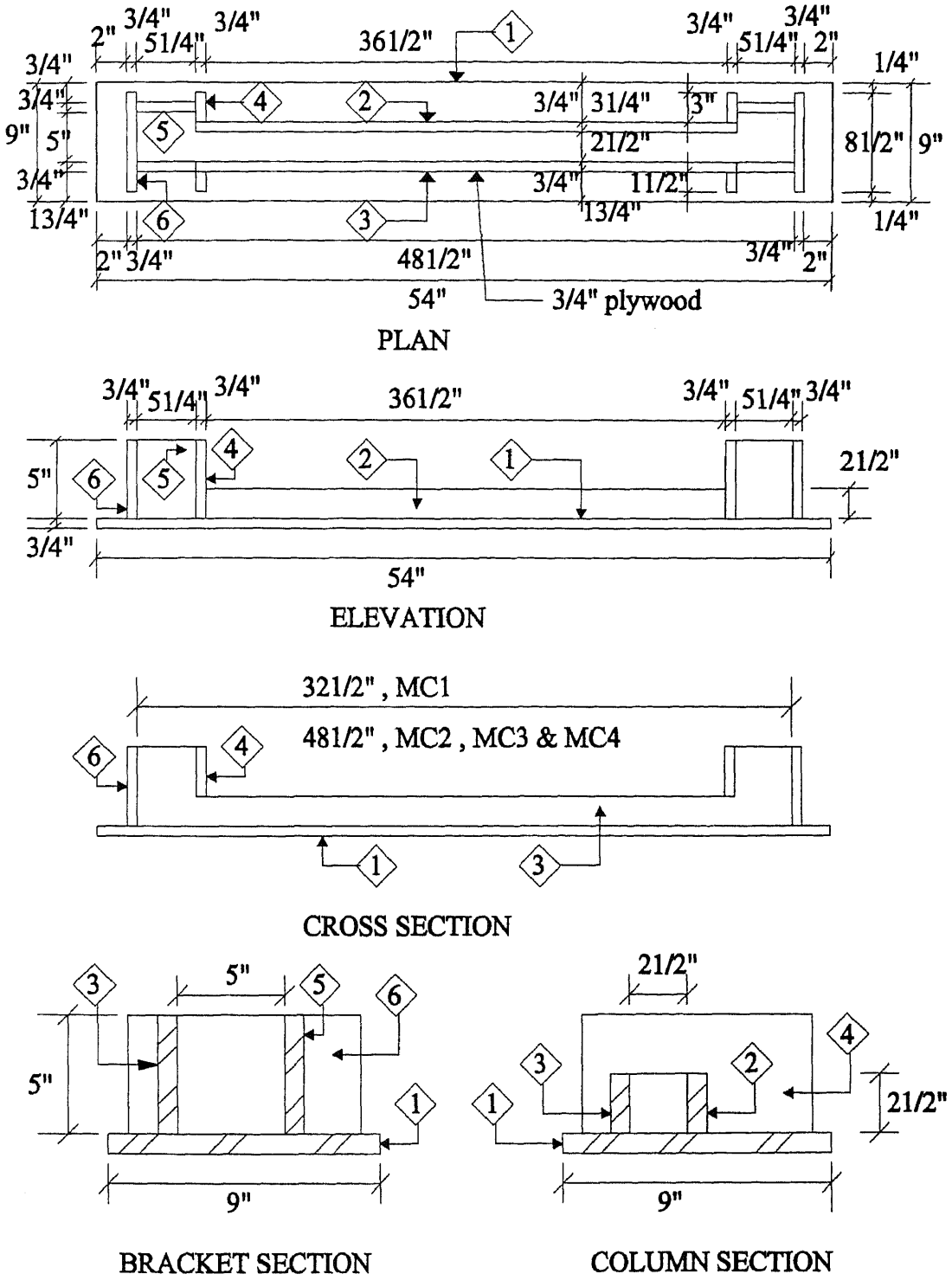


**Figure 4.2** Typical Formwork dimensions and details

The structural steel of 1 in. x 1 in. solid bar was obtained from a local steel shop supplier. The bars were cut in pieces long enough to build the specimens and to have a short sample for a tensile test.

One sample of each different type of reinforcements was tested under monotonic tensile axial load in the Strength of Materials Laboratory of NJIT.

A Tinius and Olsten Universal Hydraulic Testing Machine with a 120,000 Newton ( 27,000 lbs) capacity was used to perform the tensile tests for two 20 in. long samples of No. 2 (1/4 in. diameter) smooth and deformed bars and two 1/2 in. circular shaped samples of the structural steel bars, respectively.

**Table 4.1** Physical properties of the reinforcing rods and bars

| Rebar Type | $E_s$ x$10^3$ (ksi) | $f_{su}$ (ksi) | $\epsilon_u$ (in/in) | $f_y$ (ksi) |
|---|---|---|---|---|
| SB | 28.06 | 100.94 | 0.0428 | 89.92 |
| DB | 28.91 | 101.62 | 0.1248 | 77.02 |
| CR | 27.10 | 90.57 | 0.0467 | 88.16 |
| HR | 32.81 | 68.58 | 0.2133 | 43.75 |
| SB : Smooth Reinforcing Steel Rod<br>DB : Deformed Reinforcing Steel Rod<br>CR : Cold-Rolled Structural Steel Bar<br>HR : Hot-Rolled StructuralSteel Bar | | | | |

The typical stress-strain curves of the four steel samples are given in Figs. 4.3, 4.4, 4.5, and 4.6, respectively. A summary of their physical properties are shown in Table 4.1. The longitudinal reinforcing bars were tied with 14 gauge wire at uniform spacing along the corner bars. The 1 in. x 1 in.structural steel bars were shaped to an I-shaped section at the steel shop of the Mechanical Engineering Department of NJIT by using a milling machine.

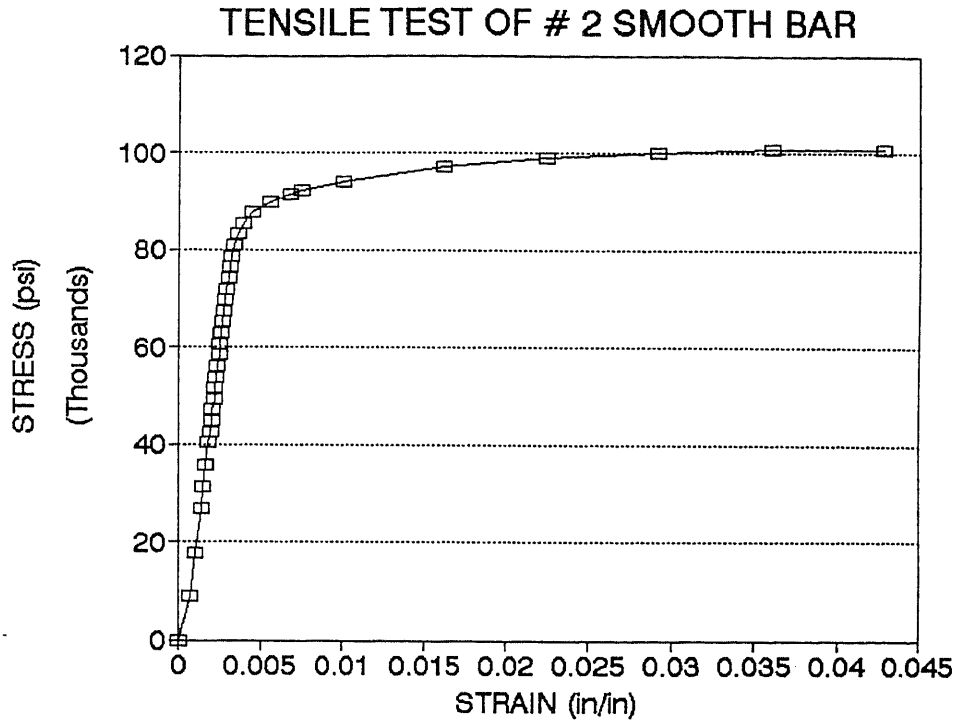


**Figure 4.3** Stress-Strain curve of #2 smooth bar for MC1, MC2 and MC3 test

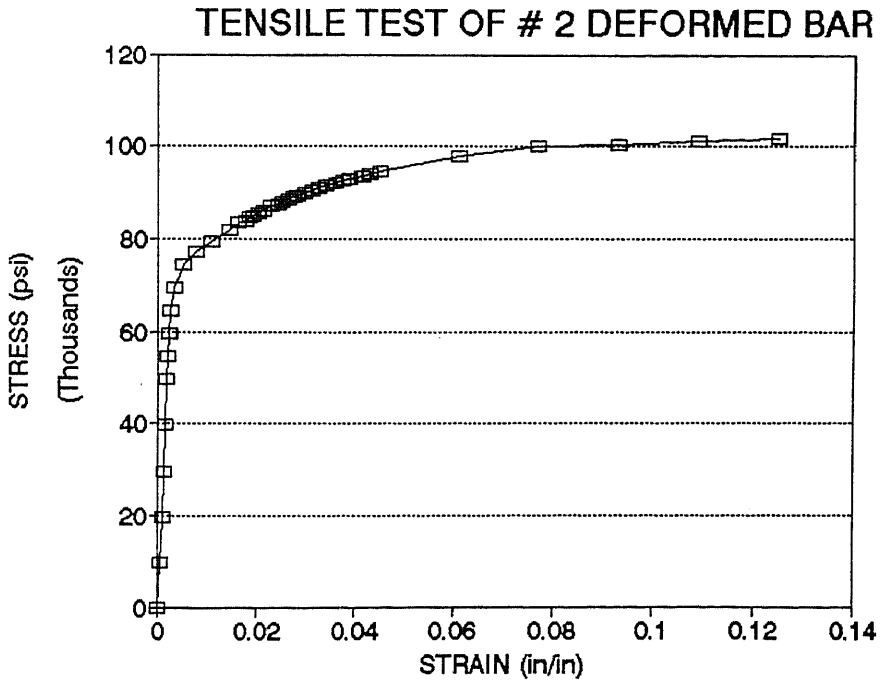


**Figure 4.4** Stress-Strain curve of #2 deformed bar for MC4 test

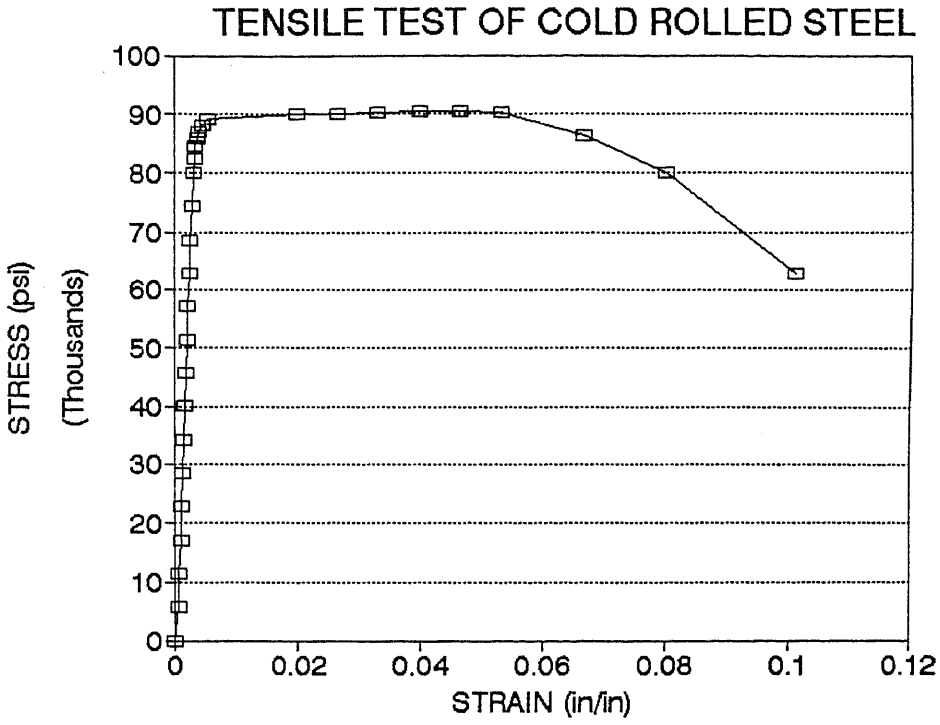


**Figure 4.5** Stress-Strain curve of cold-rolled steel for MC2 and MC3 test

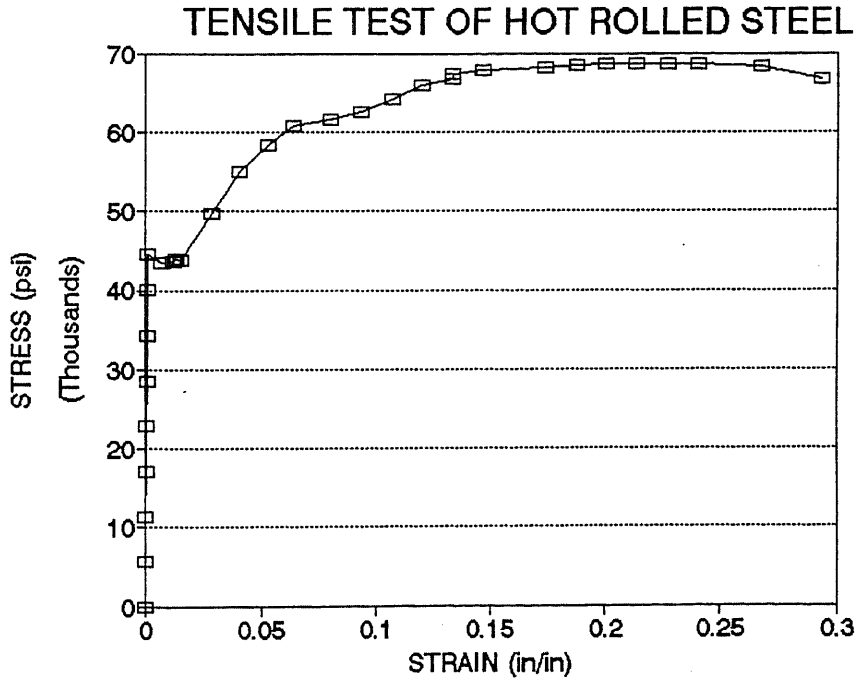


**Figure 4.6** Stress-Strain curve of hot-rolled steel for MC1 and MC4 test

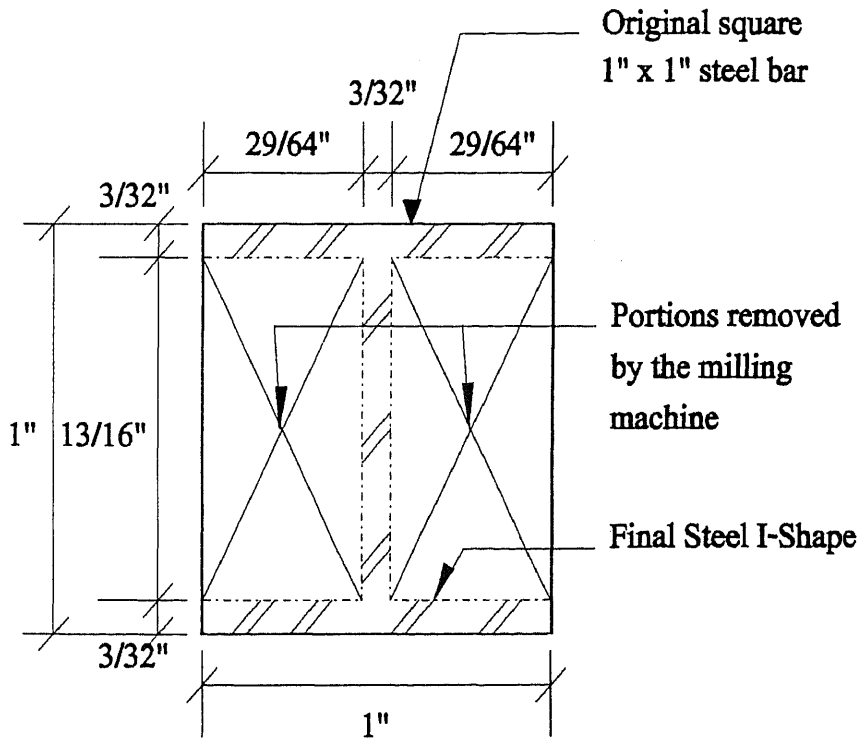


**Figure 4.7** Typical fabricated steel I-Section

The final thickness of the steel I-section flanges were within acceptable tolerances. The structural steel I-section is shown in Fig. 4.7.

### 4.3.3 Microconcrete

In general, a model is defined as a physical replica of a prototype structure which is normally smaller in size and which may be used and tested experimentally to forecast the behavior of the prototype.

The stress strain diagrams and the failure mode for the prototype and model materials must be compatible.

In this testing program the model material used was one with the most compatible characteristics with the prototype, normal weight concrete with very fine aggregate.

A one-eighth scale model of a 20 in. x 20 in. composite column prototype was fabricated using cement, small size aggregates, sand, and water and defined herein as microconcrete. The following materials were used in the fabrication of the concrete for the column specimens:

a) A high-early-strength Portland Cement Type III confirming to the ASTM C150, a type of cement characterized by producing earlier strength in mortar or concrete than the regular cement.

b) The fine aggregate, a washed and dried natural very fine sand obtained from local sources.

c) The coarse aggregate consisted of a mixture of very small rounded and crushed gravel with a maximum size of 0.0937 in. (3/32 in.+/-), obtained by gradation of gravel that passed the U.S.A. Standard Testing sieve or

screen No. 8, conforming to the ASTM specification No. E-11. (maximum opening in mm = 2.36 mm, and maximum opening in inch.= 0.0937 in.)

d) Tap water.

The microconcrete mix design was done in conformance with the ACI Standard 211.1-81 for selecting proportions for normal, heavyweight, and mass concrete (11) and according to the recommended guidelines for microconcrete mix design by Tsui and Mirza (211).

The basic parameter in the microconcrete mix design is the aggregate size. Aggregates used in the structural concrete for the prototype consist of particles whose size ranges from fine sand to coarse particles of a maximum average dimension according to the bar spacing and concrete workability.

For the model specimen, a well-graded sand is used with scaling of the coarsest particles. Table 4.2 shows the details of the final microconcrete mix proportions.

The water-cement-aggregate ratio used was 0.66:1:3.07 to obtain a column specimen with microconcrete of an ultimate compressive strength $f'_c$ in the range of 4,000 to 5,000 psi.

Five control cylinders (3 x 6 in.) were cast from each batch of microconcrete that was used to build each one of the composite column specimens.

These cylinders were capped on both ends with sulphur capping compound in the Environmental Laboratory of NJIT and were left to cure under the same indoor conditions as the column specimens.

**Table 4.2** Microconcrete design mix proportions

| Design Mix Proportions | | | |
|---|---|---|---|
| Materials | Weight ($lbs/yd^3$) | Weight ratio | Remarks |
| Water | 539.36 | W/C = 0.66 | Potable |
| Cement | 816.33 | 1.0 | TYPE III High-Early-Strength |
| Aggregate | 2507.29 | A/C = 3.07 | Includes fine and coarse particles |
| $f'_c$ Expected = 4000 to 5000 psi | | | |

The control cylinders were later tested the same day as that of the column specimen and their compressive strength calculated for later use in the analysis.

The workability of the fresh microconcrete was good and was found to be appropriate to cast the column specimens without the use of any admixture.

According to several investigators, the typical stress-strain behavior of model concrete cylinders with the same height-diameter ratio of 2 but of smaller dimension than the standard 6 x 12 in. cylinders is very similar to ordinary concrete of the same ultimate strength. Sabnis and Mirza (191) among others compared the stress-strain curves of prototype and model concrete by using the 3 x 6 in control cylinders. They reported a very good correlation between them.

Table 4.3 shows the obtained average compressive strength of the control cylinders for the different column specimens tested at present study.

### 4.3.4 Specimen Fabrication and Details

The four composite column specimens MC1, MC2, MC3, and MC4 were fabricated and tested in the Structural Laboratory of NJIT.

The composite column specimens had a square cross-section with nominal dimensions of 2 1/2 x 2 1/2 in. with both ends enlarged to a cross-section of 5 in. x 5 in. by 5 in. long bracket to accommodate the point of application of the biaxially eccentric applied compressive axial load.

The brackets were heavily reinforced in order to avoid premature splitting at the ends of the column and to allow for a consistent biaxial bending condition. Also they allow the loads to be transferred to the cross-section along the length of the specimen.

**Table 4.3** Compressive strength of control cylinders for column specimens MC1, MC2, MC3, and MC4

| Column Specimen | No. of Control Cylinders | Date Cast | Date Test | Average Ultimate Compressive Strength(psi) |
|---|---|---|---|---|
| MC1 | 5 | 4/13/92 | 5/4/92 | 5,332 |
| MC2 | 5 | 4/13/92 | 5/4/92 | 4,491 |
| MC3 | 5 | 3/27/92 | 4/10/92 | 3,745 |
| MC4 | 5 | 3/27/92 | 4/10/92 | 3,989 |
| Average unit weight of control cylinders = 130.50 lbs. per cu. ft. | | | | |

The structural steel I-shape had a 1/4 in. thick square plate of the same size of the bracket welded at each end to serve as a receiving plate for the loading mechanism. Diagonal No. 3 (3/8 in. diameter) bars were welded connecting the end plate and the I-shape bar in order to add more rigidity to the bracket.

The column specimens were cast horizontally inside a preassembled oiled plywood formwork. The fine aggregates, cement, and water were batched by weight and mixed in a metal pan mixer. Water was added gradually until all the materials were mixed to a uniform color and consistency.

Five 3 in. x 6 in. control specimens were cast from each specimen mix to determine the average ultimate compressive strength. Each column specimen and all control specimens were vibrated on a 1 ft.-8 in. x 1 ft.-8 in. Syntron Vibrating Table until full compaction was obtained.

Special care was taken to assure the alignment and position of the reinforcement and to have the mix evenly spread and flowing around the bars. Following the casting, the column specimens and control cylinders specimens were stored in a horizontal position under normal laboratory conditions of about 70°F until the time of testing.

Table 4.4 shows the column specimens dimensions, material properties and the point of application of the biaxially eccentric load.

Two column specimens were cast at the same day and were stripped from their formwork after 24 hours of casting. The specimens were periodically wetted to keep its moisture content under normal conditions. The typical reinforcement details and end loading plates are shown in Fig. 4.8.

**Table 4.4** Column specimens dimensions and material properties

| Column Specimen | Cross Section Dim. (in.xin.) | Height (in.) | Height / Width | No., Sizeand Typeof Reinf. | | Concrete (psi) | Eccentricity (in.) | |
|---|---|---|---|---|---|---|---|---|
| | | | | Bars | Shape | $f'_c$ | $e_x$ | $e_y$ |
| MC1 | 2.5x2.5 | 32 | 12.8 | 4#2SB | 1x1 HR | 5,332 | 1.5 | 1.5 |
| MC2 | 2.5x2.5 | 48 | 19.2 | 4#2SB | 1x1 CR | 4,491 | 1.25 | 1.25 |
| MC3 | 2.5x2.5 | 48 | 19.2 | 4#2SB | 1x1 CR | 3,745 | 1 | 1 |
| MC4 | 2.5x2.5 | 48 | 19.2 | 4#2DB | 1x1 HR | 3,989 | 1.5 | 1.5 |

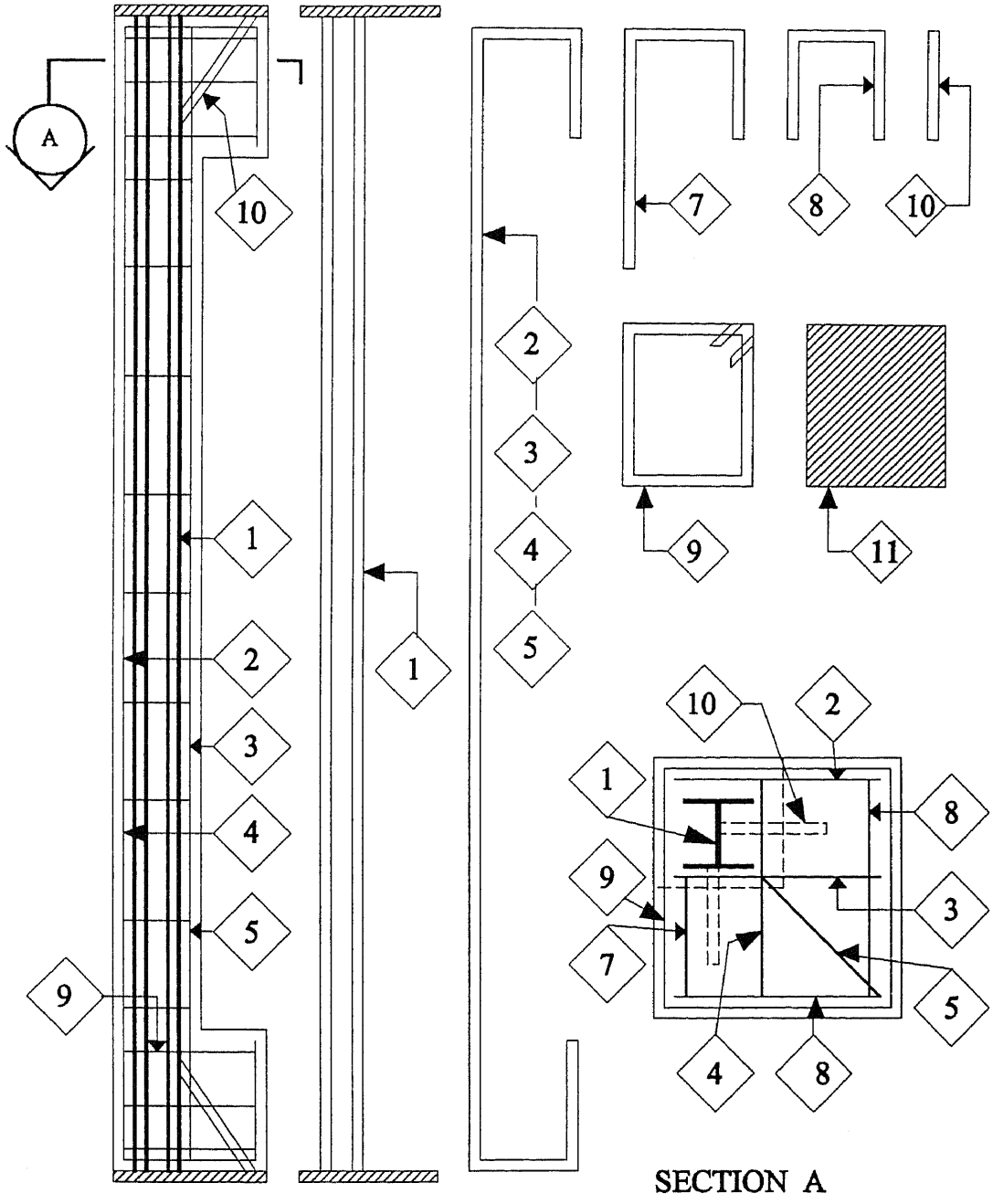


**Figure 4.8** Typical Reinforcement details of the composite column specimen

## 4.4 Test Setup and Instrumentation

The column specimens were prepared for testing by installing small circular brass plates (mechanical strain gage points) glued to the surface of the column under biaxial bending loading condition and axial compression.

Two sets of six brass plates were mounted on two perpendicular faces at the midheight of each specimen with a gage length of 6 in. These brass plates were used as marked reference points to measure the surface axial deformations for a later calculation of the axial strains and the curvatures with respect to the main column axis.

The concrete surface was cleaned off by removing any loose dirt and the irregularities were smoothed out by brushing it with sand paper before placing of the brass plates. The location of the point of application of the axial testing load was marked up on the surface of the loading plates at each end of the specimen. The approximate total weights of the final cast specimens 48 in. and 32 in. long were 48.37 lbs. and 36.56 lbs., respectively, for a given unit weight of the composite column of approximately 145 lbs. per cu. ft.

A 3 in. diameter circular 1-1/2 in. thick beveled plate was glued to the end loading plates of the specimen at the selected position of the applied load.

Every composite column specimen was carefully measured for their cross-section and the overall length. The bracket dimensions were taken and found within the tolerable limits of the projected model dimensions.

A mechanical device with a dial indicator and two sliding conical points was used to take the initial readings between each pair of the mechanical strain gage

points. Lateral displacements of the column specimens were measured using the Dial Gages.

The column specimen was then placed in a vertical position between the loading heads of the 100 kips maximum load capacity servo-controlled Material Testing System (MTS).

Two 3 in. diameter, 1-1/2 in. thick plates with a cylindrical ball at the ends of the specimen were used as hinged conditions which permitted a free rotation at the column ends.

The specimen was secured tight against the loading heads of the MTS Loading Machine. Several dial gage indicators were placed at the top, bottom and midheight of the column to measure the lateral displacements in both main directions of biaxial bending.

Fig. 4.9 shows the details of the test setup.

### 4.5 Test Procedure

The tests of four composite column specimens MC1, MC2, MC3, and MC4 were carried out in the servo-controlled MTS Testing Machine of the Structures Laboratory at New Jersey Institute of Technology, Newark, New Jersey. The axial compressive load was applied to the specimen in pre-determined increments. The digital readings of axial load and longitudinal strain were recorded during testing, after which the readings of the dial gages were taken for each set in the two perpendicular directions of the cross-section.

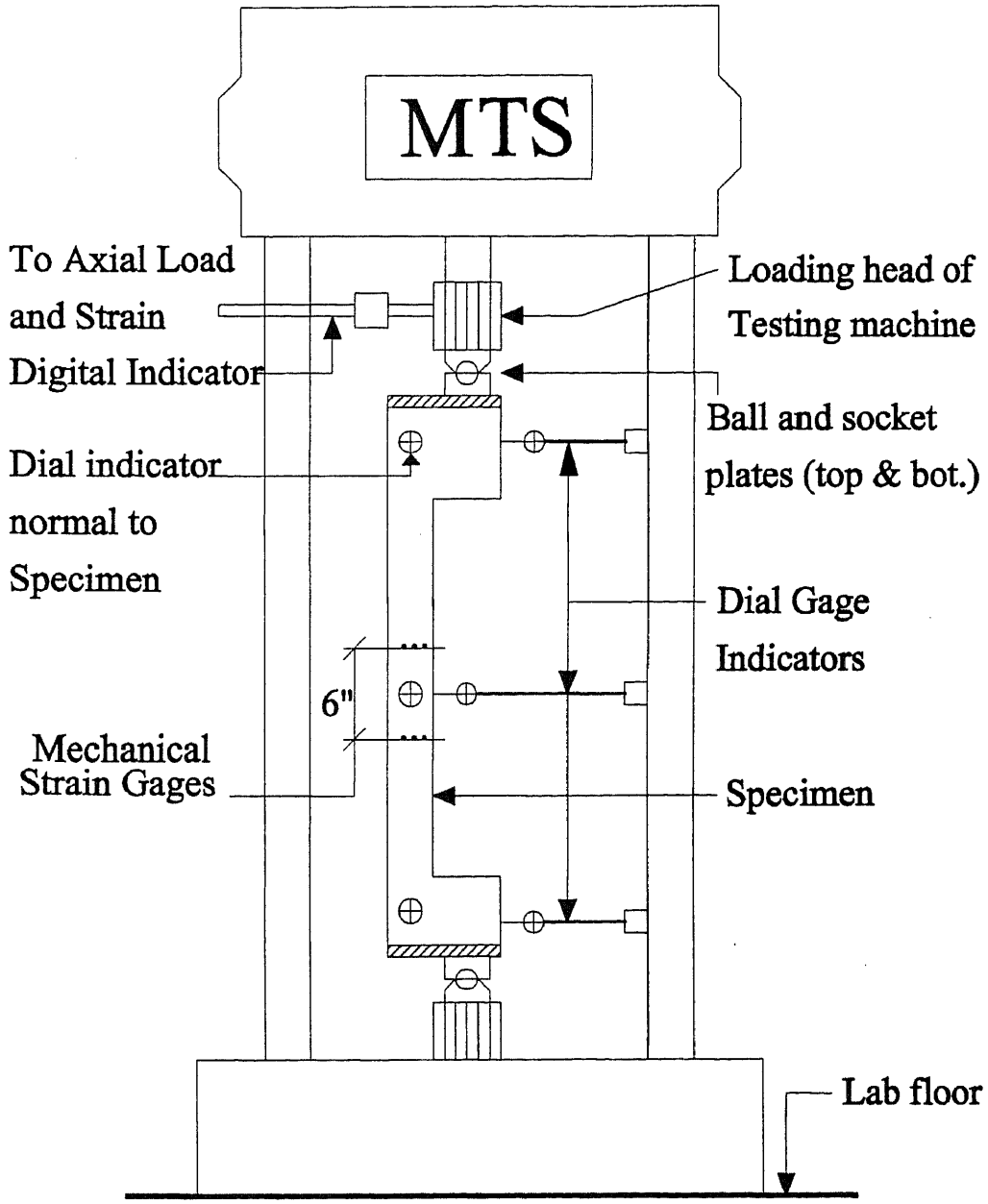


**Figure 4.9** Experimental Test Setup

The last readings recorded for each load stage were the mechanical strain gage readings, one reading for each pair of strain gage points. A total of six pairs were taken in order to calculate the surface strain and the resulting curvature.

The axial loads and the strain readings were taken right before and after collecting the data for each set of dial gages and mechanical strain gages. It was noted that the axial load dropped a small amount during this interval of time between deflection and strain measurements.

Each of the column specimens was loaded continuously and observations were made at each load stage to detect the initiation of any major cracks on the tensile faces of the specimen.

The axial loads and strain rate values were recorded directly from the memory of the MTS Testing Machine and the experiment was terminated due to concrete spall-off and formation of excessive cracking and large lateral displacements. These phenomena produced spalling of concrete at or around the midheight of the specimen. The descending branch of each specimen was attained and the crushing of the concrete on the compression face was noted at the time the test was terminated.

## 4.6 Test Results

The data collected for each specimen from the dial gages, mechanical strain gages, and the digital MTS readings of the axial load and stroke values were processed and plotted for study and comparison with the present analytical and computer model results.

The lateral displacement of the column specimens at midheight points were calculated by $d = d_i - d_o$, where $d_i$ = the dial gage reading taken at each stroke

increment, and $d_o$ = the initial dial gage reading at the time before the first stroke increment.

The axial strain values used to calculate the curvature of the column specimen about the two major axis, X and Y, were determined by $\epsilon = (l_i - l_o)/l_o$, where $l_i$ = length of the mechanical strain gage points at each loading stage, and $l_o$ = length of the mechanical strain gage points at the initial loading stage or zero loading.

The curvature for each column specimen was calculated by determining the slope of the strain values across the cross section. The linear regression method was used to give the strain distribution values obtained across the column section for the each loading stage.

**Table 4.5** Test Results for column specimens MC1, MC2, MC3, and MC4

| Column Specimen | Maximum Axial Load (Kips) | Eccentricity of applied axial load | | Eccentricity of load at balanced condition | |
|---|---|---|---|---|---|
| | | $e_x$ | $e_y$ | $e_{bx}$ | $e_{by}$ |
| MC1 | 6.33 | 1.5 | 1.5 | 1.697 | 1.896 |
| MC2 | 5.95 | 1.25 | 1.25 | 1.805 | 2.012 |
| MC3 | 6.53 | 1.0 | 1.0 | 1.977 | 3.688 |
| MC4 | 4.95 | 1.5 | 1.5 | 1.893 | 3.402 |

Plots of the load-deflection and moment-curvature test results are presented in Figs. 4.10 through 4.17.

The experimental maximum axial loads obtained for the tested specimens are presented in Table 4.5.

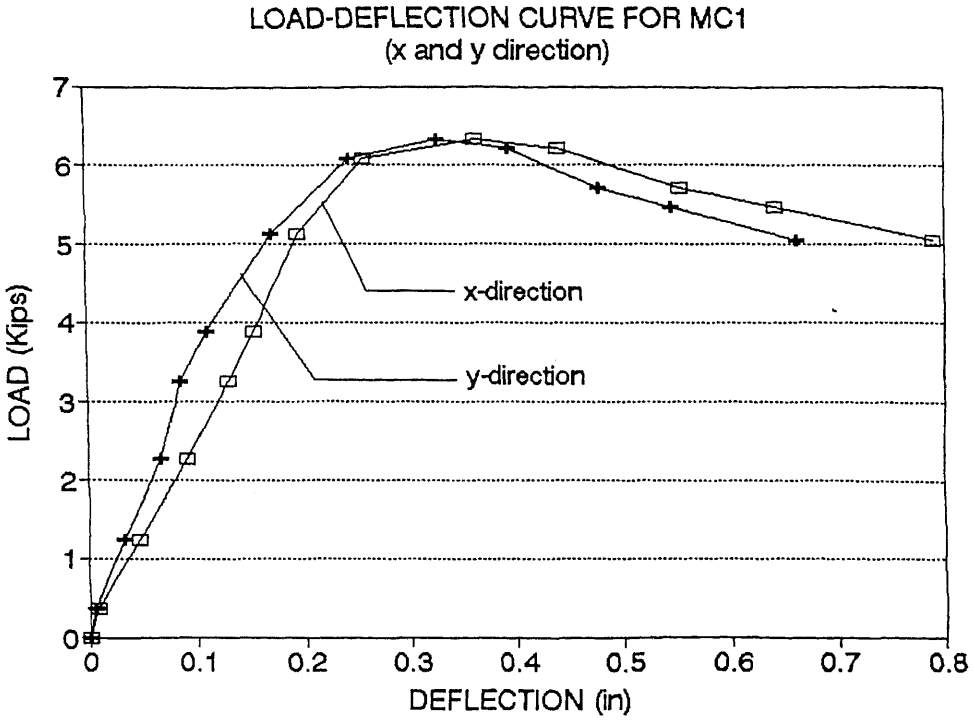


**Figure 4.10** Experimental Load-Deflection curves for column MC1

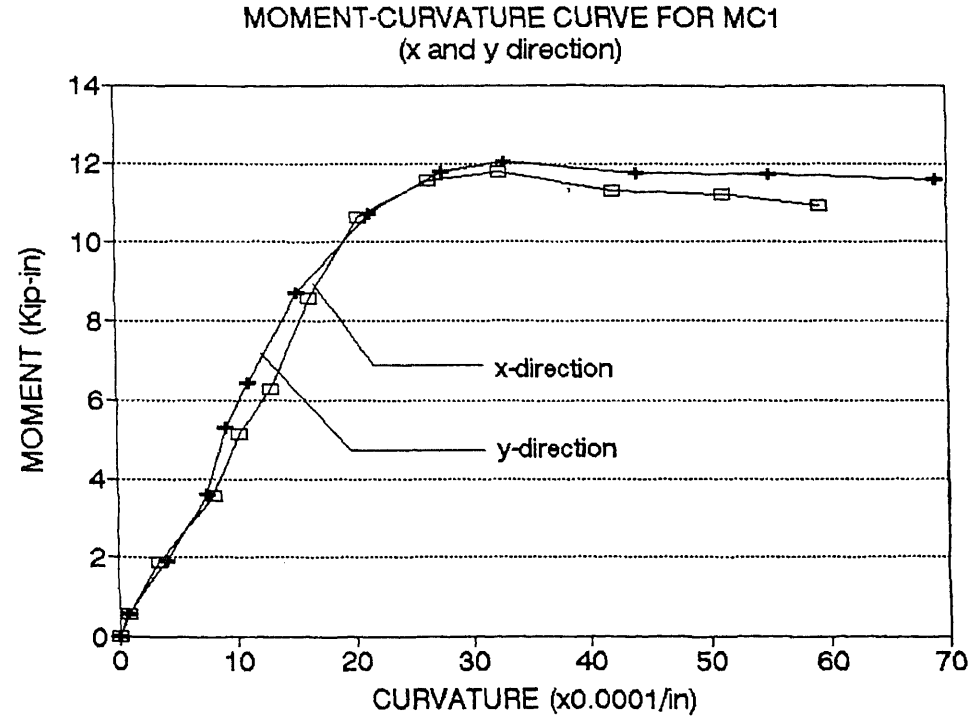


**Figure 4.11** Experimental Moment-Curvature curves for column MC1

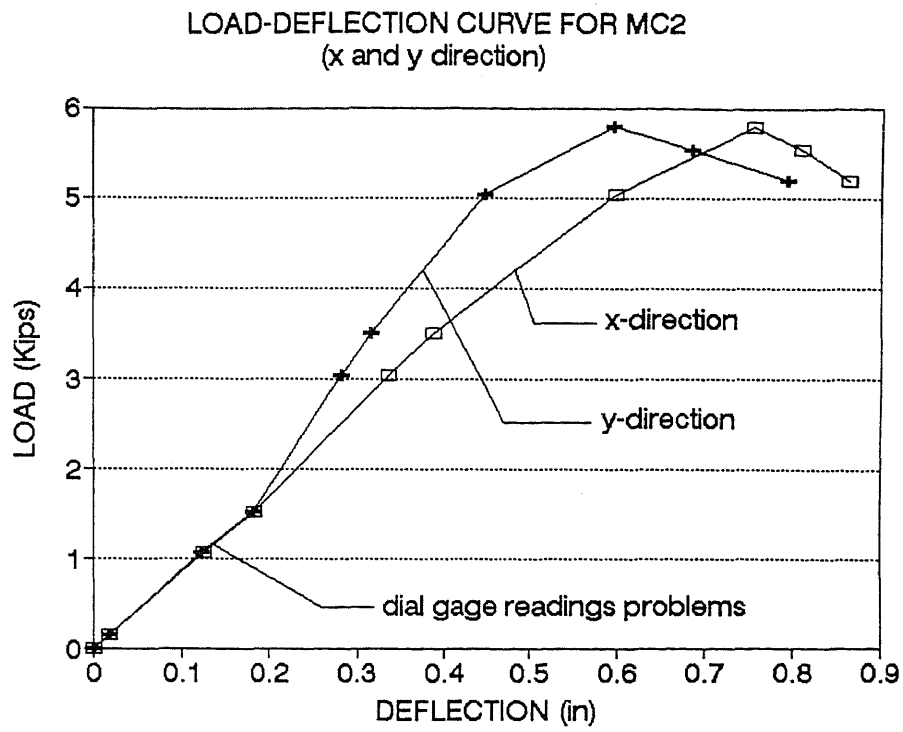


**Figure 4.12** Experimental Load-Deflection curves for column MC2

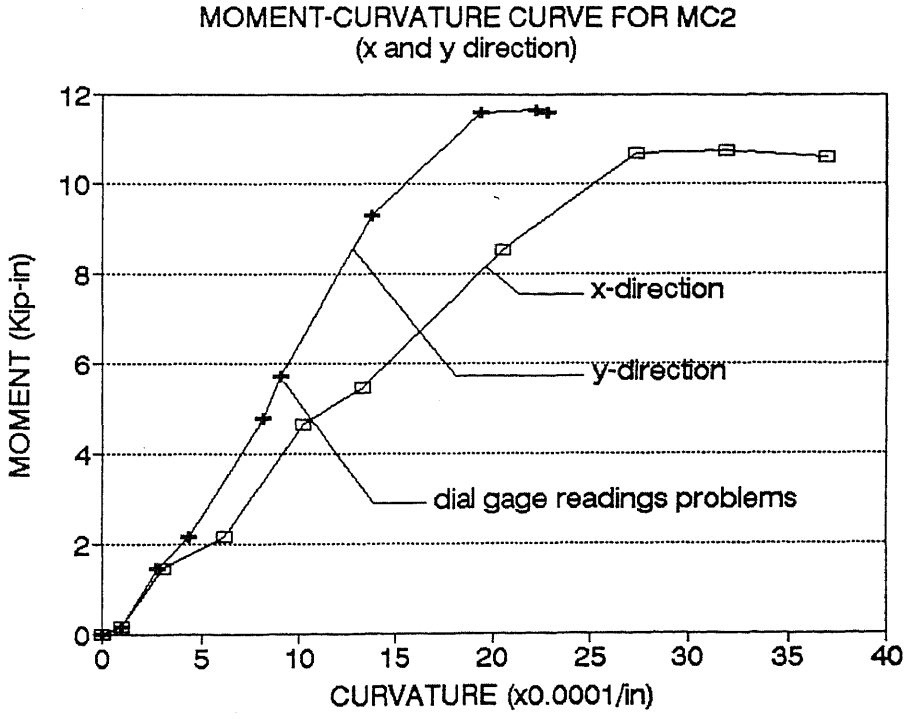


**Figure 4.13** Experimental Moment-Curvature curves for column MC2

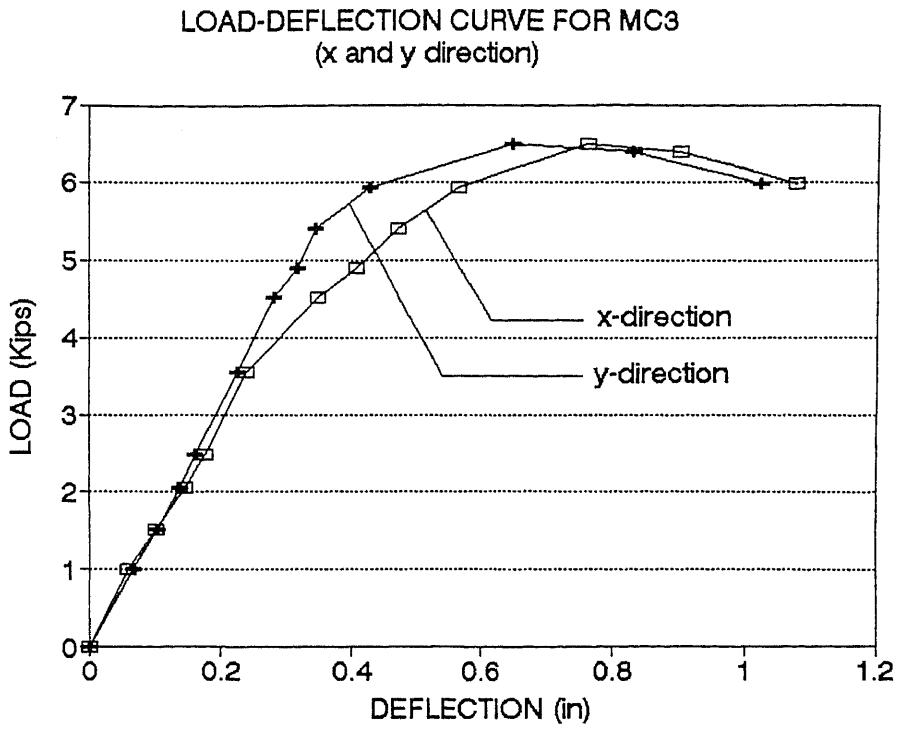


**Figure 4.14** Experimental Load-Deflection curves for column MC3

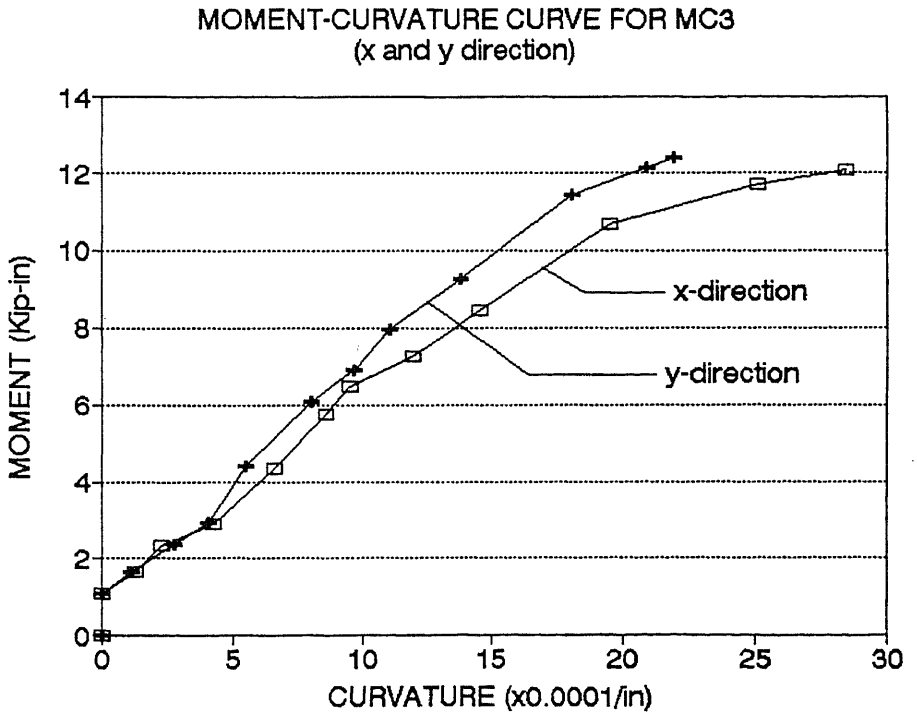


**Figure 4.15** Experimental Moment-Curvature curves for column MC3

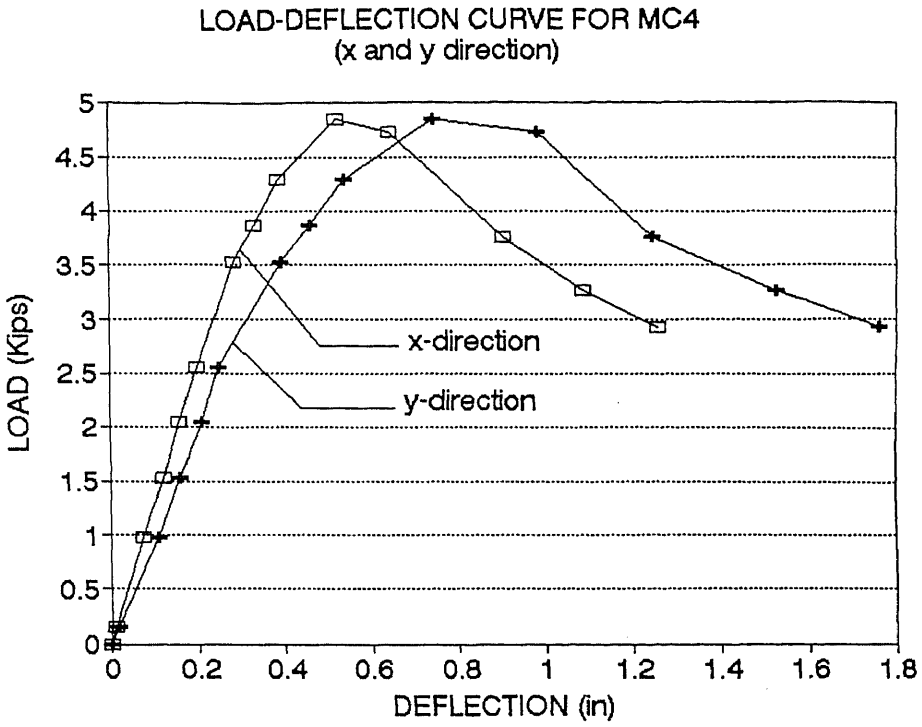


**Figure 4.16** Experimental Load-Deflection curves for column MC4

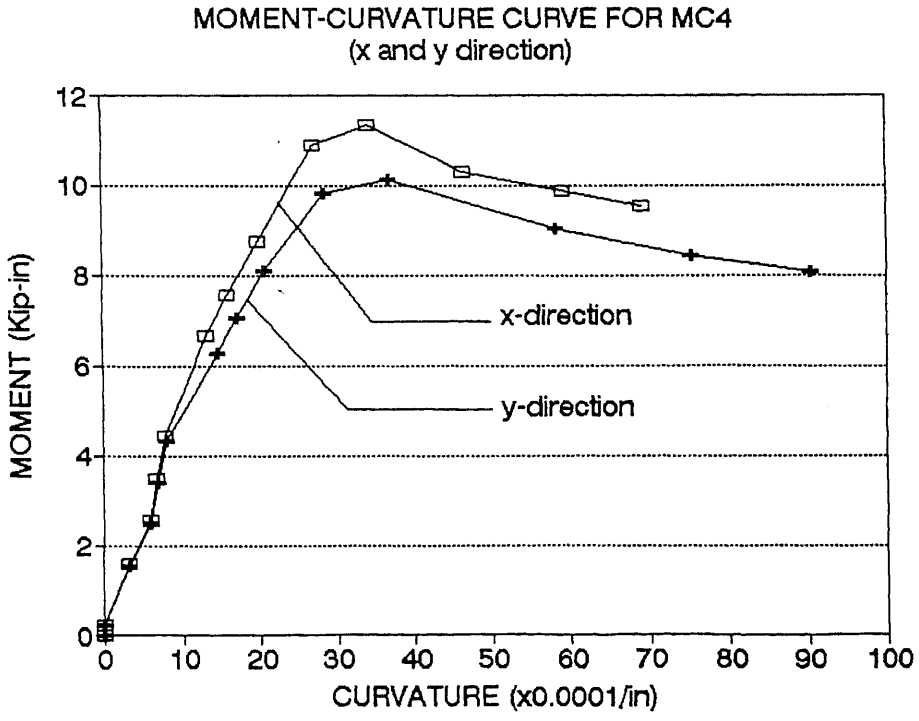


**Figure 4.17** Experimental Moment-Curvature curves for column MC4

To illustrate the validity of the computer method presented in Chapter 3 the Author calculated the theoretical loads for column specimens MC1, MC2, MC3, and MC4.

The comparative results are presented in Table 3.5 in Chapter 3, where it can be seen that a very good agreement for failure loads is obtained.

The good correlation obtained between the theoretical and experimental Failure loads confirms the validity of the proposed computer method which can accurately and safely predict the failure loads for biaxially loaded composite columns, with both ends pinned.

The comparative plots of the Load-Displacement and Moment-Curvature curves of the Analytical and Experimental results obtained for the four specimens MC1, MC2, MC3, and MC4 are presented in Figs. 4.18 through 4.25.

### 4.7 Analysis of Test Results and Failure Modes

A photographical record of the equipment that was used to build and test the composite column specimens, the experimental set-up and the specimens after testing are presented for illustration in Appendix E.

Morino, Matsui, and Watanabe (147), in their report on Strength of Biaxially loaded composite columns, discussed the phenomenon of deflection reversal occurring in long composite columns tested in Biaxial bending. The Author observed that the deflection reversal phenomenon described by Morino et al. also occurred during testing of column specimens MC1, MC2, MC3, and MC4. The deflection v along the y-axis appeared to be decreasing while the u-deflection along the x-axis increased more rapidly in the large deflection range.

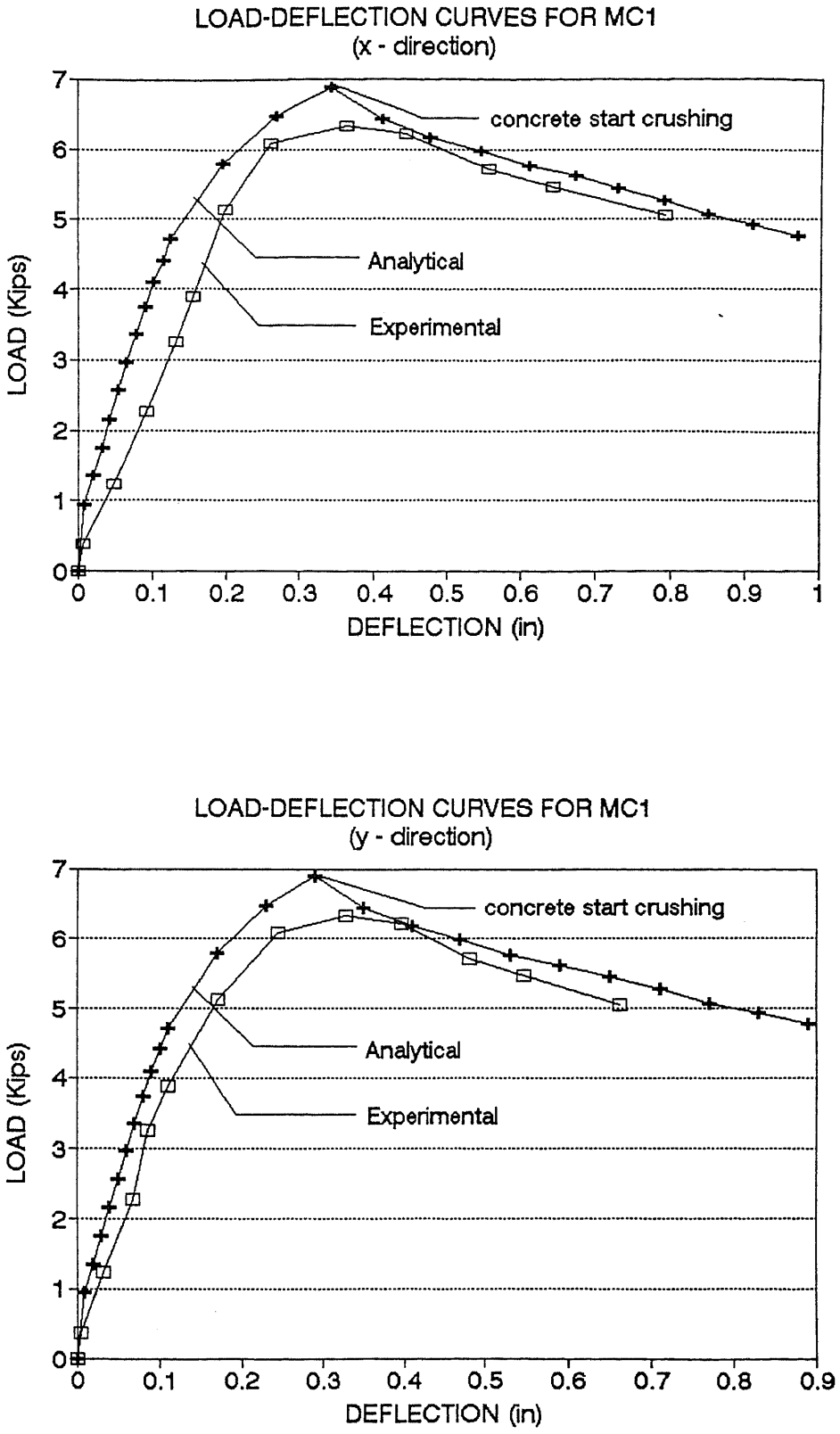


**Figure 4.18** Comparative X and Y Load-Deflection curves for column MC1

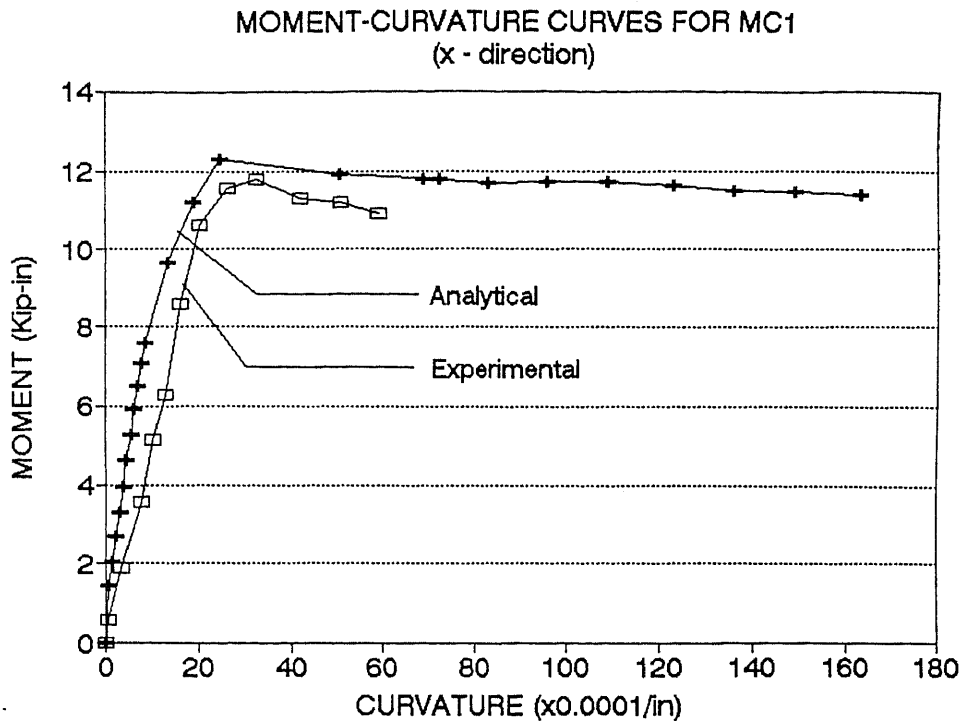


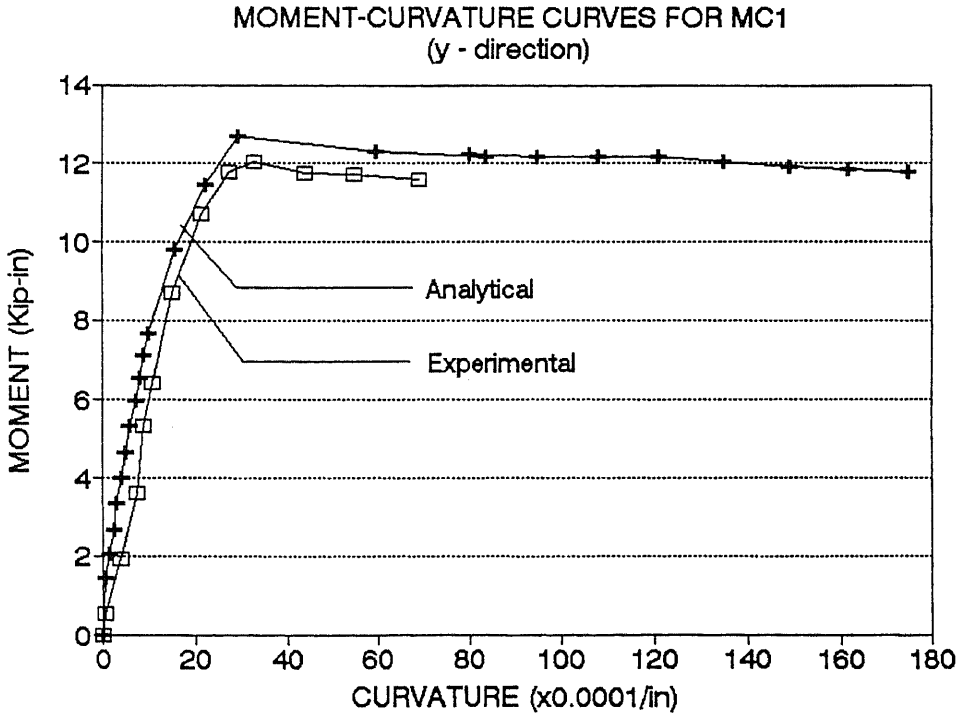


**Figure 4.19** Comparative X and Y Moment-Curvature curves for column MC1

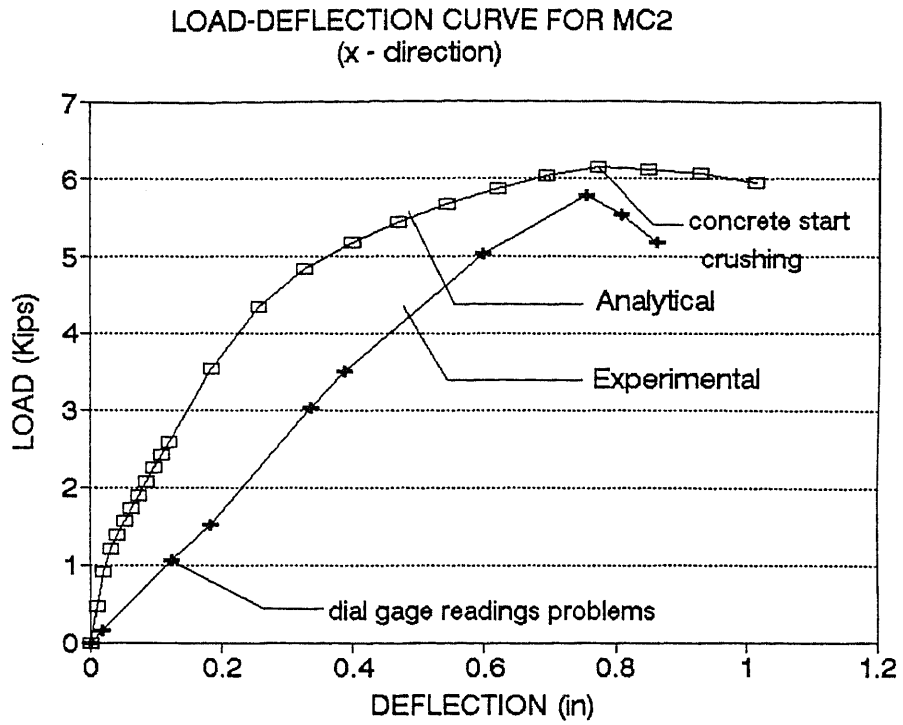


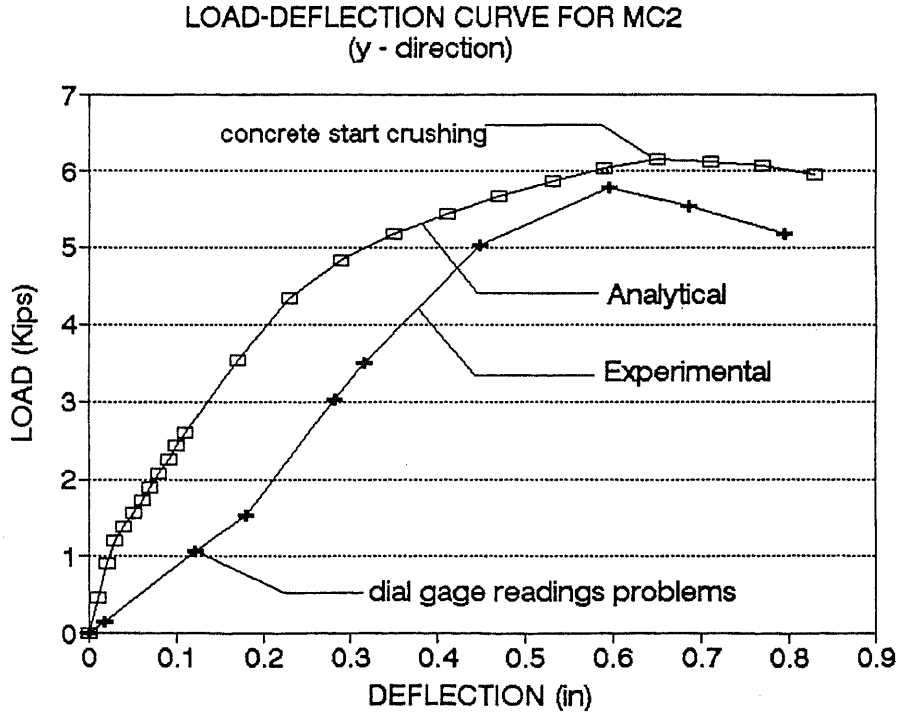


**Figure 4.20** Comparative X and Y Load-Deflection curves for column MC2

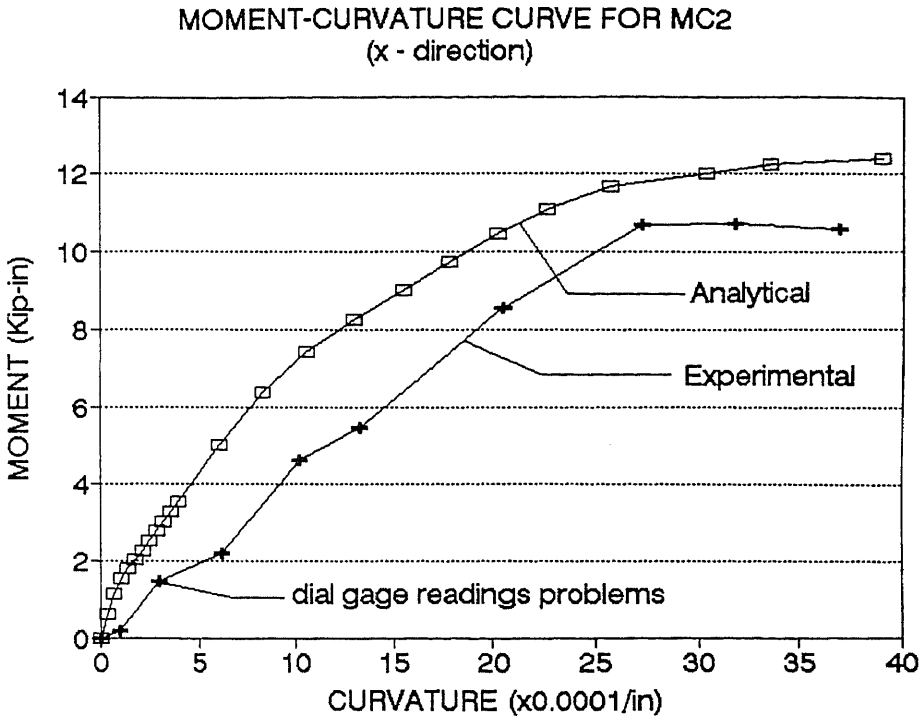


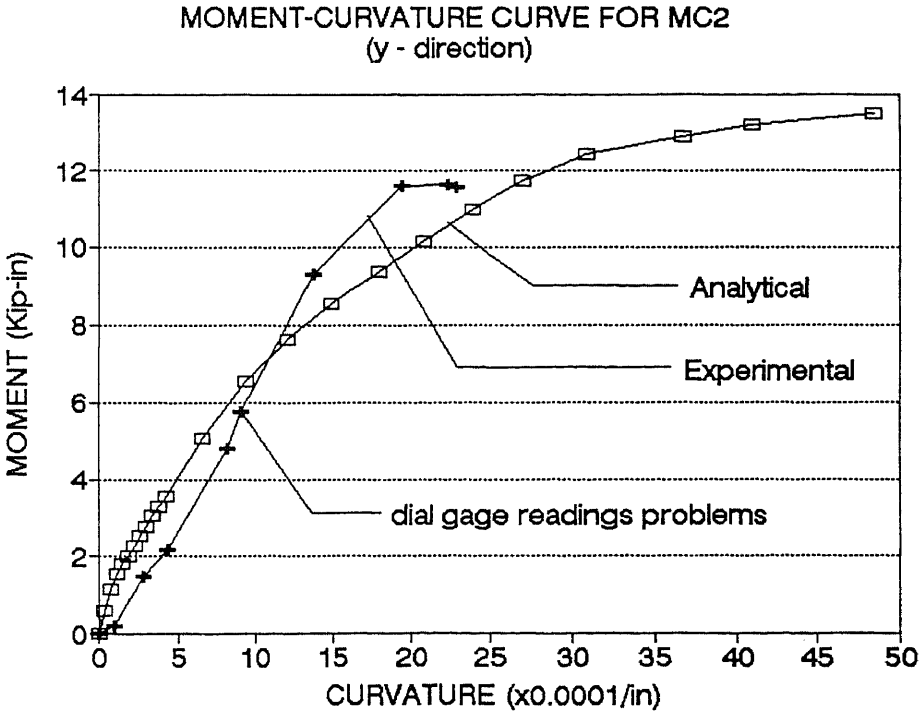


**Figure 4.21** Comparative X and Y Moment-Curvature curves for column MC2

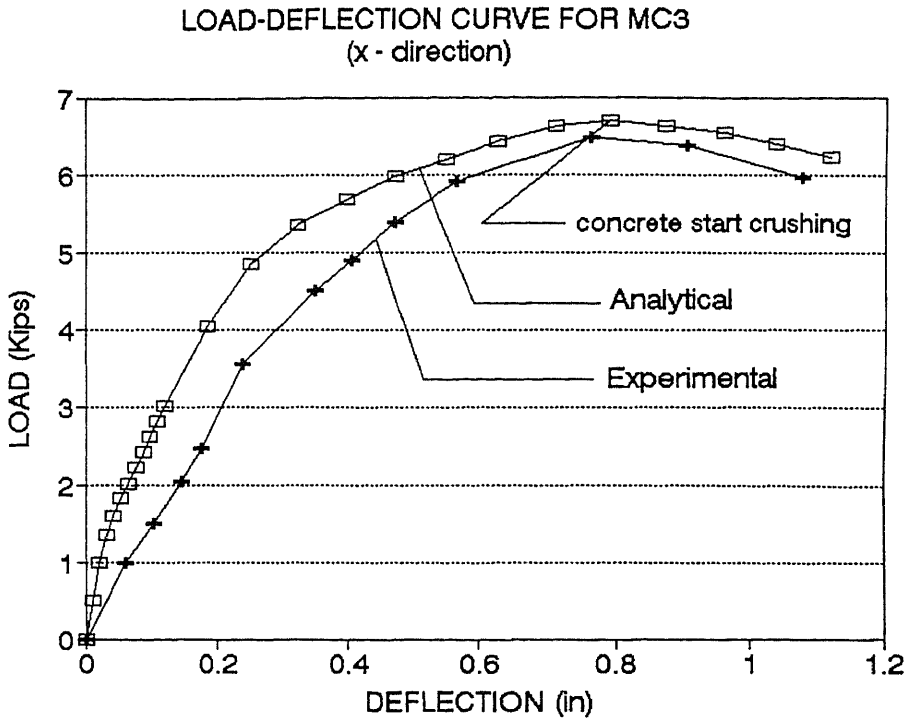


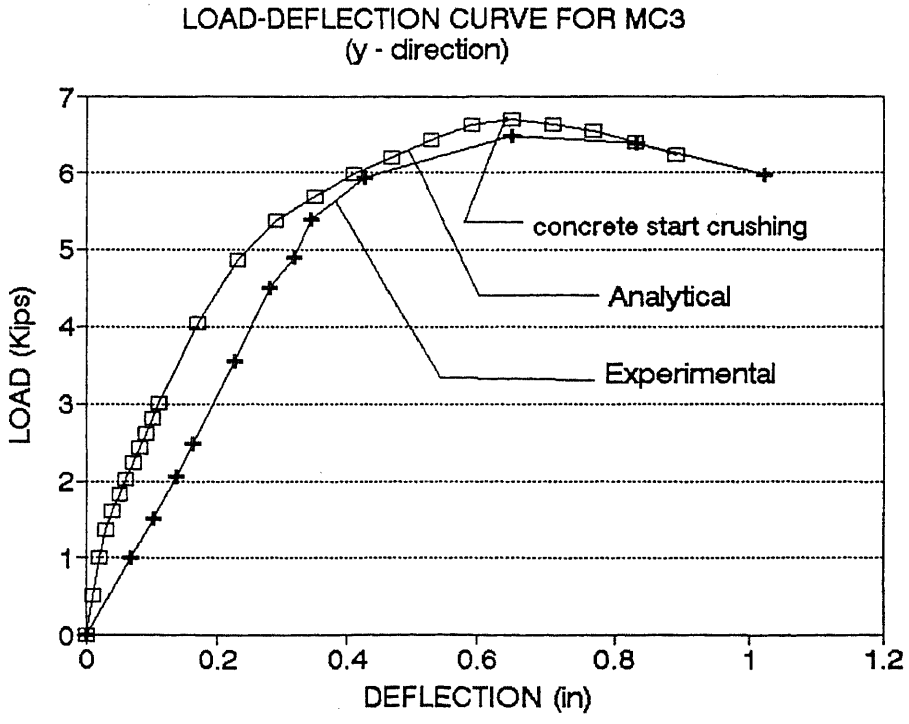


**Figure 4.22** Comparative X and Y Load-Deflection curves for column MC3

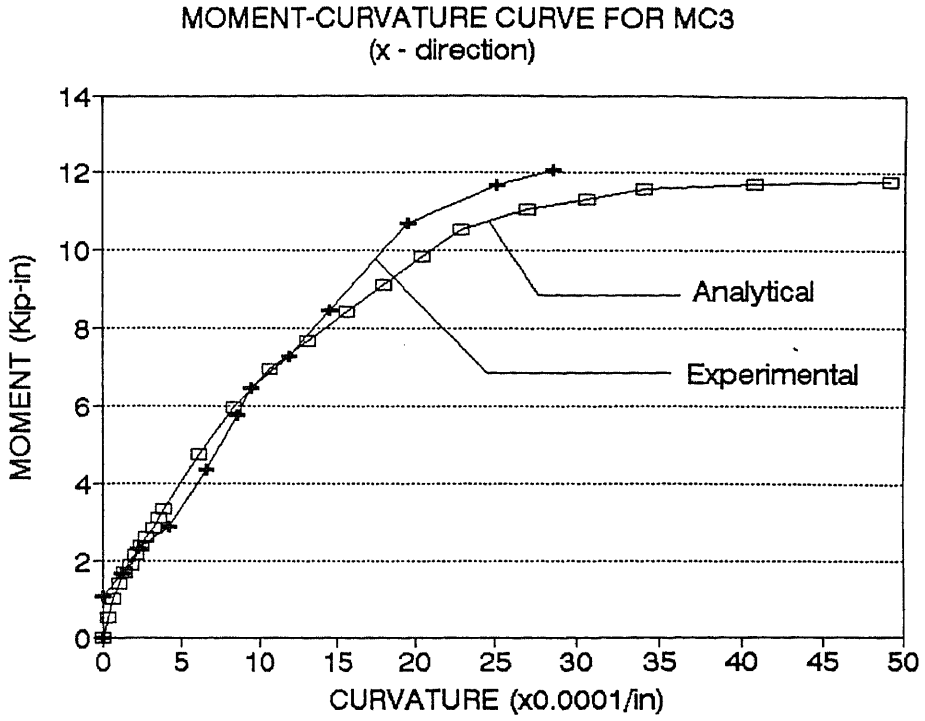


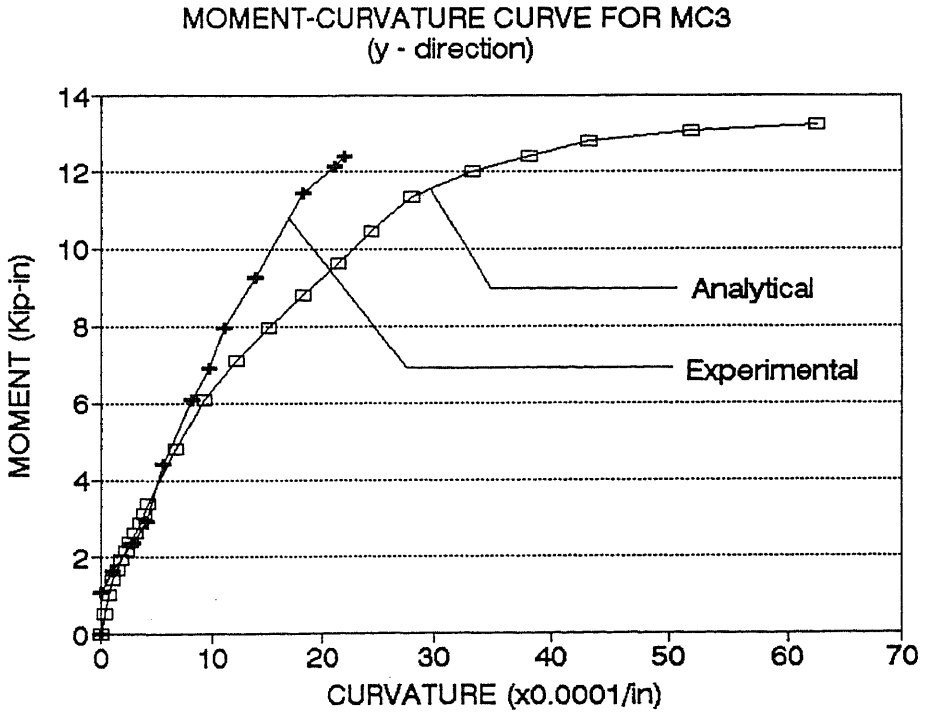


**Figure 4.23** Comparative X and Y Moment-Curvature curves for column MC3

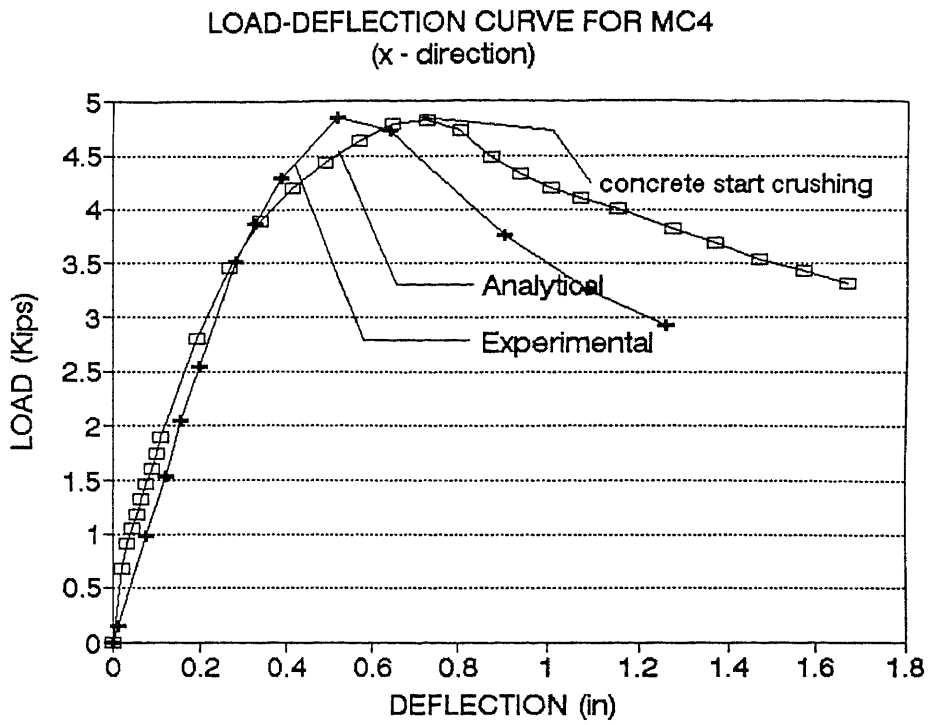


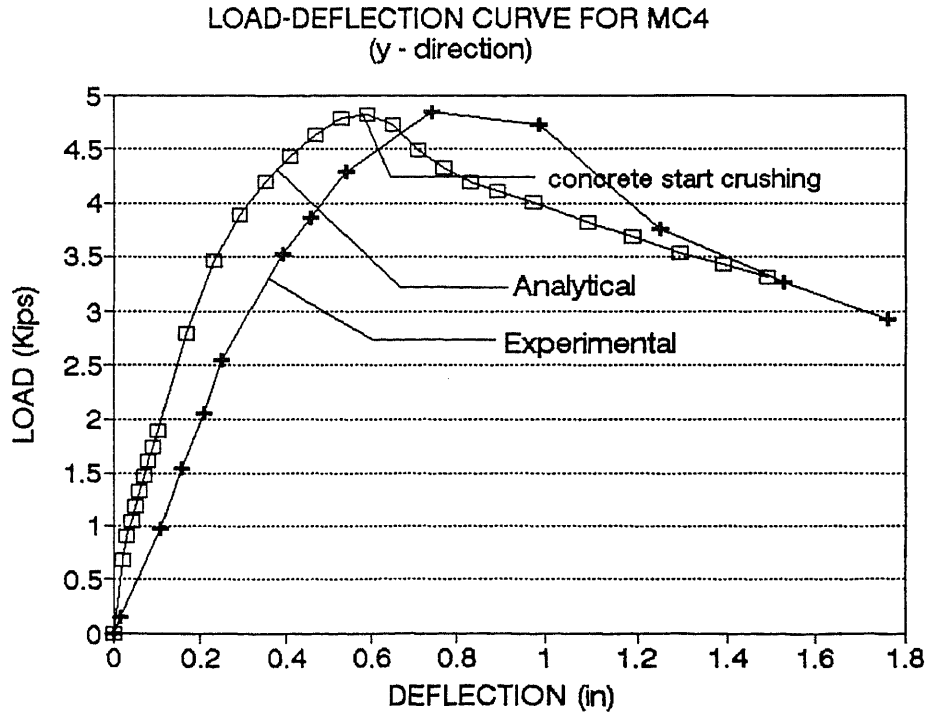


**Figure 4.24** Comparative X and Y Load-Deflection curves for column MC4

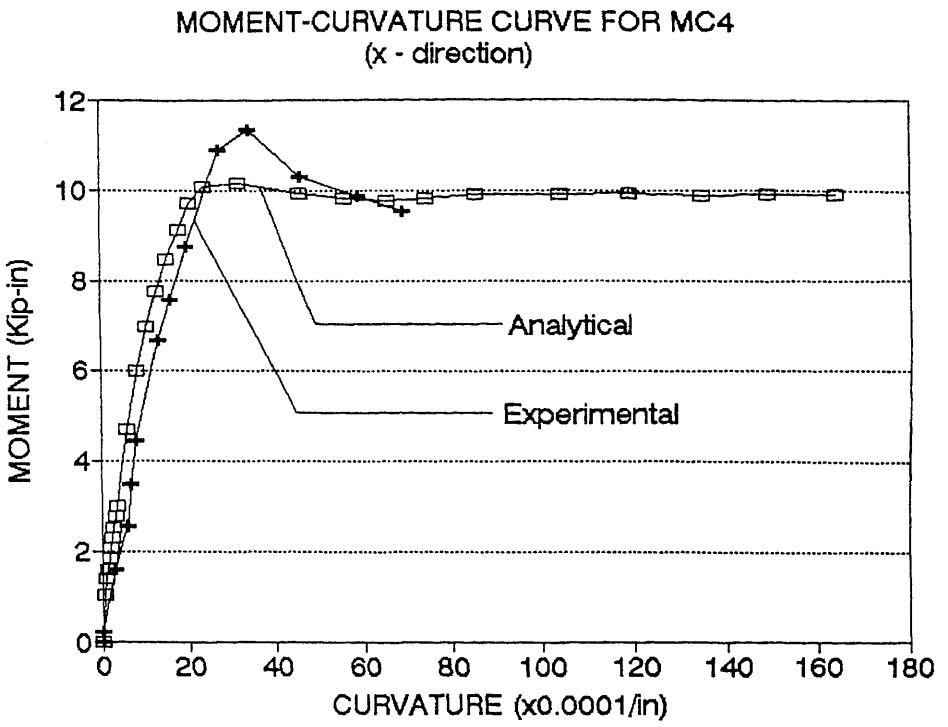


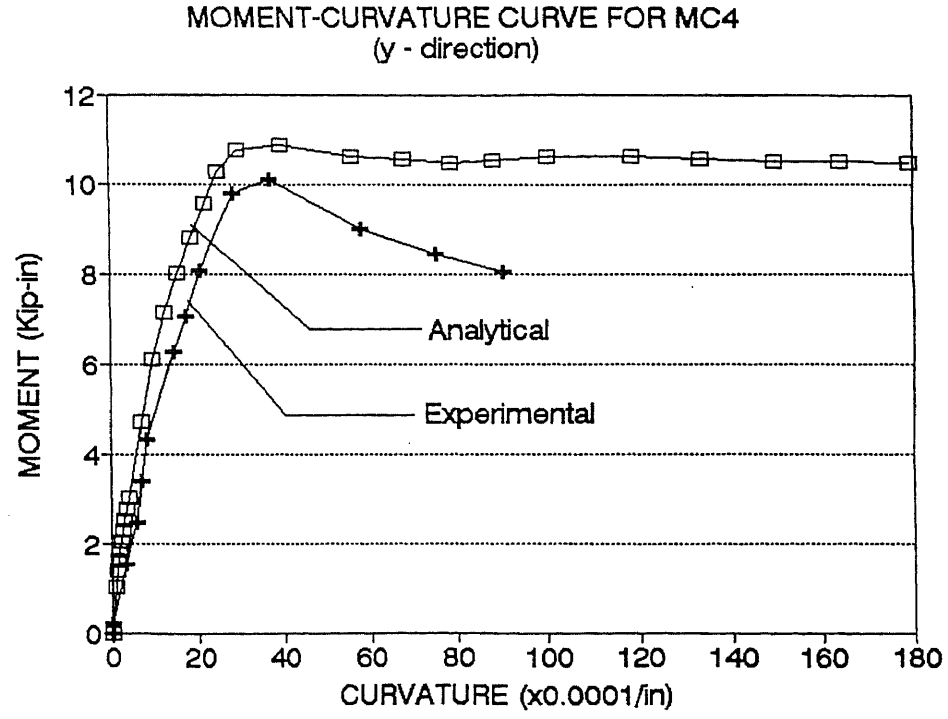


**Figure 4.25** Comparative X and Y Moment-Curvature curves for column MC4

Morino et al. (147) also discussed for the composite columns under biaxial bending and axial compressive load with different stiffness in the x and y-directions. In the large deflection range, the deflection corresponding to the weak axis increases, and the deflection in the other direction ceases increasing or sometimes decreases due to the second order P-δ effect.

It appears that the column in the large deflection range or in a final stage behaves like a member being subjected to uniaxial bending alone about the weak axis.

The type of failure observed for the column specimens at the time of testing was typically that of crushing of concrete on the inside corner of the column (the corner on the concave side of the column) with some noticeable cracking on the tensile faces of the column on the convex side.

**Table 4.6** Failure modes for column specimens MC1, MC2, MC3, and MC4

| Column specimen | Inelastic hinge location | Inelastic hinge length | REMARKS |
|---|---|---|---|
| MC1 | close to middle | +/- 4.5" | inside corner bar buckled and concrete crushed |
| MC2 | below top bracket | +/- 4.0 | concrete crushed |
| MC3 | above middle | +/- 3.75 | concrete crushed |
| MC4 | close to middle | +/- 3.5 " | concrete crushed |
| The descending branch for all column specimens was attained and the test was stopped when excessive deflection was noted. | | | |

It was difficult to obtain the formation of the inelastic hinge right at the midheight of the column specimens, as it was supposed to have occurred due to the

symmetry conditions. For two of the four specimens tested in this research, a relatively very close location of the hinging region near the middle of the column specimen was observed; Thus the test results may be found useful for comparative study of the load-deflection and moment-curvature relationships.

The Behavior of the composite column specimens under biaxial bending moments and axial compressive load can be summarized as follows:

- **Column Specimen MC1:** Minor hairline cracks started to appear at a load level of about 50% of the Maximum load on tensile or convex side of the specimen. Beyond the maximum load level, major cracks started to appear on the convex side of the specimen and at locations near the middle of the column. As the axial load was dropping and the lateral displacement increased, concrete on the concave side of the column started to spall-off. At this time the test was terminated, the corner bar on the concave side was noticed to have buckled, but the ties were not broken. Two dial gages measuring the lateral displacements around the middle of the column had to be reset due to the dislocation resulting from the concrete spall-off.
- **Column Specimen MC2:** Hairline cracks started to appear at a load level of about 30% of the maximum load on the convex side and the dial gages had to be reset at a load level right beyond the maximum load. A premature formation of an inelastic hinge occurred somewhere close to the top bracket possibly due to a misalignment of the top and bottom eccentricities that could have created an unsymmetrical pinned-ended condition.
- **Column Specimen MC3:** Hairline cracks started to appear at a load level of about 40% of the Maximum load. Signs of concrete crush appeared on the concave side of the specimen were observed at a load level near the Maximum load. Dial

gages were reset at the Maximum load level stage and final concrete crushing near the middle of the column height disabled some of the dial gages measuring the lateral displacements. Afterwards the test was terminated.

- **Column Specimen MC4:** Hairline cracks started to appear at a load level of about 40% of the maximum axial load. Dial gages had to be reset at a load level close to the maximum load and later at load levels in the descending branch.

No strain measurements of the steel bars and the steel shape were taken for the column specimens tested in the present experimental investigation. The four composite column specimens presented a zone around the midheight of the specimen where the concrete crushed giving an indication of a typical compression failure of the column in the compression side. That observation corroborated the results of the computer analysis done for the same column specimens. During the course of each column test, it was noted that the magnitude of the axial load was dropped during the dial gage and mechanical strain gage readings. The maximum difference between these readings never exceeded more than 3% of the first load reading. No major separation of the encased steel section was noted to have occurred from the surrounding concrete.

A photographical record of the different aspects of the experimental testing of the composite column specimens MC1, MC2, MC3 and MC4 at the New Jersey Institute of Technology Structures and Concrete Laboratory is presented in Appendix E. Each photo is accompanied by a brief description of the picture contents and can be considered as a diagrammatical representation of each step that takes place during the process of preparing the specimen, casting, curing and physically testing on each one of the composite column specimens.

# CHAPTER 5

# CONCLUSIONS AND DESIGN RECOMMENDATIONS

## 5.1 Conclusions

The following conclusions are presented as a result of this dissertation work:

a.- The Literature Review presented in Chapter 1 reveals that there are two different design methods currently being used in the United States for the Analysis and Design of composite columns. Their differences and in some cases inconsistences were discussed and highlighted.

The Author has found that there is a procedure to incorporate the basic concepts of the two design methods into a unified and consistent design approach.

As part of the critical review of the fundamental equations to evaluate the strength of a composite column cross section, the Author has found that the interaction diagrams and load contours of any column cross section can be mathematically represented by a continuous equation. This equation incorporates all the geometrical and material properties of the cross section and can be particularly defined by interaction coefficients that control the shape of the Failure Surface Diagram of every cross section.

A computer program to study the strength and to calculate the interaction coefficients $\alpha$ and $\beta$ that define the failure surface of the composite cross section has been found to provide all the required column parameters to process the Generalized Equation of Failure Surface for biaxially loaded composite columns presented in Chapter 2.

A study of the calculated values of the coefficient β that defines the shape of the load-contour diagram for a specified composite column cross section reveals that the variation of the coefficient β may be approximated by two straight lines, one linear relationship of the ratio $P_n/P_o^{(+)}$ for the points is above the balanced load and in the compression failure region and the second one is also a linear relationship of the ratio $P_n/P_o^{(-)}$ for the points below the balanced point and in the tensile failure region.

b.- The Author has developed in Chapter 2 a Generalized Interaction Equation of Failure Surface for the Analysis and Design of composite columns. The interaction equation is applicable to the case of columns under biaxial and uniaxial bending in combination with axial compressive or tensile loads. This proposed equation to predict the ultimate load of an eccentrically loaded short or slender composite column has proved to provide very accurate results when compared with experimental results of different researchers. The interaction equation is also used to predict the failure load of the column specimens tested as part of this dissertation and presented in Chapter 4. The calculated analytical loads show very close agreement with the experimental ultimate loads for short, slender, square and rectangular column specimens tested with small and large eccentricities.

The Author has also found that the steel reinforcement bars in a composite column provide a significant contribution of stiffness to the total stiffness value of the composite section.

It is recommended that the expression of the EI used to calculate the critical load and the critical stress of the composite section should include the effect of the reinforcing bars.

The current expressions given by the ACI (1) and the AISC (13) to calculate the flexural stiffness parameter EI of a composite section, seem to be very conservative and in many cases leading to unrealistic values of the critical load and the magnification factor for the case of very slender composite columns. It is a fact that the creep effect due to sustained loads creates a reduction of the flexural stiffness of the composite cross section. However a bottom line value of the usable flexural stiffness should be compatible with the realistic values of ultimate load that the composite column can actually sustain during the lifetime usable period of the structural frame.

c.- A computational method to determine the complete load-deformation behavior of a pinned-ended composite column subjected to biaxial bending moments and axial loads has been presented in Chapter 3. The method has been proved to provide very reasonable and accurate predictions of the ultimate load, ascending and descending profile of the load-displacement and moment-curvature curves for a composite column in a single curvature.

The computational method takes into account the nonlinear behavior of the materials that form the composite section and includes the second order effects due to the additional eccentricity of the applied axial load when the column deforms laterally. The accuracy of the predicted ultimate load depends on the number of segments or subdivisions along the column length and the initial parameters are established for the step load increment and the convergence criteria. The applicability of the computational method to a number of composite columns with a variety of steel shape sections encased in concrete has been demonstrated and proved to provide very accurate results.

The computer method can also be extended to study composite columns reinforced with other materials, such as fiberglass reinforced plastics, aluminum, and other reinforcing materials.

d.- The experimental testing of four small scale pinned-ended composite columns with biaxial bending and axial load in a single curvature proves that very reasonable conclusions can be drawn from the experimental results obtained from the testing and very good agreement has been obtained as compared to the analytical values calculated by the computational method presented in Chapter 3.

## 5.2 Design Recommendations

The last section of this dissertation presents some specific Design Recommendations applicable to the Analysis and Design of Composite Columns and particularly to the case of steel shapes embedded in square or rectangular concrete section with or without longitudinal reinforcing bars.

The experimental testing of four composite column specimens and the computational method implemented to study the behavior of composite columns under biaxial bending and axial loads have provided the Author a way to verify that short and slender columns can be easily modeled and their load-deflection and moment-curvature curves can be determined.

An extensive verification of available test results for composite column specimens under biaxial bending and axial loads shows that some of the current design parameters proposed in the ACI and the AISC should be slightly modified to reflect a more consistent approximation and correlation of the design equation with the experimental data.

The proposed Generalized Interaction Equation of Failure Surface is:

$$\left(\frac{P_n - P_{nb}}{P_o - P_{nb}}\right)^{\alpha} + \left[\left(\delta_{mfx}\frac{M_{nx}}{M_{nb}}M_{fx}\right)^{\beta} + \left(\delta_{mfy}\frac{M_{ny}}{M_{nb}}M_{fy}\right)^{\beta}\right]^{1/\beta} = 1 \tag{5.1}$$

$$\delta_{mfx} = \frac{C_{mx}}{\left(1 - \frac{P_n}{P_{crx}}\right)} \quad ; \quad \delta_{mfy} = \frac{C_{my}}{\left(1 - \frac{P_n}{P_{cry}}\right)} \tag{5.2}$$

with some of the terms shown above defined as follows:

$$M_{fx} = \frac{M_{b1y}}{M_{b1x}} \quad ; \quad M_{fy} = \frac{M_{b2x}}{M_{b2y}} \tag{5.3}$$

$$A_g = b\,t \quad ; \quad C_m = 0.6 + 0.4\frac{M_{1b}}{M_{2b}} \tag{5.4}$$

$$EI_{mc} = \frac{(E_c I_g/2.5)}{1 + \beta_d} + E_s I_s + E_{sr} I_{sr} \quad ; \quad P_{mcr} = \frac{\pi^2\, EI_{mc}}{(kL)^2} \tag{5.5}$$

$$P_o = A_g\, F_{mcr} \tag{5.6}$$

$$F_{mc} = k_1 f_c' (A_c/A_g) + k_2 F_{yr} (A_{sr}/A_g) + k_3 F_y (A_s/A_g) \tag{5.7}$$

$$E_{mc} = E_{sr}(A_{sr}/A_g) + E_s(A_s/A_g) + k_4 E_c (A_c/A_g) \tag{5.8}$$

$$r_{mc} = \sqrt{\frac{E_c I_g/2.5 + E_s I_t + E_{sr} I_{sr}}{E_c A_g/2.5 + E_s A_t + E_{sr} A_{sr}}} \quad ; \quad r_{mc} \le 0.3\,b \tag{5.9}$$

$$\lambda_{mc} = \frac{K\,l}{r_{mc}\pi}\sqrt{\frac{F_{mc}}{E_{mc}}} \tag{5.10}$$

$$for \quad \lambda_{mc} \le 1.5 \;;\; F_{mcr} = \left(0.658^{\lambda_{mc}^{2}}\right) F_{mc} \tag{5.11}$$

$$for \quad \lambda_{mc} > 1.5 \;;\; F_{mcr} = \left[\frac{0.877}{\lambda_{mc}^{2}}\right] F_{mc} \tag{5.12}$$

The above equations provide the nominal axial load and bending moment capacities that are applicable to the case of composite columns as part of a framing system with sidesway prevented.

For the case of compression composite columns not braced against sidesway as part of a Lateral Load Resisting Framing System, the applicable ACI Moment Magnification factors that include the effects of the gravity loads and the lateral loads should be included when evaluating the total moment to be used in the Equation of Failure Surface.

The ACI Building Code (1), Section 10.11.5.1, defines the gravity and lateral load moment magnification factors $\delta_b$ and $\delta_s$, and the applicable bending moments $M_{2b}$ and $M_{2s}$ for gravity and lateral loads, respectively.

The coefficients $\alpha$ and $\beta$ in the Equation of Failure Surface, Eq. 5.1, define the shape of the load-moment (P-M) interaction diagram and the load-contour ($M_x$-$M_y$) diagram of a composite column cross section, respectively.

The coefficient $\alpha$ depends primarily on the shape of the cross section, material properties and the steel layout.

The coefficient $\beta$ defines the ratio of the nominal load capacity of the cross section to the maximum allowable axial load capacity. They can be easily found by using the Author's computer program "INTRDIAG" presented in Appendix A.

In the absence of access to the "INTRDIAG" computer program, the Author recommends the use of the following values for $\alpha_c$ and $\alpha_t$:

(i) For lightly reinforced composite columns, say $1\% \le \rho \le 6\%$,

Bending about the strong axis: $1.4 \le \alpha_c \le 1.9$ ; $1.3 \le \alpha_t \le 1.75$

Bending about the weak axis: $1.75 \le \alpha_c \le 3.0$ ; $2.0 \le \alpha_t \le 3.0$

(ii) For heavily reinforced composite columns, say $6\% \le \rho \le 12\%$,

Bending about the strong axis: $1.25 \le \alpha_c \le 1.4$ ; $1.4 \le \alpha_t \le 1.55$

Bending about the weak axis: $2.2 \le \alpha_c \le 2.7$ ; $2.3 \le \alpha_t \le 2.7$

The coefficient $\beta$ presents its greatest variation when the two ratios of steel shape dimension to composite cross section dimension $b_f/b$ and d/t change.

The Author has found that the values of $f'_c$, $F_y$ and $\rho$ do not affect greatly the coefficients that define the relationship between $\beta$ and the ratio of $P_n/P_o$.

Tabulated values of the coefficients $c_1^c$, $c_2^c$, $c_1^t$ and $c_2^t$ are presented in Table 2.12 to illustrate their variation with respect to the composite section material properties and dimensional ratios.

The following preliminary design recommendations are suggested to estimate the load-contour exponent $\beta$:

(i) For composite cross sections with $0.4 \le d/t \le 0.65$ and $0.4 \le b_f/b \le 0.65$, the exponent $\beta$ of the load-contour diagrams in the compression region is given in the following expression:

$$\beta = c_1^c + c_2^c (P_n / P_o) \; ; \; 1.1 \le c_1^c \le 1.35 \; ; \; 0.35 \le c_2^c \le 1.1 \; ; \; 1.4 \le \beta \le 2$$

For the load-contour diagrams in the tensile region:

$\beta = c_1^t + c_2^t (P_n / P_o)$ ; $1.3 \leq c_1^t \leq 2.15$ ; $0.35 \leq c_2^t \leq 1.4$ ; $1.4 \leq \beta \leq 2.25$

(ii) For composite cross sections with $0.65 < d/t \leq 0.95$ and $0.65 \leq b_f/b \leq 0.95$, the exponent $\beta$ of the load-contour diagrams in the compression region can be found by using the following expression:

$\beta = c_1^c + c_2^c (P_n / P_o)$ ; $2.4 \leq c_1^c \leq 3.45$ ; $-0.25 \leq c_2^c \leq -1.65$ ; $1.6 \leq \beta \leq 2$

For the load-contour diagrams in the tensile region:

$\beta = c_1^t + c_2^t (P_n / P_o)$ ; $2.1 \leq c_1^t \leq 2.85$ ; $0.1 \leq c_2^t \leq -0.9$ ; $1.6 \leq \beta \leq 3.5$

The values presented above are suggested as preliminary design parameters. The more accurate values of the coefficient $\beta$ can be easily computed by using the Author's computer program "INTRDIAG" presented in Appendix A.

The proposed Generalized Interaction Equation of Failure Surface may be used in the two following design situations: Firstly, to examine the adequacy of a particular short or slender composite column cross section for a given set of externally applied axial load and biaxial bending moments. Secondly, to predict the maximum allowable axial load applied to a given composite column cross section at the specified values of eccentricity about the x and y axis.

# APPENDIX

# APPENDIX A

## Listing of BASIC Computer Program "INTRDIAG"

```
10 REM NEW JERSEY INSTITUTE OF TECHNOLOGY; DATE: 02-07-94
15 REM PROGRAM INTRDIAG.BAS
20 REM INTERACTION DIAGRAM FOR COMPOSITE COLUMNS
25 REM SQUARE AND RECTANGULAR CONCRETE-ENCASED STEEL SHAPES
30 REM CALCULATES INTERACTION DIAGRAMS FOR MAJOR AND MINOR AXIS.
40 KEY OFF: CLS : COLOR 1, 10, 4: CLS
50 DIM AB(20), X(50), Y(50), AY(50), AX(50), PN(50), MN(50),
55 DIM PX(50), MX(50)
60 DIM PY(50), MY(50), DI(50), AK(50), C(50), EN(50), EI(50),
62 TS(50), E2(50), CI(50)
65 DIM CX(50), CY(50), XX(50), XY(50), M2(50), M4(50), R1(5)
67 DIM V2(65), V4(65), PH(65), PK(65),MK(65),VA(5),CXY(50)
68 DIM M6(2500), ZX(2500), ZY(2500), PT(50), RX(5), RY(5)
69 DIM M7(60, 5), M8(60, 5), XB(5), YB(5), CS(60), V5(60),
70 V6(60), MZX(60), MZY(60),R2(5),QX(50,2),QY(50,2),DR(50)
71 DIM MRX(60), MRY(60), XZ(50), YZ(50), AC(50), AD(50),
72 DIM MNX(60), MNY(60), ENX(50), ENY(50), EXY(50), XXY(50)
73 DIM DCP(50), DCB(50), MXZ(50), MYZ(50), MXY(10, 50)
74 DIM PBN(10), MBN(10), MLC(10, 50), MOX(10, 50),PXY(10,50)
76 DIM PNO(50), KXP(50), PLC(10, 50),MOY(10,50),BTC(50)
77 PRINT "INTERACTION DIAGRAM PROGRAM FOR COMPOSITE COLUMNS"
78 PRINT "CONCRETE-ENCASED STRUCTURAL STEEL I-SHAPE SECTIONS"
80 PRINT "NEW JERSEY INSTITUTE OF TECHNOLOGY - SPRING 1993"
90 PRINT "BY: PEDRO RICARDO MUNOZ-ARIAS, MSCE": PRINT
100 REM INPUT GEOMETRY OF COMPOSITE COLUMN CROSS SECTION
102 INPUT "COLUMN FILE NAME (WITHOUT EXTENSION) = "; F9$
103 NF$ = F9$: F9$ = F9$ + ".RES"
104 OPEN "O", #9, F9$
105 PI = 3.141593
107 PRINT : PRINT "COMPOSITE COLUMN OVERALL DIMENSIONS"
110 INPUT "COLUMN WIDTH (SHORT DIMENSION inch.) = "; B
120 INPUT "COLUMN DEPTH (LONG DIMENSION inch.) = "; T: PRINT
121 INPUT "STEEL I-SHAPE AND CONCRETE MAJOR AXIS PARALLEL (Y/N):"; WF$
122 INPUT "STEEL WIDE FLANGE WIDTH (inch.) = "; BW
123 INPUT "STEEL WIDE FLANGE DEPTH (inch.) = "; DW
124 IF WF$ = "Y" OR WF$ = "y" THEN 125 ELSE 126
125 IF BW > B OR DW > T THEN 122 ELSE 128
126 IF DW > B OR BW > T THEN 122
128 INPUT "STEEL FLANGE THICKNESS (inch.) = "; TF
130 INPUT "STEEL WEB THICKNESS (inch.) = "; TW: PRINT
135 REM INPUT MATERIAL PROPERTIES
140 INPUT "ULT. COMPRESSIVE STRENGTH OF CONCRETE (ksi) = "; FC
150 INPUT "YIELD STRENGTH OF REBARS (ksi) = "; FY
160 INPUT "MODULUS OF ELASTICITY OF STEEL REBARS (ksi) = "; ES
162 INPUT "YIELD STRENGTH OF THE STEEL SHAPE (ksi) = "; FYS
```

```
164 INPUT "MOD. OF ELASTICITY OF THE STEEL SHAPE (ksi) = "; ESS
166 NFE = 11: NWE = 11: NSE = 2 * NFE + NWE
170 EC = 57 * SQR(FC * 1000): EY = FY / ES: EYS = FYS / ESS
180 IF FC < = 4 THEN B1 = .85 ELSE IF FC < = 8 THEN B1 = 1.05-.05*FC ELSE B1 = .65
190 REM INPUT STEEL REINFORCEMENT SIZE AND LOCATION
200 INPUT "NUMBER OF BARS ALONG LONG SIDE/PER FACE  = "; NL
205 INPUT "ALL BARS ALONG LONG SIDE SAME DIAMETER(Y/N)"; YL$
207 IF YL$ = "N" THEN 215
210 INPUT "DIAMETER OF BAR ALONG LONG SIDE  (No. )  = "; DL
212 IF DL<2 OR DL=12 OR DL=13 OR DL=15 OR DL=16 OR DL=17
    OR DL>18 THEN 210
215 INPUT "COVER OF REBARS ALONG LONG SIDE (inch.) = ";D2:PRINT
220 INPUT "No. OF INTERIOR BARS ALONG SHORT SIDE/FACE = " NS
225 IF NS = 0 THEN 240
227 INPUT "ALL BARS ALONG SHORT SIDE SAME DIAMETER(Y/N)";YS$
228 IF YS$ = "N" THEN 240
230 INPUT "DIAMETER OF BAR ALONG SHORT SIDE  (No. )  = "; DS
235 IF DS<2 OR DS=12 OR DS=13 OR DS=15 OR DS=16 OR
    DS=17 OR DS>18 THEN 230
240 AB(2) = .05:AB(3) = .11:AB(4) = .2:AB(5) = .31: AB(6) = .44
250 AB(7) = .6: AB(8) = .79: AB(9) = 1!: AB(10) = 1.27
260 AB(11) = 1.56: AB(14) = 2.25: AB(18) = 4!
270 REM INPUT COORD. OF REBARS ALONG LONG & SHORT DIRECTION
280 AT = 0: A1 = 0: A2 = 0
285 PRINT "COORDINATES OF STEEL REBARS ALONG LONG SIDE"
290 FOR I = 1 TO NL
300 PRINT "BAR # "; I;
301 INPUT "DISTANCE FROM BOTTOM EDGE (inch.) = "; Y(I)
302 IF YL$ < > "N" THEN 310
303 IF I = NL THEN DL = DC: GOTO 310
304 PRINT "BAR #";I;:INPUT "DIAMETER OF BAR(No.) = ";DL 305 IF I=1 THEN DC = DL
306 IF DL < 2 OR DL = 12 OR DL = 13 OR DL = 15 OR
    DL = 16 OR DL = 17 OR DL > 18 THEN 304
310 AY(I) = AB(DL): A1 = A1 + 2 * AY(I)
315 NEXT I
318 D3 = Y(1): D4 = Y(NL): D5 = (T - D4)
320 AT = AT + A1
325 IF NS = 0 THEN A2 = 0: GOTO 370
330 PRINT : PRINT "COORD. OF INTERIOR STEEL REBARS ALONG SHORT SIDE"
340 FOR I = 1 TO NS
350 PRINT "BAR # ";I;
351 INPUT "DISTANCE FROM LEFT EDGE(inch.) = "; X(I)
352 IF YS$ < > "N" THEN 360
354 PRINT "BAR # "; I; : INPUT "DIAMETER OF BAR (No.) = "; DS
356 IF DS < 2 OR DS = 12 OR DS = 13 OR DS = 15 OR
    DS = 16 OR DS = 17 OR DS > 18 THEN 354
360 AX(I) = AB(DS): A2 = A2 + 2 * AX(I)
365 NEXT I
370 AT = AT + A2: ATB = AT
381 REM DEFINE PARAMETERS FOR STEEL SHAPE ELEMENT COORDINATES
382 NTB = 2 * (NL + NS)
384 TNS = NTB + NSE
385 GOSUB 1500
386 AT = ATB + ATS: AG = B * T: RO = AT / AG
```

```
388 PO = .85 * FC * (AG - ATB - ATS) + FY * ATB + FYS * ATS:
389 PF = -(FY * ATB + FYS * ATS): PN(0) = PO: MN(0) = 0!
390 PRINT "DEFINE NO. OF POINTS FOR REGIONS OF THE INTERACTION DIAGRAM"
400 INPUT "NUMBER OF POINTS FOR REGION I =";N1
410 INPUT "NUMBER OF POINTS FOR REGION II =";N2
420 INPUT "NUMBER OF POINTS FOR REGION III=";N3
430 INPUT "NUMBER OF POINTS FOR REGION IV =";N4: PRINT
440 K1 = N1 + N2: K2 = N1 + N2 + N3
460 REM DEFINE INPUT DATA FOR INTERACTION DIAGRAM-Pnx * Mnx
470 JZ = K2: BB = B: H = T:NE = NL: NI = NS: NT = NE: MMX = 0
480 FOR I = 1 TO NE: DI(I) = H - Y(I): DI(I + NE) = DI(I)
482 AK(I) = AY(I): AK(I + NE) = AK(I): NEXT I
490 D = DI(1): D1 = DI(NE)
500 IF NI = 0 THEN 530
502 FOR I = 1 TO NI
504 DI(2 * NE + I) = DI(1): DI(2 * NE + I + NI) = DI(NE)
506 AK(2 * NE + I) = AX(I): AK(2 * NE + I + NI) = AX(I)
508 NEXT I
530 FOR I = IWF TO TNS: DI(I) = H - Y(I): NEXT I
531 REM FOR I = 1 TO TNS: PRINT I, DI(I), AK(I): INPUT Z$:
532 NEXT I :DDC = DI(1)
533 PRINT "CALCULATION OF INTERACTION VALUES FOR X-X BENDING...WAIT"
534 GOSUB 2000
535 JX = K5: J = JX - 1: X3 = NZ: JX3 = JZ: K1X = KX
540 REM CALCULATED VALUES OF Pnx* Mnx
550 PX(0) = PN(0): PX(JX) = PN(K5): MX(0) = 0!: MX(JX) = 0!
555 CX(0) = 9999!: CX(JX) = 9999!: XX(0) = 0!: XX(JX) = 0!
560 FOR I = 1 TO J: PX(I) = PN(I): MX(I) = MN(I): XX(I) =0
565 EN(I): CX(I) = C(I): NEXT I
1000 REM DEFINE INPUT DATA FOR INTERACTION DIAGRAM-Pny*Mny
1010 JZ = K2: BB = T: H = B: MMX = 0
1020 FOR I = 1 TO NL
1030 DI(I)=H-D2:DI(I+NL)=D2:AK(I) = AY(I): AK(I + NL) = AY(I)
1040 NEXT I
1042 D = DI(1): D1 = DI(2 * NL)
1045 IF NS = 0 THEN 1070
1047 FOR I = 1 TO NS
1049 DI(2 * NL + I) = H - X(I): DI(2 * NL + I + NS) = H - X(I)
1050 AK(2 * NL + I) = AX(I): AK(2 * NL + I + NS) = AX(I)
1060 NEXT I
1070 FOR I = IWF TO TNS: DI(I) = H - X(I): NEXT I
1072 REM FOR I =1 TO TNS:PRINT I,DI(I),AK(I):INPUT Z$: NEXT I
1074 DDC = DI(1): PRINT
1076 PRINT "CALCULATION OF INTERACTION VALUES FOR Y-Y BENDING...WAIT"
1078 GOSUB 2000
1080 JY = K5: J = JY - 1: Y3 = NZ: JY3 = JZ: K1Y = KX
1085 REM CALCULATED VALUES OF  Pny & Mny
1090 PY(0) = PN(0): PY(JY) = PN(K5): MY(0) = 0!: MY(JY) = 0!
1100 CY(0) = 9999!: CY(JY) = 9999!: XY(0) = 0!: XY(JY) = 0!
1110 FOR I = 1 TO J: PY(I) = PN(I): MY(I) = MN(I): XY(I) = EN(I): CY(I)= C(I): NEXT I
1125 GOSUB 3000: PRINT
1130 INPUT "COLUMN DATA AND INTERACTION DIAGRAM POINTS
     OUTPUT TO FILE (Y/N) ="; YN$
1140 IF YN$ = "Y" OR YN$ = "y" THEN GOSUB 4000
```

```
1150 REM CALCULATION OF DESIGN INTERACTION EQUATION
1160 GOSUB 5000
1162 GOSUB 4500
1165 GOSUB 8000
1170 GOSUB 7000
1180 CLS : PRINT "*** UNIAXIAL  INTERACTION  DIAGRAM  ***"
1182 PRINT "*** PROGRAM  COMPLETED AND TERMINATED ***"
1185 PRINT:INPUT"RUN UNIAXIAL PROGRAM AGAIN FOR ANOTHER SECTION"; YN$
1187 IF YN$ = "Y" OR YN$ = "y" THEN 10
1190 PRINT : INPUT "RUN PROGRAM FOR BIAXIAL INTERACTION
     DIAGRAMS <Y/N>:";YN$
1192 IF YN$ = "Y" OR YN$ = "y" THEN GOSUB 9000
1194 INPUT "RUN PROGRAM FOR ANOTHER COLUMN SECTION (Y/N):";YN$
1196 CLOSE #9
1198 IF YN$ = "Y" OR YN$ = "y" THEN 10
1200 END
1500 REM SUBROUTINE TO GENERATE THE X AND Y COORDINATES OF STEEL
     SHAPE ELEMENTS
1515 IWF = (NTB + 1):AFE = (BW*TF)/NFE:AWE = (DW - 2 * TF) * TW / NWE
1517 DWW = (DW - 2 * TF): IWN = (NTB + 2 * NFE + 1)
1520 IF WF$ = "Y" OR WF$ = "y" THEN 1530 ELSE 1800
1525 REM AREA, X AND Y COORDINATES FOR THE I-SHAPE SECTION
     STEEL ELEMENTS
1527 REM AREA AND X - COORDINATES
1530 FOR I = IWF TO (NTB + NFE)
1540 X(I) = B/2 -BW/2 + BW/(2 * NFE) + (BW/NFE)*(I-IWF): AK(I) = AFE
1550 X(I + NFE) = X(I): AK(I + NFE) = AFE
1560 NEXT I
1570 FOR I = IWN TO TNS: X(I) = B / 2: AK(I) = AWE: NEXT I
1572 REM Y - COORDINATES
1575 YI = (T / 2 - DW / 2) + TF / 2
1580 FOR I = IWF TO (NTB + NFE)
1590 Y(I) = YI: Y(I + NFE) = YI + DW - TF
1600 NEXT I
1610 FOR I = IWN TO TNS
1620 Y(I) = YI + TF / 2 + DWW / (2 * NWE) + (DWW/NWE)*(I - IWN)
1630 NEXT I
1640 GOTO 1900
1800 REM AREA, X AND Y COORDINATES FOR THE H-SHAPE SECTION
     STEEL ELEMENTS
1810 REM AREA AND Y - COORDINATES
1820 FOR I = IWF TO (NTB + NFE)
1825 Y(I) = T/2-BW/2 + BW/(2*NFE) + (BW/NFE)*(I- IWF): AK(I) = AFE
1830 Y(I + NFE) = Y(I): AK(I + NFE) = AFE
1835 NEXT I
1845 FOR I = IWN TO TNS: Y(I) = T / 2: AK(I) = AWE: NEXT I
1850 REM X - COORDINATES
1855 XI = (B / 2 - DW / 2) + TF / 2
1860 FOR I = IWF TO (NTB + NFE)
1865 X(I) = XI: X(I + NFE) = XI + DW - TF
1870 NEXT I
1875 FOR I = IWN TO TNS
1880 X(I) = XI + TF/2 + DWW/ (2 * NFE) + (DWW / NWE) * (I - IWN)
1885 NEXT I
```

```
1900 REM CALCULATING TOTAL AREA OF STEEL SHAPE ELEMENTS
1920 ATS = 2 * BW * TF + DWW * TW
1950 RETURN
2000 REM SUBROUTINE TO CALCULATE INTERACTION DIAGRAM POINTS
2005 REM CALCULATION OF INTERACTION POINTS IN THE
     COMPRESSION REGION
2010 C(1) = H: C(N1) = D: N0 = N1 - 1: CD = (C(N1) - C(1)) / N0
2020 FOR I = 2 TO N0: C(I) = C(I - 1) + CD: NEXT I
2030 CB = .003 * DDC / (.003 + EY): J = N1 + 1: K = N1 + N2-1  2032
     CD = (CB - C(N1)) / N2: C(K1) = CB
2040 FOR I = J TO K: C(I) = C(I - 1) + CD: NEXT I
2050 J = K1 + 1: K = N1 + N2 + N3 - 1: C(K2) = .1 * D1 / B1
2052 CM = C(K2): CD = (CM - CB) / N3
2060 FOR I = J TO K: C(I) = C(I - 1) + CD: NEXT I
2070 J = 1: W = K2: FG = 0!: TL = .95
2080 FOR I = J TO W
2090 A = B1 * C(I): CI = C(I): PN(I) = .85 * FC * A * BB:
2092 CC = PN(I): MN(I) = CC * (H / 2 - A / 2)
2100 FOR K = 1 TO TNS
2105 IF K > NTB THEN ES = ESS: FY = FYS: EY = EYS
2110 EK = .003 * (CI - DI(K)) / CI: SG = SGN(EK): EZ = ABS(EK)
2115 IF EZ >= EY THEN ET = SG * EY ELSE ET = EK
2120 IF DI(K) <= A THEN FS = (ET*ES - .85 * FC) ELSE FS = ET * ES
2130 CS(K) = AK(K) * FS: PN(I) = PN(I) + CS(K)
2140 MN(I) = MN(I) + CS(K) * (H / 2 - DI(K))
2150 NEXT K
2160 EN(I) = MN(I) / PN(I): MTM = MN(I)
2165 IF MTM > MMX THEN MMX = MTM: KX = I
2170 IF I <= K1 THEN 2290
2175 IF I > JZ THEN 2290
2180 IF FG = 1! THEN 2220
2190 S1 = SGN(PN(I - 1)): S2 = SGN(PN(I)): IF S1 = S2 THEN 2290
2200 TP = PN(I - 1): BP = PN(I): C1 = C(I - 1): C2 = C(I)
2202 C(I) = (C(I - 1) + C(I)) / 2: FG = 1!
2210 GOTO 2090
2220 PZ = PN(I): MZ = MN(I): CZ = C(I)
2230 IF ABS(PZ) <= TL THEN 2270
2240 S1 = SGN(TP): S2 = SGN(BP): S3 = SGN(PZ)
2250 IF S3 = S1 THEN TP = PZ: C1 = CZ ELSE C2 = CZ: BP = PZ
2260 C(I) = (C1 + C2) / 2: GOTO 2090
2270 NZ = I - (N1 + N2): JZ = N1 + N2 + NZ: PN(JZ) = 0!
2272 MN(JZ) = MN(I): C(JZ) = C(I)
2275 EN(JZ) = 9999!
2280 GOTO 2300
2290 NEXT I
2295 GOTO 2350
2297 REM CALCULATION OF INTERACTION POINTS IN THE TENSILE REGION
2300 K3 = JZ + 1: K4 = JZ + N4: J = K3: W = K4: K5 = K4 + 1
2310 C(K4) = .85 * D1 / B1: CD = (C(K4) - C(JZ)) / N4
2320 FOR I = J TO W: C(I) = C(I - 1) + CD: NEXT I
2330 GOTO 2080
2350 PN(K5) = PF: MN(K5) = 0!
2360 RETURN
3000 REM SUBROUTINE TO OUTPUT RESULTS
```

```
3002 A$ = "###.##^^^^    ": CLS : PRINT
3004 PRINT "COMPOSITE COLUMN INTERACTION DIAGRAM"
3006 PRINT "NOMINAL AXIAL LOAD AND BENDING MOMENTS": PRINT
3010 PRINT "MAXIMUM AXIAL COMPRESSIVE LOAD (kips) = "; PO
3020 PRINT "MAXIMUM AXIAL TENSILE LOAD     (kips) = "; PF: PRINT
3030 PRINT "INTERACTION DIAGRAM POINTS*BENDING ABOUT X-X"
3040 PRINT "BALANCED LOAD      Pnbx (kips)  = "; PX(K1X)
3050 PRINT "BALANCED MOMENT    Mnbx (kip-in) = "; MX(K1X)
3052 PRINT "BALANCED ECCENTRICITY enby (in.) = "; XX(K1X)
3055 PRINT : INPUT "PRESS ANY KEY TO CONTINUE ..."; Z$
3060 PRINT : PRINT "I", "Pnx", "Mnx", "eny", "Cny"
3070 FOR I = 0 TO JX:PRINT I,PX(I), MX(I), XX(I), CX(I): NEXT I
3080 PRINT : INPUT "PRESS ANY KEY TO CONTINUE ..."; Z$
3090 CLS : PRINT
3092 PRINT "INTERACTION DIAGRAM POINTS*BENDING ABOUT Y-Y"
3100 PRINT "BALANCED LOAD      Pnby (kips)  = "; PY(K1Y)
3110 PRINT "BALANCED MOMENT    Mnby (kip-in) = "; MY(K1Y)
3112 PRINT "BALANCED ECCENTRICITY enbx (in.) = "; XY(K1Y)
3115 PRINT : INPUT "PRESS ANY KEY TO CONTINUE ..."; Z$
3120 PRINT : PRINT "I", "Pny", "Mny", "enx", "Cnx"
3130 FOR I = 0 TO JY: PRINT I,PY(I),MY(I), XY(I), CY(I): NEXT I
3150 RETURN
4000 PRINT #9, "INTERACTION DIAGRAM PROGRAM FOR
     COMPOSITE COLUMNS"
4001 PRINT #9, "COLUMN FILE NAME :"; F9$
4002 PRINT #9, "COLUMN SECTION GEOMETRY AND MATERIAL
     PROPERTIES"
4003 PRINT #9, "COLUMN WIDTH (SHORT DIMENSION inch.) = "; B
4004 PRINT #9, "COLUMN DEPTH (LONG  DIMENSION inch.) = "; T
4005 PRINT #9, "STEEL WIDE FLANGE WIDTH (inch.) = "; BW
4006 PRINT #9, "STEEL WIDE FLANGE DEPTH (inch.) = "; DW
4008 PRINT #9, "STEEL FLANGE THICHNESS (inch.) = "; TF
4010 PRINT #9, "STEEL WEB   THICKNESS (inch.) = "; TW
4012 PRINT #9, "ULT. COMPR. STRENGTH OF CONCRETE (ksi) = "; FC
4014 PRINT #9, "YIELD STRENGTH OF STEEL REBARS (ksi) = "; FY
4016 PRINT #9, "MOD. OF ELASTICITY OF CONCRETE (ksi) = "; EC
4018 PRINT #9, "MOD. OF ELASTICITY OF STEEL REBARS (ksi) = "; ES
4020 PRINT #9, "YIELD STRENGTH OF THE STEEL SHAPE (ksi) = "; FYS
4022 PRINT #9, "MOD. OF ELASTICITY OF STEEL SHAPE (ksi) = "; ESS
4028 PRINT #9, "COLUMN SECTION REINFORCEMENT"
4030 PRINT #9, "NUMBER OF BARS ALONG LONG SIDE/FACE = "; NL
4032 PRINT #9, "NO. OF INT. BARS ALONG SHORT SIDE/FACE = "; NS
4035 PRINT #9, "DIAMETER OF BARS ALONG LONG  SIDE (inch.) = ";DL
4040 PRINT #9, "DIAMETER OF BARS ALONG SHORT SIDE (inch.) = ";DS
4050 PRINT #9, "COVER OF REBARS ALONG LONG SIDE (inch) = "; D2
4060 PRINT #9, "NUMBER OF POINTS FOR REGION I  = "; N1
4070 PRINT #9, "NUMBER OF POINTS FOR REGION II = "; N2
4080 PRINT #9, "NO. OF POINTS FOR REGION III - ABOUT X-X = "; X3
4085 PRINT #9, "NUMBER OF POINTS FOR REGION III-ABOUT Y-Y = ";Y3
4090 PRINT #9, "NUMBER OF POINTS FOR REGION IV = "; N4
4100 PRINT #9, "MAXIMUM AXIAL COMPRESSIVE LOAD (kips) = "; PO
4110 PRINT #9, "MAXIMUM AXIAL TENSILE LOAD     (kips) = "; PF
4120 PRINT #9, "INTERACTION DIAGRAM POINTS FOR X-X BENDING"
4130 PRINT #9, "BALANCED LOAD      Pnbx (kips)  = "; PX(K1X)
```

```
4140 PRINT #9, "BALANCED MOMENT    Mnbx (kip-in) = "; MX(K1X)
4145 PRINT #9, "BALANCED ECCENTRICITY enby (in.) = "; XX(K1X)
4150 PRINT #9, "POINT", "Pnx", "Mnx", "eny", "Cny"
4160 FOR I = 0 TO JX:PRINT #9,I,PX(I),MX(I),XX(I),CX(I):4165 NEXT I
4170 PRINT #9, "INTERACTION DIAGRAM POINTS FOR Y-Y BENDING"
4180 PRINT #9, "BALANCED LOAD      Pnby (kips)  = "; PY(K1Y)
4190 PRINT #9, "BALANCED MOMENT    Mnby (kip-in) = "; MY(K1Y)
4195 PRINT #9, "BALANCED ECCENTRICITY enbx (in.) = "; XY(K1Y)
4200 PRINT #9, "POINT", "Pny", "Mny", "enx", "Cnx"
4210 FOR I = 0 TO JY:PRINT #9,I,PY(I),MY(I),XY(I),CY(I):  4215 NEXT I
4220 RETURN
4500 REM SUBROUTINE TO PRINT DESIGN INTERACTION MOMENT VALUES
4505 PRINT #9, "INTERACTION DIAGRAM POINTS BY MUNOZ'S
     INTERACTION EQUATION"
4515 PRINT #9, "X-X BENDING-BEST COMPRESSION SIDE-ALPHA = "; XC
4517 PRINT #9, "X-X BENDING BEST TENSILE SIDE - ALPHA = "; XT
4520 PRINT #9, "POINT", "Pnx", "Mnx", "M'nx", "M'nx/Mnx"
4540 FOR I = 0 TO JX
4550 IF I = 0 OR I = JX THEN M9 = 1 ELSE M9 = MRX(I)
4560 PRINT #9, I, PX(I), MX(I), MZX(I), M9: NEXT I
4575 PRINT #9, "Y-Y BENDING-BEST COMPRESSION SIDE-ALPHA = "; YC
4577 PRINT #9, "Y-Y BENDING-BEST COMPRESSION SIDE-ALPHA = "; YT
4580 PRINT #9, "POINT", "Pny", "Mny", "M'ny", "M'ny/Mny"
4600 FOR I = 0 TO JY
4610 IF I = 0 OR I = JY THEN M9 = 1 ELSE M9 = MRY(I)
4620 PRINT #9, I, PY(I), MY(I), MZY(I), M9: NEXT I
4630 RETURN
5000 REM SUBROUTINE TO CALCULATE DESIGN INTERACTION
     EQUATIONS
5010 L = .25: Q = 3!: API = .05: M = (Q - L) / API + 1
5020 REM UNIAXIAL BENDING ABOUT X-X
5025 CLS : PRINT
5027 PRINT "CALCULATION OF COEFFICIENT ALPHA(COMP/TENS) FOR
     BENDING ABOUT X-X"
5029 PRINT : PRINT "*** CALCULATIONS IN PROGRESS ... ,PLEASE WAIT !!! ***"
5030 J = JX: P0 = PX(0): P1 = PX(K1X): M0 = MX(K1X)
5040 FOR I = 0 TO J: PK(I) = PX(I): MK(I) = MX(I): NEXT I
5042 MV$ = "N": YN$ = "N": GOTO 5050
5045 INPUT "SCREEN/OUTPUT OF MOMENTS FOR ALPHA = 0.25 TO 3.00 (Y/N) = "; MV$
5047 INPUT "SAVE FILE OF MOMENT DEVIATIONS ALPHA = .25 TO 3.0 (Y/N) = ";YN$
5050 KXY = K1X
5051 GOSUB 5500
5052 FOR K = 1 TO M:FOR I = 0 TO J: LL = I + (K - 1) * (J + 1)
5054 ZX(LL) = M6(LL): NEXT I: NEXT K
5056 VX = AH: VA(1) = VX: XC = AHC: XT = AHT
5060 REM UNIAXIAL BENDING ABOUT Y-Y
5065 CLS : PRINT
5066 PRINT "CALCULATION OF COEFFICIENT ALPHA(COMP/TENS)
     FOR BENDING ABOUT Y-Y"
5067 PRINT : PRINT "*** CALCULATIONS IN PROGRESS ... ,PLEASE WAIT !!! ***"
5070 J = JY: P0 = PY(0): P1 = PY(K1Y): M0 = MY(K1Y)
5080 FOR I = 0 TO J: PK(I) = PY(I): MK(I) = MY(I): NEXT I
5085 KXY = K1Y
5090 GOSUB 5500
```

```
5092 FOR K=1TO M: FOR I = 0 TO J: LL = I + (K - 1) * (J + 1)
5094 ZY(LL) = M6(LL): NEXT I: NEXT K
5096 VY = AH: VA(2) = VY: YC = AHC: YT = AHT
5100 GOTO 6050
5500 REM SUBROUTINE TO CALCULATE INTERACTION VALUES
5510 FO R K= 1 TO M:V4(K)= 0!: V5(K) = 0!: V6(K) = 0!: NEXT K
5520 FOR K = 1 TO M
5525 L1 = (K - 1) * (J + 1): L2 = (K - 1) * (J + 1) + J
5527 M6(L1) = 0!: M6(L2) = 0!
5530 PH(K) = L + (K - 1) * API: AP = PH(K)
5540 FOR I = 1 TO J - 1
5545 LL = I + (K - 1) * (J + 1)
5550 P2 = PK(I): IF I > KXY THEN P0 = PK(J)
5570 M2(I) = M0 * (1 - ((P2 - P1) / (P0 - P1)) ^ AP)
5580 M4(I) = M2(I) / MK(I)
5590 V2(I) = ((M2(I) - MK(I)) / 1000) ^ 2
5600 V4(K) = V4(K) + V2(I)
5602 IF I < = KXY THEN V5(K) = V5(K) + V2(I): GOTO 5610
5604 V6(K) = V6(K) + V2(I)
5610 M6(LL) = M2(I)
5700 NEXT I
5705 IF MV$ = "Y" OR MV$ = "y" THEN 5710 ELSE 5870
5710 FYN$ = "Y"
5720 PRINT "ALPHA="; AP
5730 PRINT "I", "Pn", "Mn", "Mnz"
5740 IF FYN$ = "Y" OR FYN$ = "y" THEN 5750 ELSE 5760
5750 PRINT #9, "ALPHA="; AP: PRINT #9, "I", "Pn", "Mn", "Mnz"
5760 FOR I = 1 TO J - 1
5770 PRINT I, PK(I), MK(I), M2(I)
5780 IF FYN$ = "Y" OR FYN$ = "y" THEN 5790 ELSE 5800
5790 PRINT #9, I, PK(I), MK(I), M2(I)
5800 NEXT I
5810 PRINT "I", "Mnz/Mn", "dz^2": PRINT
5820 IF FYN$="Y" OR FYN$="y" THEN PRINT #9,"I","Mnz/Mn","dz^2"
5825 A$ = "##.####^^^^  "
5830 FOR I = 1 TO J - 1
5840 PRINT I, M4(I), : PRINT USING A$; V2(I)
5850 IF FYN$="Y" THEN PRINT #9,I,M4(I),
5855 PRINT #9,USING A$;V2(I)
5860 NEXT I
5870 P0 = PK(0)
5871 IF K = 1 THEN AH = PH(K): AHC = PH(K): AHT = PH(K)
5872 IF K=1 THEN VM = V4(K): V7 = V5(K): V8 = V6(K): GOTO 5880
5874 IF V4(K) < VM THEN VM = V4(K): AH = PH(K)
5875 IF V5(K) < V7 THEN V7 = V5(K): AHC = PH(K)
5876 IF V6(K) < V8 THEN V8 = V6(K): AHT = PH(K)
5880 NEXT K
5900 IF YN$ < > "Y" THEN 6035
5910 PRINT #9,"ALPHA","SUM(dz^2)", "COMP(dz^2)", "TENS(dz^2)"
6000 FOR K = 1 TO M
6020 PRINT #9, PH(K), V4(K), V5(K), V6(K)
6030 NEXT K
6035 PRINT
6037 PRINT "BEST COMPRESSION SIDE - ALPHA ="; AHC
```

```
6038 PRINT "BEST TENSILE    SIDE - ALPHA ="; AHT: PRINT
6039 PRINT : INPUT "PRESS ANY KEY TO CONTINUE"; Z$
6040 RETURN
6050 J = JX: MZX(0)  = 0!: MZX(JX)  = 0!
6060 FOR I = 1 TO J - 1
6070 IF I < = K1X THEN AP = XC ELSE AP = XT
6080 K = 1 + (AP - L) / API: LL = I + (K - 1) * (J + 1)
6090 MZX(I)  = ZX(LL):  MRX(I)  = MZX(I)  / MX(I)
6100 NEXT I
6110 J = JY: MZY(0)  = 0!: MZY(JY)  = 0!
6120 FOR I = 1 TO J - 1
6130 IF I < = K1Y THEN AP = YC ELSE AP = YT
6140 K = 1 + (AP - L) / API: LL = I + (K - 1) * (J + 1)
6150 MZY(I)  = ZY(LL):  MRY(I)  = MZY(I)  / MY(I)
6160 NEXT I
6170 RETURN
7000 REM SUBROUTINE TO SAVE INTERACTION DIAGRAM  VALUES TO DISK
7010 PRINT : INPUT "** SAVE RESULTS TO DISK (Y/N)  ** ="; YN$
7020 IF YN$  = "Y"  OR YN$  = "y" THEN 7030 ELSE 7190
7030 F1$ = NF$ + ".DAT":F2$ = NF$ + "PMX.PRN"F3$ = NF$ + "PMY.PRN"
7060 OPEN "O", #1, F1$: OPEN "O", #2, F2$: OPEN "O", #3, F3$
7075 REM DATA  0  1 2 3  4  5  6  7  8  9  10  11
7080 PRINT #1, JX; JY; L; M; VX; VY; XC; XT; YC; YT; ABC; ABT
7082 REM DATA  12  13  14  15  16  17  18      19
7085 PRINT #1, PO; PF; BX; BY; UX; UY; RX(IYX);  RY(IXY)
7086 REM  DATA 20     21     22      23      24   25
7088 PRINT #1, XX(K1X); XY(K1Y); XB(IYX); YB(IXY); JX3; JY3
7090 FOR I = 0 TO JX:PRINT #2,PX(I);MX(I);MZX(I);XX(I):NEXT  I
7100 FOR I = 0 TO JY:PRINT #3,PY(I);MY(I);MZY(I);XY(I):NEXT  I
7185 CLOSE #1, #2, #3
7190 RETURN
8000 REM SUBROUTINE TO CALCULATE MOMENT RATIO VALUES
     (Mox/Mbxy) & (Moy/Mbyx)
8010 BX = PX(K1X): BY = PY(K1Y):  UX = MX(K1X):  UY = MY(K1Y)
8012 PO = PX(0): PF = PX(JX)
8015 VAC(1)  = XC: VAT(1)  = XT: VAC(2)  = YC: VAT(2)  = YT: I=1
8016 IF VAC(I)  < = VAC(I  + 1) THEN IAC  = I ELSE IAC  = I + 1
8018 IF VAT(I)  < = VAT(I  + 1) THEN IAT  = I ELSE IAT  = I + 1
8019 ABC  = VAC(IAC):  ABT  = VAT(IAT)
8020 IF BX  > BY THEN 8022 ELSE 8025
8022 FG = 1:J = JX:AH = VX:IYX = IAT:IXY  = IAC:  KXY  = K1X:  GOTO 8030
8025 FG  = 2:  J = JY:  AH  = VY:  IYX  = IAC:  IXY  = IAT:  KXY  = K1Y
8030 K = (AH - L) / API + 1
8040 FOR I = 0 TO J
8050 IF FG  > 1 THEN PT(I)  = PY(I):  QY(I,  2)  = MZY(I)  ELSE
     PT(I)  = PX(I):  QX(I,  1)  = MZX(I)
8060 NEXT I
8070 FOR I = 1 TO 2
8080 IF FG  > 1 THEN P3  = PO:  P4  = PF:  APX  = VAC(I):
     APY  = VAT(I):  GOTO 8090
8085 P3  = PF:  P4  = PO:  APX  = VAT(I):  APY  = VAC(I)
8090 RX(I)  = UX  * (1 - ((BY - BX) / (P3 - BX))  ^ APX)
8100 RY(I)  = UY  * (1 - ((BX - BY) / (P4 - BY))  ^ APY)
8105 NEXT I
```

```
8110 IF FG > 1 THEN P1 = BX: KXY = K1X: GOTO 8130
8120 P1 = BY: KXY = K1Y
8130 FOR K = 1 TO 2
8140 FOR I = 0 TO J
8150 P2 = PT(I)
8160 IF I > KXY THEN P5 = PF ELSE P5 = PO
8170 IF FG > 1 THEN 8210
8172 IF P2>BY THEN P5=PO:APY=VAC(K) ELSE P5 = PF: APY = VAT(K)
8174 P1 = BY
8180 QY(I, K) = UY * (1 - ((P2 - P1) / (P5 - P1)) ^ APY)
8190 IF K = 1 THEN 8230
8192 IF P2>BX THEN P5=PO:APX=VAC(K) ELSE P5 = PF: APX = VAT(K)
8194 P1=BX:QX(I, K) = UX * (1 - ((P2 - P1) / (P5 - P1)) ^ APX)
8200 GOTO 8230
8210 IF P2>BX THEN P5=PO:APX=VAC(K) ELSE P5 = PF: APX = VAT(K)
8212 P1 = BX
8215 QX(I, K) = UX * (1 - ((P2 - P1) / (P5 - P1)) ^ APX)
8220 IF K > 1 THEN 8230
8222 IF P2>BY THEN P5=PO:APY=VAC(K) ELSE P5=PF:APY = VAT(K)
8224 P1=BY:QY(I, K)= UY * (1 - ((P2 - P1) / (P5 - P1)) ^ APY)
8230 NEXT I
8240 NEXT K
8250 IF FG > 1 THEN B3 = BY: B4 = BX ELSE B3 = BX: B4 = BY
8260 FOR K = 1 TO 2
8270 FOR I = 0 TO J
8280 P2 = PT(I)
8290 IF P2 < B3 THEN 8310
8300 IF FG > 1 THEN R1(K) = RX(K): R2(K) = UY ELSE R1(K) = UX
     R2(K) = RY(K): GOTO 8340
8310 IF P2 < B4 THEN 8330
8320 R1(K) = UX: R2(K) = UY: GOTO 8340
8330 IF FG > 1 THEN R1(K) = UX: R2(K) = RY(K) ELSE R1(K) = RX(K)
     R2(K) = UY
8340 M7(I, K) = QX(I, K) / R1(K): M8(I, K) = QY(I, K) / R2(K)
8350 NEXT I
8360 NEXT K
8365 IF BY = 0 THEN XB(1) = 9999: XB(2) = 9999: GOTO 8367
8366 XB(1) = RX(1) / BY: XB(2) = RX(2) / BY
8367 IF BX = 0 THEN YB(1) = 9999: YB(2) = 9999: GOTO 8390
8370 YB(1) = RY(1) / BX: YB(2) = RY(2) / BX
8390 PRINT : INPUT "MOMENT RATIO VALUES ABOUT X-X AND Y-Y
     OUTPUT TO FILE (Y/N)"; YN$
8410 IF YN$ = "Y" OR YN$ = "y" THEN 8420 ELSE 8640
8420 PRINT #9, "CALCULATED INTERACTION BENDING MOMENT
     RELATIONSHIPS"
8430 PRINT #9, "BALANCED LOAD ABOUT X-X (Kips) ="; BX
8440 PRINT #9, "BALANCED LOAD ABOUT Y-Y (Kips) ="; BY
8450 PRINT #9, "BALANCED MOMENT ABOUT X-X (Kip-in)="; UX
8460 PRINT #9, "BALANCED MOMENT ABOUT Y-Y (Kip-in)="; UY
8462 PRINT #9, "BALANCED ECCENTR. ABOUT X-X (in.)="; XX(K1X)
8464 PRINT #9, "BALANCED ECCENTR. ABOUT Y-Y (in.)="; XY(K1Y)
8470 PRINT #9, "X-X BENDING MOMENTS FOR BEST ALPHA ="; XC; XT
8480 PRINT #9, "MOMENT X-X Mbyx FOR Pnby (Kip-in)="; RX(1)
8490 PRINT #9, "MOMENT Y-Y Mbxy FOR Pnbx (Kip-in)="; RY(1)
```

```
8492 PRINT #9, "X-X ECCENTRICITY AT Pnby (in.) = "; XB(1)
8494 PRINT #9, "Y-Y ECCENTRICITY AT Pnbx (in.) = "; YB(1)
8500 PRINT #9, "Y-Y BENDING MOMENTS FOR BEST ALPHA = "; YC; YT
8510 PRINT #9, "MOMENT X-X Mbyx FOR Pnby (Kip-in) = "; RX(2)
8520 PRINT #9, "MOMENT Y-Y Mbxy FOR Pnbx (Kip-in) = "; RY(2)
8522 PRINT #9, "X-X ECCENTRICITY AT Pnby (in.) = "; XB(2)
8524 PRINT #9, "Y-Y ECCENTRICITY AT Pnbx (in.) = "; YB(2)
8530 PRINT #9, "INTERACTION DIAGRAM MOMENT RATIO VALUES
     (Mox/Mnb & Moy/Mnb)"
8535 PRINT #9, "BEST X-X ALPHA - COMPRESSION SIDE = "; XC
8537 PRINT #9, "BEST X-X ALPHA - TENSILE SIDE = "; XT
8540 PRINT #9, "Pn", "Mox", "Moy", "Mox/Mnbyx", "Moy/Mnbxy"
8550 FOR I = 0 TO J
8560 PRINT #9, PT(I), QX(I, 1), QY(I, 1), M7(I, 1), M8(I, 1)
8570 NEXT I
8580 PRINT #9, "INTERACTION DIAGRAM MOMENT RATIO VALUES
     (Mox/Mnb & Moy/Mnb)"
8585 PRINT #9, "BEST Y-Y ALPHA - COMPRESSION SIDE = "; YC
8587 PRINT #9, "BEST Y-Y ALPHA - TENSILE SIDE = "; YT
8590 PRINT #9, "Pn", "Mox", "Moy", "Mox/Mnbyx", "Moy/Mnbxy"
8600 FOR I = 0 TO J
8610 PRINT #9, PT(I), QX(I, 2), QY(I, 2), M7(I, 2), M8(I, 2)
8620 NEXT I
8640 RETURN
9000 REM * SUBROUTINE TO GENERATE THE BIAXIAL
     INTERACTION REM DIAGRAMS AND
9002 REM * THE LOAD CONTOURS FOR SQUARE AND RECTANGULAR
     REM COMPOSITE COLUMNS
9004 PRINT:INPUT"No. OF INTERACTION DIAGRAM PLANES:"; NPL
9006 ANG = 90 / (NPL + 1): TNE = NTB + NSE
9010 DG = SQR(B ^ 2 + T ^ 2)
9015 BET = ATN(T / B) * 180 / PI: PHI = (90 - BET)
9017 REM PRINT ANG, DG, BET, PHI: INPUT Z$
9018 DD = D2/COS(BET * PI / 180): DDT = D5 / SIN(BET * PI / 180)
9019 DDG = DG - DD
9020 REM * X AND Y COORDINATES OF THE STEEL BARS AND THE STEEL
     REM SHAPE ELEMENTS
9022 FOR I = 1 TO NL
9025 XZ(I) = D2:XZ(I+NL) = (B-D2): YZ(I) = Y(I): YZ(I + NL) = Y(I)
9030 NEXT I
9035 FOR I = 1 TO NS: J = 2 * NL + I
9040 XZ(J) = X(I): XZ(J + NS) = X(I):YZ(J) = D3: YZ(J + NS) = D4
9045 NEXT I
9050 FOR I = IWF TO TNE
9055 XZ(I) = X(I): YZ(I) = Y(I)
9060 NEXT I
9061 REM PRINT NTB,NSE,TNS:INPUTZ$
9062 REM FOR I = 1 TO TNE:PRINT I,XZ(I),YZ(I):INPUT Z$ 9064 NEXT I
9065 REM*CALCULATION FOR INTERACTION DIAGRAM/EACH PLANE
9068 FOR IP = 1 TO NPL
9069 JZ = K2: MMX = 0: KX = 0
9070 ALP = IP * ANG
9071 PRINT : PRINT "CALCULATIONS FOR INCLINED PLANE AT :";
     ALP;"(DEGREES)"
```

```
9072 PRINT : PRINT "CALCULATIONS IN PROGRESS, PLEASE WAIT.."
9073 IF ALP < PHI THEN 9074 ELSE 9078
9074 DGP = DG * SIN((BET + ALP) * PI / 180)
9075 DDB = DDG * SIN((BET + ALP) * PI / 180)
9076 DDP = DD * SIN((BET + ALP) * PI / 180)
9077 D1P = DDT * SIN((BET + ALP) * PI / 180): GOTO 9082
9078 DGP = DG * SIN((180 - BET - ALP) * PI / 180)
9079 DDP = DD * SIN((180 - BET - ALP) * PI / 180)
9080 D1P = DDT * SIN((180 - BET - ALP) * PI / 180)
9081 DDB = DDG * SIN((180 - BET - ALP) * PI / 180)
9082 REM * GENERATING THE VALUES OF POSITION OF NEUTRAL AXIS
9083 C(1)=DGP:C(N1)=DGP-DDP:N0=N1-1:CD = (C(N1) - C(1)) / N0
9084 FOR I = 2 TO N0: C(I) = C(I - 1) + CD: NEXT I
9090 DDC = DDB
9092 CB = .003 * DDC / (.003 + EY):J= N1 + 1: K = N1 + N2 - 1
9093 CD = (CB - C(N1)) / N2: C(K1) = CB
9094 FOR I = J TO K: C(I) = C(I - 1) + CD: NEXT I
9096 K3 = JZ + 1: K4 = JZ + N4
9098 C(K4) = D1P / .9: C(K2) = (CB + C(K4)) / 2
9100 J=K1+1:K=N1+N2 + N3 - 1: CM = C(K2): CD = (CM - CB) / N3
9102 FOR I = J TO K: C(I) = C(I - 1) + CD: NEXT I
9110 REM CALCULATION OF INTERACTION POINTS IN THE TENSILE
     REM REGION
9112 J = K3: W = K4: K5 = K4 + 1
9114 CD = (C(K4) - C(K2)) / N4
9116 FOR I = J TO W: C(I) = C(I - 1) + CD: NEXT I
9118 REM **************
9120 J = 1: W = K4
9121 REM PRINT IP, BET, ALP, DG, DGP: INPUT Z$
9122 REM CALCULATIONS OF THE COMPRESSIVE STRESS BLOCK
9125 FOR I = J TO W
9130 AC(I) = B1 * C(I)
9135 REM PRINT I, C(I), AC(I): INPUT Z$
9140 IF ALP < PHI THEN 9142 ELSE 9150
9142 AD(I) = AC(I) / SIN((BET + ALP) * PI / 180)
9143 DCP(I) = C(I) / SIN((BET + ALP) * PI / 180)
9144 GOTO 9155
9150 AD(I) = AC(I) / SIN((180 - BET - ALP) * PI / 180)
9152 DCP(I) = C(I) / SIN((180 - BET - ALP) * PI / 180)
9155 DCB(I) = DG - DCP(I): DR(I) = DG - AD(I)
9158 NEXT I
9159 APR = ALP * PI / 180
9160 REM CALCULATIONS OF THE COMPRESSIVE STRESS BLOCK
9162 FOR I = J TO W
9164 XC1=DR(I)*COS(BET*PI/180):YC1=DR(I)*SIN(BET* PI / 180)
9166 XCZ = B - XC1: YCZ = T - YC1
9168 AP1=(ATN(YCZ/XC1))*180/PI:AP2=(ATN(YC1 / XCZ)) * 180 / PI
9170 IF AP1 > AP2 THEN 9172 ELSE 9178
9172 IF ALP > 0 AND ALP <=AP2 THEN 9500
9174 IF ALP > AP2 AND ALP <=AP1 THEN 9200
9176 IF ALP > AP1 AND ALP <=90 THEN 9300 ELSE STOP: END
9178 IF ALP > 0 AND ALP <=AP1 THEN 9500
9180 IF ALP > AP1 AND ALP <=AP2 THEN 9400
9182 IF ALP > AP2 AND ALP <=90 THEN 9300 ELSE STOP: END
```

```
9200 XC2 = YC1 / TAN(APR): YC2 = XC1 * TAN(APR)
9205 XC3 = B - XC1 - XC2: YC3 = T - YC1 - YC2
9210 AR1 = B * YC3: AR2 = XC3 * (YC1 + YC2)
9215 ACT = (XC1+XC2) * (YC1 + YC2) / 2: ACS = AR1 + AR2 + ACT
9220 XCG = (AR1*B/2+AR2*XC3/2+ACT*(XC3+(XC1+XC2) / 3)) / ACS
9225 YCG = (AR1 * YC3 / 2 + AR2 * (YC3 + (YC1 + YC2) / 2) +
     ACT * (YC3 + (YC1 + YC2) / 3)) / ACS
9230 GOTO 9600
9300 XC2=YC1/TAN(APR): XC3 = B - XC1 - XC2: XC5 = T / TAN(APR)
9305 AR1 = T * XC3: ACT = T * XC5 / 2: ACS = AR1 + ACT
9310 XCG = (AR1 * XC3 / 2 + ACT * (XC3 + XC5 / 3)) / ACS
9315 YCG = (AR1 * T / 2 + ACT * T / 3) / ACS
9320 GOTO 9600
9400 XC2 = B - XC1: YC2 = T - YC1: YC3 = XC2 * TAN(APR)
9405 YC4 = YC2 +YC3:XC4 = YC4 / TAN(APR): ACS = XC4 * YC4 / 2
9410 XCG = XC4 / 3: YCG = YC4 / 3
9420 GOTO 9600
9500 XC2=B - XC1: YC2 = XC1 * TAN(APR): YC3 = (T - YC1 - YC2)
9505 YC4 = XC2 * TAN(APR)
9510 AR1 = B * YC3: ACT = B * (YC2 + YC4) / 2: ACS = AR1 + ACT
9515 XCG = (AR1 * B / 2 + ACT * B / 3) / ACS
9520 YCG=(AR1 * YC3 / 2 + ACT * (YC3 + (YC2 + YC4) / 3)) / ACS
9525 REM CALCULATING CONCRETE COMPRESSIVE AXIAL FORCE
9600 PN(I) = .85 * FC * ACS: CI = C(I)
9700 CC=PN(I):MNX(I)=CC*(T/2-YCG):MNY(I) = CC * (B / 2 - XCG)
19000 REM **************
19005 FOR K = 1 TO TNS
19010 THT = (ATN(YZ(K) / XZ(K))) * 180 / PI
19015 DXY = SQR(XZ(K) ^ 2 + YZ(K) ^ 2)
19020 IF THT > BET THEN 19030 ELSE 19050
19030 DT1=(BET+ALP)*PI/180:DT2= (180 - ALP - THT) * PI / 180
19035 DD2 = DXY * SIN(DT2) / SIN(DT1): GOTO 19060
19050 DT2=(ALP+THT)*PI/180:DT1= (180 - BET - ALP) * PI / 180
19055 DD2 = DXY * SIN(DT2) / SIN(DT1)
19060 DDI = DG - DD2: CI = C(I)
19065 IF ALP<PHI THEN DIP=DDI*SIN((BET+ALP)*PI/180):GOTO19140
19070 DIP = DDI * SIN((180 - BET - ALP) * PI / 180)
19140 IF K > NTB THEN ES = ESS: FY = FYS: EY = EYS
19145 EK = .003 * (CI - DIP) / CI: SG = SGN(EK): EZ = ABS(EK)
19150 IF EZ >=EY THEN ET = SG * EY ELSE ET = EK
19155 IF DDI <=AD(I) THEN FS=(ET*ES-.85*FC)ELSE FS = ET * ES
19160 CS(K) = AK(K) * FS: PN(I) = PN(I) + CS(K)
19165 MNX(I) = MNX(I) + CS(K) * (T / 2 - (T - YZ(K)))
19168 MNY(I) = MNY(I) + CS(K) * (B / 2 - (B - XZ(K)))
19170 NEXT K
19175 ENX(I) = MNX(I) / PN(I): ENY(I) = MNY(I) / PN(I)
19180 PXY(IP, I) = PN(I)
19185 MXY(IP, I) = SQR(MNX(I) ^ 2 + MNY(I) ^2):MTM=MXY(IP, I)
19190 EXY(I) = SQR(ENX(I) ^ 2 + ENY(I) ^ 2): CXY(I) = C(I)
19195 IF MTM > MMX THEN MMX = MTM: KX = I
19250 NEXT I
19255 PBN(IP) = PXY(IP, KX): MBN(IP) = MMX
19290 PXY(IP, K5) = PF: PXY(IP, 0) = PN(0)
19320 MXY(IP, 0) = 0: MXY(IP, K5) = 0
```

```
19325 CXY(0) = 9999: CXY(K5) = 9999: EXY(0) = 0: EXY(K5) = 0
19330 KXP(IP) = KX
19360 GOSUB 20000
19365 NEXT IP
19368 KXP(0) = K1X: KXP(NPL + 1) = K1Y
19370 MXY(0, K1X) = MX(K1X): MXY(NPL + 1, K1Y) = MY(K1Y)
19375 GOSUB 30000
19380 REM END OF PROGRAM
19400 RETURN
19500 REM **********
20000 REM SUBROUTINE TO OUTPUT INTERACTION DIAGRAM VALUES FOR
      REM EACH PLANE
20005 CLS : PRINT
20010 PRINT "COMPOSITE COLUMN BIAXIAL INTERACTION DIAGRAM"
20015 PRINT "AXIAL LOAD AND MOMENTS FOR PLANE AT :"; ALP;
      "(DEGREES)"
20020 PRINT "MAXIMUM AXIAL COMPRESSIVE LOAD (Kips) ="; PO
20025 PRINT "MAXIMUM AXIAL TENSILE LOAD (Kips) ="; PF
20030 PRINT "BALANCED LOAD Pnb (Kips) ="; PXY(IP, KX)
20045 PRINT "BALANCED MOMENT Mnb(Kip-in) =";MXY(IP, KX)
20060 PRINT "BALANCED NOMINAL ECCENTRICITY eb(in.) ="; EXY(KX)
20065 PRINT : INPUT "PRESS ANY KEY TO CONTINUE ..."; Z$
20066 PRINT #9, "AXIAL LOAD AND MOMENTS FOR PLANE AT :"; ALP;"
      (DEGREES)"
20070 PRINT : PRINT "I", "Pn", "Mn"
20075 FOR I = 0 TO K5: PRINT I, PXY(IP, I), MXY(IP, I)
20076 PRINT #9, I, PXY(IP, I), MXY(IP, I)
20078 NEXT I
20080 PRINT : INPUT "PRESS ANY KEY TO CONTINUE ...."; Z$
20085 PRINT "CALCULATIONS IN PROGRESS, PLEASE WAIT ...!!!"
20090 RETURN
30000 REM SUBROUTINE TO GENERATE THE LOAD CONTOURS AT
      CONSTANT AXIAL LOAD
30005 JK = JX - 1: JL = K5 - 1
30010 FOR I = 1 TO (NPL + 1)
30015 ILT = 1: ILB = 0
30020 FOR IL = 1 TO JK
30021 PXX = PX(IL)
30022 IF I > NPL THEN 30026
30024 PTP = PXY(I, ILT): PBT = PXY(I, ILB): GOTO 30030
30026 PTP = PY(ILT): PBT = PY(ILB)
30030 IF PXX < = PBT AND PXX > = PTP THEN 30040
30032 ILT = ILT + 1: ILB = ILB + 1
30033 IF I > NPL THEN 30034 ELSE 30036
30034 IF ILB > (JY - 1) THEN ILT = JY: ILB = JY - 1
30036 GOTO 30022
30040 IF I > NPL THEN 30044
30042 MTP = MXY(I, ILT): MBT = MXY(I, ILB): GOTO 30045
30044 MTP = MY(ILT): MBT = MY(ILB)
30045 MMM = ((MTP-MBT)*(PXX-PBT)/(PTP-PBT)):MMP =MBT + MMM
30050 MLC(I, IL) = MMP
30060 NEXT IL
30065 MLC(I, 0) = 0: MLC(I, JX) = 0
30070 NEXT I
```

```
30075 PRINT : INPUT "PRESS ANY KEY TO CONTINUE ...!!!"; Z$
30080 FOR I = 0 TO JX
30082 MLC(0, I) = MX(I)
30085 PRINT I
30090 FOR K = 0 TO NPL + 1: PRINT MLC(K, I); : NEXT K: PRINT
30095 NEXT I
30100 PRINT : INPUT "PRESS ANY KEY TO CONTINUE ...!!!"; Z$
30102 BTM = 0: SDM = 0
30104 PRINT "CALCULATIONS OF COEFFICIENT BETA FOR EACH LOAD CONTOUR":
30105 FOR I = 1 TO (JX - 1)
30108 BTC(I) = 0
30110 FOR J = 1 TO NPL
30115 ALP = J * (ANG * PI / 180)
30120 MOX(J,I) = MLC(J,I)*COS(ALP):MOY(J,I) = MLC(J,I) * SIN(ALP)
30122 NEXT J
30125 L = 1.05: Q = 3.5: API = .05
30130 M = (Q - L) / API + 1
30140 MPX = MLC(0, I): MPY = MLC(NPL + 1, I)
30145 FOR K = 1 TO M
30150 BTA = L + (K - 1) * API:  OBT = 1 / BTA
30152 SD2 = 0
30155 FOR J = 1 TO NPL
30160 MCI = MOY(J, I): MCX = MOX(J, I)
30162 IF MCX > MPX THEN BTM = 2!: SDM = 0: GOTO 30204
30165 MCY = MPY * ((1 - (MCX / MPX) ^ BTA) ^ OBT)
30170 SD2 = SD2 + ((MCY - MCI) / MCI) ^ 2
30175 NEXT J
30180 IF K = 1 THEN SDM = SD2: BTM = BTA: GOTO 30200
30185 IF SD2 < SDM THEN BTM = BTA: SDM = SD2
30200 NEXT K
30204 IF I > (N1+N2+X3)THEN PNO(I) = PX(I) / PF: GOTO 30210
30205 PNO(I) = PX(I) / PO
30210 BTC(I) = BTM: PRINT I; PNO(I); SDM; BTM
30215 NEXT I
30217 PRINT : INPUT "PRESS ANY KEY TO CONTINUE ...!!!"; Z$
30220 PRINT : INPUT "SAVE BIAXIAL INTERACTION VALUES TO DISK(Y/N):"; YN$
30225 IF YN$ = "N" OR YN$ = "n" THEN 30700
30230 F4$ = NF$ + "BPM.PRN"
30235 OPEN "O", #4, F4$
30240 FOR I = 1 TO JX - 1
30245 FOR J = 0 TO (NPL + 1)
30250 PRINT #4, MLC(J, I);
30255 NEXT J
30260 PRINT #4, PX(I); BTC(I)
30265 NEXT I
30270 FOR I = 0 TO (NPL + 1): PRINT #4, KXP(I); : NEXT I
30272 PRINT #4, PO; PF
30274 FOR I = 0 TO (NPL + 1): PRINT #4, MXY(I,KXP(I));:NEXT I
30275 PRINT #4, NPL; JX
30280 CLOSE #4
30285 CLS : PRINT :PRINT "PROGRAM  COMPLETED AND TERMINATED"
30300 INPUT "PRESS ANY KEY TO RETURN TO PROGRAM  !!!"; Z$: CLS 30305 PRINT
30700 RETURN
```

# APPENDIX B

## Sample Results from computer program "INTRDIAG"

INTERACTION DIAGRAM PROGRAM FOR COMPOSITE COLUMNS
PROGRAM NAME: "INTRDIAG"
COLUMN FILE NAME :A:AISC3.RES
COLUMN SECTION GEOMETRY AND MATERIAL PROPERTIES
COLUMN WIDTH (SHORT DIMENSION inch.) = 16
COLUMN DEPTH (LONG DIMENSION inch.) = 16
STEEL WIDE FLANGE WIDTH (inch.) = 8.11
STEEL WIDE FLANGE DEPTH (inch.) = 8.5
STEEL FLANGE THICHNESS (inch.) = .685
STEEL WEB THICKNESS (inch.) = .4
ULTIMATE COMPRESSIVE STRENGTH OF CONCRETE (ksi) = 3.5
YIELD STRENGTH OF THE STEEL REINFORCEMENT (ksi) = 60
MODULUS OF ELASTICITY OF CONCRETE (ksi) = 3372.166
MODULUS OF ELASTICITY OF STEEL REBARS (ksi) = 30000
YIELD STRENGTH OF THE STEEL SHAPE (ksi) = 50
MODULUS OF ELASTICITY OF THE STEEL SHAPE (ksi) = 29000
COLUMN SECTION REINFORCEMENT
NUMBER OF BARS ALONG LONG SIDE PER FACE = 2
NUMBER OF INTERIOR BARS ALONG SHORT SIDE PER FACE = 0
DIAMETER OF BARS ALONG LONG SIDE (No.) = 7
DIAMETER OF BARS ALONG SHORT SIDE (No.) = 0
COVER OF STEEL REBARS ALONG LONG SIDE (inch.) = 2
NUMBER OF POINTS FOR REGION I = 10
NUMBER OF POINTS FOR REGION II = 10
NUMBER OF POINTS FOR REGION III - ABOUT X-X = 4
NUMBER OF POINTS FOR REGION III - ABOUT Y-Y = 3
NUMBER OF POINTS FOR REGION IV = 10
MAXIMUM AXIAL COMPRESSIVE LOAD (kips) = 1555.056
MAXIMUM AXIAL TENSILE LOAD (kips) = -842.135
INTERACTION DIAGRAM POINTS FOR BENDING ABOUT X-X
BALANCED LOAD Pnbx (kips) = 217.7067
BALANCED MOMENT Mnbx (kip-in) = 4177.391
BALANCED ECCENTRICITY enby (in.) = 19.18815

| POINT | Pnx | Mnx | eny | Cny |
|---|---|---|---|---|
| 0 | 1555.056 | 0 | 0 | 9999 |
| 1 | 1207.151 | 1757.194 | 1.455654 | 16 |
| 2 | 1178.066 | 1766.819 | 1.499762 | 15.77778 |
| 3 | 1161.083 | 1844.722 | 1.588794 | 15.55556 |
| 4 | 1143.86 | 1921.785 | 1.680088 | 15.33333 |
| 5 | 1126.395 | 1998.061 | 1.773855 | 15.11111 |
| 6 | 1108.677 | 2073.591 | 1.87033 | 14.88889 |
| 7 | 1090.694 | 2148.415 | 1.969769 | 14.66667 |
| 8 | 1072.435 | 2222.584 | 2.072465 | 14.44444 |
| 9 | 1053.874 | 2296.122 | 2.178743 | 14.22222 |
| 10 | 1051.397 | 2304.246 | 2.191604 | 14 |
| 11 | 1002.036 | 2485.326 | 2.480276 | 13.44 |
| 12 | 951.1244 | 2661.653 | 2.798427 | 12.88 |
| 13 | 897.2667 | 2836.592 | 3.16137 | 12.32 |

| | | | | |
|---|---|---|---|---|
| 14 | 839.4579 | 3013.4 | 3.589698 | 11.76 |
| 15 | 778.905 | 3190.542 | 4.096189 | 11.2 |
| 16 | 713.7861 | 3370.402 | 4.721865 | 10.64 |
| 17 | 643.8541 | 3556.813 | 5.524253 | 10.08 |
| 18 | 565.2765 | 3744.103 | 6.623489 | 9.519997 |
| 19 | 469.9942 | 3902.104 | 8.302451 | 8.959996 |
| 20 | 374.527 | 4013.731 | 10.7168 | 8.4 |
| 21 | 217.7067 | 4177.391 | 19.18815 | 7.583529 |
| 22 | 122.1512 | 4011.957 | 32.84419 | 6.767058 |
| 23 | 21.48587 | 3759.75 | 174.9871 | 5.950588 |
| 24 | 0 | 3697.33 | 9999 | 5.784742 |
| 25 | -50.86052 | 3542.863 | -69.65841 | 5.406268 |
| 26 | -105.3658 | 3363.476 | -31.9219 | 5.027794 |
| 27 | -147.5962 | 3220.461 | -21.8194 | 4.64932 |
| 28 | -214.4467 | 2963.357 | -13.81862 | 4.270845 |
| 29 | -287.9915 | 2668.174 | -9.264766 | 3.892371 |
| 30 | -370.5898 | 2326.121 | -6.276808 | 3.513897 |
| 31 | -465.5197 | 1924.303 | -4.133665 | 3.135423 |
| 32 | -577.8602 | 1442.736 | -2.496688 | 2.756948 |
| 33 | -648.8591 | 1110.842 | -1.711993 | 2.378474 |
| 34 | -677.2148 | 938.5768 | -1.385937 | 2 |
| 35 | -842.135 | 0 | 0 | 9999 |

INTERACTION DIAGRAM POINTS FOR BENDING ABOUT Y-Y
BALANCED LOAD Pnby (kips) = 139.5333
BALANCED MOMENT Mnby (kip-in) = 2823.21
BALANCED ECCENTRICITY enbx (in.) = 20.23323

| POINT | Pny | Mny | enx | Cnx |
|---|---|---|---|---|
| 0 | 1555.056 | 0 | 0 | 9999 |
| 1 | 1252.251 | 1272.062 | 1.01582 | 16 |
| 2 | 1235.095 | 1338.025 | 1.083338 | 15.77778 |
| 3 | 1217.707 | 1402.76 | 1.151969 | 15.55556 |
| 4 | 1200.05 | 1466.25 | 1.221825 | 15.33333 |
| 5 | 1181.614 | 1527.781 | 1.292962 | 15.11111 |
| 6 | 1162.895 | 1588.125 | 1.365665 | 14.88889 |
| 7 | 1143.882 | 1647.305 | 1.440101 | 14.66667 |
| 8 | 1124.561 | 1705.345 | 1.516454 | 14.44444 |
| 9 | 1104.917 | 1762.273 | 1.594937 | 14.22222 |
| 10 | 1084.935 | 1818.115 | 1.675783 | 14 |
| 11 | 1040.286 | 1930.741 | 1.855972 | 13.48905 |
| 12 | 989.3851 | 2046.728 | 2.068687 | 12.9781 |
| 13 | 939.0112 | 2148.877 | 2.288447 | 12.46715 |
| 14 | 885.8425 | 2248.78 | 2.538577 | 11.9562 |
| 15 | 825.0901 | 2347.318 | 2.844923 | 11.44525 |
| 16 | 763.3254 | 2437.093 | 3.192731 | 10.93431 |
| 17 | 694.2327 | 2528.494 | 3.642142 | 10.42336 |
| 18 | 622.2836 | 2612.624 | 4.198446 | 9.912407 |
| 19 | 551.8041 | 2693.822 | 4.881845 | 9.401458 |
| 20 | 462.7903 | 2774.88 | 5.995977 | 8.890511 |
| 21 | 312.8841 | 2812.439 | 8.988756 | 8.024989 |
| 22 | 139.5333 | 2823.21 | 20.23323 | 7.159468 |
| 23 | 0 | 2762.341 | 9999 | 6.490041 |
| 24 | -96.40091 | 2675.594 | -27.75487 | 6.041037 |

| | | | | |
|---|---|---|---|---|
| 25 | -191.8553 | 2568.87 | -13.38962 | 5.592032 |
| 26 | -292.7695 | 2426.852 | -8.289292 | 5.143028 |
| 27 | -361.768 | 2272.317 | -6.281146 | 4.694024 |
| 28 | -429.9804 | 2060.604 | -4.792322 | 4.24502 |
| 29 | -494.3636 | 1830.83 | -3.703408 | 3.796016 |
| 30 | -553.3768 | 1591.031 | -2.875132 | 3.347012 |
| 31 | -604.5235 | 1354.228 | -2.240157 | 2.898007 |
| 32 | -643.4773 | 1142.986 | -1.776265 | 2.449003 |
| 33 | -677.2149 | 938.5775 | -1.385937 | 1.999999 |
| 34 | -842.135 | 0 | 0 | 9999 |

INTERACTION DIAGRAM POINTS BY NJIT'sINTERACTION EQUATION
BENDING ABOUT X-X - BEST COMPRESSION SIDE - ALPHA= 1.7
BENDING ABOUT X-X - BEST TENSILE SIDE - ALPHA= 1.4

| POINT | Pnx | Mnx | M'nx | M'nx/Mnx |
|---|---|---|---|---|
| 0 | 1555.056 | 0 | 0 | 1 |
| 1 | 1207.151 | 1757.194 | 1674.428 | .952899 |
| 2 | 1178.066 | 1766.819 | 1798.217 | 1.017771 |
| 3 | 1161.083 | 1844.722 | 1869.297 | 1.013322 |
| 4 | 1143.86 | 1921.785 | 1940.474 | 1.009724 |
| 5 | 1126.395 | 1998.061 | 2011.711 | 1.006832 |
| 6 | 1108.677 | 2073.591 | 2083.009 | 1.004542 |
| 7 | 1090.694 | 2148.415 | 2154.362 | 1.002768 |
| 8 | 1072.435 | 2222.584 | 2225.766 | 1.001432 |
| 9 | 1053.874 | 2296.122 | 2297.262 | 1.000497 |
| 10 | 1051.397 | 2304.246 | 2306.721 | 1.001074 |
| 11 | 1002.036 | 2485.326 | 2491.085 | 1.002318 |
| 12 | 951.1244 | 2661.653 | 2672.912 | 1.00423 |
| 13 | 897.2667 | 2836.592 | 2855.864 | 1.006794 |
| 14 | 839.4579 | 3013.4 | 3041.237 | 1.009238 |
| 15 | 778.905 | 3190.542 | 3222.867 | 1.010132 |
| 16 | 713.7861 | 3370.402 | 3403.417 | 1.009796 |
| 17 | 643.8541 | 3556.813 | 3579.612 | 1.00641 |
| 18 | 565.2765 | 3744.103 | 3754.664 | 1.002821 |
| 19 | 469.9942 | 3902.104 | 3932.196 | 1.007712 |
| 20 | 374.527 | 4013.731 | 4068.128 | 1.013553 |
| 21 | 217.7067 | 4177.391 | 4177.391 | 1 |
| 22 | 122.1512 | 4011.957 | 4033.535 | 1.005379 |
| 23 | 21.48587 | 3759.75 | 3783.468 | 1.006308 |
| 24 | 0 | 3697.33 | 3721.786 | 1.006614 |
| 25 | -50.86052 | 3542.863 | 3566.108 | 1.006561 |
| 26 | -105.3658 | 3363.476 | 3385.641 | 1.00659 |
| 27 | -147.5962 | 3220.461 | 3237.057 | 1.005153 |
| 28 | -214.4467 | 2963.357 | 2987.627 | 1.00819 |
| 29 | -287.9915 | 2668.174 | 2694.819 | 1.009986 |
| 30 | -370.5898 | 2326.121 | 2345.066 | 1.008144 |
| 31 | -465.5197 | 1924.303 | 1918.172 | .9968141 |
| 32 | -577.8602 | 1442.736 | 1381.533 | .9575782 |
| 33 | -648.8591 | 1110.842 | 1026.09 | .9237047 |
| 34 | -677.2148 | 938.5768 | 880.7881 | .9384294 |
| 35 | -842.135 | 0 | 0 | 1 |

BENDING ABOUT Y-Y - BEST COMPRESSION SIDE - ALPHA= 2.5
BENDING ABOUT Y-Y - BEST COMPRESSION SIDE - ALPHA= 2.35

| POINT | Pny | Mny | M'ny | M'ny/Mny |
|---|---|---|---|---|
| 0 | 1555.056 | 0 | 0 | 1 |
| 1 | 1252.251 | 1272.062 | 1276.482 | 1.003475 |
| 2 | 1235.095 | 1338.025 | 1335.415 | .9980496 |
| 3 | 1217.707 | 1402.76 | 1393.748 | .9935756 |
| 4 | 1200.05 | 1466.25 | 1451.555 | .9899776 |
| 5 | 1181.614 | 1527.781 | 1510.394 | .9886189 |
| 6 | 1162.895 | 1588.125 | 1568.555 | .9876769 |
| 7 | 1143.882 | 1647.305 | 1626.023 | .9870808 |
| 8 | 1124.561 | 1705.345 | 1682.77 | .9867619 |
| 9 | 1104.917 | 1762.273 | 1738.782 | .98667 |
| 10 | 1084.935 | 1818.115 | 1794.029 | .9867525 |
| 11 | 1040.286 | 1930.741 | 1911.273 | .9899168 |
| 12 | 989.3851 | 2046.728 | 2034.697 | .9941215 |
| 13 | 939.0112 | 2148.877 | 2146.399 | .9988466 |
| 14 | 885.8425 | 2248.78 | 2253.376 | 1.002044 |
| 15 | 825.0901 | 2347.318 | 2362.36 | 1.006408 |
| 16 | 763.3254 | 2437.093 | 2459.252 | 1.009093 |
| 17 | 694.2327 | 2528.494 | 2551.819 | 1.009225 |
| 18 | 622.2836 | 2612.624 | 2631.45 | 1.007206 |
| 19 | 551.8041 | 2693.822 | 2693.967 | 1.000054 |
| 20 | 462.7903 | 2774.88 | 2752.851 | .9920612 |
| 21 | 312.8841 | 2812.439 | 2808.393 | .9985611 |
| 22 | 139.5333 | 2823.21 | 2823.21 | 1 |
| 23 | 0 | 2762.341 | 2794.395 | 1.011604 |
| 24 | -96.40091 | 2675.594 | 2724.198 | 1.018166 |
| 25 | -191.8553 | 2568.87 | 2603.212 | 1.013368 |
| 26 | -292.7695 | 2426.852 | 2412.318 | .994011 |
| 27 | -361.768 | 2272.317 | 2241.297 | .9863484 |
| 28 | -429.9804 | 2060.604 | 2037.864 | .9889644 |
| 29 | -494.3636 | 1830.83 | 1813.097 | .9903143 |
| 30 | -553.3768 | 1591.031 | 1578.074 | .9918562 |
| 31 | -604.5235 | 1354.228 | 1351.235 | .9977906 |
| 32 | -643.4773 | 1142.986 | 1163.7 | 1.018122 |
| 33 | -677.2149 | 938.5775 | 990.7554 | 1.055593 |
| 34 | -842.135 | 0 | 0 | 1 |

CALCULATED INTERACTION BENDING MOMENT RELATIONSHIPS

BALANCED LOAD ABOUT X-X (Kips) = 217.7067
BALANCED LOAD ABOUT Y-Y (Kips) = 139.5333
BALANCED MOMENT ABOUT X-X (Kip-in) = 4177.391
BALANCED MOMENT ABOUT Y-Y (Kip-in) = 2823.21
BALANCED ECCENTRICITY ABOUT X-X (in.) = 19.18815
BALANCED ECCENTRICITY ABOUT Y-Y (in.) = 20.23323

X-X BENDING MOMENTS FOR BEST (COMP/TENS) ALPHA = 1.7 1.4

MOMENT X-X Mbyx FOR Pnby (Kip-in) = 4068.785
MOMENT Y-Y Mbxy FOR Pnbx (Kip-in) = 2802.68

X-X ECCENTRICITY AT Pnby (in.) = 29.15996
Y-Y ECCENTRICITY AT Pnbx (in.) = 12.87365

Y-Y BENDING MOMENTS FOR BEST (COMP/TENS) ALPHA = 2.5 2.35
MOMENT X-X Mbyx FOR Pnby (Kip-in) = 4168.265
MOMENT Y-Y Mbxy FOR Pnbx (Kip-in) = 2821.186

X-X ECCENTRICITY AT Pnby (in.) = 29.8729
Y-Y ECCENTRICITY AT Pnbx (in.) = 12.95865

INTERACTION DIAGRAM MOMENT RATIO VALUES (Mox/Mnb & Moy/Mnb)
BEST X-X ALPHA - COMPRESSION SIDE = 1.7
BEST X-X ALPHA - TENSILE SIDE = 1.4

| Pn | Mox | Moy | Mox/Mnbyx | Moy/Mnbxy |
|---|---|---|---|---|
| 1555.056 | 0 | 0 | 0 | 0 |
| 1207.151 | 1674.428 | 1075.411 | .4008312 | .383708 |
| 1178.066 | 1798.217 | 1155.583 | .4304642 | .4123137 |
| 1161.083 | 1869.297 | 1201.677 | .4474797 | .4287599 |
| 1143.86 | 1940.474 | 1247.877 | .4645181 | .4452444 |
| 1126.395 | 2011.711 | 1294.165 | .4815712 | .4617598 |
| 1108.677 | 2083.009 | 1340.541 | .4986387 | .478307 |
| 1090.694 | 2154.362 | 1387.006 | .5157195 | .4948857 |
| 1072.435 | 2225.766 | 1433.56 | .5328124 | .5114961 |
| 1053.874 | 2297.262 | 1480.233 | .5499275 | .5281491 |
| 1051.397 | 2306.721 | 1486.412 | .5521919 | .530354 |
| 1002.036 | 2491.085 | 1607.087 | .5963257 | .5734109 |
| 951.1244 | 2672.912 | 1726.585 | .639852 | .616048 |
| 897.2667 | 2855.864 | 1847.406 | .6836477 | .659157 |
| 839.4579 | 3041.237 | 1970.558 | .7280231 | .7030978 |
| 778.905 | 3222.867 | 2092.129 | .7715025 | .7464744 |
| 713.7861 | 3403.417 | 2214.15 | .8147233 | .7900118 |
| 643.8541 | 3579.612 | 2334.798 | .8569014 | .833059 |
| 565.2765 | 3754.664 | 2456.995 | .898806 | .8766592 |
| 469.9942 | 3932.196 | 2585.148 | .9413043 | .9223844 |
| 374.527 | 4068.128 | 2689.864 | .9738442 | .959747 |
| 217.7067 | 4177.391 | 2802.68 | 1 | 1 |
| 122.1512 | 4033.535 | 2813.252 | .9913364 | .9964731 |
| 21.48587 | 3783.468 | 2677.707 | .9298765 | .9484619 |
| 0 | 3721.786 | 2639.327 | .9147167 | .9348674 |
| -50.86052 | 3566.108 | 2539.087 | .8764552 | .8993617 |
| -105.3658 | 3385.641 | 2419.03 | .8321012 | .8568368 |
| -147.5962 | 3237.057 | 2318.198 | .795583 | .8211215 |
| -214.4467 | 2987.627 | 2146.25 | .7342798 | .7602164 |
| -287.9915 | 2694.819 | 1941.474 | .6623153 | .6876833 |
| -370.5898 | 2345.066 | 1694.097 | .5763553 | .6000606 |
| -465.5197 | 1918.172 | 1389.361 | .4714361 | .4921211 |
| -577.8602 | 1381.533 | 1003.287 | .3395443 | .3553712 |
| -648.8591 | 1026.09 | 746.232 | .2521859 | .2643204 |
| -677.2148 | 880.7881 | 640.9028 | .2164744 | .2270121 |
| -842.135 | 0 | 0 | 0 | 0 |

INTERACTION DIAGRAM MOMENT RATIO VALUES (Mox/Mnb & Moy/Mnb)

BEST Y-Y ALPHA - COMPRESSION SIDE = 2.5
BEST Y-Y ALPHA - TENSILE SIDE = 2.35

| Pn | Mox | Moy | Mox/Mnbyx | Moy/Mnbxy |
|---|---|---|---|---|
| 1555.056 | 0 | 0 | 0 | 0 |
| 1207.151 | 2210.539 | 1428.478 | .5291674 | .5063395 |
| 1178.066 | 2351.91 | 1521.538 | .5630094 | .5393257 |
| 1161.083 | 2431.546 | 1574.102 | .582073 | .5579575 |
| 1143.86 | 2510.142 | 1626.087 | .6008875 | .576384 |
| 1126.395 | 2587.635 | 1677.455 | .6194382 | .594592 |
| 1108.677 | 2664.002 | 1728.193 | .6377192 | .6125766 |
| 1090.694 | 2739.213 | 1778.284 | .6557235 | .6303819 |
| 1072.435 | 2813.238 | 1827.711 | .6734439 | .6478521 |
| 1053.874 | 2886.093 | 1876.49 | .6908842 | .6651421 |
| 1051.397 | 2895.635 | 1882.889 | .6931685 | .6674103 |
| 1002.036 | 3077.02 | 2005.023 | .736589 | .7107022 |
| 951.1244 | 3246.987 | 2120.47 | .7772764 | .7516237 |
| 897.2667 | 3408.504 | 2231.318 | .8159409 | .7909148 |
| 839.4579 | 3561.74 | 2337.833 | .8526231 | .8286701 |
| 778.905 | 3700.868 | 2436.1 | .8859281 | .8635018 |
| 713.7861 | 3827.308 | 2527.266 | .9161958 | .8958168 |
| 643.8541 | 3937.953 | 2609.306 | .9426824 | .9248967 |
| 565.2765 | 4033.545 | 2683.148 | .9655656 | .9510707 |
| 469.9942 | 4112.82 | 2748.865 | .9845429 | .9743649 |
| 374.527 | 4157.721 | 2791.507 | .9952914 | .98948 |
| 217.7067 | 4177.391 | 2821.186 | 1 | 1 |
| 122.1512 | 4162.762 | 2822.994 | .9986799 | .9999235 |
| 21.48587 | 4098.042 | 2803.758 | .983153 | .9931101 |
| 0 | 4076.096 | 2794.395 | .9778879 | .9897935 |
| -50.86052 | 4011.484 | 2763.395 | .9623871 | .9788132 |
| -105.3658 | 3921.271 | 2715.13 | .9407441 | .9617173 |
| -147.5962 | 3835.55 | 2666.134 | .9201791 | .9443627 |
| -214.4467 | 3670.005 | 2566.332 | .8804636 | .9090123 |
| -287.9915 | 3443.327 | 2422.91 | .8260817 | .8582112 |
| -370.5898 | 3129.925 | 2216.945 | .750894 | .785257 |
| -465.5197 | 2688.662 | 1917.81 | .6450314 | .6793012 |
| -577.8602 | 2048.375 | 1472.208 | .4914214 | .5214661 |
| -648.8591 | 1574.701 | 1136.771 | .3777834 | .4026519 |
| -677.2148 | 1370.126 | 990.756 | .3287042 | .3509325 |
| -842.135 | 0 | 0 | 0 | 0 |

AXIAL LOAD AND MOMENTS FOR PLANE AT : 18 (DEGREES)

| | | |
|---|---|---|
| 0 | 1555.056 | 0 |
| 1 | 1302.246 | 1107.047 |
| 2 | 1287.476 | 1185.4 |
| 3 | 1271.927 | 1266.607 |
| 4 | 1255.573 | 1350.415 |
| 5 | 1238.297 | 1436.413 |
| 6 | 1220.209 | 1524.643 |
| 7 | 1201.298 | 1614.941 |
| 8 | 1181.554 | 1707.174 |
| 9 | 1160.963 | 1801.234 |

| | | |
|---|---|---|
| 10 | 1139.616 | 1895.217 |
| 11 | 1093.016 | 2082.57 |
| 12 | 1043.911 | 2257.662 |
| 13 | 989.6236 | 2429.148 |
| 14 | 934.1216 | 2582.341 |
| 15 | 871.3059 | 2733.576 |
| 16 | 801.6302 | 2874.992 |
| 17 | 726.6633 | 3005.692 |
| 18 | 645.5871 | 3126.157 |
| 19 | 557.4056 | 3236.986 |
| 20 | 461.0358 | 3342.674 |
| 21 | 397.6835 | 3388.679 |
| 22 | 330.5808 | 3433.41 |
| 23 | 258.4811 | 3475.998 |
| 24 | 182.3678 | 3519.62 |
| 25 | 105.4664 | 3538.298 |
| 26 | 36.40857 | 3515.206 |
| 27 | -24.20273 | 3438.171 |
| 28 | -78.11779 | 3306.491 |
| 29 | -130.6695 | 3148.822 |
| 30 | -185.184 | 2972.454 |
| 31 | -242.6571 | 2771.504 |
| 32 | -304.8557 | 2541.424 |
| 33 | -371.678 | 2282.866 |
| 34 | -445.1025 | 1989.526 |
| 35 | -523.6585 | 1677.338 |
| 36 | -602.6059 | 1361.004 |
| 37 | -668.7744 | 1071.969 |
| 38 | -715.27 | 828.4013 |
| 39 | -740.6482 | 662.0157 |
| 40 | -754.2418 | 555.3944 |
| 41 | -842.135 | 0 |

AXIAL LOAD AND MOMENTS FOR PLANE AT : 36 (DEGREES)

| | | |
|---|---|---|
| 0 | 1555.056 | 0 |
| 1 | 1340.204 | 918.2711 |
| 2 | 1326.659 | 982.1849 |
| 3 | 1312.309 | 1048.139 |
| 4 | 1297.165 | 1115.998 |
| 5 | 1281.229 | 1185.615 |
| 6 | 1264.482 | 1256.743 |
| 7 | 1246.812 | 1328.883 |
| 8 | 1228.407 | 1402.405 |
| 9 | 1209.135 | 1476.775 |
| 10 | 1188.769 | 1551.128 |
| 11 | 1141.896 | 1709.585 |
| 12 | 1088.358 | 1875.606 |
| 13 | 1029.631 | 2039.97 |
| 14 | 966.8492 | 2195.236 |
| 15 | 897.1071 | 2346.902 |
| 16 | 822.2078 | 2486.418 |
| 17 | 741.436 | 2612.257 |
| 18 | 653.1236 | 2724.488 |

| | | |
|---|---|---|
| 19 | 557.2385 | 2820.287 |
| 20 | 453.3371 | 2901.953 |
| 21 | 385.298 | 2925.155 |
| 22 | 314.5624 | 2944.505 |
| 23 | 239.3228 | 2956.246 |
| 24 | 159.8748 | 2965.262 |
| 25 | 78.64893 | 2954.607 |
| 26 | -1.250163 | 2920.054 |
| 27 | -81.01713 | 2855.993 |
| 28 | -159.8083 | 2765.067 |
| 29 | -235.5897 | 2641.525 |
| 30 | -305.8076 | 2479.293 |
| 31 | -369.0332 | 2278.807 |
| 32 | -434.4934 | 2063.937 |
| 33 | -504.0109 | 1826.326 |
| 34 | -565.4791 | 1588.124 |
| 35 | -618.1232 | 1355.873 |
| 36 | -662.305 | 1134.977 |
| 37 | -700.6585 | 923.8812 |
| 38 | -730.7026 | 738.532 |
| 39 | -749.771 | 601.1187 |
| 40 | -761.1395 | 505.4735 |
| 41 | -842.135 | 0 |

AXIAL LOAD AND MOMENTS FOR PLANE AT : 54 (DEGREES)

| | | |
|---|---|---|
| 0 | 1555.056 | 0 |
| 1 | 1350.371 | 818.3287 |
| 2 | 1336.106 | 879.2012 |
| 3 | 1321.07 | 941.967 |
| 4 | 1305.234 | 1006.366 |
| 5 | 1288.691 | 1072.445 |
| 6 | 1271.359 | 1139.786 |
| 7 | 1253.082 | 1207.762 |
| 8 | 1234.051 | 1276.763 |
| 9 | 1214.251 | 1346.582 |
| 10 | 1193.666 | 1417.011 |
| 11 | 1144.142 | 1569.997 |
| 12 | 1090.016 | 1723.062 |
| 13 | 1030.388 | 1871.474 |
| 14 | 965.5173 | 2015.238 |
| 15 | 894.2832 | 2149.058 |
| 16 | 817.679 | 2272.254 |
| 17 | 736.3041 | 2379.238 |
| 18 | 650.2512 | 2473.635 |
| 19 | 557.2377 | 2552.875 |
| 20 | 456.3421 | 2622.424 |
| 21 | 389.0742 | 2635.252 |
| 22 | 319.8412 | 2645.369 |
| 23 | 244.6015 | 2650.733 |
| 24 | 163.6511 | 2649.206 |
| 25 | 81.42529 | 2633.992 |
| 26 | -1.365314 | 2594.897 |
| 27 | -86.81509 | 2528.39 |

| | | |
|---|---|---|
| 28 | -172.421 | 2446.347 |
| 29 | -259.7924 | 2343.275 |
| 30 | -345.6474 | 2205.791 |
| 31 | -422.2694 | 2050.539 |
| 32 | -490.5518 | 1877.437 |
| 33 | -550.7564 | 1680.832 |
| 34 | -598.751 | 1476.068 |
| 35 | -638.5581 | 1277.778 |
| 36 | -674.8302 | 1082.234 |
| 37 | -706.8654 | 895.0328 |
| 38 | -732.0507 | 731.6769 |
| 39 | -749.7711 | 601.1182 |
| 40 | -761.1395 | 505.473 |
| 41 | -842.135 | 0 |

AXIAL LOAD AND MOMENTS FOR PLANE AT : 72 (DEGREES)

| | | |
|---|---|---|
| 0 | 1555.056 | 0 |
| 1 | 1336.855 | 843.9913 |
| 2 | 1321.052 | 911.9249 |
| 3 | 1304.236 | 981.7592 |
| 4 | 1286.596 | 1053.322 |
| 5 | 1267.95 | 1125.926 |
| 6 | 1248.345 | 1199.513 |
| 7 | 1227.871 | 1274.145 |
| 8 | 1206.415 | 1349.487 |
| 9 | 1183.869 | 1425.21 |
| 10 | 1160.651 | 1500.507 |
| 11 | 1106.728 | 1657.682 |
| 12 | 1052.297 | 1799.663 |
| 13 | 993.3472 | 1937.447 |
| 14 | 929.529 | 2068.314 |
| 15 | 865.1194 | 2180.421 |
| 16 | 794.1234 | 2281.779 |
| 17 | 719.99 | 2371.318 |
| 18 | 641.3449 | 2451.922 |
| 19 | 557.4056 | 2522.173 |
| 20 | 465.5836 | 2588.199 |
| 21 | 404.505 | 2604.656 |
| 22 | 338.9048 | 2617.61 |
| 23 | 268.3076 | 2625.99 |
| 24 | 192.9254 | 2631.911 |
| 25 | 114.3203 | 2624.041 |
| 26 | 34.4105 | 2594.415 |
| 27 | -47.62686 | 2534.569 |
| 28 | -131.3804 | 2461.778 |
| 29 | -216.8479 | 2358.893 |
| 30 | -298.9577 | 2244.849 |
| 31 | -379.3311 | 2092.881 |
| 32 | -449.9219 | 1927.067 |
| 33 | -512.4589 | 1737.572 |
| 34 | -566.4361 | 1539.717 |
| 35 | -614.3107 | 1341.499 |
| 36 | -654.9758 | 1149.221 |

| | | |
|---|---|---|
| 37 | -693.0526 | 963.6953 |
| 38 | -720.9827 | 799.8153 |
| 39 | -740.6483 | 662.0151 |
| 40 | -754.2419 | 555.3935 |
| 41 | -842.135 | 0 |

BENDING MOMENTS AT SELECTED PLANES, AXIAL LOAD AND COEFFICIENT β FOR LOAD CONTOUR DIAGRAMS

| $M_x$ | $M_1$ | $M_2$ | $M_3$ | $M_4$ | $M_y$ | P | β |
|---|---|---|---|---|---|---|---|
| 4597.619 | 4352.351 | 4082.281 | 3592.073 | 3260.851 | 3343.489 | 2123.267 | 1.9 |
| 4730.358 | 4566.518 | 4250.699 | 3739.965 | 3383.897 | 3477.125 | 2082.508 | 2.05 |
| 4625.528 | 4493.358 | 4192.815 | 3689.135 | 3341.607 | 3431.411 | 2096.517 | 2.1 |
| 4797.714 | 4661.842 | 4326.802 | 3799.110 | 3440.061 | 3536.273 | 2063.903 | 2.1 |
| 4970.111 | 4827.887 | 4455.317 | 3902.293 | 3539.366 | 3633.195 | 2030.719 | 2.1 |
| 5142.843 | 4992.960 | 4586.140 | 4007.329 | 3636.345 | 3723.777 | 1996.940 | 2.1 |
| 5316.039 | 5161.070 | 4717.136 | 4110.458 | 3735.108 | 3818.414 | 1962.539 | 2.1 |
| 5477.316 | 5314.970 | 4835.154 | 4206.526 | 3829.758 | 3909.110 | 1929.571 | 2.1 |
| 5651.068 | 5482.803 | 4964.487 | 4311.802 | 3919.917 | 4003.199 | 1893.442 | 2.1 |
| 5825.700 | 5651.658 | 5093.994 | 4414.932 | 4011.419 | 4097.817 | 1856.591 | 2.15 |
| 6275.360 | 6074.361 | 5400.918 | 4670.241 | 4241.900 | 4330.814 | 1759.587 | 2.1 |
| 6744.852 | 6503.060 | 5713.675 | 4921.915 | 4470.228 | 4569.483 | 1654.403 | 2.1 |
| 7219.967 | 6916.981 | 6015.387 | 5162.784 | 4684.583 | 4797.600 | 1544.581 | 2.1 |
| 7718.511 | 7343.596 | 6322.998 | 5403.135 | 4906.367 | 5023.220 | 1424.052 | 2.05 |
| 8236.054 | 7741.000 | 6623.336 | 5633.933 | 5120.251 | 5248.429 | 1297.156 | 2 |
| 8788.658 | 8147.270 | 6921.519 | 5868.661 | 5322.577 | 5481.768 | 1157.716 | 1.9 |
| 9373.162 | 8551.199 | 7208.836 | 6106.561 | 5532.948 | 5718.956 | 1007.823 | 1.85 |
| 10005.92 | 8973.279 | 7500.733 | 6339.033 | 5751.905 | 5985.333 | 841.0243 | 1.75 |
| 10698.40 | 9391.007 | 7782.829 | 6567.001 | 5973.748 | 6188.749 | 666.6849 | 1.7 |
| 11379.36 | 9791.054 | 8037.359 | 6780.468 | 6154.651 | 6354.539 | 476.8357 | 1.65 |
| 11376.43 | 9972.086 | 8169.449 | 6886.607 | 6224.357 | 6388.608 | 347.8978 | 1.75 |
| 11283.60 | 10072.85 | 8263.986 | 6944.869 | 6247.086 | 6403.616 | 214.1894 | 1.85 |
| 10952.05 | 9996.055 | 8297.464 | 6971.133 | 6227.619 | 6405.698 | 54.09562 | 1.9 |
| 10776.52 | 9922.179 | 8293.340 | 6972.955 | 6212.145 | 6394.185 | 00.00000 | 1.95 |
| 10411.38 | 9646.398 | 8243.537 | 6926.803 | 6180.140 | 6308.572 | -107.1580 | 2 |
| 10001.95 | 9306.680 | 8157.612 | 6860.343 | 6095.189 | 6221.824 | -215.7357 | 2 |
| 9520.487 | 8948.030 | 8039.793 | 6783.084 | 6005.816 | 6107.123 | -316.9958 | 2.05 |
| 8956.088 | 8499.175 | 7840.603 | 6647.476 | 5890.655 | 5981.008 | -427.8365 | 2.05 |
| 8310.653 | 7967.527 | 7504.590 | 6472.938 | 5744.583 | 5823.946 | -548.9604 | 2.1 |
| 7541.234 | 7313.389 | 7013.330 | 6225.414 | 5541.168 | 5634.864 | -686.9766 | 2.1 |
| 6909.378 | 6766.334 | 6540.106 | 5969.681 | 5346.208 | 5431.855 | -797.9093 | 2.1 |
| 5799.372 | 5790.301 | 5682.688 | 5455.503 | 4914.451 | 4966.010 | -985.6180 | 2.2 |
| 4404.496 | 4516.298 | 4571.197 | 4556.762 | 4177.347 | 4064.450 | -1217.050 | 2.6 |
| 2607.486 | 2848.743 | 2944.635 | 2939.252 | 2843.005 | 2612.795 | -1512.030 | 2.6 |

## APPENDIX C

### Sample MathCad Documents for Interaction Equations

MathCad Document for the Uniaxial Interaction Equation.

$\alpha := 2.75$ $e := 8"$ $P_n := 1$

$P_o := 1139.052$ kip $P_{nb} := 122.948$ kip $P_{cr} := 1537.145$ kip $M_{nb} := 1559.476$ kip-in

GIVEN :

$$\left(\frac{P_n - P_{nb}}{P_o - P_{nb}}\right)^{\alpha} + \frac{e\, P_n\, P_{cr}}{M_{nb}\,(P_{cr} - P_n)} \approx 1 \qquad \text{(C.1)}$$

$P_n := \text{Find}(P_n)$ $P_n = 172.957$ kips

MathCad Document for the Biaxial Interaction Equation

MATHCAD FILENAME : COMPBEQ.MCD

$P_{nbx} := 355.868$ kip $M_{nbx} := 4.083 \times 10^3$ k-in $e_{nbx} := 11.474"$ $\alpha_c := 1.55$

$P_{nby} := 279.998$ kip $M_{nby} := 2.044 \times 10^3$ k-in $e_{nby} := 7.299"$ $\alpha_t := 1.6$

$P_{oc} := 1.174 \times 10^3$ kip $M_{byx} := 3.975 \times 10^3$ k-in $e_{byx} := 14.198"$ $\alpha := 1.6$

$P_{ot} := -379.2$ kip $M_{bxy} := 1.999 \times 10^3$ k-in $e_{bxy} := 5.617"$ $\beta := 1.5$

$P_o := -379.2$ kip $P_{nb} := 355.868$ kip $M_{nb} := 4.083 \times 10^3$ k-in MFX:= 1

$P_n := P_{nb}$ $e_x := 10.5"$ $e_y := 15"$ $\delta_x := 1$ $\delta_y := 1$ MFY:= 1.945

GIVEN : BIAXIAL EQUATION OF FAILURE SURFACE

$$\left(\frac{P_n - P_{nb}}{P_o - P_{nb}}\right)^{\alpha} + \left(\left(\delta_{mfx}\, P_n\, e_y\, \frac{M_{fx}}{M_{nb}}\right)^{\beta} + \left(\delta_{mfy}\, P_n\, e_x\, \frac{M_{fy}}{M_{nb}}\right)^{\beta}\right)^{\frac{1}{\beta}} \approx 1 \qquad \text{(C.2)}$$

$P_n := \text{Find}(P_n)$ $P_n = 121.134$ kip

# APPENDIX D

## Analysis and Design of Biaxially Loaded Reinforced Concrete Columns

The Author have used the Generalized Equation of Failure Surface developed in Chapter 2 to study its applicability to the Analysis and Design of Biaxially loaded reinforced concrete columns.

Tables D.1 and D.2 shows the results of the evaluation for coefficient $\alpha$. The values are obtained by using the computer program "INTRDIAG" for the reinforced concrete column sections presented by Hsu (85). They were studied and tested by the following investigators: Anderson and Lee (8), Bresler (19), Hsu (85), Ramamurthy (171), Heimdahl and Bianchini (97), Ansari (9), Hudson (98), Hoegnestad (99), Wang and Salmon (224), Leet (126), Winter and Nilson (225), Nawy (155), and Smith (189). The detailed dimensions and reinforcement of the column sections presented in Tables D.1 and D.2 are shown in Figs. D.1a to D.1v.

The Author found a wide variation of the values for coefficient $\alpha$, ranging from as low as 1.1 to as high as 3.25, depending on the main column parameters such as number and position of bars (N), column cross section dimensions (width b, depth t), modulus of elasticity of steel rebars ($E_s$), steel yield strength ($f_y$, ksi), ultimate concrete compressive strength ($f'_c$, ksi), steel ratio ($\rho_s$) and concrete cover (d). The relationship of the coefficient $\alpha$ with the column parameters may be written as follows:

$$\alpha = f\,(\,N,\ b,\ t,\ E_s\ ,\ f_y\ ,\ f'_c\ ,\ \rho_s\ ,\ d\,) \qquad (D.1)$$

**Table D.1** Calculated coefficients $\alpha$ for columns of Figs. D.1a to D.1m.

| Column No. | Figure No. | Size in.xin. | $E_s \times 10^3$ ksi | $f_y$ ksi | $f'_c$ psi | $\rho_g$ % | $\alpha$ | | | |
|---|---|---|---|---|---|---|---|---|---|---|
| | | | | | | | $\alpha_{cx}$ | $\alpha_{tx}$ | $\alpha_{cy}$ | $\alpha_{ty}$ |
| HS-1 | D.1a | 4 x 4 | 29.0 | 44.5 | 3426 | 2.75 | 1.55 | 1.35 | 1.55 | 1.35 |
| S-1 | D.1b | 4 x 4 | 29.0 | 44.5 | 3200 | 2.75 | 1.40 | 1.40 | 1.40 | 1.40 |
| S-2 | D.1b | 4 x 4 | 29.0 | 44.5 | 4095 | 2.75 | 1.45 | 1.45 | 1.45 | 1.45 |
| U-1 | D.1c | 4 x 4 | 29.2 | 73.0 | 3905 | 2.81 | 1.95 | 1.55 | 1.95 | 1.55 |
| U-5 | D.1c | 4 x 4 | 29.2 | 73.0 | 3715 | 2.81 | 1.90 | 1.55 | 1.90 | 1.55 |
| H-1 | D.1d | $4\frac{1}{4} \times 4\frac{1}{4}$ | 29.0 | 44.5 | 3545 | 4.87 | 1.70 | 1.65 | 1.70 | 1.65 |
| H-3 | D.1d | $4\frac{1}{4} \times 4\frac{1}{4}$ | 29.0 | 44.5 | 4227 | 4.87 | 1.75 | 1.65 | 1.75 | 1.65 |
| SC-9 | D.1e | 4 x 4 | 29.0 | 45.6 | 5435 | 5.0 | 1.45 | 1.30 | 1.45 | 1.30 |
| AR-1 | D.1f | 5 x 5 | 28.0 | 71.6 | 4633 | 3.2 | 1.90 | 1.25 | 1.90 | 1.25 |
| AR-3 | D.1f | 5 x 5 | 28.0 | 71.6 | 5376 | 3.2 | 2.0 | 1.25 | 2.0 | 1.25 |
| DR-1 | D.1f | 5 x 5 | 28.0 | 71.6 | 3666 | 3.2 | 1.75 | 1.25 | 1.75 | 1.25 |
| BR-3 | D.1f | 5 x 5 | 28.0 | 71.6 | 4997 | 3.2 | 1.95 | 1.25 | 1.95 | 1.25 |
| ER-1 | D.1f | 5 x 5 | 28.0 | 71.6 | 3480 | 3.2 | 1.70 | 1.25 | 1.70 | 1.25 |
| HD-2 | D.1g | 6 x 6 | 29.0 | 40.0 | 3400 | 4.44 | 1.45 | 1.90 | 1.45 | 1.90 |
| HD-3 | D.1g | 6 x 6 | 29.0 | 40.0 | 4200 | 6.89 | 1.40 | 1.95 | 1.40 | 1.95 |
| B-1 | D.1h | 6 x 8 | 30.0 | 53.5 | 3700 | 2.58 | 1.65 | 1.30 | 2.0 | 1.40 |
| B-4 | D.1h | 6 x 8 | 30.0 | 53.5 | 4600 | 2.58 | 1.75 | 1.35 | 2.0 | 1.45 |
| B-5 | D.1h | 6 x 8 | 30.0 | 53.5 | 3200 | 2.58 | 1.60 | 1.30 | 2.0 | 1.40 |
| AN-1 | D.1i | 7 x 8 | 29.0 | 40.0 | 3830 | 1.43 | 1.50 | 1.75 | 1.55 | 1.70 |
| AN-2 | D.1i | 7 x 8 | 29.0 | 40.0 | 4882 | 1.43 | 1.65 | 1.70 | 1.70 | 1.65 |
| AN-5 | D.1i | 7 x 8 | 29.0 | 40.0 | 4112 | 1.43 | 1.55 | 1.75 | 1.60 | 1.70 |
| RB-1 | D.1j | 8 x 8 | 30.0 | 46.79 | 4230 | 3.88 | 1.50 | 1.90 | 1.50 | 1.90 |
| RB-2 | D.1j | 8 x 8 | 30.0 | 46.79 | 3735 | 3.88 | 1.45 | 1.95 | 1.45 | 1.95 |
| RB-3 | D.1j | 8 x 8 | 30.0 | 46.79 | 4860 | 3.88 | 1.55 | 1.85 | 1.55 | 1.85 |
| RB-5 | D.1j | 8 x 8 | 30.0 | 46.79 | 2805 | 3.88 | 1.40 | 1.95 | 1.40 | 1.95 |
| D-1 | D.1k | 6 x 9 | 30.0 | 46.79 | 4590 | 4.59 | 1.50 | 1.80 | 1.50 | 1.80 |
| D-2 | D.1k | 6 x 9 | 30.0 | 46.79 | 3690 | 4.59 | 1.45 | 1.85 | 1.45 | 1.85 |
| D-3 | D.1k | 6 x 9 | 30.0 | 46.79 | 3546 | 4.59 | 1.45 | 1.90 | 1.45 | 1.90 |
| D-5 | D.1k | 6 x 9 | 30.0 | 46.79 | 4482 | 4.59 | 1.50 | 1.85 | 1.50 | 1.85 |

**Table D.1** (cont.) Calculated coefficients $\alpha$ for columns of Figs. D.1a to D.1m.

| Column No. | Figure No. | Size in.xin. | $E_s$ x$10^3$ ksi | $f_y$ ksi | $f'_c$ psi | $\rho_g$ % | $\alpha$ $\alpha_{cx}$ | $\alpha_{tx}$ | $\alpha_{cy}$ | $\alpha_{ty}$ |
|---|---|---|---|---|---|---|---|---|---|---|
| D-6 | D.1k | 6 x 9 | 30.0 | 46.79 | 3465 | 4.59 | 1.40 | 1.90 | 1.40 | 1.90 |
| E-1 | D.1l | 6 x 12 | 30.0 | 46.79 | 3402 | 3.44 | 1.50 | 1.85 | 1.50 | 1.85 |
| E-2 | D.1l | 6 x 12 | 30.0 | 46.79 | 3105 | 3.44 | 1.45 | 1.85 | 1.45 | 1.85 |
| E-3 | D.1l | 6 x 12 | 30.0 | 46.79 | 4023 | 3.44 | 1.55 | 1.85 | 1.55 | 1.85 |
| A-15a | D.1m | 10 x 10 | 29.0 | 43.6 | 5100 | 4.80 | 1.75 | 2.0 | 1.35 | 1.35 |

**Table D.2** Calculated coefficients $\alpha$ for columns of Figs. D.1n to D.1v.

| Column No. | Figure No. | Size in.xin. | $E_s$ x $10^3$ ksi | $f_y$ ksi | $f'_c$ psi | $\rho_g$ % | $\alpha$ $\alpha_{cx}$ | $\alpha_{tx}$ | $\alpha_{cy}$ | $\alpha_{ty}$ |
|---|---|---|---|---|---|---|---|---|---|---|
| EX-1, 2 | D.1n | 15 x 24 | 29.0 | 50 | 3000 | 1.32 | 1.50 | 1.60 | 1.80 | 1.85 |
| EX-3 | D.1o | 17 x 17 | 29.0 | 40 | 3000 | 2.77 | 1.65 | 2.00 | 1.35 | 1.50 |
| EX-4 | D.1p | 14 x 20 | 29.0 | 50 | 4500 | 3.34 | 1.40 | 1.40 | 1.80 | 1.80 |
| EX-5 | D.1q | 16 x 16 | 29.0 | 40 | 3000 | 3.97 | 1.45 | 1.95 | 1.45 | 1.95 |
| EX-6 | D.1r | 18 x 18 | 29.0 | 60 | 4000 | 2.47 | 1.60 | 1.65 | 1.60 | 1.65 |
| EX-7 | D.1s | 12 x 18 | 29.0 | 60 | 4000 | 4.39 | 1.45 | 1.65 | 1.80 | 1.65 |
| EX-8 | D.1t | 16 x 20 | 29.0 | 60 | 4000 | 1.74 | 1.65 | 1.65 | 1.75 | 1.60 |
| EX-9 | D.1u | 12 x 20 | 29.0 | 60 | 4000 | 3.33 | 1.45 | 1.70 | 1.90 | 1.60 |
| EX-10 | D.1v | 12 x 20 | 29.0 | 60 | 4000 | 2.63 | 1.55 | 1.70 | 1.95 | 1.60 |

A special-purpose computer program was implemented to study the correlation between the different variables involved in the calculations of coefficient $\alpha$. A reinforcing steel bar with a modulus of elasticity $E_s$ of 29,000 ksi and Grade 60 yield strength of 60,000 psi was selected for the study, reducing the relationship of the column parameter to the following function:

$$\alpha = f ( N, b, t, f'_c , \rho_s , d ) \qquad (D.2)$$

A typical column cross-section with reinforcement symmetrically placed and

evenly distributed along all four faces of the column was used. The number of bars was changed in increments of four, starting with a column cross-section with one bar at each corner, for a total of four bars. It is found that for column cross-sections with 12 and 16 bars, the values of coefficient $\alpha$ do not change significantly; The results lead the Author to the following conclusions. For a column cross-section with a constant steel ratio, the position and number of bars do not have a significant change in the value of coefficient $\alpha$ for the columns doubled the number of bars with the same steel ratio. As the number of bars increases but with the same steel ratio, the value of coefficient $\alpha$ converges to a constant number. The correlation of values in this study is done for column sections with a d/b ratio ranging from 0.10 to 0.225 and concrete ultimate strength f'c from 3,000 psi to 6,000 psi.

For the compression controlled portion of the load-moment uniaxial interaction diagram, the following equation is presented by the Author after studying the correlation of the different column parameters:

$$\alpha_c = (\alpha_{c1})\ (\alpha_{c2})^{d/b}\ (\alpha_{c3} + \alpha_{c4})^{\rho} \tag{D.3}$$

$$\alpha_{c1} = K_1 + K_2\ N + K_3\ (K_4)^N\ f_c' \tag{D.4}$$

$$\alpha_{c2} = K_5 + K_6\ N + (K_7 + K_8\ N)\ln f_c' \tag{D.5}$$

$$\alpha_{c3} = K_9 + K_{10}N + K_{11}K_{12}^N\ f_c' \tag{D.6}$$

$$\alpha_{c4} = (K_{13} + K_{14}\ N + K_{15}K_{16}^N\ f_c')\ln\ (d/b) \tag{D.7}$$

The values of constants $K_1$ through $K_{16}$ have the following values:

**Table D.3** Values of Constants $K_1$ to $K_{16}$ for the compression controlled region.

| Constant (K) | Value | Constant (K) | Value |
|---|---|---|---|
| $K_1$ | 0.05435 | $K_9$ | 1.2938375 |
| $K_2$ | -0.006154 | $K_{10}$ | -0.02060702 |
| $K_3$ | 0.104692 | $K_{11}$ | -0.072965 |
| $K_4$ | 1.022738 | $K_{12}$ | 0.8320365 |
| $K_5$ | 145.253479 | $K_{13}$ | 024708945 |
| $K_6$ | 14.4063218 | $K_{14}$ | -0.0131314625 |
| $K_7$ | -23.949535 | $K_{15}$ | -0.048928305 |
| $K_8$ | -9.260418075 | $K_{16}$ | 0.7914431 |

A similar expression can be derived to estimate the value of the coefficient $\alpha_t$ that will define the shape of the tension controlled portion of the load-moment interaction diagram.

The Author recommends the use of the computer program "INTRDIAG" to find the proper values of coefficients $\alpha_c$ and $\alpha_t$. The program accepts a wide range of input values of the main column parameters and provides the complete load-interaction diagram for both main axes as well.

For columns subjected to biaxial bending and axial loads the Author proposes to use a single coefficient $\alpha$ by taking the lowest of the two values which define the compression controlled or tension controlled regions.

Depending on the location of the nominal axial load $P_n$, one can obtain a lower bound solution, which is conservative and practical.

The coefficient $\beta$ in the load-contour equation for a given reinforced concrete column under axial load and biaxial bending moments varies with the magnitude of the axial load $P_n$.

Several investigators have studied the variation of the coefficient $\beta$. Hsu (85), in his proposed equation of failure surface recommends a value of $\beta = 1.5$. Amirthanandan and Rangan (4) presented the equation adopted by The British Standard BS8220 (21):

$$\beta = 0.7 + 1.7( P_n / 0.6 P_o ) \qquad (D.8)$$

where: $1.0 < \beta < 2.0$

An analytical formulation for $\beta$, was presented by Gowens (77) where $\beta$ was taken as a function of the number of bars, the reinforcement index $q = A_{st}f_y/bhf'_c$ and the uniaxial load $P_n$.

Towfighi (209) developed a condensation procedure, that led to the tabulation of axial load, moment capacities and the $\beta$ values with minimum error. He used a regression analysis and the exact points of the load-contour plane and load-moment interaction diagrams.

The Author studies the validity of the Generalized Equation of Failure Surface for the analysis and design of reinforced concrete columns under axial loads and biaxial bending. The value of the coefficient $\beta$ used in this study is 1.50, and the coefficient $\alpha$ will be calculated by the use of the computer program "INTRDIAG'.

The special-purpose computer program "INTRDIAG" generates all the main

column parameters required to process the generalized equation of failure surface.

The MathCAD® software (138), was used to create a mathematical document to manipulate the variables involved in the calculations of the uniaxial and biaxial equations of failure surface.

Hsu (85), in 1988 proposed an interaction equation of failure surface for the analysis and design of square and rectangular reinforced concrete columns, the equation for the combined biaxial bending and axial load case can be written as follows:

$$\left(\frac{P_n - P_{nb}}{P_o - P_{nb}}\right) + \left(\frac{M_{nx}}{M_{nbx}}\right)^{1.5} + \left(\frac{M_{ny}}{M_{nby}}\right)^{1.5} = 1.0 \qquad \text{(D.9)}$$

The Author proposes herein the following generalized expression of the interaction equation of failure surface:

$$\left(\frac{P_n - P_{nb}}{P_o - P_{nb}}\right)^{\alpha} + \left[\left(\frac{M_{nx}}{M_{nb}}\ M_{fx}\right)^{\beta} + \left(\frac{M_{ny}}{M_{nb}}\ M_{fy}\right)^{\beta}\right]^{1/\beta} = 1 \qquad \text{(D.10)}$$

The different column sections studied by Hsu (85) were checked by using the Author's proposed interaction equation of failure surface for both uniaxial bending and biaxial bending cases. The results are presented in Tables D.4, D.5 and D.6.

A sample of the MathCAD documents used to calculate the uniaxial and biaxial interaction equations are presented in Appendix C.

**Table D.4** Comparative test and analytical loads for columns of Figs. D.1a,f,g,h, i.

| Col. No. | Fig. No. | $e_x$ in. | $e_y$ in. | h/b | $P_n$, Kips $P_t$ | $P_1$ | $P_2$ | Fail. Mode | $P_t/P_2$ |
|---|---|---|---|---|---|---|---|---|---|
| A-15a | D.1m | 12.5 | 0 | 7.5 | 88.0 | 79.0 | 82.69 | Tens. | 1.06 |
| B-1 | D.1h | 6.0 | 0 | 8 | 24.0 | 25.4 | 26.52 | Tens. | 0.905 |
| B-2 | D.1h | 3.0 | 0 | 8 | 60.0 | 56.0 | 57.99 | Com. | 1.03 |
| B-3 | D.1h | 0 | 4.0 | 8 | 70.0 | 68.5 | 70.58 | Com. | 0.992 |
| B-4 | D.1h | 0 | 8.0 | 8 | 32.0 | 32.0 | 30.70 | Tens. | 1.04 |
| HS-1 | D.1a | 5.0 | 0 | 15 | 6.445 | 6.55 | 6.69 | Tens. | 0.963 |
| HS-2 | D.1a | 3.0 | 0 | 15 | 11.91 | 12.50 | 13.08 | Tens. | 0.911 |
| HD-1 | D.1g | 2.0 | 0 | 8 | 72.0 | 69.0 | 71.30 | Com. | 1.009 |
| HD-2 | D.1g | 2.0 | 0 | 8 | 80.0 | 74.0 | 76.33 | Com. | 1.048 |
| HD-3 | D.1g | 2.0 | 0 | 8 | 100.0 | 100.2 | 102.61 | Com. | 0.975 |
| HD-4 | D.1g | 2.0 | 0 | 8 | 106.0 | 101.5 | 104.43 | Com. | 1.015 |
| AN-1 | D.1i | 0 | 0 | 2.57 | -32.0 | -32.0 | -31.52 | Tens. | 1.015 |
| AN-2 | D.1i | 0 | 2.0 | 2.57 | -19.0 | -22.5 | -20.86 | Tens. | 0.911 |
| AN-3 | D.1i | 0 | 2.0 | 2.57 | -19.0 | -21.5 | -20.87 | Tens. | 0.910 |
| AN-4 | D.1i | 0 | 5.0 | 2.57 | -13.0 | -13.6 | -13.55 | Tens. | 0.959 |
| AN-5 | D.1i | 0 | 5.0 | 2.57 | -12.0 | -13.4 | -13.54 | Tens. | 0.886 |
| AN-6 | D.1i | 0 | 0 | 2.57 | -33.0 | -32.0 | -31.8 | Tens. | 1.038 |
| AN-7 | D.1i | 0 | 0 | 2.57 | -34.0 | -32.0 | -31.52 | Tens. | 1.079 |
| AN-8 | D.1i | 0 | 5.0 | 2.57 | -14.2 | -13.5 | -13.52 | Tens. | 1.05 |
| AR-1 | D.1f | 1.03 | 0 | 3.2 | 78.0 | 80.5 | 87.79 | Com. | 0.888 |
| AR-2 | D.1f | 1.06 | 0 | 3.2 | 81.5 | 80.0 | 86.54 | Com. | 0.942 |
| AR-3 | D.1f | 2.8 | 0 | 6 | 42.3 | 43.0 | 45.92 | Com. | 0.921 |
| AR-4 | D.1f | 2.72 | 0 | 6 | 46.0 | 44.0 | 47.07 | Com. | 0.977 |
| AR-5 | D.1f | 5.25 | 0 | 6 | 23.6 | 24.7 | 24.84 | Tens. | 0.95 |
| AR-6 | D.1f | 5.24 | 0 | 6 | 23.7 | 24.8 | 24.89 | Tens. | 0.952 |
| DR-1 | D.1f | 2.73 | 0 | 6 | 42.6 | 36.7 | 39.20 | Com. | 1.087 |
| DR-2 | D.1f | 5.27 | 0 | 6 | 19.7 | 20.9 | 21.42 | Com. | 0.919 |

average for specimens in tension controls = 0.975 $P_t$ : Test Load

average for specimens in compression controls = 0.984 $P_1$ : Load by Hsu's Eq. D.9

overall Average = 0.979 $P_2$ : Load by Author's Eq.D.10

**Table D.5** Comparative test and analytical loads for columns of Figs. D.1b to D.1l.

| Col. No. | Figure No. | e, in. | | h/b | $P_n$, Kips | | | Fail. Mode | $P_t/P_2$ |
|---|---|---|---|---|---|---|---|---|---|
| | | $e_x$ | $e_y$ | | Test Load $P_t$ | Load $P_1$ | Load $P_2$ | | |
| SC-9 | G.1e | 2.82 | 2.82 | 12.5 | 14.3 | 15.1 | 15.4 | Tens. | 0.929 |
| B-5 | G.1h | 3.0 | 4.0 | 8 | 35.3 | 33.9 | 32.97 | Tens. | 1.071 |
| B-6 | G.1h | 6.0 | 8.0 | 8 | 17.0 | 15.6 | 15.57 | Tens. | 1.092 |
| B-7 | G.1h | 6.0 | 4.0 | 8 | 21.0 | 20.0 | 20.161 | Tens. | 1.042 |
| B-8 | G.1h | 3.0 | 8.0 | 8 | 24.0 | 22.0 | 22.29 | Tens. | 1.077 |
| S-1 | G.1b | 1.0 | 1.5 | 7.5 | 21.0 | 22.0 | 22.67 | Comp. | 0.926 |
| S-2 | G.1b | 1.0 | 1.5 | 7.5 | 24.8 | 25.8 | 26.05 | Comp. | 0.952 |
| U-1 | G.1c | 2.5 | 3.5 | 10 | 9.6 | 9.0 | 9.32 | Tens. | 1.03 |
| U-2 | G.1c | 3.0 | 3.5 | 10 | 8.7 | 8.2 | 8.5 | Tens. | 1.023 |
| U-3 | G.1c | 3.5 | 3.5 | 10 | 8.0 | 7.6 | 7.902 | Tens. | 1.012 |
| U-4 | G.1c | 2.0 | 2.0 | 10 | 14.30 | 14.35 | 14.45 | Comp. | 0.99 |
| U-5 | G.1c | 0.5 | 5.5 | 10 | 10.80 | 7.40 | 7.71 | Tens. | 1.40 |
| U-6 | G.1c | 0.5 | 7.0 | 10 | 6.24 | 5.70 | 5.94 | Tens. | 1.051 |
| H-1 | G.1d | 3.0 | 2.0 | 15 | 13.9 | 13.15 | 13.99 | Tens. | 0.994 |
| H-2 | G.1d | 3.25 | 2.25 | 15 | 11.8 | 12.0 | 13.02 | Tens. | 0.906 |
| H-3 | G.1d | 2.5 | 3.0 | 15 | 13.6 | 12.4 | 13.54 | Tens. | 1.004 |
| RB-1 | G.1j | 0.8282 | 3.091 | 10 | 141.4 | 134.0 | 137.96 | Comp. | 1.025 |
| RB-2 | G.1j | 0.764 | 1.848 | 10 | 173.5 | 166.0 | 170.22 | Comp. | 1.019 |
| RB-3 | G.1j | 2.0 | 3.464 | 10 | 120.0 | 113.0 | 115.77 | Tens. | 1.037 |
| RB-4 | G.1j | 2.5 | 4.33 | 10 | 89.0 | 81.0 | 88.65 | Tens. | 1.004 |
| RB-5 | G.1j | 1.414 | 1.414 | 10 | 134.5 | 139.0 | 141.61 | Comp. | 0.950 |
| RB-6 | G.1j | 2.545 | 2.545 | 10 | 112.5 | 113.5 | 115.54 | Comp. | 0.974 |
| RB-7 | G.1j | 2.828 | 2.828 | 10 | 116.0 | 105.0 | 107.42 | Tens. | 1.079 |
| RB-8 | G.1j | 4.0 | 4.0 | 10 | 83.125 | 68.0 | 76.95 | Tens. | 1.08 |
| D-1 | G.1k | 0.9987 | 1.4975 | 12.5 | 176.5 | 175.2 | 186.07 | Comp. | 0.949 |

$P_t$: Test Load

$P_1$: Analytical Load, by Hsu's Eq. D.9

$P_2$: Analytical Load, by Author's Eq. D.10

**Table D.5** (cont.) Comparative test and analytical loads for columns of Figs. D.1b to D.1l.

| Column No. | Figure No. | e, in. | | h/b | $P_n$, Kips | | | Fail. Mode | $P_t/P_2$ |
|---|---|---|---|---|---|---|---|---|---|
| | | $e_x$ in. | $e_y$ in. | | Test Load $P_t$ | Load $P_1$ | Load $P_2$ | | |
| D-2 | D.1k | 2.1938 | 3.3278 | 12.5 | 90.0 | 91.5 | 86.42 | Comp. | 1.041 |
| D-3 | D.1k | 2.9916 | 4.4926 | 12.5 | 70.0 | 67.0 | 62.16 | Tens. | 1.126 |
| D-4 | D.1k | 1.2728 | 1.2728 | 12.5 | 153.0 | 145.5 | 153.14 | Comp. | 0.999 |
| D-5 | D.1k | 3.182 | 3.182 | 12.5 | 85.0 | 78.0 | 86.54 | Tens. | 0.982 |
| D-6 | D.1k | 3.1177 | 1.8 | 12.5 | 90.0 | 83.5 | 86.52 | Comp. | 1.04 |
| E-1 | D.1l | 2.3645 | 4.4719 | 12.5 | 104.5 | 91.2 | 114.99 | Tens. | 0.909 |
| E-2 | D.1l | 3.0 | 6.0 | 12.5 | 70.0 | 60.0 | 86.96 | Tens. | 0.805 |
| E-3 | D.1l | 3.3941 | 3.3941 | 12.5 | 98.0 | 76.2 | 96.83 | Tens. | 1.012 |
| E-4 | D.1l | 2.5981 | 1.5 | 12.5 | 122.0 | 116.0 | 124.30 | Comp. | 0.982 |
| BR-1 | D.1f | 0.4087 | 0.9867 | 3.2 | 73.0 | 75.5 | 82.59 | Comp. | 0.884 |
| BR-2 | D.1f | 0.4076 | 0.9839 | 3.2 | 77.0 | 75.8 | 82.72 | Comp. | 0.931 |
| BR-3 | D.1f | 2.624 | 1.087 | 6 | 38.0 | 38.5 | 40.83 | Comp. | 0.931 |
| BR-5 | D.1f | 4.89 | 2.025 | 6 | 19.1 | 21.7 | 22.0 | Tens. | 0.868 |
| BR-6 | D.1f | 5.028 | 2.083 | 6 | 17.6 | 21.0 | 21.3 | Tens. | 0.826 |
| CR-1 | D.1f | 0.7623 | 0.7623 | 3.2 | 78.2 | 73.8 | 80.43 | Comp. | 0.972 |
| CR-2 | D.1f | 0.7545 | 0.7545 | 3.2 | 75.5 | 74.21 | 80.91 | Comp. | 0.933 |
| CR-3 | D.1f | 1.897 | 1.897 | 6 | 38.7 | 39.7 | 42.22 | Comp. | 0.917 |
| CR-4 | D.1f | 1.947 | 1.947 | 6 | 37.0 | 38.8 | 41.22 | Comp. | 0.898 |
| CR-5 | D.1f | 3.7844 | 3.7844 | 6 | 18.5 | 20.7 | 20.97 | Tens. | 0.882 |
| CR-6 | D.1f | 3.725 | 3.725 | 6 | 18.9 | 21.0 | 21.37 | Tens. | 0.885 |
| ER-1 | D.1f | 2.505 | 1.037 | 6 | 42.1 | 33.7 | 35.86 | Comp. | 1.174 |
| ER-2 | D.1f | 4.889 | 2.025 | 6 | 18.5 | 19.0 | 19.36 | Comp. | 0.956 |
| FR-1 | D.1f | 1.9177 | 1.9177 | 6 | 38.2 | 33.4 | 35.66 | Comp. | 1.071 |
| FR-2 | D.1f | 3.7123 | 3.7123 | 6 | 18.2 | 18.9 | 19.21 | Comp. | 0.947 |

average for specimens in compression controls = 0.977; $P_t$: Test Load

average for specimens in tension controls = 1.005; $P_1$: Analytical Load by Eq. D.9

overall Average for Specimens = 0.991; $P_2$: analytical Load by Eq. D.10

**Table D.6** Comparative analytical loads for columns of Figs. D.1n to D.1v

| Column Specimen No. | Figure No. | e, in. | | $P_n$, Kips | | | Failure Mode | $P_{th}/P_2$ |
|---|---|---|---|---|---|---|---|---|
| | | $e_x$ in. | $e_y$ in. | $P_{th}$(1) by Authors | $P_1$ by Eq. G.9 | $P_2$ by Eq. G.10 | | |
| EX-1 | D.1n | 0 | 8 | 560 | 555 | 560.22 | Comp. | 0.999 |
| EX-2 | D.1n | 0 | 20 | -80.0 | -87.8 | -85.34 | Tens. | 0.937 |
| EX-3 | D.1o | 2.4 | 0 | 755 | 750 | 754.1 | Comp. | 1.001 |
| EX-4 | D.1p | 0 | 29.12 | 164 | 168.4 | 175.42 | Tens. | 0.935 |
| EX-5 | D.1q | 4.485 | 10 | 216.7 | 206 | 240.93 | Tens. | 1.11 |
| EX-6 | D.1r | 4 | 3 | 709 | 685.7 | 747.81 | Comp. | 0.948 |
| EX-7 | D.1s | 3.972 | 9.972 | 291 | 284 | 310.32 | Tens. | 0.938 |
| EX-8 | D.1t | 3 | 4 | 634 | 630 | 673.08 | Comp. | 0.942 |
| EX-9 | D.1u | 3 | 6 | 401.5 | 410 | 455.5 | Comp. | 0.881 |
| EX-10 | D.1v | 4.67 | 8 | 331.5 | 270 | 285.97 | Tens. | 1.159 |

NOTE (1): The axial loads $P_{th}$ calculated by authors are theoretical values obtained by Bresler'sreciprocal load method and principles of statics.

| | | |
|---|---|---|
| average for specimens in compression controls | = | 0.954 |
| average for specimens in tension controls | = | 1.016 |
| overall average for specimens | = | 0.985 |

The reinforced concrete column sections with the dimensions, reinforcement information and corresponding investigator's name are shown in the following pages.

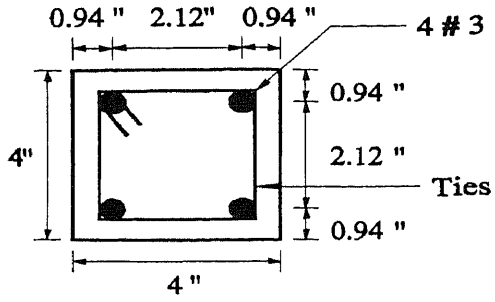


Fig. D.1a - Column cross section HS-1
Hsu (85)

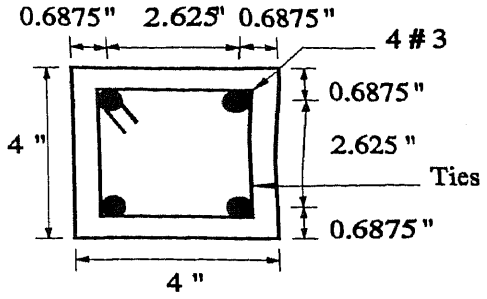


Fig. D.1b - Column cross section S-1
Hsu (85)

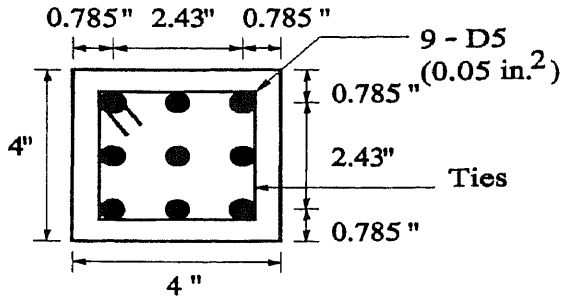


Fig. D.1c - Column cross section U-1
Hsu (85)

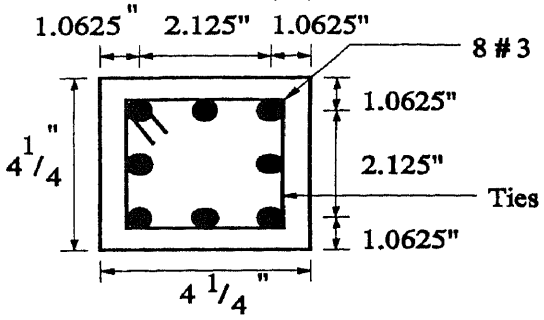


Fig. D.1d - Column cross section H-1
Hsu (85)

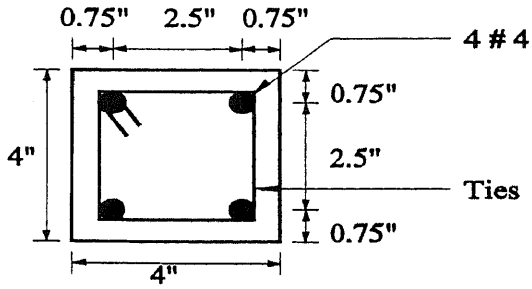


Fig. D.1e - Column cross section SC-9
Anderson & Lee (8)

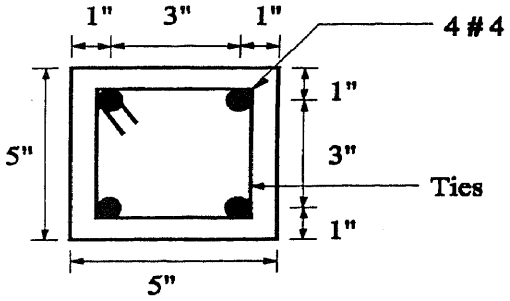


Fig. D.1f - Column cross section AR-1
Heimdahl et. al. (97)

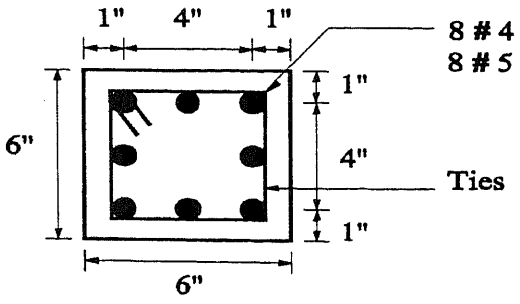


Fig. D.1g - Column cross section HD-2
Hudson (98)

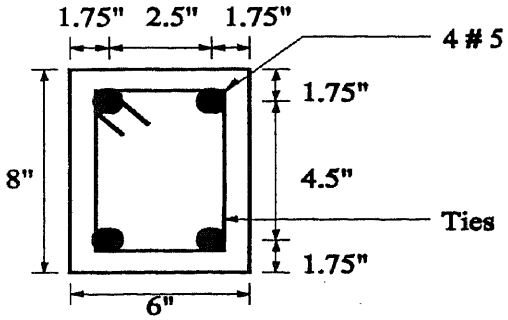


Fig. D.1h - Column cross section B-1
Bresler (19)

**Figure D.1** Column cross sections D.1a to D.1h

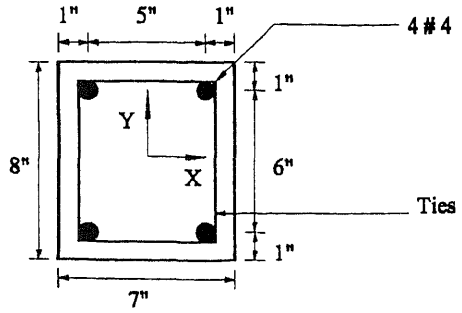


Fig. D.1i - Column cross section AN-1
Ansari (9)

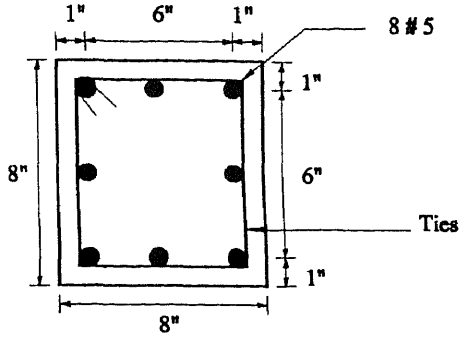


Fig. D.1j - Column cross section RB-1
Ramamurthy (171)

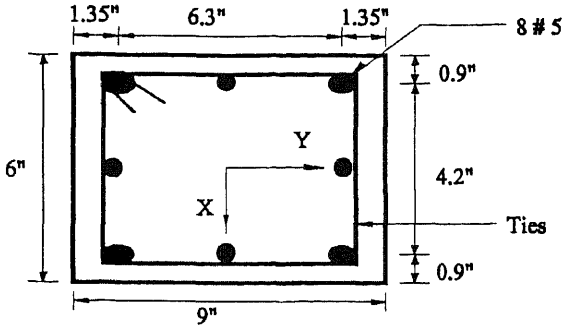


Fig. D.1k - Column cross section D-1
Ramamurthy (171)

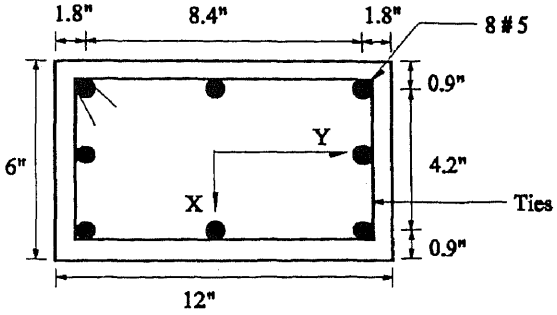


Fig. D.1i - Column cross section E-1
Ramamurthy (171)

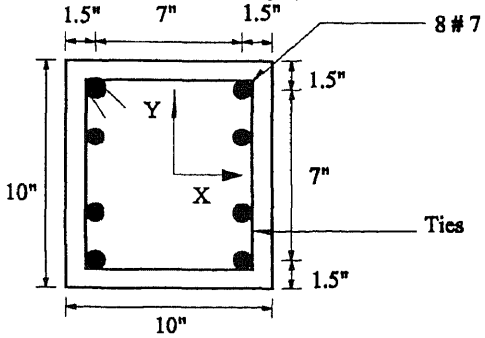


Fig. D.1m - Column cross section A-15a
Hoegnestad (99)

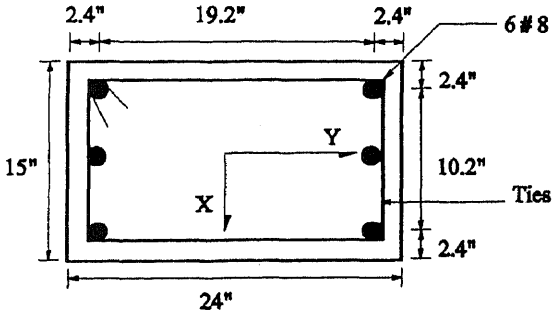


Fig. D.1n - Column cross section EX-1
Wang & Salmon (224)

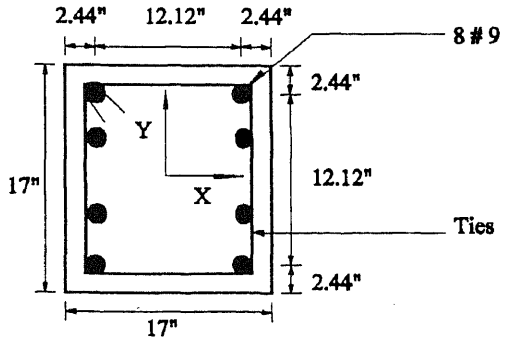


Fig. D.1o - Column cross section EX-3
Wang and Salmon (224)

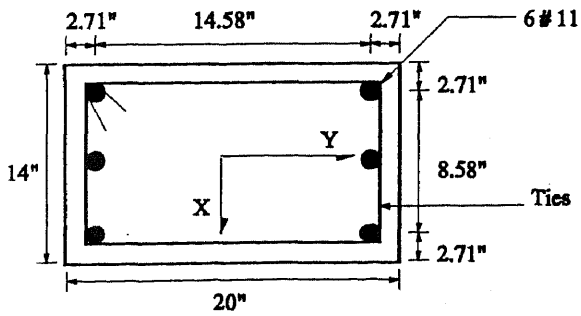


Fig. D.1p - Column cross section EX-4
Wang and Salmon (224)

**Figure D.2** Column cross sections D.1i to D.1p

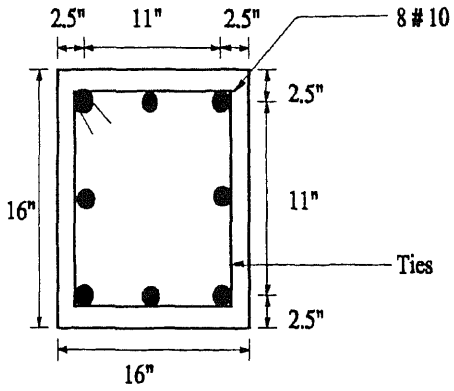


Fig. D.1q - Column cross section EX-5
Wang and Salmon (224)

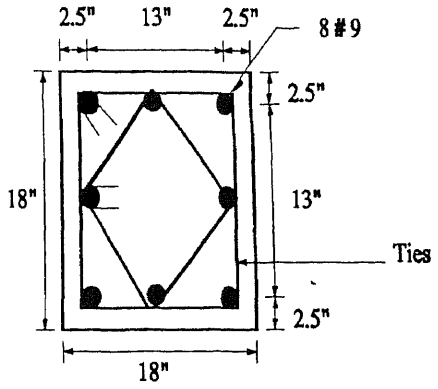


Fig. D.1r - Column cross section EX-6
Leet (126)

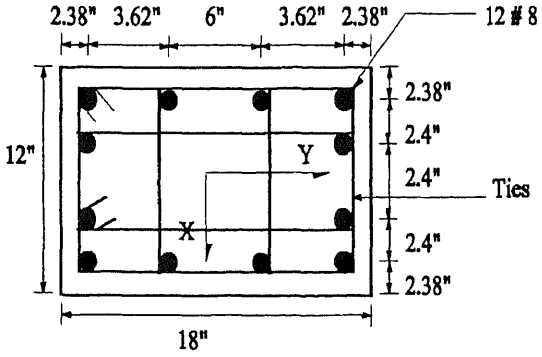


Fig. D.1s - Column cross section EX-7
Smith (189)

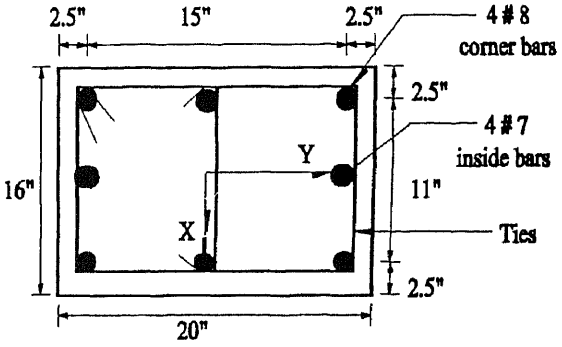


Fig. D.1t - Column cross section EX-8
Leet (126)

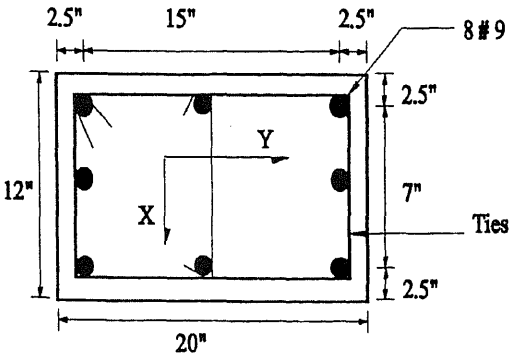


Fig. D.1u - Column cross section EX-9
Winter and Nilson (225)

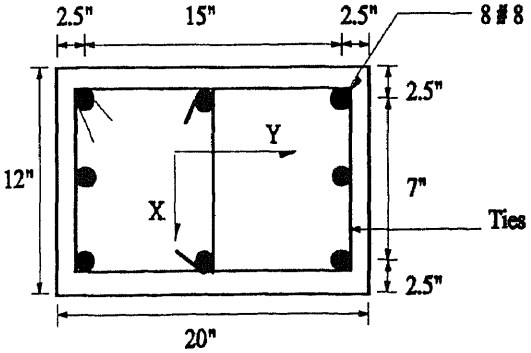


Fig. D.1v - Column cross section EX-10
Nawy (155)

**Figure D.3** Column cross sections D.1q to D.1v

# APPENDIX E

## Photographs

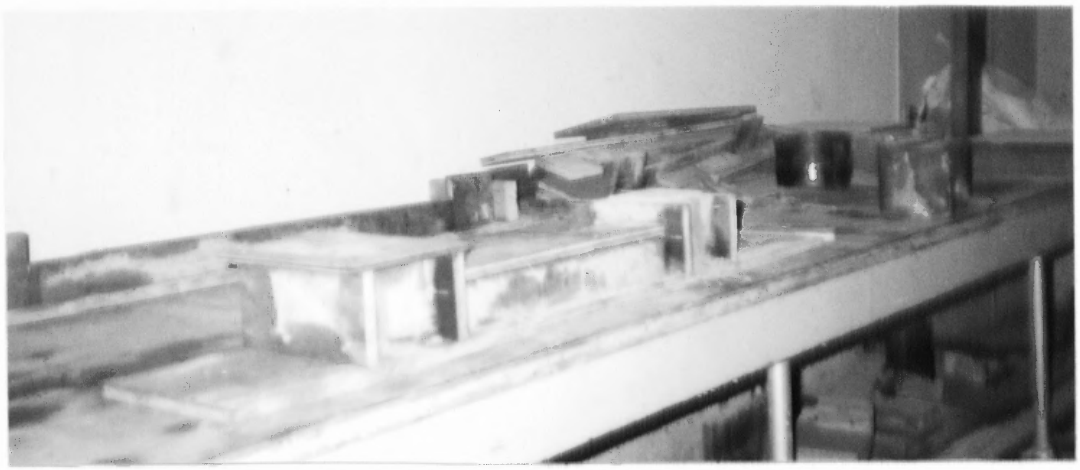

**Photo No. 1** Formwork, Short and Slender specimens with control cylinders after casting


**Photo No. 2** Tensile and Compressive tests of samples; Short and Slender composite column specimens before testing

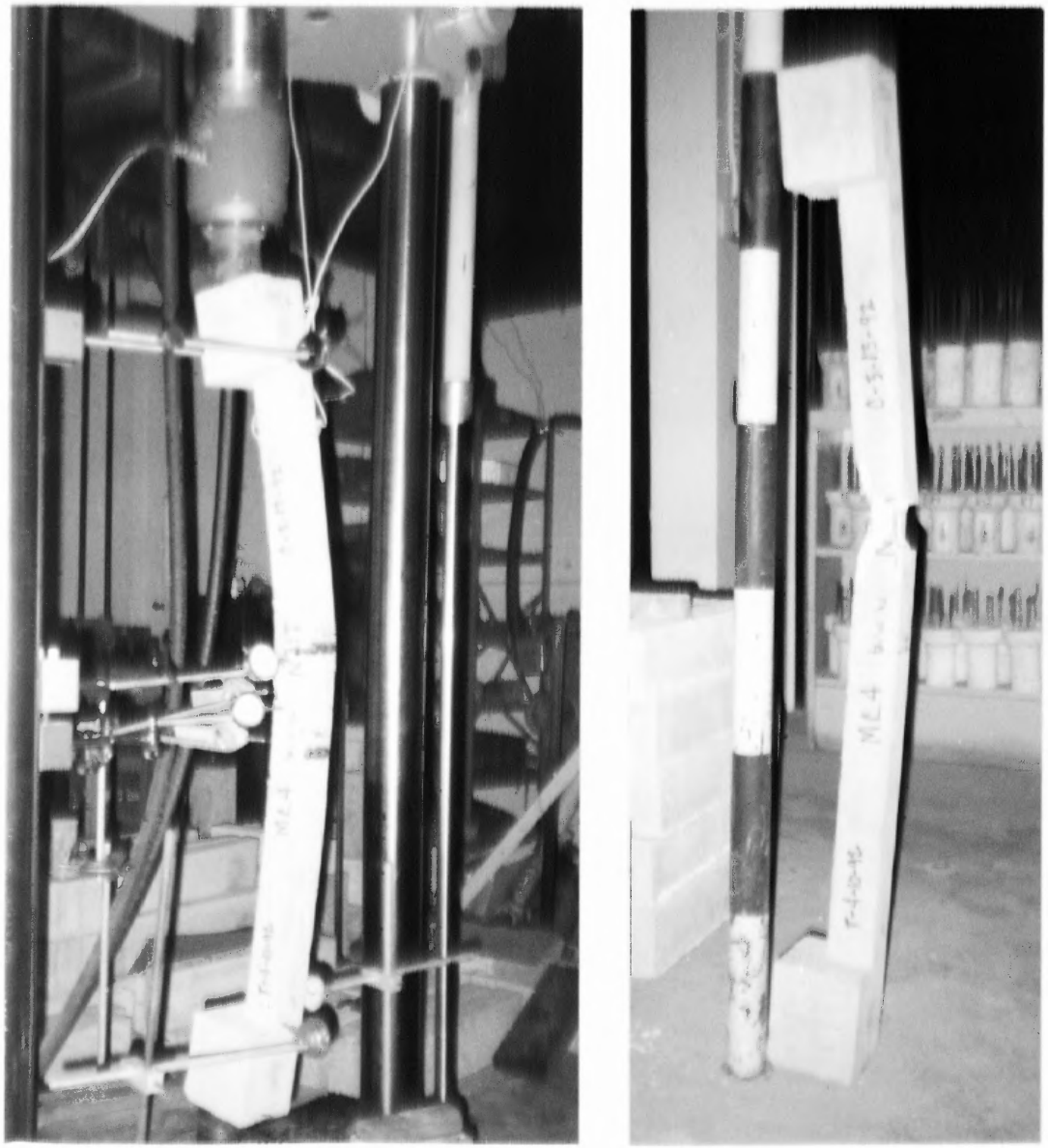

**Photo No. 3** Composite column MC4 with instrumentation during and after test

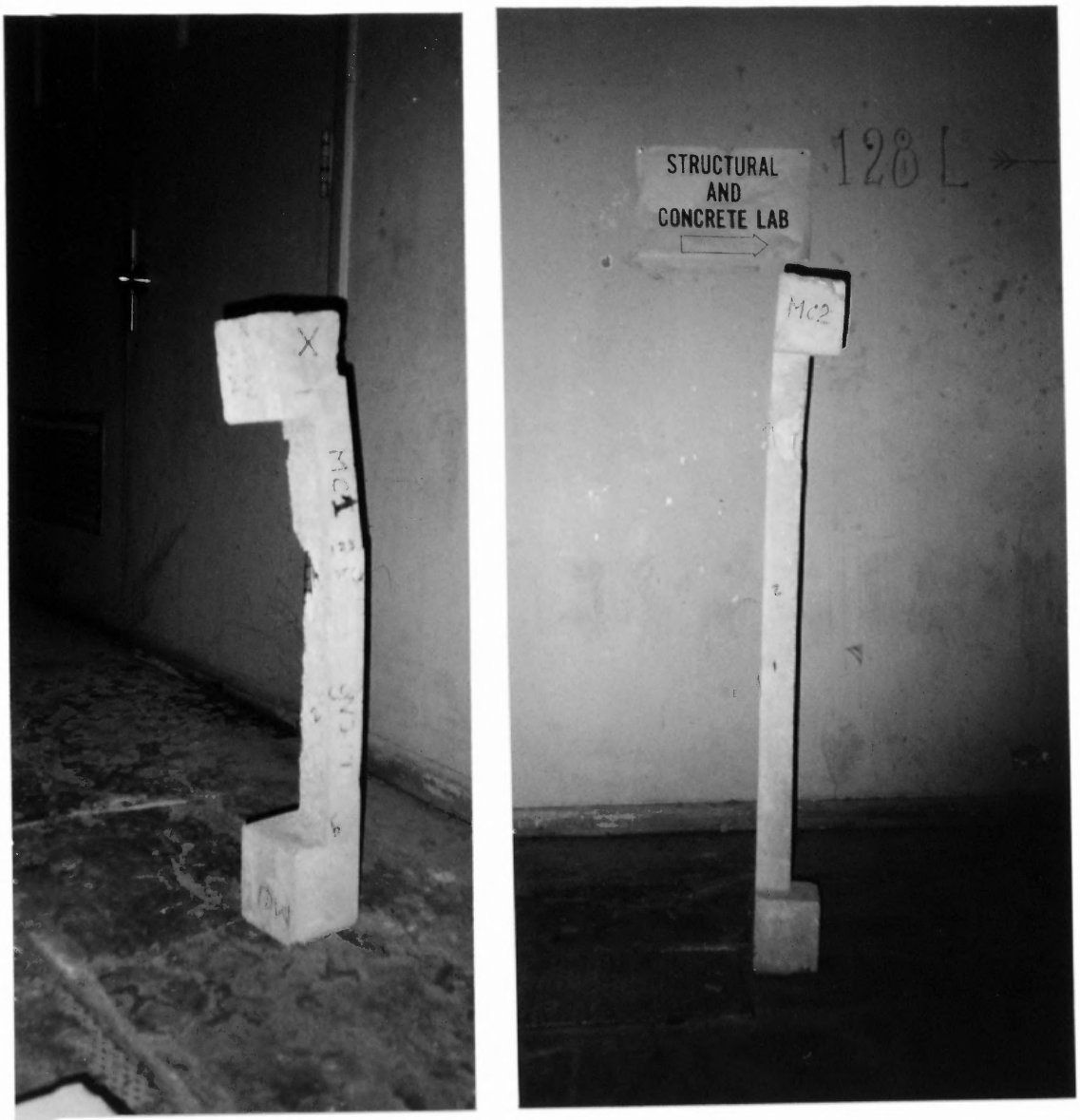


**Photo No. 4** Composite columns MC1 and MC2 after test

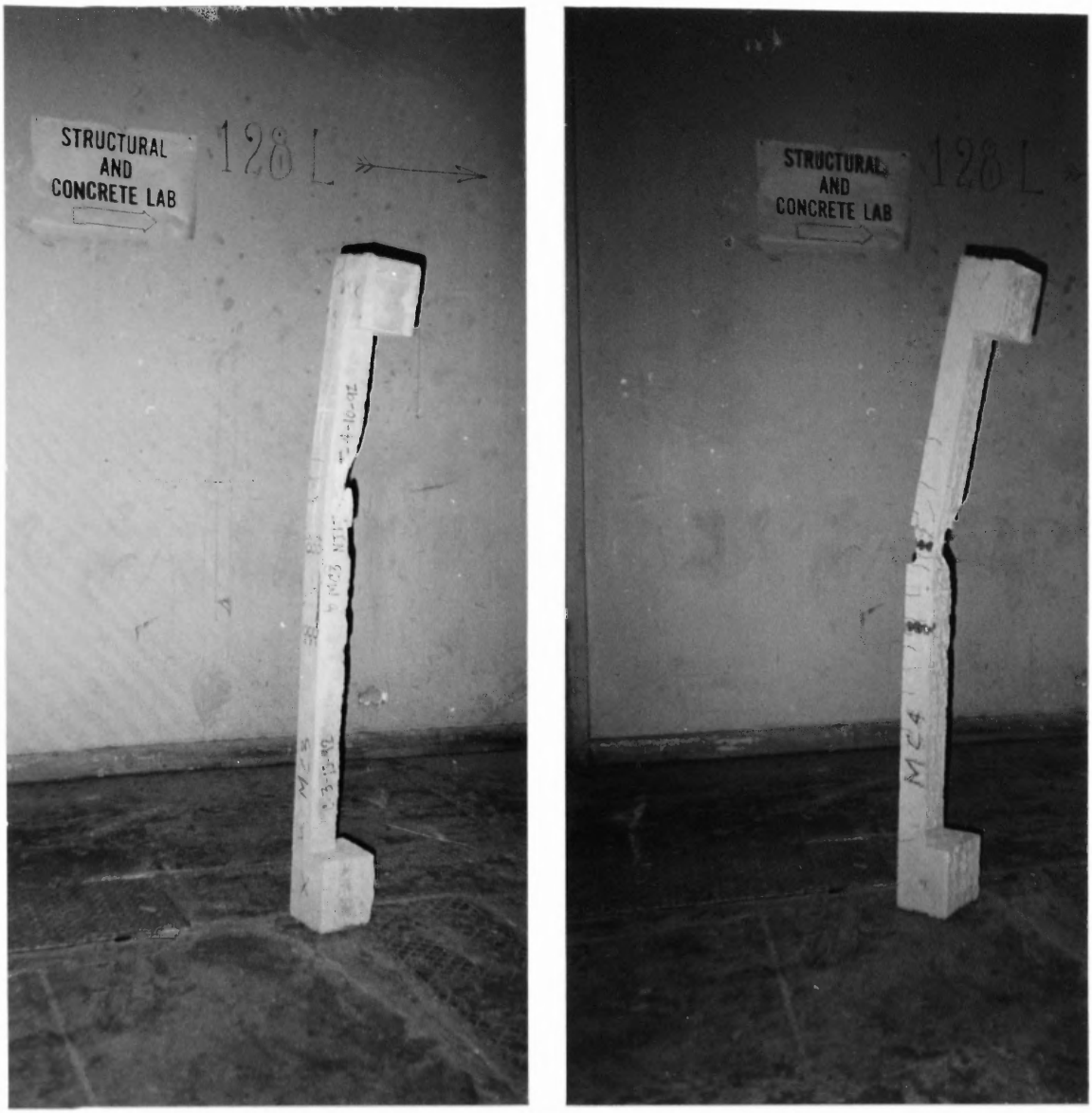


**Photo No. 5** Composite columns MC3 and MC4 after test

## BIBLIOGRAPHY


1. ACI Committee 318. *Building Code Requirements for Reinforced Concrete (ACI 318-89) and Commentary (ACI 318R-89).* American Concrete Institute, Detroit (1989): 107-130.

2. ACI-ASCE Committee 441. *Symposium on Reinforced Concrete Columns. Publication SP-13.* American Concrete Institute, Detroit (1966).

3. ACI Committee 441. *Reinforced Concrete Columns., Publication SP-50.* American Concrete Institute, Detroit (1975).

4. Amirthanandan, K., and B.V. Rangan. "Strength of Reinforced Concrete Columns in Biaxial Bending." *Institutions of Engineers-Civil Engineering Transactions.* Paper No. C89847, Vol. CE33, Australia (1991).

5. Aas-Jakobsen, A. "Biaxial Eccentricities in Ultimate Load Design." *ACI Journal.* March:(1964).

6. ACI Committee 340. *Design Handbook in Accordance with The Strength Design Method of ACI 318-89: Vol. 2 - Columns.* American Concrete Institute, Detroit (1990).

7. ACI. *1992 Publications Catalog.* American Concrete Institute, Detroit (1992).

8. Anderson, P., and H.N. Lee. "A Modified Plastic Theory of Reinforced Concrete." *Bulletin No. 33.* V. 54, No. 19, University of Minnesota, Minneapolis (1951).

9. Ansari, F. *Design of Reinforced Concrete Members Subjected to Tension with Small Eccentricities.* MSc Thesis, University of Colorado, Boulder (1978).

10. ACI Publication SP-24. *Models for Concrete Structures.* American Concrete Institute, Detroit, Michigan (1970): 65-159.

11. ACI Standard 211.1-81. "Standard Practice for Selecting Proportions for Normal, Heavyweight, and Mass Concrete." *ACI Manual of Concrete Practice 1992-Part 1.* American Concrete Institute, Detroit (1992).

12. AISC 1990. *ASD Manual of Steel Construction, 9th Edition.* American Institute of Steel Construction, Chicago, Illinois (1990).

13. AISC 1986. *Manual of Steel Construction, Load and Resistance Factor Design, First Edition.* American Institute of Steel Construction, Chicago, (1986).

14. Abe, H. "SRC Elevated Station Structures for New Bullet Trains." *Composite and Mixed Construction, Proceedings of the U.S.A./Japan Joint Seminar.* University of Washington, Seattle, Washington, July 18-20, (Edited by Charles W. Roeder),(1984): 163-175.

15. Abe, H., and Nakanao, T. "Experimental Investigation of Composite Rigid Frames." *State of the Art Report on Composite or Mixed Steel-Concrete Construction for Buildings.* Structural Specification Liaison Committee, ASCE (1977): 123-130.

16. Al-Noury, S.I., and Chen, W.F. "Finite Segment Method for Biaxially Loaded RC Columns." *Journal of the Structural Division, Proc. of the ASCE.* Vol. 108, ST4. (1982): 780-799.

17. Al-Noury, S.I., and Chen, W.F. "Behavior and Design of Reinforced and Composite Concrete Sections." *Journal of the Structural Division, Proc. of the ASCE.* Vol. 108, No. ST6, June (1982): 1266-1284.

18. Abel-Sayed, G., and Chung, K. "Composite Cold-Formed Steel Concrete Columns." *Canadian Journal of Civil Engineers.* v. 14, n. 3, June (1987): 295 301.

19. Bresler, B. "Design Criteria for Reinforced Columns under Axial Load and Biaxial Bending." *ACI Journal.* Proceedings 57, November (1960): 481-490.

20. Bresler, B., (Editor). *Reinforced Concrete Engineering-Volume I.* New York, John Wiley & Sons (1974): 217-219.

21. British Standards Institution. *Structural Use of Concrete - Part 1: Code of Practice for Design and Construction BS 8110.* London (1985).

22. Basu, A.K. "Computation of Failure Loads of Composite Columns." *Proceedings, Institution of Civil Engineers.* Vol. 36, March (1967): 557-578.

23. Basu, A.K. and W. Sommerville. "Derivation of Formulae for the Design of Rectangular Composite Columns." *Institution of Civil Engineers.* Paper 72065, Supplementary Volume (1969).

24. Burr, W.H. "The Reinforced Concrete Work of the McGraw Building.", *ASCE Transactions.* Vol. 60, No. 1075 (1908): 443 et seq.

25. Bondale, D.S. "Column theory with special reference to composite columns." *Consulting Engineer.* Vol. 30, No. 7, London, July (1966): 72-77; Vol. 30, No. 8 August (1966): 43-48; Vol. 30, No. 9, September (1966): 68-70.

26. Bradford, M.A., and Gilbert, R.I. "Time-Dependent Analysis and Design of Composite Columns." *Journal of Structural Engineering.* Vol. 116, No. 12, December, (1990): 3338-3357.

27. Bergmann, R. "Tubular Steel Columns filled with Concrete." *Acier-Stahl-Steel.* March (1981):107-109.

28. Belford, D. "Composite Steel-Concrete Building Frame." *Civil Engineering Magazine of ASCE.* July (1972): 61-65.

29. Bridge, R.Q., and Roderick, J.W. "Behavior of Built-Up Composite Columns." *Journal of the Structural Division, Proc. of the ASCE.* Vol. 104, No. ST7, July (1978): 1141-1155

30. Bode, H., and Bergmann, R. "Concrete filled structural hollow sections." *Stahl, Beratungsstelle Für Stahlverwendung.* 167, 2, Auflage (1985): 1-20.

31. Bridge, R.Q. "Effect of Pre-cracking on the Behavior of Composite Steel-Concrete Columns." *Institute of Engineers of Australia Civil Engineers Transactions.* v. CE 23, n. 2, May (1981) : 104-109.

32. Basu, A.K. "Restrained Composite Columns in Uniaxial Bending." *Proc. Journal of Construction Steel Research.* v. 2, n. 3, (1982): 2-10.

33. Bossart, R. "Possibilities of Use of Steel-Core Columns." *Stahlbau Rundsh.* n. 65, October (1985): 13-15.

34. Bondale, D.S. and Clark, P.J. "Composite Construction in the Almondsbury Interchange." *Proceedings of Conference on Structural Steelwork.* British Constructional Steelwork Association, Sept. (1966): 91-100.

35. Burr, W.H. "Composite Columns of Concrete and Steel." *Proceedings, The Institution of Civil Engineers.* Vol. 188, (1912): 114-126.

36. Basu, A.K., and Hill, W.F. "A More Exact Computation of Failure Loads of Composite Columns." *Proceedings, The Institution of Civil Engineers.* Vol. 40, May (1968): 37-60.

37. Brettle, R.Q. "Ultimate Strength Design of Composite Columns." *Journal of the Structural Division,* ASCE, Vol. 99, No. ST9, Proc. Sept. (1973): 1931-1951.

38. Chu, K.H., and A. Pabarcius. "Biaxially Loaded Reinforced Concrete Columns." *Proceedings ASCE.* Vol. 84, ST8, December (1958): 1-27.

39. Concrete Reinforcing Steel Institute. *CRSI Handbook.* Chicago (1984).

40. Chen, W.F., and L. Duan. "Design Interaction Equation for Steel Beam-Columns." *Journal of Structural Division, Proceedings ASCE.* Vol. 115, No. 5, May (1989): 1225-1243.

41. Cook, J.P. *Composite Construction Methods.* Chapter 10, The Composite Column. John Wiley & Sons, Inc., New York (1977): 206-321.

42. Cranston, W.B. "A Computer Method for the Analysis of Restrained Columns." *Technical Report TRA 402.* Cement and Concrete Association, London, April (1967).

43. Cai, S. and Jiao, Z. "Behavior and Ultimate Strength of Short Concrete-Filled Steel Tubular Columns." *Jian Zhu Jie Gou Xue Bao.* v. 5, n. 6, (1984): 13-29.

44. Cai, S. and Di, X. "Behavior and Ultimate Strength of Concrete-Filled Steel Tubular Columns under Eccentric Loading." *Jian Zhu Jie Gou Xue Bao.* v. 6, n. 4, (1985): 32-42.

45. Cai, S. and Gu, L. "Behavior and Ultimate Strength of Long Concrete-Filled Steel Tubular Columns " *Jian Zhu Jie Gou Xue Bao.* v. 6, n. 1, (1985): 32-40.

46. CIDECT. *Design Manual for Concrete-Filled Hollow Section Steel Columns.* Cidect Monograph No. 1, British Steel Corporation (1970).

47. Chen, W.F. "Analysis of Concrete-Filled Steel Tubular Beam-Columns.", *Fritz Engineering Laboratory Report No. 370.10.* Lehigh University (1970).

48. Chen, W.F., and Atsuta, T. *Theory of Beam-Columns.* Vol. 2, McGraw-Hill Book Co., Inc., New York, N.Y. (1976).

49. Dunham, C.W. *Advanced Reinforced Concrete.* McGraw-Hill Book Co., New York (1965).

50. Dundar, C. "Concrete Box Sections under Biaxial Bending and Axial Load." *Journal of Structural Engineering, ASCE.* Vol. 116, No. 3, March (1990): 860-865.

51. Davister, M.D. "A Computer Program for Exact Analysis." *Concrete International: Design and Construction.* Vol. 8, No. 7, July (1986): 56-61.

52. DIN 18 806, *Deutsche Norm.* Normenausschuß Bauwesen (NABau) im DIN Deutsches Institut für Normung e.V., März (1984): 1-10.

53. D'Huart, Jacques, and Wuerker, KarlGerd "Design of concrete-filled HSS Columns." International Symposium on Hollow Structural Sections, Toronto, May 25 (1977), Sponsored by CIDECT

54. Dunberry, E., Le-blanc, D., and Redwood, R.G. "Cross-Section Strength of Concrete-Filled HSS Columns at Simple Beam Connections." *Canadian Journal of Civil Engineering*. v. 14, n. 3, June (1987): 408-417.

55. Duan, L., and Chen, W.F. "Design Interaction Equations for Cylindrical Tubular Beam Columns." *Journal of Structural Engineering, ASCE*. Vol. 116, No. 7, July (1990): 1794-1812.

56. Duan, L., and Chen, W.F. "Design Interaction Equation for Steel Beam-Columns." *Journal of Structural Engineering, ASCE*. Vol. 115, No. 5, May (1989): 1225-1243.

57. Ehsani, M. "CAD for Columns" *Concrete International: Design and Construction*. Vol. 8, No. 9, September (1986): 43-47.

58. Emperger, F. V. "Welche statische Bedeutung hat die Einbetonierungeiner Eisensaule." *Beton Eisen*. Berlin (1907): 172-174.

59. Elnashai, A.S. (Imperial College of Science and Technology, London, (England), El-Ghazouli, A.Y., and Dowling, P.J. "International assesment of design guidance for composite columns." *Journal of Construction Steel Research*. v. 15 n 3 (1990): 191-213.

60. Elnasfi, A.S., El-ghazouli, A.Y., and Dowling, P.J. "International assessment of design guidance for composite columns." *Journal of Construction Steel Research*. Vol. 15, (1990): 191-213.

61. Fling, R.S. *Practical Design of Reinforced Concrete*. John Wiley & Sons, New York (1987): 253-309.

62. Fintel, M. (Editor). *Handbook of Concrete Engineering*. Van Nostrand Reinhold Co., 2nd Ed., New York (1985): 5-41.

63. Fergusson, P.M., and J. Breen, and J.O. Jirsa. *Reinforced Concrete Fundamentals*. 5th ed. John Wiley & Sons, New York (1985).

64. Furlong, R.W. "Concrete Columns under Biaxially Eccentric Thrust." *ACI Journal, Proceedings*. Vol. 76, October (1979): 1,093-1,118.

65. Furlong, R.W. "Strength of steel-encased concrete beam-columns." *Journal of the Structural Division, ASCE*. Vol. 93, ST10, October (1967): 113-124.

66. Furlong, R.W. "Design of steel-encased concrete beam-columns." *Journal of the Structural Division, ASCE*. Vol. 94, ST1, January (1968): 267-282.

67. Furlong, R.W. *Design tables for composite columns.* Preprint 1531, ASCE Annual meeting, St. Louis, Missouri, October 18-22 (1971).

68. Furlong, R.W. "Steel-concrete composite columns." *Handbook of composite construction Engineering.* (Ed. by Gajanan Sabnis), New York, Van Nostrand Reinhold, (1979)

69. Furlong, R.W. "AISC Column design logic makes sense for composite columns too." *Engineering Journal, AISC.* Vol. 13, 1(First Quarter), (1976): 1-7.

70. Furlong, R.W. "A recommendation: Composite column design rules consistent with specifications of the American Institute of Steel Construction." *Structural Stability Research Council.* Boston, Massachusetts, May (1978).

71. Faber, O. "Savings to be affected by the more rational design of encased stanchions as a result of recent full size tests." *Structural Engineer.* Vol. 34, No. 3, March, London (1956): 88-109.

72. Furlong, R.W. "Comparison of AISC, SSLC, and ACI Specifications for Composite Columns." *ASCE Journal of Structural Division.* Vol. 109, No. ST9, (1983): 1784-1803.

73. Furlong, R.W. "Column Rules of ACI, SSLC, and LRFD Compared." *Journal of Structural Engineering, ASCE.* Vol. 109, No. 10, October (1983): 2375-2386.

74. Furlong, R.W. "Composite Columns - A Bridge between AISC and ACI Regulations." *International Colloquium on Stability of Structures under Static and Dynamic Loads.* Washington, D.C., May 17-19, National Science Foundation and ASCE (1977): 709-717.

75. Furlong, R.W. "Binding and Bonding Concrete to Composite Columns.", *State of the Art Report on Composite or Mixed Steel-Concrete Construction for Buildings.* Structural Specification Liaison Committee, ASCE (1977): 330-336.

76. Ghosh, S.K., and B.G. Rabbat (Editors). *Notes on ACI 318-89, Building Code Requirements for Reinforced Concrete with Design Applications.* PCA, Portland Cement Association, 5th ed., (1990): 11.1-13.47.

77. Gowens, A.J. "Biaxial Bending Simplified." *Reinforced Concrete Columns (SP-50).* American Concrete Institute, Detroit (1975): 233-261.

78. Gardener, N.J. "Use of Spiral welded steel tubes in Pipe columns." *Journal of the ACI.* Vol. 65, No. 11, Nov. (1968): 937-942.

79. Gardener, N.J., and Jacobson, E.R. "Structural behavior of concrete-filled steel tubes." *Journal of ACI.* Vol. 64, No. 7, July (1967): 404-413.

80. Galambos, T.V.(Editor). *Guide to the Stability Design Criteria for Metal Structures, 4th Edition.* John Wiley & Sons, New York (1988): 359-386.

81. Griffis, L.G. "Some Design Considerations for Composite-Frame Structures." *Engineering Journal of the AISC.* Second Quarter, (1986): 59-64.

82. Grimault, J.P., and Mouty, J. "Prediction of Fire Resistance of Steel Columns with Concrete-filled Hollow Sections." *Journal of Construction Metals.* v. 21, n. 3, September (1984): 45-57.

83. Guiaux, P., and Dehouse, N.M. "Tests on 22 Eccentrically-Loaded Square and Rectangular Concrete-Filled Tubular Columns." *Laboratories d'Essais des Constructions du Genie Civil et d'Hydraulique Fluviale, University of Liege, Test Report No. R766.* September (1968).

84. Hassoun, M.N. *Design of Reinforced Concrete Structures.* PWS Engineering, Boston (1985).

85. Hsu, Cheng-Tsu T. "Analysis and Design of Square and Rectangular Columns by Equation of Failure Surface." *ACI Structural Journal.* V. 85, No. 2, March-April (1988): 167-179.

86. Hsu, Cheng-Tzu T. "Reinforced Concrete Members Subject to Combined Biaxial Bending and Tension." *ACI Journal Proceedings.* V. 83, No. 1, Jan.-Feb. (1986): 137-144.

87. Hsu, Cheng-Tzu T. "Biaxially Loaded L-Shaped Reinforced Concrete Columns." *Journal of Structural Engineering, ASCE.* V. 111, No. 12, Dec. (1985): 2576-2595.

88. Hsu, Cheng-Tzu T. "T-Shaped Reinforced Concrete Members under Biaxial Bending and Axial Compression." *ACI Structural Journal.* V. 86, No. 4, July-August (1989): 460-468.

89. Hsu, Cheng-Tzu T. "Channel-Shaped Reinforced Concrete Compression Members under Biaxial Bending." *ACI Structural Journal.* V. 84, No. 3, May-June (1987): 201-211.

90. Hsu, Cheng-Tzu T., et al. *Design of Biaxially Loaded Irregular Shaped Column Sections. Technical Report Structural Series No. 89-2.* Department of Civil and Environmental Engineering, New Jersey Institute of Technology, September (1989).

91. Hsu, Cheng-Tzu T. "Design of Reinforced Concrete Columns by Modified Load Contour Method." *Proceedings of NJIT-ASCE-ACI Structural Concrete Design Conference.* New Jersey Institute of Technology, March (1983): 285-299.

92. Hartley, G.A. "Radial Contour Methods of Biaxial Short Column Design." *ACI Journal Proceedings.* Vol. 82, No. 5, Sept.-Oct. (1985): 693-700.

93. Harik, I.E., and H. Gesund. "Flow Charts for Biaxial Bending in R/C Tied Columns." *Journal of Structural Engineering, ASCE.* Vol. 114, No. 6, June (1988): 1230-1249.

94. Huang, C., Harik, E.E., and H. Gesund. "CADCO: Analysis and Design of Uniaxially and Biaxially Bent Nonslender and Slender R/C Tied Columns in Braced and Unbraced Frames." *Design of Structural Concrete/Computer Publication COM-3.* American Concrete Institute, Detroit, Michigan (1987).

95. Horowitz, B. "Design of Columns Subjected to Biaxial Bending." *ACI Structural Journal.* Vol. 86, No. 6, November-December (1989): 717-722.

96. Hsu, Cheng-Tsu Thomas. *Behavior of Structural Concrete Subjected to Biaxial Flexure and Axial Compression.* Ph.D. Thesis, McGill University, Montreal, August (1974).

97. Heimdahl, P.D., and A.C. Bianchini. "Ultimate Strength of Biaxially Eccentrically Loaded Concrete Columns Reinforced with High Strength Steel." *Reinforced Concrete Columns, SP-50.* ACI, Detroit (1975): 93-117.

98. Hudson, F.M. "Reinforced Concrete Columns: Effects of Lateral Tie Spacing on Ultimate Strength." *Symposium on Reinforced Concrete Columns, SP-13.* American Concrete Institute, Detroit (1966): 235-244.

99. Hoegnestad, E. *A Study of Combined Bending and Axial Load in Reinforced Concrete Members. Bulletin No. 399.* Engineering Experiment Station, University of Illinois, Urbana (1951).

100. Hunaiti, Y. "Bond Strength in Battened Composite Columns." *Journal of Structural Engineering.* Vol. 117, No. 3, March (1991): 699-714.

101. Hanbin, G., and Tsutomu, U. "Strength of Concrete-Filled Thin-Walled Steel Box Columns: Experiment." *Journal of Structural Engineering, ASCE.* Vol. 118, No. 11, November (1992): 3036-3054.

102. Iyengar, S.H., and M. Iqbal. "Composite Construction-Chapter 23." *Building Structural Design Handbook.* (Edited by R. White and C. Salmon) John Wiley & Sons, (1987): 787-820.

103. Iyengar, S.H. *State of the Art Report on Composite or Mixed Steel-Concrete Construction for Buildings.* Structural Specification Liaison Committee, ASCE (1977): 1-32.

104. Iida, T. and Takada, K. "Studies on concrete-filled tubular steel columns." *Sumitomo Met.* v 41 n 4, October (1989): 43-52.

105. Johnson, R.P. *Composite Structures of Steel and Concrete, Vol. 1.* Chapter Five, Composite Columns and Frames, Constrado Monographs, A. Halsted Press Book, John Wiley & Sons, New York (1975): 145-206.

106. Johnston, B.G.(Editor). *Guide to the Stability Design Criteria for Metal Structures, Third Edition.* Structural Stability Research Council, John Wiley & Sons, New York (1976): 524-551

107. Jones, R., and Rizk, A.A. "An investigation of the behavior of encased steel columns under load." *Structural Engineer.* London, Vol. 41, No. 1, January (1963): 21-33.

108. Japan Society of Civil Engineers. *Steel-Concrete Composite Structures in Japan - State of the Art 1984.* Subcommittee on Steel-Concrete Composite Construction, JSCE, July (1984).

109. Johnson, R.P., and May, I.M. "Tests on Restrained Composite Columns." *The Structural Engineer.* Vol. 56B, No. 2, June (1978): 21-28.

110. Johnson, R.P., and Smith, D.G.E. "Simple Design Method for Composite Columns." *Structural Engineer.* Part A, v. 58A n. 3, March (1980): 85-93.

111. Juchniewicz, J., and Gorak, B. "Studies of Eccentrically Compressed Concrete-Filled Tubular Steel Columns." *Zesz Nauk Politech Lodz Budownictwo.* n. 33, (1984): 193-205.

112. Janss, J. *Composite Steel-Concrete Construction Part 3, Tests on Concrete Filled Tubular Columns.* Center of Scientific Research and Industrial Fabrication (CRIF), Brussels.

113. Kwan, K.H., and T.C. Liauw. "Computer Aided Design of Reinforced Concrete Members Subjected to Axial Compression and Biaxial Bending." *The Structural Engineer.* Vol, 63B, No. 2, June (1985): 34-40.

114. Kawakami, M., Tokuda H., Kagaya M., and M. Hirata. "Limit States of Cracking and Ultimate Strength of Arbitrary Concrete Sections under Biaxial Loading." *ACI Structural Journal, Proceedings.* Vol. 82, No. 2, March-April (1985): 203-212.

115. Kent, D.C., and R. Park. (1971) "Flexural Members with Confined Concrete." *Journal of Structural Division, ASCE.* Vol. 97, No. 7, (1971): 1969-1990.

116. Knowles, R.B., and Park, R. "Axial load design for concrete filled steel tubes." *Journal of the Structural Division, ASCE.* Vol. 96, ST10, October (1970): 2125-2153.

117. Knowles, R.B. and Park, R. "Strength of Concrete filled steel tubular columns." *Journal of the Structural Division, ASCE.* Vol. 95, No. ST12, Dec. (1969): 2565-2587.

118. Klöppel, K., and Goder, W. "Traglastversuche mit Ausbetonierton Stahlrohen and Aufstellung einer Bemessungsformel." *Der Stahlbau.* Berlin, Vol. 26 January-March (1957).

119. Kong, F.K., Evans, R.H., Cohen, E., and Roll, F., (Editors). *Handbook of Structural Concrete.* Chapter 17, McGraw-Hill Book Company, New York (1983): 17.38-17.56.

120. Kato, B., and Tagami, J. "Beam-to-Column Connection of a Composite Structure." *State of the Art Report on Composite or Mixed Steel-Concrete Construction for Buildings.* Structural Specification Liaison Committee, ASCE (1977): 205-214.

121. Knowles, P.R. *Composite Steel and Concrete Construction.* A Halsted Press book, John Wiley & Sons, (1973): 123-127.

122. Kennedy, S.J., and MacGregor, J.G. "End Connection Effects on the Strength of Concrete Filled HSS Beam Columns." *University of Alberta, Department of Civil Engineering, Structural Engineering Report n. 115.* April (1984)

123. Kato, B., and Kanatani, H. "Experimental Studies on Concrete-Filled Tubular Columns." *Steel Structures Laboratory Report.* Department of Architecture, Faculty of Engineering, Tokyo University, October (1966).

124. Kerensky, O.A., and Dallard, N.J. "The Four-Level Interchange between M4 and M5 Motorways at Almondsbury." *Proceedings, The Institution of Civil Engineers*. Vol. 40, July (1968): 295-322.

125. Kato, B., Sato, K., Kohyama, K., et al. "A study on Cast T-Stub Connections in Composite Strucutres, No. 1 and No. 2." *Abstracts of the Annual Congress of AIJ*. Sept. (1983): 2531-2533 (In Japanese).

126. Leet, K. *Reinforced Concrete Design*. McGraw-Hill Book Co.: (1982).

127. Lachance, L. "Stress Distribution in Reinforced Concrete Sections Subjected to Biaxial Loading." *ACI Structural Journal, Proceedings*. Vol. 77, No. 2, March-April (1980): 11-23.

128. Lu, L., Slutter, R., and Yen, B.T. "Recent Research on Composite Structures for Building and Bridge Applications." *Composite and Mixed Construction, Proceedings of the U.S.A./Japan Joint Seminar*. University of Washington, Seattle, Washington, July 18-20 (1984) Edited by Charles W. Roeder, ASCE (1985): 150-162.

129. Lachance, L. "Ultimate Strength of Biaxially Loaded Composite Sections." *Journal of the Structural Division, Proceedings of the ASCE*. Vol. 108, No. ST10, October (1982): 2313-2329.

130. Liu, X.L., and Chen, W.F. "Behavior and Design of Reinforced Concrete Pipe Columns." *Purdue University, School of Civil Engineering Technical Report CE-STR n. 82-28*. (1982)

131. Laredo, M., and Bard, J. "A Study of Steel-Concrete Composite Columns and their Application in High-Rise Buildings." (in French) *Annales de L'Institut du Batiment et des Travaux Publics*. Paris, Vol. 22, No. 254, February, (1969): 388-421.

132. Lally Column Co. *Lally Column Handbook*. File 13-C, New York: (1962).

133. Lu, L., and Kato, B. "Seminar Summary and Research Needs." *Composite and Mixed Construction, Proceedings of the U.S.A./Japan Joint Seminar*. University of Washington, Seattle, Washington, July 18-20 (1984), Edited by Charles W. Roeder, ASCE (1985): 323-329.

134. MacGregor, J.G. *Reinforced Concrete, Mechanics and Design*. Prentice Hall, Englewood Cliffs, New Jersey: (1988).

135. Meek, J.L. "Ultimate Strength of Columns with Biaxially Eccentric Loads." *ACI Journal, Proceedings*. Vol. 60, August (1963): 1053-1064.

136. Moran, F. "Design of Reinforced Concrete Sections under Normal Loads and Stresses in the Ultimate Limit State." *Bulletin d'Information No. 83, Comité Européen Du Béton*. Paris, April (1972).

137. MacGregor, J.G. "Simple Design Procedures for Concrete Columns." *Introductory Report, Symposium on Design and Safety of Reinforced Concrete Members*. Reports of the Working Commissions, Vol. 15, International Association of Bridge and Structural Engineering, Zurich, April (1973): 23-49.

138. MathCAD. *MathCAD V. 2.5.* Registered Trademark of MathSoft, Inc., (1989).

139. Mirza, S.A., and B.W. Shrabek. "Statistical Analysis of Slender Composite Beam-Columns Strength." *Journal of Structural Division, ASCE*. Vol. 118, No. 5, May (1992): 1312-1332.

140. Mensch, J.L. "Tests on Columns with Cast Iron Core." *ACI Proceedings*. Vol. 13, (1917)

141. Mensch, J.L. "Discussion of the Final Report of the Committee on Steel Columns and Struts." *Transactions ASCE*. Vol. 83, No. 1456 (1919-1920): 1667-1686.

142. Molitor, D. "Discussion of Composite Columns." *ACI Proceedings*. Vol. 27 (1930-1931): 947-950.

143. Mensch, J.L. "Composite Columns." *ACI Proceedings*. Vol. 27 (1930-1931): 263-280.

144. Metwally, A. "Slender Composite Beam-Columns." *Journal of Structural Engineering, ASCE*. Vol. 114, No. 10, October (1988): 2254-2267.

145. Mirza, S.A., and Skrabek, B.W. "Reliability of Short Composite Beam-Column Strength Interaction." *Journal of Structural Engineering, ASCE*. Vol. 117, No. 8, (1991): 2320-2339.

146. Moore, W.P., and Gosain, N.K. "Mixed Systems, Past Practices, Recent Experience and Future Direction." *Composite and Mixed Construction, Proceedings of the U.S.A./Japan Joint Seminar*. University of Washington, Seattle, Washington, July 18-20 (1984) Edited by Charles W. Roeder, ASCE (1985).

147. Morino, S., Matsui, C., and Watanabe, H. "Strength of Biaxially Loaded SRC Columns." *Proceedings U.S./Japan Joint Seminar on Composite and Mixed Construction,* ASCE (1984): 185-194.

148. Minami, K. "Beam to Column Stress Transfer in Composite Structures." *State of the Art Report on Composite or Mixed Steel-Concrete Construction for Buildings.* Structural Specification Liaison Committee, ASCE (1977): 215-225.

149. McDevitt, C.F., and Viest, I.M. "(a) Interaction of different materials." *Introductory Report, 55-79.* (b) "A Survey of using steel in combination with other materials." *Final Report, 101-117.* Ninth Congress, Int. Assoc. for Bridge and Struct. Eng., Amsterdam: (1972).

150. Malhorta, H.L., and Stevens, R.F. "Fire Resistance of Encased Steel Stanchions." *Proceedings, The Institution of Civil Engineers.* Vol. 27, No. 1, January, (1964): 77-98.

151. Matsui, C., Morino, S., et al. "Restraining Effect of Reinforced Concrete Portion on the Local Buckling of Steel Section in SRC Beam-Columns." *Abstracts of the Annual Congress of AIJ.* Oct. (1982): 2237-2238 (In Japanese).

152. Masuda, K., and Hirasaka, T. "Connections in Steel Reinforced Concrete Structures - Column Bases, Part 2 and 3." *Transactions AIJ.* No. 287, Jan. (1980): 39-50. No. 290, April (1980): 39-50. No. 290, April (1980): 33-44 (In Japanese).

153. Mirza, S.A. (Lakehead University, Thunder Bay, Ontario, Canada). "Parametric study of composite column strength variability." *Journal of Construction Steel Research.* v 14 n 2 (1989): 121-137

154. Matsumura, H., Ito, S., et al. "Concrete-filled rectangular tubular column with inner ribs." *NKK Tech Rev.* n 59 August (1990): 30-37.

155. Nawy, E.G. *Reinforced Concrete.* 2nd ed., Prentice Hall, Englewood Cliffs, New Jersey: (1990): 297-375.

156. Neogi, P.K., Sen, H.K., and Chapman, J.C. "Concrete-filled tubular steel columns under eccentric loading." *The Structural Engineer.* Vol. 47, No. 5, May (1969): 187-195

157. Nakai, H., Yoshikawa, O. "Experimental Study on Strength of Concrete-Filled Steel Pier." *Doboku Gakkai Rombun Hokokushu.* n. 344/I-1 (1984): 195-204

158. Nakai, H., Kitada, T., and Yoshikawa, O. "Design Method of Steel Plate Elements in Concrete Filled Square Steel Tubular Columns." *Doboku Gakkai Rombun Hokokushu.* n. 356/I-3 April (1985): 405-413.

159. Narayanan, R.(Editor). *Steel-concrete composite structures: Stability and Strength.* Elsevier Applied Science, New York, N.Y. (1988).

160. Nakai, H., Yoshikawa, O., and Terada, H. "An experimental study on ultimate strength of composite columns for compression or bending." *Proceedings, JSCE, Structural Engineering/Earthquake Engineering.* Japan Society of Civil Engineers (JSCE), 3(2), (1986): 235-245.

161. Park, R., and T. Paulay. *Reinforced Concrete Structures.* Wiley-Interscience, New York: (1975).

162. Pannell, F.N. "Failure Surfaces for Members in Compression and Biaxial Bending." *ACI Journal, Proceedings.* Vol. 60, January (1963): 129-140.

163. Parme, A.L., J.M. Nieves, and A. Gouwens. "Capacity of Reinforced Rectangular Columns Subject to Biaxial Bending." *ACI Journal, Proceedings.* Vol. 63, September (1966): 911-923.

164. Pannell, F.N. "Discussion of Biaxially Loaded Reinforced Concrete Columns." *Proceedings ASCE.* Vol. 85, ST6, June (1959): 47-54.

165. PCA Publication EB009D. *Strength Design of Reinforced Concrete Columns.* Portland Cement Association, Skokie, Illinois (1978).

166. PCA. *1991 Catalog, Publications, Computer Software, Audiovisual Materials.* Portland Cement Associations, Skokie, Illinois (1991).

167. Park, R., M.J.N. Priestley, and W. D. Gills. "Ductility of Square Confined Concrete Columns." *Journal of Structural Division, ASCE.* Vol. 108, No. 4, (1982): 929-950.

168. Pham, L. "Reliability Analysis of Reinforced Concrete and Composite Column Sections under Concentric Loads." *Institute of Civil Engineers of Australia, Transactions.* v. 27, n. 1, February (1985): 68-72.

169. Quast, U. "Investigations on the Fire Behavior of Composite Columns and Solid Steel Section Columns." *Stahlbau Rundsch.* n 53, Oct. (1979): 12-13.

170. Rice, P.F. and E.S. Hoffman. *Structural Design Guide to the ACI Building Code. 2nd ed.* Van Nostrand Reinhold Co., New York (1978): 276-317.

171. Ramamurthy, L.N. "Investigation of the Ultimate Square and Rectangular Columns under Biaxially Eccentric Loads." *Symposium on Reinforced Concrete Columns, SP-13.* American Concrete Institute, Detroit (1966): 263-298.

172. Ramamurthy, L.N. and T.A. Hafeez Khan. "L-Shaped Column Design for Biaxial Eccentricity." *Journal of Structural Engineering, ASCE.* Vol. 109, No. 8, August (1983): 1903-1917.

173. Row, D.G. and T. Paulay. "Biaxial Flexure and Axial Load Interaction in Short Rectangular Reinforced Concrete Columns." *Bulletin of the New Zealand Society for Earthquake Engineering.* Vol. 6, No. 3, September (1973): 110-121.

174. Ross, D.A., and J.R. Yen. "Interactive Design of Reinforced Concrete Columns with Biaxial Bending." *ACI Structural Journal, Proceedings.* Vol. 83, No. 6, Nov.-Dec. (1986): 988-993.

175. Roderick, J.W., and Rogers, D.F. "Load-carrying capacity of simple composite columns." *Journal of the Structural Division, ASCE.* Vol. 95, ST2 ,February (1969): 209-228.

176. Roik, K., and Bergmann, R. "Composite Columns - Design and Examples for Construction." *State of the Art Report on Composite or Mixed Steel-Concrete Construction for Buildings.* 2nd. US-Japan Seminar on Composite Structures.", Seattle, Wa. July (1984).

177. Rangan, B.V. "Design of Slender Hollow Steel Columns Filled with Concrete." *International Conference on Steel and Aluminum Strucutres.* Singapore, May 22-24 (1991).

178. Roberts, E.H., and Yam, L.C.P. "Some Recent Methods for the Design of Steel, Reinforced Concrete, and Composite Steel-Concrete Columns in the U.K." *ACI Journal.* March-April, (1983): 139-149.

179. Roeder, C.W. "Bond Stress of Embedded Steel Shapes in Concrete." *State of the Art Report on Composite or Mixed Steel-Concrete Construction for Buildings.* Structural Specification Liaison Committee, ASCE, (1977).

180. Roik, K., and Schwalbenhofer, K. "Experimental and Theoretical Examinations on the Plastic Behavior and the Rotation Capacity of Composite Beam-Columns." *Wilhelm Ernst & Sohn Verlag für Architektur und technische Wissenschaften, Stahlbau 58.* Berlin (1989).

181. Roik, K., and Bergmann, R. "Zur Traglastberechnung von Verbundstützen." *Der Stahlbau,* 51 Jahrgang, Heft 1, Jan. (1982): 8-16.

182. Roik, K., Bode, H., and Bergmann, R. "Bearing Capacity of Concrete-filled Hollow Steel Columns with allowance for the Creep Behavior of the Concrete." *Stahlbau.* v. 51, n. 7, July (1982): 207-212.

183. Roik, K., and Hanswille, G. "Studies of Load Introduction in Composite Columns with Encased I-Sections." *Stahlbau*. v. 53, n. 12, Dec. (1984): 353-358.

184. Roik, K., Diekmann, C., and Schwalbenhofer, K. "Composite Columns with Steel Fiber Reinforced Concrete." *Bauingenieur*. v. 62, n.4, April (1987): 179-182.

185. Roderick, J.W. "Further Studies of Composite Steel and Concrete Structures." *Preliminary Report, International Association for Bridge and Structural Engineering, Ninth Congress*. Amsterdam, May, (1972): 157-164.

186. Roik, K. (Ruhr-Univ Bochum, West Germany), and Bergmann, R. "Design Method for composite columns with unsymmetrical cross-sections." *Journal of Construction Steel Research*. v. 15 n 1-2 (1990): 153-168.

187. Shanmughasundaram, N. "Biaxial Interaction Exponent for Concrete Columns." *Journal of The Structural Division, Proceedings ASCE*. Vol. 103, No. ST12, December (1977): 2295-2305.

188. Sallah, A.Y. "Analysis of Short Rectangular Reinforced Concrete Columns Subjected to Biaxial Moments." *M. Eng. Thesis, Department of Civil Engineering, Carleton University*. Ottawa, January (1983).

189. Smith, J.C. "Biaxially Loaded Concrete Interaction Curve." *Computers and Structures*. Vol. 3, (1973): 1461-1464.

190. Sabnis, G.M., H. G. Harris, et al. *Structural Modeling and Experimental Techniques*. Prentice-Hall, Inc., Englewood Cliffs, New Jersey (1983).

191. Sabnis, G.M., and M.S. Mirza. "Size Effects in Model Concretes." *ASCE Journal of Structural Division*. V. 105, No. ST6, June (1979): 1007-1020.

192. Saatcioglu, M., and S.R. Razvi. "Strength and Ductility of Confined Concrete." *Journal of Structural Division, ASCE*. Vol. 118, No. 6, June (1992): 1590-1607.

193. Samra, R.M. "Ductility Analysis of Confined Columns." *Journal of Structural Div., ASCE*. Vol. 116, No. 11, November (1990): 3148-3162.

194. Stevens, R.F. "The Strength of Encased Stanchions" *Research Paper 38*. National Building Studies, HMSO, London (1965).

195. Stevens, R.F. "Encased Stanchions" *Structural Engineer*. Vol. 43, London, Feb. (1965).

196. Structural Stability Research Council, (Task Group 20). "A Specification for the Design of Steel-Concrete Composite Columns." *Engineering Journal of AISC.* Vol. 16, No. 4, (1979): 101-115.

197. Sharma, A., and Pandit, G.S. "Tests on Concrete Beams in Biaxial Bending, Axial Compression, and Torsion." *Proceedings, Institute of Civil Engineers.* Part 2, Technical Note 361, 75, June (1983): 297-306.

198. Smith, D.G.E.(Scott Wilson Kirpatrick & Partners) "Slenderness Effects in Reinforced Concrete, Steel, and Composite Columns." *Proceedings of the Institution of Civil Engineers.* London, v. 69, pt. 2, June (1980): 343-357

199. Suzuya, J. and Kawana, H. "Experimental Studies on Steel Reinforced Concrete Beam-Columns." *Tohoku Kogyo Daigaku Kiyo.* 1, n. 4, March (1984): 23-40.

200. Schleich, J.B. "Fire Safety, design of Composite Columns." *Rev. Tech. Luxemburg.* v. 77, n. 1, January-March (1985): 1-24.

201. Stevens, R.F. "Encased Stanchions and BS 449." *Structural Engineer.* 188, October (1959).

202. Salani, H.J., and Sims, J.R. "Behavior of Mortar Filled Steel Tubes in Compression." *Journal of American Concrete Institute.* Vol. 61, No. 10, October (1964): 1271-1283.

203. Suzuki, T., Takiguchi, K., Ichinose, T., and Okamoto, T. "Effect of Hoop Reinforcement in Steel and R/C Composite." *Preprints of the Third South Pacific Regional Conference on the Earthquake Engineering.* Wellington, New Zealand, 9-12 May (1983).

204. Shakir-Khalil, H. (University of Manchester, Manchester, England), and Mouli, M. "Further tests on concrete-filled rectangular hollow-section columns." *Structural Engineer.* v 68 n 20 October 16 (1990): 405-413.

205. Skrabek, B.W., and Mirza, S.A. "Strength reliability of short and slender composite steel-concrete columns." *Report No. CE-90-1,* Lakehead University, Thunder Bay, Ontario, Canada (1990).

206. Shakir-Khalil, H., and Hunaiti,Y.M. "Battened composite columns." *Steel in Buildings: IABSE-ECCS Symposium.* Luxembourg (1985): 325-333.

207. Sohal, I.S., Duan, L., and Chen, W.F. "Design Interaction Equations for Steel Members." *Journal of Structural Engineering, ASCE.* Vol. 115, No. 7, July (1989): 1650-1665.

208. Tsao, W.H. "Behavior of Square and L-shaped Slender Reinforced Concrete Columns under Combined Biaxial Bending and Axial Compression." *Ph.D. Thesis, New Jersey Institute of Technology*. December (1991).

209. Towfighi, Sa'id. "Design Aids for Reinforced Concrete Columns." *Concrete International: Design & Construction*. Vol. 10, No. 3, March (1988): 49-54.

210. Taylor, M.A. "Direct Biaxial Design of Columns." *Journal of Structural Engineering, ACI*. Vol. 111, No. 1, January (1985): 158-173.

211. Tsui, S.H. and M.S. Mirza. (1969) "Model Microconcrete Mixes." *Structural Concrete Series No. 23*. McGill University, Montreal, November (1969).

212. Taranath, B.S. *Structural Analysis and Design of Tall Buildings.* McGraw-Hill Book Co., New York: (1973): 341-379.

213. Talbot, A. N., and Lord, A.R. "Tests of Columns: An Investigation of the Value of Concrete as Reinforcement for Structural Steel Columns." *Engineering Experimental Station Bulletin, No. 56*. University of Illinois at Urbana (1912).

214. Tucker, J. "Reinforced Concrete Columns." *Transactions ASCE*. Vol. 86, No. 1523 (1923):1074-1148.

215. Tomii, M., Matsui, C., and Sakino, K. "Concrete-filled steel tube structures." *Tokyo Regional Conference*. IABSE-ASCE Tall Buildings Conference, August (1973).

216. Tomii, M., Yoshimura, K., and Morishita, Y. "Experimental Studies on Concrete-Filled Steel Tubular Stub Columns under Concentric Loading." *International Colloqium on Stability of Structures*. Washington, D.C., May 17-19 (1977): 718-741.

217. Taylor, R., Shakir-Khalil, H., and Yee, K.M. "Some Tests on a new type of Composite Column." *Proceedings Institute of Civil Engineers*. Part 2, Technical Note 355, June (1983): 283-296.

218. Virdi, K.S. and Dowling, P.J. "A Unified Design Method for Composite Columns." *CESUC Report CC11*. Imperial College, London, July (1975).

219. Varghese, P.C. "Ultimate strength of encased steel members subjected to combined bending and axial loads." *Journal of Institution of Civil Engineers.* India, Vol. XLI, No. 6, Pt. 1 February (1961): 225-237.

220. Viest, I.M., Chmn. "Composite Steel-Concrete Construction, by the Subcommittee on the State-of-the-Art Survey, of the Task Committee on Composite Construction, of the Committee on Metals, Structural Division." *Journal of the Structural Division, ASCE.* Vol. 100, No. ST5, Proc. Paper 10561, May (1974): 1085-1139.

221. Virdi, K.S., and Dowling, P.J. "The Ultimate Strength of Biaxially Restrained Columns." *Proceedings of Institution of Civil Engineers.* Part 2, 61, March (1976): 41-58.

222. Virdi, K.S., and Dowling, P.J. "The Ultimate Strength of Composite Columns in Biaxial Bending." *Proceedings of Institution of Civil Engineers.* Part 2, March (1973): 251-272.

223. Virdi, K.S., and Dowling, P.J. "Bond strength in concrete-filled steel tubes." *Proceedings IABSE.* (1980): 125-139.

224. Wang, Chu-kia, and C. G. Salmon. *Reinforced Concrete Design.* 4th ed. Harper & Row, New York: (1985): 400-486.

225. Winter, G. and A. Nilson. *Design of Concrete Structures. 10th ed.* McGraw-Hill, New York (1986): 259-301.

226. Wang, G., and Cheng-Tzu T. Hsu. "Complete Load Deformation Behavior of Biaxially Loaded Reinforced Concrete Columns." *Technical Report, Structural Series No. 90-2.* Department of Civil and Environmental Engineering, New Jersey Institute of Technology, September (1990)

227. Weber, D.C. "Ultimate Strength Design Charts for Columns with Biaxial Bending." *ACI Structural Journal.* Vol, 63, No. 11, November (1966): 1205-1230.

228. White, R.N., and M.S. Mirza, et al. *Structural Modeling and Experimental Techniques.* Prentice-Hall, Inc., Englewood Cliffs, New Jersey (1983).

229. Withey, M.O. "Tests of Plain and Reinforced Concrete Columns." *Bulletin No. 300 Engineering Series.* Vol. 5, No. 2, University of Wisconcin (Madison) (1909): 143-188

230. Wakabayashi, M. "Recent Research Activities on Composite Steel Reinforced Concrete Building Structures and Design Practices in Japan." *2nd. US-Japan Seminar on Composite Structures.* Seattle, Wa. July (1984).

231. Wakabayashi, M. "Seismic Design of Mixed Steel Concrete Structures in Japan." *International Colloqium on Stability of Structures.* Washington, D.C., May 17-19 (1977): 40-58.

232. Wakabayashi, M. "A New Design Method of Long Composite Beam-Columns." *International Colloqium on Stability of Structures.* Washington, D.C., May 17-19 (1977): 742-756.

233. Wakabayashi, M. "Recent Developments for Composite Buildings in Japan." *Composite and Mixed Construction, Proceedings of the U.S.A./Japan Joint Seminar.* University of Washington, Seattle, Washington, July 18-20 (1984) (Edited by Charles W. Roeder) ASCE, (1985): 241-253.

234. Watanabe, Y. "A Study of the Strength of Axially Loaded Composite Columns made with Steel H-Sections Embedded in Concrete." (In Japanese) *Transactions, Architectural Institute of Japan.* (1966).

235. Wakabayashi, M., Nakamura, T., et al. "Experimental Study on the Inelastic Stability of Steel Reinforced Concrete Columns." *Abstracts of the Annual Congress of AIJ.* Sept. (1983): 2473-2474 (In Japanese).

236. Xi-min, S., Guanzao, T., and Bingguan, Z. "Building with Concrete-filled Steel Columns." *Batim Institute of Building Research Practice.* v. 16 n. 5 Sep-Oct (1983): 311-316.

237. Yen, J.Y.R. "Quasi-Newton Method for Reinforced-Concrete Column Analysis and Design." *Journal of Structural Engineering, ASCE.* Vol. 117, No. 3, March (1991): 657-666.

238. Yee, K.M., Shakir-Khalil, H., and Taylor, R. "Design Expressions for a new type of Composite Column." *Journal of Construction Steel Research.* v. 2, n. 2, June (1982): 26-32.

239. Yamada, M., Kawamura, H., et al. "A Study on the Elasto-Plastic Deformation and Collapse Characteristics of SRC Unit Rigid Frames Under Constant Axial Compression." *Abstracts of the Annual Congress of AIJ.* Oct. (1982): 2297-2298 (In Japanese).

240. Zahn, F.A., R. Park, and J.N. Priestley. "Strength and Ductility of Square Reinforced Concrete Column Sections Subjected to Biaxial Bending." *ACI Structural Journal.* Vol. 56, No. 2, March-April (1989): 123-131.

241. Zhong, S. and Miao, R. "Research on the Computation of Bearing Capacity of Concrete-Filled Steel Tubular members subjected to Axial Compressive Loading." *Jian Zhu Jie Gou Xue Bao.* v.5, n. 6, (1984): 38-48.

242. Zhong, S. "Research on the Calculation of Load Bearing Capacity of Concrete-Filled Steel Tubular Columns Under Eccentric Loading." *Jian Zhu Jie Gou Xue Bao.* v. 6, n. 4, (1985): 21-31.

243. Zhou, S.P., and Chen, W.F. "Design Criteria for Box Columns under Biaxial Bending." *Journal of Structural Engineering, ASCE.* Vol. 111, No. 12, December (1985): 2643-2658.